

UPPER PALEOCENE-LOWERMOST EOCENE PLANKTONIC
FORAMINIFERAL BIOSTRATIGRAPHY AND RECORD OF
THE PALEOCENE-EOCENE THERMAL MAXIMUM
IN THE HAYMANA BASIN (ANKARA, TURKEY)

A THESIS SUBMITTED TO
THE GRADUATE SCHOOL OF NATURAL AND APPLIED SCIENCES
OF
MIDDLE EAST TECHNICAL UNIVERSITY

BY
GAMZE TANIK

IN PARTIAL FULFILLMENT FOR THE REQUIREMENTS
FOR
THE DEGREE OF MASTER OF SCIENCE
IN
GEOLOGICAL ENGINEERING

AUGUST 2017

Approval of the thesis:

**UPPER PALEOCENE-LOWERMOST EOCENE PLANKTONIC
FORAMINIFERAL BIOSTRATIGRAPHY AND RECORD OF
THE PALEOCENE-EOCENE THERMAL MAXIMUM
IN THE HAYMANA BASIN (ANKARA, TURKEY)**

Submitted by **GAMZE TANIK** in partial fulfillment of the requirements for the degree of **Master of Science in Geological Engineering Department, Middle East Technical University** by,

Prof. Dr. Gülbin DURAL
Dean, Graduate School of **Natural and Applied Sciences**

Prof. Dr. Erdin BOZKURT
Head of Department, **Geological Engineering**

Prof. Dr. Sevinç ALTINER
Supervisor, **Geological Engineering Dept., METU**

Examining Committee Members:

Prof. Dr. İsmail Ömer YILMAZ
Geological Engineering Dept., METU

Prof. Dr. Sevinç ALTINER
Geological Engineering Dept., METU

Prof. Dr. Veysel IŞIK
Geological Engineering Dept., Ankara University

Assist. Prof. Dr. Fatma KÖKSAL TOKSOY
Geological Engineering Dept., METU

Assist. Prof. Dr. Ayşe ÖZDEMİR
Geophysical Engineering Dept., Yüzüncüyıl University

Date: 11.08.2017

I hereby declare that all information in this document has been obtained and presented in accordance with academic rules and ethical conduct. I also declare that, as required by these rules and conduct, I have fully cited and referenced all material and results that are not original to this work.

Name, Last Name: Gamze TANIK

Signature :

ABSTRACT

UPPER PALEOCENE-LOWERMOST EOCENE PLANKTONIC FORAMINIFERAL BIOSTRATIGRAPHY AND RECORD OF THE PALEOCENE-EOCENE THERMAL MAXIMUM IN THE HAYMANA BASIN (ANKARA, TURKEY)

Tanık, Gamze
M.Sc., Department of Geological Engineering
Supervisor: Prof. Dr. Sevinç ALTINER

August 2017, 258 pages

A rapid global warming event, called the Paleocene-Eocene Thermal Maximum (PETM), took place ca. 56 Ma, marking the Paleocene/Eocene boundary. This event is recorded by a turnover of planktonic foraminifera in deep marine settings, with occurrence of three species so-called planktonic foraminifera excursion taxa (PFET). This work was carried out in order to determine the record of this event in the Haymana Basin, Central Anatolia.

The Haymana Basin provides a continuous sedimentary succession starting with Upper Cretaceous up to middle Eocene, where upper Paleocene-lower Eocene succession is represented by a deep marine shale succession, known as the Eskipolatlı Formation. A 33 meter thick stratigraphic section was measured from this formation, and 41 samples were taken. The samples were prepared by standard

washing method, and planktonic foraminifera were picked from >63 and >106 μm fractions, and analyzed.

Planktonic foraminifera were studied for biostratigraphic framework, 40 species belonging to 11 genera were identified, and 4 biozones were distinguished spanning through the late Thanetian and earliest Ypresian. In ascending order these biozones are as follows: *Globanomalina pseudomenardii* Zone, *Morozovella subbotinae* Zone, *Acarinina sibiyaensis* Zone, and *Pseudohastigerina wilcoxensis* Zone.

A quantitative study was conducted on 26 of the samples in order to establish the generic relative abundance changes throughout the measured section. As is in similar latitudes, the section withholds a dominance of *Acarinina*, accompanied by *Subbotina* and *Morozovella* genera. A smaller fraction of the assemblage is represented by Globanomalinids and Igorinids. A reworking/transportation problem is identified in the samples, causing difficulties determining the zonal boundaries. This situation, along with the quantitative results, can be interpreted to be related to the phases of turbiditic activity.

With this study one representative of PFET, hence the chronostratigraphically short *A. sibiyaensis* Zone was detected in the Haymana Basin, Turkey, for the first time. The PFET, apart from *Acarinina sibiyaensis*, were not discovered, which may be due to large sampling interval, preservational complexities, or their preferred geographical distribution. Through the identification of *A. sibiyaensis* Zone, position of the PETM is designated. With planktonic foraminiferal biozonation, chronostratigraphic position of the Eskipolatlı Formation is better visualized.

Keywords: Paleocene/Eocene boundary, Paleocene-Eocene Thermal Maximum, planktonic foraminifera, biostratigraphy, Haymana Basin

ÖZ

HAYMANA HAVZASI'NDA (ANKARA, TÜRKİYE) ÜST PALEOSEN-EN ALT EOSEN PLANKTONİK FORAMİNİFER BİYOSTRATİGRAFİSİ VE PALEOSEN-EOSEN TERMAL MAKSİMUM'UN KAYDI

Tanık, Gamze
Yüksek Lisans, Jeoloji Mühendisliği Bölümü
Tez Yöneticisi: Prof. Dr. Sevinç ALTINER

Ağustos 2017, 258 sayfa

Yaklaşık 56 Ma önce gerçekleşmiş ani bir küresel ısınma (Paleosen-Eosen Termal Maksimum) Paleosen/Eosen sınırını simgeler. Bu olay derin deniz ortamlarında planktonik foraminifer topluluklarında planktonik foraminifer sapma taksonları (PFET) olarak adlandırılan üç planktonik foraminifer türünün ortaya çıkışı ile bir dönüşüm olarak kaydedilmiştir. Tez çalışması bu olayın Orta Anadolu'da Haymana Havzası'ndaki kaydını incelemeyi amaçlamaktadır.

Haymana Havzası Üst Kretase-orta Eosen aralığında sürekli çökelmiş olan bir sedimanter istif özelliği nedeniyle bu çalışma için uygun bir ortam sunmaktadır. Üst Paleosen-alt Eosen aralığı Eskipolatlı Formasyonu olarak bilinen derin deniz şeyl birimiyle temsil edilmektedir. Bu formasyondan ölçülen 33 metrelik stratigrafik kesit üzerinden alınan 41 örnek yıkama metodu ile hazırlanarak planktonik foraminiferler toplanarak çalışılmıştır.

Planktonik foraminiferler biyostratigrafik çatı için çalışılmış olup 11 cinse ait toplam 40 tür tanımlanmıştır. Kesit boyunca 4 adet biyozon belirlenmiş olup bunlar gençleşen sırayla şöyledir: *Globanomalina pseudomenardii* Zonu, *Morozovella subbotinae* Zonu, *Acarinina sibiyaensis* Zonu, and *Pseudohastigerina wilcoxensis* Zonu. Bu biyozonlar geç Tanesiyen ve en erken İpresiyen'i temsil etmektedir.

Cins bazında bollukların ölçülü kesit boyunca incelenmesi amacıyla 26 adet örnekten sayısal analiz yapılmıştır. Benzer enlemlerde de görüldüğü gibi *Acarinina* cinsinin baskınlığı kaydedilmiş olup *Subbotina* ve *Morozovella* cinslerinin bolluğu eşlik etmektedir. Topluluğun küçük bir kısmını ise Globanomalinid ve Igorinid gruplar oluşturmaktadır. Örneklerde belirlenen taşınma/yeniden işleme sorunu zon sınırlarının belirlenmesinde zorluklara sebep olmuştur. Sayısal analizle birlikte incelendiğinde bu durum türbit akıntı fazlarına bağlı olarak yorumlanabilir.

Bu çalışma ile PFET'den bir tür olan *A. sibiyaensis* Türkiye'de ilk defa Haymana Havzası'nda belirlenmiş ve biyozon oluşturulmuştur. Diğer PFET türlerine örneklerde rastlanmamış olması geniş örnek aralığı, korunmaya dair problemler veya bu türlerin tercih ettiği coğrafi dağılım ile açıklanabilir. *A. sibiyaensis* Zonu'nun bulunuşuyla PETM'in yeri belirlenmiştir. Çalışma ile oluşturulan biyostratigrafik çatı Eskipolatlı Formasyonu'nun kronostratigrafik pozisyonunu belirginleştirmiştir.

Keywords: Paleosen/Eosen sınırı, Paleosen-Eosen Termal Maksimum, planktonik foraminifer, biyostratigrafi, Haymana Havzası

*To women who dreamt of
having a career in science*

ACKNOWLEDGEMENTS

I would like to express my gratitude to my supervisor Prof. Dr. Sevinç ÖZKAN-ALTINER, without her guidance this thesis could not have been produced. I am also very grateful for the discussions and encouragement of Prof. Dr. Demir ALTINER. They have been there whenever I felt discouraged and in doubt; they supported and guided my work, as well as my passion.

I would like to thank to Dr. Aynur HAKYEMEZ for her precious insight of Cenozoic planktonic foraminifera, she stepped in right when needed and pushed just as necessary.

I would like to thank to Serkan YILMAZ for his hours of time in the SEM laboratory; and to Orhan KARAMAN for preparation of the thin sections needed for this study. Moreover, I would like to thank to METU Scientific Research Projects Coordination (BAP) for giving financial support for this study.

This thesis would not have been realized if it weren't for my colleagues Serdar Görkem ATASOY, Uygur KARABEYOĞLU, Ezgi VARDAR, and the other members of the Stratigraphy, Sedimentology and Micropaleontology Research Group, who'd helped and supported me in so many aspects of this study from the field to the microscope. Their help is precious and I hope to have been such help to them as well.

Lastly, I would like to mention my appreciation of the support of my beloved friends Emre TOPÇU and Yunus TERZİOĞLU, and my mother Naciye Tendu TİMURTAŞ and my brother Nahit Doğan TANIK who have been there for me during all this time, comforting me and easing my nerves. And my dear friend Mustafa KANGÜL is also highly appreciated for showing up just at the right moment to keep me up and going.

TABLE OF CONTENTS

ABSTRACT.....	v
ÖZ	vii
ACKNOWLEDGEMENTS	x
TABLE OF CONTENTS	xi
LIST OF TABLES	xv
LIST OF FIGURES	xvii
ABBREVIATIONS	xxiii
CHAPTERS	
1. INTRODUCTION	1
1.1 Purpose and Scope	1
1.2 Geographic Setting	3
1.3 Method of Study	6
1.4 Previous Works in the Haymana Basin	10
1.5 Regional Geology	17
2. STRATIGRAPHY	25
2.1 Lithostratigraphy.....	25
2.2 Biostratigraphy.....	47
2.2.1 Planktonic foraminiferal biostratigraphy of late Paleocene-early Eocene in literature	47

2.2.2 Planktonic foraminiferal events throughout the Paleocene and the Eocene	52
2.2.3 Planktonic foraminiferal biostratigraphy of the measured section.....	55
2.2.3.1 Globanomalina pseudomenardii Zone	55
2.2.3.2 Morozovella subbotinae Zone	59
2.2.3.3 Acarinina sibiyaensis Zone.....	61
2.2.3.4 Pseudohastigerina wilcoxensis Zone.....	62
3. QUANTITATIVE ANALYSIS	65
3.1 Size Fraction	65
3.2 Relative Abundance	74
3.3 Paleoenvironmental Interpretations	77
4. THE PALEOCENE/EOCENE BOUNDARY AND THE PALEOCENE-EOCENE THERMAL MAXIMUM	83
4.1 Stable Oxygen and Carbon Isotopic Record.....	84
4.2 Hypotheses.....	86
4.3 Marine Micropaleontological Record.....	88
4.5 Planktonic Foraminiferal Studies on the P/E Boundary and the PETM.....	92
5. SYSTEMATIC TAXONOMY	101
5.1 Family Globigerinidae Carpenter, Parker, and Jones, 1862	106
5.1.1 Genus <i>Parasubbotina</i> Olsson, Hembleben, Berggren, and Liu, 1992	107
5.1.2 Genus <i>Subbotina</i> Brotzen and Pozaryska, 1961.....	111
5.2 Family Truncorotaloididae Loeblich and Tappan, 1961.....	121

5.2.1 Genus <i>Morozovella</i> McGowran in Luterbacher, 1964.....	121
5.2.2 Genus <i>Acarinina</i> Subbotina, 1953	135
5.2.3 Genus <i>Igorina</i> Davidzon, 1976.....	156
5.2.4 Genus <i>Pearsonites</i> Soldan, Petrizzo & Premoli Silva, 2014	160
5.2.5 Genus <i>Planorotalites</i> Morozova, 1957	163
5.3 Family Hedbergellidae Loeblich and Tappan, 1961.....	165
5.3.1 Genus <i>Globanomalina</i> Haque, 1956.....	166
5.3.2 Genus <i>Pseudohastigerina</i> Banner and Blow, 1959.....	174
5.4 Family Chiloguembelinidae Reiss, 1963	177
5.4.1 Genus <i>Chiloguembelina</i> Loeblich and Tappan, 1956.....	177
5.5 Family Heterohelicidae Cushman, 1927.....	180
5.5.1 Genus <i>Zeauvigerina</i> Finlay, 1939.....	181
5.6 Triserial Tests	183
5.7 High Trochospired Tests.....	183
5.8. Reworked Tests.....	183
6. DISCUSSION AND CONCLUSIONS	185
REFERENCES.....	191
APPENDICES	221
APPENDIX A	221
APPENDIX B.....	225
APPENDIX C.....	229

PLATE 1	230
PLATE 2	232
PLATE 3	234
PLATE 4	236
PLATE 5	238
PLATE 6	240
PLATE 7	242
PLATE 8	244
PLATE 9	246
APPENDIX D.....	249

LIST OF TABLES

Table 1: GPS points of start and end points of the measured section (UTM 36S)	4
Table 2: Planktonic foraminiferal count, mass and the split for >63µm fraction	8
Table 3: Planktonic foraminiferal count, mass and the split for >106µm fraction	9
Table 4: Summary table for paleontological works in the Haymana Basin: PF: Planktonic Foraminifera, BF: Benthic Foraminifera	14
Table 5: Grain size distribution of the measured section: weight of different size intervals for 100 g dry sample.....	32
Table 6: Reference table for recent quantitative planktonic foraminiferal analyses on Paleocene-Eocene units. Size: sieve size studied; S/G: counted taxonomical rank, Species or Genus	66
Table 7: Estimated number of planktonic foraminifera individuals in 1 gr of rock. .	68
Table 8: Classification schemes of several authors, the ones marked with asterisk are as compiled in Lipps (1966).....	103
Table 9: Rapid recognition chart for species of genus <i>Parasubbotina</i> . * for species identified in this study.....	108
Table 10: Rapid recognition chart for species of genus <i>Subbotina</i> . * for species identified in this study.....	112
Table 11: Rapid recognition chart for species of genus <i>Morozovella</i> . * for species identified in this study.....	124
Table 12: Rapid recognition chart for species of genus <i>Acarinina</i> . * for species identified in this study.....	137

Table 13: Rapid recognition chart for species of genera <i>Igorina</i> and <i>Pearsonites</i> . * for species identified in this study.....	158
Table 14: Rapid recognition chart for species of genera <i>Planorotalites</i> . * for species identified in this study.....	164
Table 15: Rapid recognition chart for species of genus <i>Globanomalina</i> . * for species identified in this study.....	168
Table 16: Rapid recognition chart for species of genus <i>Pseudohastigerina</i> . * for species identified in this study.....	176
Table 17: Rapid recognition chart for species of genus <i>Chiloguembelina</i> . * for species identified in this study.....	178
Table 18: Rapid recognition chart for species of genus <i>Zeauvigerina</i> . * for species identified in this study.....	182
Table 19: Quantitative data and percent relative abundances of genera for >106 μm	222
Table 20: Quantitative data and percent relative abundances of genera for >63 μm	223
Table 21: Page and Plate-Figure addresses of planktonic foraminifera identified in this study.....	225

LIST OF FIGURES

Figure 1: Location map of the study area indicated by the hatched rectangle.....	3
Figure 2: Google earth image showing the location of the study area (red rectangle)	4
Figure 3: A panoramic view of the study area. Yellow lines indicate the formation boundaries, to the east Çayraz, to the west Iğnıkdere Formations are seen. The red line indicates the approximate position of measured section line.....	5
Figure 4: Field photo (looking southeast) showing the upper part of the measured section line with sample points indicated on.....	5
Figure 5: Summary of the lithostratigraphic schemes from Haymana and Polatlı basins.....	12
Figure 6: Geological map of the study area taken from Çiner et al. (1996a). Red line indicates the measured section.	18
Figure 7: Generalized columnar section of the Haymana Basin, modified from Ünalın et al. (1976). Red line indicates the measured section.....	19
Figure 8: Paleogeographical sketch cross sections of the area (Ünalın et al., 1976).	21
Figure 9: Facies map of Kartal, Çaldağ, Yeşilyurt Formations (Ünalın et al. 1976)	22
Figure 10: Sketch cross section along A-A' profile in Figure 11. Thick red line indicates the approximate position of the measured section. Blue line indicates the approximate location of P/E boundary.....	26
Figure 11: Close up view of study area taken from Google Earth with formation boundaries and measured section (red line) indicated.	27

Figure 12: Lithostratigraphy and planktonic foraminiferal biozones of the measured section. *A. sib.* stands for *A. sibaiaensis* Zone..... 28

Figure 13: Field photograph from the second field work. Sampling points indicated on the figure 29

Figure 14: Photographs belonging to sampling pits of samples GT-17.125 and 17.25. Note the color difference..... 30

Figure 15: Photograph belonging to GT-24 sample pit showing the lamination and color of the rock 31

Figure 16: Grain size distribution of initial samples. Sand size refers to the weight of residue over 63 μm sieve after washing, out of 100 g dry sample. Right-hand side graph is enlarged image of the first 10% of the left-hand side graph for better visualization of the changes in sand size fraction 33

Figure 17: Thin section microphotographs of several samples. p: planktonic foraminifera, b: benthic foraminifera. Sample numbers indicated at the right bottom corner of the microphotographs, along with scale. 34

Figure 18: Microphotographs of samples of several biogenic elements recovered from various samples; A: Echinoid spines, B: Micromollusca, C: Unknown elements, D: Benthic foraminifera, E: Ostracoda, F: Planktonic foraminifera 39

Figure 19: Milky white spheres from the samples GT-16 (A) and GT-4 (B, C, and D). Left-hand side: binocular light microscope microphotograph; right-hand side: SEM images with scale bar representing 200 μm . EDS analysis results can be found in Appendix D:Figure 48, Figure 49 40

Figure 20: Amber colored globular grains: tailed cysts. Left- hand side: binocular light microscope microphotograph from the sample GT-16; right-hand side: SEM images with scale bar representing 100 μm : A, B and D from GT-15.5, and C from GT-16. EDS analysis results can be found in Appendix D: Figure 50 and Figure 51 41

Figure 21: Several calcitic (A and B) and siliceous (C and D) grains from the sample GT-16. Left-hand side: binocular light microscope microphotograph; right-hand side: SEM images with scale bar representing 100 μm . EDS analysis results can be found in Appendix D: Figure 52, Figure 53, Figure 54, Figure 55	42
Figure 22: A: Several mineral aggregate grains of unknown origin probably iron oxide in composition. B: Close-up view of the grain in white rectangle; note the reddish crystals.....	43
Figure 23: Octahedral iron oxide crystals from the sample GT-18. Left-hand side: binocular light microscope microphotograph; right-hand side: SEM images with scale bar representing 200 μm . EDS analysis results can be found in Appendix D: Figure 47	44
Figure 24: Field photo of the last two samples GT-26 (shale) and GT-27 (limestone). Uppermost limit of the Eskipolatlı Formation and the lowermost beds of the Çayraz Formation are also seen. Dashed line showing the position of the limestone tongue that the sample GT-27 was taken from.	45
Figure 25: Thin section microphotographs of the sample GT-27. p: planktonic foraminifera, m: Morozovellid, a: agglutinated foraminifera, f: foraminifera of undetermined type, D: Discocyclinidae, N: Nummulitidae.....	46
Figure 26: Comparison of several planktonic foraminiferal zonation schemes of upper Paleocene (P) and part of lower Eocene (E) interval with respect to zonation scheme and stratigraphic ranges by Berggren & Pearson (2005).	48
Figure 27: Summary of the Paleocene-Eocene major planktonic foraminiferal events with respect to biozonation scheme of Berggren and Pearson (2005).....	53
Figure 28: Summary of the biostratigraphic schemes and their correlation with this study	56
Figure 29: Stratigraphical distribution of the planktonic foraminifera in the measured section	57

Figure 30: SEM images of pre-adult (left-hand side) and adult (right-hand side) specimens of 1. *Globigerinoides ruber* (magnification: a: x449, b: x469, c: x120, d: x147), 2. *Neogloboquadrina dutertrei* (e: x290, f:x304, g: x74, h: x62), 3. *Globigerinita juvenilis* (i: x653, j: x805, k: x143, l: x136) (taken from Brummer et al.,1986)..... 70

Figure 31: Relative abundance of genera and groups for >63 µm fraction. *Globa.:* *Globanomalina*, *Pse.:* *Pseudohastigerina*, *Igor.:* *Igorina*, *Pear.:* *Pearsonites* 71

Figure 32: Relative abundance of genera and groups for >106 µm fraction, abbreviations as in Figure 31 72

Figure 33: Comparison of relative abundance of genera and groups for >63 µm, and >106 µm fraction, abbreviations as in Figure 31 73

Figure 34: Relative abundances of planktonic foraminifera groups and carbon isotope plotted against lithology and biostratigraphy. *Subbotina* gr. stands for genera *Subbotina*, *Parasubbotina* and *Globorotaloides* of similar habitat. (Luciani et al., 2007)..... 76

Figure 35: Relative abundances and diversity in Kaurtakapy section (Kazakstan) (Pardo et al., 1999) 77

Figure 36: Distribution of the Paleogene planktonic foraminifera in the neritic environment (BouDagher-Fadel, 2015) 78

Figure 37: Simplified scheme showing the inferred life strategies and depth ranking of middle Eocene planktonic foraminifera (Luciani, et al., 2010) 80

Figure 38: Climate zones in Paleogene (BouDagher-Fadel, 2015), red star indicates the estimated position of the measured section 80

Figure 39: Geochemical data from DSDP Site 401 from Bay of Biscay, North Atlantic. Isotopic studies conducted on benthic foraminifera species *Nuttallides truempyi* (for bottom water conditions), and planktonic foraminifera species

<i>Subbotina patagonica</i> (for thermocline waters), <i>Morozovella subbotinae</i> and <i>Acarinina soldadoensis</i> (for surface water conditions) (Bornemann et al. 2014).....	85
Figure 40: Correlation of planktonic foraminiferal, shallow benthic foraminiferal, and calcareous nannofossil biostratigraphy along Paleocene and lower Eocene (Vandenberghé et al., 2012).....	89
Figure 41: Dinoflagellate cysts and radiolarian biostratigraphy along Paleocene and lower Eocene (Vandenberghé et al., 2012)	91
Figure 42: Several P/E planktonic foraminiferal investigation sites including the study area. ODP sites: 1. Kerguelen Island, 2. Shatsky Rise (Central Pacific). Tethyan sites: 3. Pakistan, 4. India, 5. Dababiya (Egypt), 6. Sinai (Egypt), 7. Haymana, Central Anatolia (Turkey), 8. Western Black Sea Region (Turkey), 9. Tunisia, 10. Forada, Possagno (Italy), 11. Zumaya (Spain), 12. Alamedilla, Caravaca (Spain), 13: Kaurtakapy (Kazakhstan).....	92
Figure 43: Paleogeographic map for 56 Ma with marine and continental sites of studied P/E boundary interval indicated with red circles, as compiled by McInerney and Wing (2011) (site numbers are keyed in Supplemental Table 1 of McInerney and Wing, 2011). Yellow star indicates approximate position of study area.	93
Figure 44: Base of the Ypresian Stage of the Paleogene System at Dababiya, Egypt (Vandenberghé et al., 2012).....	95
Figure 45: Details of pre-, within, and post-CIE intervals in Dababiya (DBH section) (Berggren & Ouda, 2003a).....	97
Figure 46: Hand sketched figure showing chamber shape, apertural position, and peripheral geometry variety in genus <i>Globabanomalina</i>	167
Figure 47: Octahedral iron oxide crystal from GT-18, Figure 23.....	250
Figure 48: Milky white sphere from GT-4, Figure 19-B	251
Figure 49: Milky white sphere from GT-16, Figure 19-A.....	252

Figure 50: Amber colored globular grain from GT-16, Figure 20-C..... 253

Figure 51: Amber colored globular grain from GT-15.5, Figure 20-A..... 254

Figure 52: Calcitic grain from GT-16, Figure 21-A..... 255

Figure 53: Calcitic grain from GT-16, Figure 21-B..... 256

Figure 54: Siliceous grain from GT-16, Figure 21-C..... 257

Figure 55: Siliceous grain from GT-16, Figure 21-D 258

ABBREVIATIONS

HOD: Highest occurrence datum, HO for short

LOD: Lowest occurrence datum, LO for short

PETM: Paleocene-Eocene Thermal Maximum

P/E: Paleocene/Eocene Boundary

SEM: Scanning Electron Microscopy

EDS: Energy Dispersive Spectroscopy

CIE: Carbon Isotope Excursion

PFET: Planktonic Foraminifera Excursion Taxa

BFE: Benthic Foraminifera Extinction Event

ss.: *Sensu stricto*

CHAPTER 1

INTRODUCTION

1.1 Purpose and Scope

The Paleocene/Eocene boundary is the record of a globally experienced warming event (Paleocene-Eocene Thermal Maximum - PETM), with chemical, paleontological and lithological evidence around the world. Set at 56 Ma (Vandenberghé et al., 2012), the boundary is defined by the onset of a negative shift in carbon isotope, called Carbon Isotope Excursion (CIE) (Aubry, 2000; Aubry, 2002; Aubry et al., 2007). The PETM (and CIE) is one of the peaking events that took place during an overall 5°C temperature increase from late Paleocene into early Eocene, one other being the Early Eocene Thermal Maximum (Zachos et al., 2001). The CIE is accompanied by a shift in oxygen isotope as well, which is well translated into temperature change showing a 5-6°C increase in surface, 4°C increase in bottom waters occurring rather rapidly, in less than 10 ky, and dissipating in 150 ky (Zachos et al., 1993). Hypotheses concerning the trigger of the event are being discussed, focusing around the means of injection of high amounts of isotopically light carbon into the ocean-atmosphere system.

The paleontological data surrounding the event are numerous, especially in marine realm. These were summarized well within chronological framework as secondary correlative elements to the boundary in Aubry et al. (2007) as follows:

- Deep benthic foraminifera extinction event (BFE)
- Planktonic foraminifera excursion taxa (PFET)
- Calcareous nannofossil *Rhomboaster* – *Discoaster araneus* (RD) assemblage
- Dinoflagellate *Apectodinium* acme

These events are more or less in synchronic and being used as widely as main P/E boundary criteria i.e. base of CIE.

In Haymana basin lithostratigraphical and paleontological studies had been carried out frequently (e.g. Ünalán et al., 1976; Özkan-Altınér and Özcan, 1999; Esmeray-Senlet et al., 2015). However, there are no studies concerning detailed position of the P/E boundary and the PETM record in the basin. A turbiditic to pelagic suite is found in the northern Haymana, composed of conglomerates, sandstones, and mudrocks (İlgınlıkdere and Eskipolatlı Formations, Ünalán et al., 1976) previously dated as Ilerdian-Cuisian, spanning from latest Paleocene to early Eocene, covered by middle Eocene Nummulitic limestone (Çayraz Formation).

The use of regional informal stages (namely Montian, Ilerdian and Cuisian) is widespread among previous works in the Haymana Basin, which prevents high quality correlations between works due to their non-standardized nature; moreover, the diachrony of lithostratigraphic boundaries prevents wide regional correlations.

This study aims to present the late Paleocene-earliest Eocene planktonic foraminiferal biostratigraphy of the Eskipolatlı Formation, test the PETM planktonic foraminiferal record of the Haymana Basin, and the northern Neo-Tethys, and delineate the P/E boundary in the study area. Moreover, this thesis will position the Eskipolatlı Formation in the standard chronostratigraphic scheme, providing a better constrained lithostratigraphic unit. Additionally, this thesis at hand offers the reader a comprehensive summary of the PETM literature, a detailed guide for the upper Paleocene – lower Eocene planktonic foraminiferal taxonomy and biostratigraphy, and a case study for quantitative analysis.

1.2 Geographic Setting

The study area is situated to southwest of Ankara, near the Yeşilyurt village (Figure 1, Figure 2). The location was chosen because of wide exposures of monotonous fine grained lithology that promises fairly good preservation of open marine biota.

The studied stratigraphic section was measured from the southern flank of an approximately east-west directed seasonal stream bed (see Figure 2 Figure 3, Figure 4); a total of 33 m in the Eskipolatlı Formation, starting above the Iğnıkdere / Eskipolatlı Formation boundary, ending below the Eskipolatlı / Çayraz Formation boundary (Table 1).

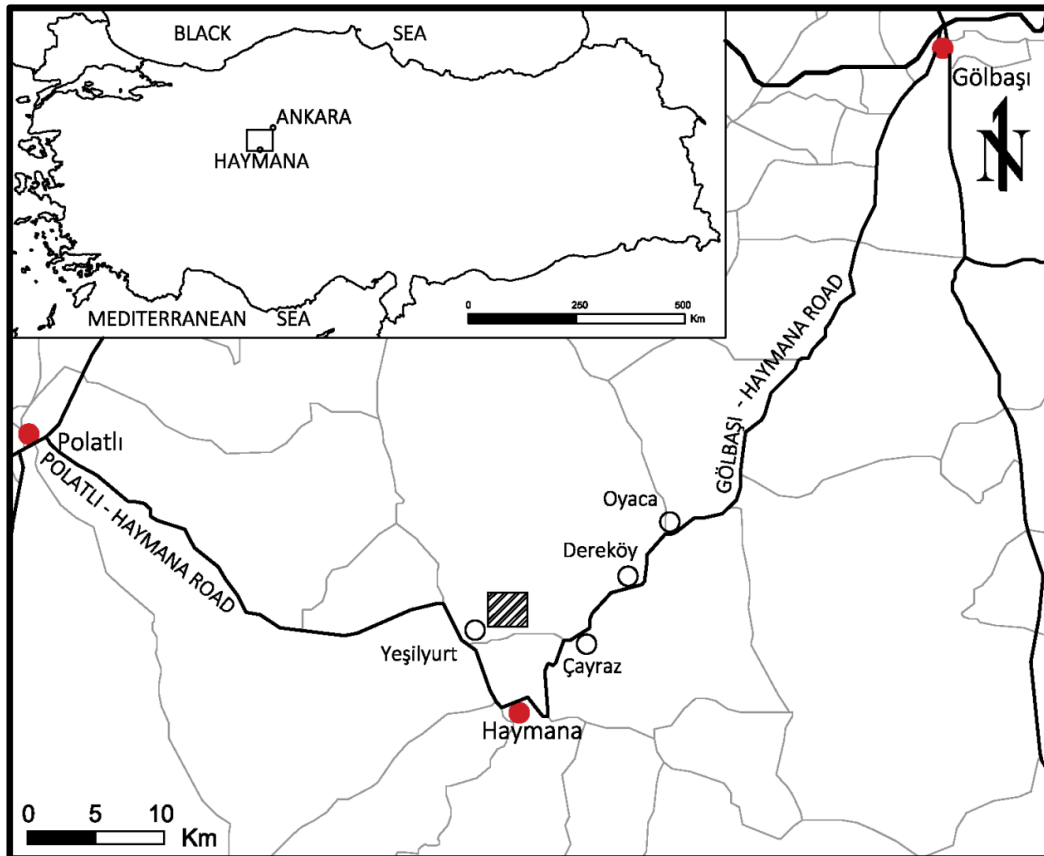


Figure 1: Location map of the study area indicated by the hatched rectangle



Figure 2: Google earth image showing the location of the study area (red rectangle)

Table 1: GPS points of start and end points of the measured section (UTM 36S)

Sample Number	Easting	Northing
GT-0	0456774	4371400
GT-27	0456997	4371537



Figure 3: A panoramic view of the study area. Yellow lines indicate the formation boundaries, to the east Çayraz, to the west Ilgınlıkdere Formations are seen. The red line indicates the approximate position of measured section line.

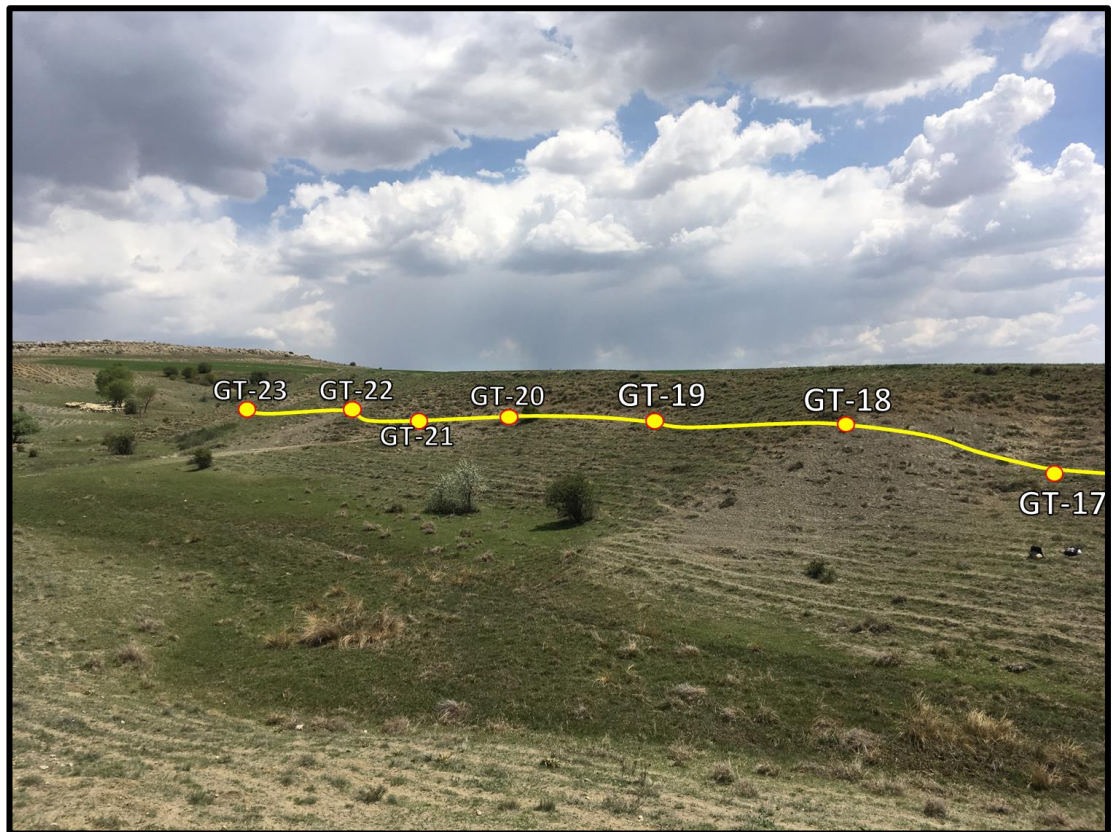


Figure 4: Field photo (looking southeast) showing the upper part of the measured section line with sample points indicated on.

The study area is positioned on a low lying portion, bounded from west by cliffs of the Ilgınlıkdere Formation and east by cliffs of the Çayraz Formation (Figure 3). Due to the lithological properties, the measured section is covered by a variable thickness of soil layer and no outcrops are seen (Figure 4).

1.3 Method of Study

A section of 33 meters in total was measured for the study from continuous shale succession of the Eskipolatlı Formation. Two phases of sampling were carried out. Initial samples were taken generally with 1 meter intervals, with two exceptions (2 meters spacing between GT-22 and GT-23, and 1.5-meter spacing between GT-25 and GT-26); adding up to a total of 27 shale samples. The uppermost sample (GT-27) is taken from the first prominent limestone tongue, right above sample GT-26. The sampled points were covered with a soil layer which was dug in order to reach fresh rock; then samples were collected from formed shallow pits, especially large pieces were chosen when possible. Approximately 1.5 kg of rock was collected for each sampling point and was numbered and bagged accordingly.

Secondary sampling of 13 samples was carried out after the initial samples were studied thoroughly for recognition of the P/E boundary. The 1-meter interval for the P/E boundary (GT-17-18 interval) was sampled with 12.5 cm spacing, and a sample was taken for each interval between samples GT-15 – 16, GT-16 – 17, GT-18 – 19, GT-19 – 20, GT-20 – 21 and GT-21 – 22. In total, 40 shale samples and 1 limestone sample were studied for this work.

Wash samples were considered as the main study method since the lithology is suitable, therefore a series of testing was conducted on the sample GT-0 in order to establish which method of washing will be implemented. At the end of the experiments it was decided to use 200 ml of H₂O₂ solution of 50% dilution for 100 grams of dry and broken sample with a soaking time of 90 minutes. All samples were prepared for washing by breaking using a hammer into a maximum of pea-sized particles, and dried for 24 hours prior to soaking. After soaking, samples were

washed under tap water from 250, 125, 63 and 38 micron sieves with slightly rubbing for removal of any clay particles. Fractions were transported from sieves into glass evaporation dishes with use of distilled water for prevention of salt precipitation on specimens. Dried sample fractions were bagged separately with appropriate labeling.

Second phase samples were washed with the same method except for one sample (GT-17.125) which was too soft for the H₂O₂ method. This sample was washed only with soaking in water for 24 hours.

Another soft sample (GT-16) showed some features which could be explained by the washing induced dissolution, yet, after a second washing (without H₂O₂) it became clear that the dissolution was not washing induced.

Quantitative analysis was done on the 26 initial phase samples (GT-1 to GT-26), and 2 size fractions were investigated for this study, namely >63µm and >106µm. The investigation of larger fraction (>106µm) was decided after the unsuccessful attempt on the smaller fraction (>63µm). The investigation of smaller fraction, although not impossible, is not an easy task for the stereomicroscope in use (max *100 magnification) due to preservational complexities and abundance of pre-adult and reworked/transported forms. If to be accounted for in the quantitative analysis, correct assignment of the pre-adult forms is crucial for the relative abundance studies; therefore, elimination of these forms is favored over the high probability of incorrect taxonomical assignments. Hence, the need for a second counting study with the larger fraction was necessary for healthier results.

For richness and relative abundance calculations, all planktonic foraminifera (around 300 individuals) were picked from aliquot (adequately split samples). For this purpose, 63, 125 and 250µm sieve residues were weighted, mixed, then split with microsplitter for >63µm fraction. For the >106µm fraction, the mixed residues were dry sieved from 106µm sieve, and then split. The weights of residues and fractions, and the studied split for each sample can be found in Table 2 and Table 3. The rest of

Table 2: Planktonic foraminiferal count, mass and the split for >63 μ m fraction

Sample no	>63 μ m			
	Residue mass (g)	Split	Counted ratio	# of specimens
GT- 26	1.61	9	1/ 512	147
GT- 25	0.35	6	1/ 64	209
GT- 24	0.52	8	1/ 256	187
GT- 23	0.35	7	1/ 128	203
GT- 22	0.52	7	1/ 128	368
GT- 21	0.50	8	1/ 256	275
GT- 20	0.55	8	1/ 256	273
GT- 19	0.40	7	1/ 128	309
GT- 18	0.65	7	1/ 128	651
GT- 17	0.88	8	1/ 256	521
GT- 16	0.14	5	1/ 32	748
GT- 15	0.85	8	1/ 256	322
GT- 14	0.71	7	1/ 128	611
GT- 13	0.96	8	1/ 256	412
GT- 12	1.24	8	1/ 256	298
GT- 11	0.70	8	1/ 256	201
GT- 10	1.39	9	1/ 512	175
GT- 9	0.62	7	1/ 128	377
GT- 8	0.69	8	1/ 256	298
GT- 7	1.07	8	1/ 256	281
GT- 6	0.24	4	1/ 16	313
GT- 5	0.35	7	1/ 128	248
GT- 4	0.77	5	1/ 32	321
GT- 3	0.44	8	1/ 256	237
GT- 2	0.77	7	1/ 128	449
GT- 1	1.07	8	1/ 256	251

Table 3: Planktonic foraminiferal count, mass and the split for >106µm fraction

Sample no	>106 µm			
	Residue mass (g)	Split	Counted ratio	# of specimens
GT- 26	0.59	5	1/ 32	334
GT- 25	0.16	2	1/ 4	335
GT- 24	0.20	5	1/ 32	291
GT- 23	0.16	3	1/ 8	439
GT- 22	0.21	3	1/ 8	506
GT- 21	0.16	5	1/ 32	270
GT- 20	0.24	4	1/ 16	470
GT- 19	0.22	4	1/ 16	283
GT- 18	0.27	5	1/ 32	348
GT- 17	0.33	6	1/ 64	250
GT- 16	0.04	2	1/ 4	327
GT- 15	0.24	5	1/ 32	405
GT- 14	0.26	5	1/ 32	432
GT- 13	0.31	6	1/ 64	341
GT- 12	0.27	4	1/ 16	350
GT- 11	0.17	3	1/ 8	446
GT- 10	0.62	4	1/ 16	524
GT- 9	0.27	3	1/ 8	259
GT- 8	0.30	5	1/ 32	287
GT- 7	0.44	4	1/ 16	368
GT- 6	0.04	2	1/ 4	379
GT- 5	0.10	3	1/ 8	374
GT- 4	0.17	4	1/ 16	275
GT- 3	0.15	4	1/ 16	330
GT- 2	0.29	4	1/ 16	420
GT- 1	0.38	4	1/ 16	371

the samples were screened for rarer species. The presence or absence of every species in every sample is marked, and planktonic foraminiferal generic abundances were counted. The raw counting data of both of the fractions can be found in the Appendix A.

SEM was used for imaging of planktonic foraminifera. The imaging was done by JSM-6400 Electron Microscope (JEOL), equipped with NORAN System 6 X-ray Microanalysis System & Semafore Digitizer, after coating with gold via HUMMLE VII Sputter Coating Device, in Scanning Electron Microscopy Laboratory of Metallurgical and Materials Engineering Department, Middle East Technical University.

During the investigations of washed samples, several grains were also found in the aliquot and imaged via SEM. Moreover, EDS analyses were carried out for some of these grains in the same facility and by the same equipment.

Thin sections were prepared from several samples in Thin Section Laboratory of Geological Engineering Department, Middle East Technical University, and were investigated via a polarized microscope for screening of facies characteristics.

1.4 Previous Works in the Haymana Basin

Earliest studies in the basin were mostly focused on the petroleum potential (e.g. Rigo de Righi and Cortesini, 1959; Recamp and Özbey, 1960; Schmidt, 1960; Yüksel, 1970; and Akarsu, 1971) which prepared a base for the later stratigraphic studies. Figure 5 is a summary table for comparison of lithostratigraphy schemes of several authors, including these unpublished works.

Sirel (1975) studied the adjacent and connected Polatlı Basin, established the lithostratigraphy and biostratigraphy (mostly benthic foraminifera) of Paleocene-Eocene successions. The author distinguished two Paleocene units, namely Kartal (semi-continental red clastics) and Kırkkavak Formations (algal limestone), and one Eocene unit, Eskipolatlı Formation (grey-green mudrocks), above a limestone unit of

Jurassic age. This Jurassic limestone was incorrectly taken as the Çaldağ Formation of Schmidt (1960), yet it correlates better with Bilecik Limestone of shallow marine platform carbonates of the Pontides. The cover rock of this area was established by this study as Ağasivri Formation of Neogene age (Figure 5).

Ünalın et al. (1976) did a comprehensive study in the northern part of the Haymana Basin, providing a widely agreed upon Upper Cretaceous-Cenozoic lithostratigraphy scheme to the area, and giving a highly detailed correlation chart with the earlier works. They acknowledged the presence of pre-Upper Cretaceous basement rocks (Temirözü Formation, Triassic metamorphics; Mollaresul Formation, Upper Jurassic-Lower Cretaceous limestones correlative with the Çaldağ Formation of Sirel (1975); and Dereköy Formation, Upper Cretaceous ophiolitic mélangé; Figure 5), although not giving detailed descriptions. Eleven formations were distinguished in the Upper Cretaceous-middle Eocene basin fill (Beyobası, Haymana, Kartal, Çaldağ, Yeşilyurt, Kırkkavak, Iğnıkdere, Eskipolatlı, Beldede, Çayraz, Yamak Formations; Figure 5; for details see section 1.5) covered unconformably by Neogene volcanics and continental deposits. The lateral and vertical relationships of the units were investigated for a paleogeographic evolution hypothesis. Though not including a biostratigraphic framework, fossil contents of the distinguished formations were also studied and documented, hence providing age control. This lithostratigraphic scheme is chosen as base for this study due to its coverage of our study area, and being generally accepted.

Gökçen (1976a, 1976b, 1977) presented another comprehensive work in three volumes, studying southern part of the Haymana Basin in terms of lithostratigraphy and sedimentology. He distinguished eight formations (Figure 5), two being pre-Upper Cretaceous rocks (Temirözü Formation of Paleozoic and Türbetepe Kireçtaşı correlative with Çaldağ Formation of Sirel, 1975; and Mollaresul Formation of Ünalın et al., 1976), five being Upper Cretaceous-middle Eocene basin fills (Germük, Karlıkdağı, Sarıdere (correlative to the Iğnıkdere Formation of Ünalın et al. (1976)), Bahçecik (correlative to the Eskipolatlı Formation of Ünalın et al.

Time	Rigo de Right & Cortesini 1959 Polatlı-Haymana	Recamp & Özbek 1960 Polatlı	Schmidt 1960 Haymana	Yüksel 1970 Haymana	Alarsu 1971 Haymana-Ş.Boğhisar	Sirel 1975 Polatlı	Unalan et al. 1976 Haymana-Polatlı	Gökçen 1976 South Haymana	
Cenozoic	Neogene	Terrigenous sediments	Terrigenous sediments	Andesite Conglomerate Marl	Çhanbeyli Fm.	Ağasıvri Fm.	Terrigenous sediments	Soğulca Fm.	
	Priabonian	Eskipolatlı Fm.	Harhor Fm.	Çayraz Fm.	Eskipolatlı Fm.	Eskipolatlı Fm.	Volcanics		
	Lutetian	Eskipolatlı Fm.	Çayraz Fm.	Karahoca Fm.	Eskipolatlı Fm.	Eskipolatlı Fm.	Eskipolatlı Fm.	Yamak Fm.	
	Ypresian/Cuisian and Ilerdian	Eskipolatlı Fm.	Kırkkavak Fm.	Gedik Fm. Kadıköy Fm.	Kırkkavak Fm.	Kırkkavak Fm.	Kırkkavak Fm.	Belde Fm.	Yamak Fm.
	Thanetian	Kırkkavak Fm.	Kırkkavak Fm.	Gedik Fm. Kadıköy Fm.	Kırkkavak Fm.	Kırkkavak Fm.	Kırkkavak Fm.	Eskipolatlı Fm.	Bahçecik Fm.
	Selandian	Kırkkavak Fm.	Kırkkavak Fm.	Gedik Fm. Kadıköy Fm.	Kırkkavak Fm.	Kırkkavak Fm.	Kırkkavak Fm.	Eskipolatlı Fm.	Sardere Fm.
Danian	Kırkkavak Fm.	Kırkkavak Fm.	Gedik Fm. Kadıköy Fm.	Kırkkavak Fm.	Kırkkavak Fm.	Kırkkavak Fm.	Eskipolatlı Fm.	Kırkkavak Fm.	
Mesozoic	Haymana Fm.	Haymana Fm.	Haymana Fm.	Kavak Fm. Haymana Fm. Yalınhisar Fm. Sevran Fm.	Haymana Fm.	Haymana Fm.	Haymana Fm.	Germük Fm.	
	Reefal Limestone	Haymana Fm.	Haymana Fm.	Çaldag Fm. and serpentinite limestone complex	Çaldag Fm.	Çaldag Fm.	Çaldag Fm.	Mollaresul Fm.	Türbetepe Fm.
	Limestone	Haymana Fm.	Haymana Fm.	Çaldag Fm. and serpentinite limestone complex	Çaldag Fm.	Çaldag Fm.	Çaldag Fm.	Mollaresul Fm.	Türbetepe Fm.
	Metamorphic rocks, Granite	Haymana Fm.	Haymana Fm.	Çaldag Fm. and serpentinite limestone complex	Çaldag Fm.	Çaldag Fm.	Çaldag Fm.	Mollaresul Fm.	Türbetepe Fm.
	Temirözü Fm.	Haymana Fm.	Haymana Fm.	Çaldag Fm. and serpentinite limestone complex	Çaldag Fm.	Çaldag Fm.	Çaldag Fm.	Mollaresul Fm.	Türbetepe Fm.
Zivariç Fm.	Haymana Fm.	Haymana Fm.	Çaldag Fm. and serpentinite limestone complex	Çaldag Fm.	Çaldag Fm.	Çaldag Fm.	Mollaresul Fm.	Türbetepe Fm.	
Temirözü Fm.	Haymana Fm.	Haymana Fm.	Çaldag Fm. and serpentinite limestone complex	Çaldag Fm.	Çaldag Fm.	Çaldag Fm.	Mollaresul Fm.	Türbetepe Fm.	
Paleozoic	Haymana Fm.	Haymana Fm.	Çaldag Fm. and serpentinite limestone complex	Çaldag Fm.	Çaldag Fm.	Çaldag Fm.	Mollaresul Fm.	Türbetepe Fm.	

Figure 5: Summary of the lithostratigraphic schemes from Haymana and Polatlı basins.

(1976)) and Yamak Formations; see section 1.5 for details), and one Neogene unit (Soğulca Formation). Fossil contents of the suitable rocks were also studied for age control. Through sedimentological studies, paleocurrent and paleoenvironmental interpretations were made concluding an ellipsoidal basin with approximately ENE-WSW directed longer axis. Structural analyses included identification of several anticlines, synclines and faults showing roughly N-S directed deformational forces after deposition.

Paleontological works in the basin were generally focused on foraminifera, and some other fossils groups were studied only sparsely (Table 4); one of these groups is mollusca which show a good abundance in several levels in the area (e.g. Güngör, 1975; Özer, 1986; Table 4). Of foraminifera, specialized studies were conducted on benthics and planktonics for taxonomical and biostratigraphic purposes. Sirel (1976a, 1976b, 1976c, 1998, 1999), Sirel and Gündüz (1976), Matsumaru (1997, 1999), Özcan et al. (2001), Özcan (2002), Çolakoğlu and Özcan (2003), and Geyikçioğlu Erbaş (2008) worked specifically on larger benthic foraminifera of Paleocene-Eocene interval describing several new species and genera. Özcan and Özkan-Altın (1997, 1999, 2001) studied the Cretaceous larger benthic foraminifera and Özkan-Altın and Özcan (1999) presented the calibration of Cretaceous larger benthics with planktonic foraminifera. Dinçer (2016) worked on larger benthics of Eocene age in terms of stable isotopes. Earliest planktonic foraminiferal works belong to Toker (1975, 1977, 1979, 1981), followed by Özkan-Altın and Özcan (1999), Huseynov (2007), Amirov (2008), Esmeray (2008), and Esmeray-Senlet et al. (2015) dealing with parts of Upper Cretaceous-middle Eocene fill of the basin. Most of these studies focus on Upper Cretaceous biostratigraphy and K/Pg boundary, while the P/E boundary and the PETM stays unknown in the Haymana region. Closest approximation is by Amirov (2007) who studied the Paleocene Yeşilyurt Formation and located the boundary in the Yeşilyurt Formation. Most recent foraminiferal paleontological study in the Haymana Basin belongs to Okay and Altın (2016) where they examined the Upper Jurassic-Lower Cretaceous carbonate successions in terms of benthic and planktonic foraminifera.

Table 4: Summary table for paleontological works in the Haymana Basin: PF: Planktonic Foraminifera, BF: Benthic Foraminifera

Foraminifera	Type	Others
Toker (1975)	PF	
Sirel (1976a)	BF	
Sirel (1976b)	BF	Nannofossil
Sirel (1976c)	BF	Toker (1975)
Sirel&Gündüz (1976)	BF	Toker (1977)
Toker (1977)	PF	Toker (1980)
Toker (1979)	PF	
Meriç&Görür (1970-80)	BF	
Toker (1981)	PF	
Matsumaru (1997)	BF	
Özcan&Özkan-Altner (1997)	BF	Ostracoda
Sirel (1998)	BF	Duru&Gökçen (1990)
Matsumaru (1999)	BF	
Özcan&Özkan-Altner (1999)	BF	
Özkan-Altner&Özcan (1999)	PF&BF	Mollusca
Sirel (1999)	BF	Güngör (1975)
Özcan&Özkan-Altner (2001)	BF	Özer (1986)
Özcan et al. (2001)	BF	Deveciler (2008)
Özcan (2002)	BF	Okan&Hoşgör (2008)
Çolakoğlu& Özcan (2003)	BF	İslamoğlu et al. (2011)
Huseynov (2007)	PF	Hoşgör (2012)
Amirov (2008)	PF	
Esmeray (2008)	PF	
Geyikçioğlu Erbaş (2008)	BF	Ichnofossil
Esmeray-Senlet et al. (2015)	PF	Eser Doğdu (2007)
Dinçer (2016)	BF	
Okay&Altner (2016)	PF&BF	

One of the first sedimentological studies in the area is by Norman and Rad (1971) who worked on the Harhor Formation (Schmidt, 1960) which was described as a coarse clastic unit with mud intercalations (turbiditic character) above the Nummulitic Çayraz Formation. Through heavy mineral and clay mineral analyses they proposed a multi-provenance model with high disintegration rates, and short travel distances. Norman and Rad (1971) concluded that the Harhor formation was made up of resedimented units, which most probably first deposited in a deltaic or neritic environment, then failed and redeposited as turbiditic clastics; a mechanism that may have been triggered by intense tectonic activities.

Gökçen (1976a, 1976b, 1977) produced a wider research of all flyschoidal deposits that outcrop in the southern Haymana; via sedimentological studies of coarse grained facies. The author concluded that these are resedimented facies that were transported and deposited by fluxoturbiditic and turbiditic flows into a continuously deepening oval shaped basin. A multi-provenance of varying distance model was proposed for coarse grained facies, and Bahçecik Formation (equivalent of the Eskipolatlı Formation of Ünalın et al., 1976) was interpreted as a pelagic sedimentation phase composed of mudrocks that was interrupted from time to time by turbiditic deposits of coarser grained material. Gökçen and Kelling (1983) studied the Yamak Formation (middle Eocene) in the southern Haymana and hypothesized a rapidly developing submarine fan system situated above the finer grained pelagic Bahçecik Formation. Later on, Çetin et al. (1986) studied the northern Haymana in terms of clastic sedimentology and shared the conclusions of a continuously deepening basin model with magmatic and metamorphic source rocks (in the north to northwest direction) for turbiditic coarse grained facies. They interpreted the basin as a forearc basin developed between the Tethys oceanic plate and the Kırşehir microplate, filled with continental and ophiolitic detrital material. Bayhan and Gökçen (1990) compared the Haymana-Polatlı, Tuz Gölü and Kırıkkale-Yahşihan basins in terms of clastic sedimentary petrology, and exhibited that these basins were fed from previously uplifted magmatic/metamorphic rocks of the two colliding plates.

Sequence stratigraphic point of view was applied to the successions of the Haymana Basin. Cyclicity of laterally related middle Eocene formations (Beldede, Çayraz and

Yamak) were studied by Çiner et al. (1993a, 1993b, 1996a, 1996b) and Çiner (1996). The authors presented divisions into several orders of sequence stratigraphic units and proposed that both autocyclic and allocyclic mechanisms were in affect at the time of deposition. They further claim an overall high rate of subsidence for this time interval with many small cycles of relative sea-level fluctuations caused by both tectonic and eustatic changes. Huseynov (2007) worked on Early to Middle Campanian of the Haymana Formation, and compared their findings with global sea-level literature; concluding a greater effect of tectonics rather than eustacy during related time interval.

Relationship of the Haymana Basin with nearby other basins was studied by several researchers. Görür et al. (1984), provided an identic stratigraphic nomenclature for Haymana and Tuzgölü basins which, as previously reported (Görür, 1981), evolved coevally but independently as parts of a single unified basin (Tuzgölü basinal complex), using mainly the Haymana Basin lithostratigraphy nomenclature. Görür et al. (1984) stated that the Haymana Basin was a forearc basin lying partly upon the Late Jurassic-Early Cretaceous sedimentary succession of the Sakarya Continent and partly on the accretionary prism of the Ankara Mélange. Koçyiğit et al. (1988) further developed the idea by classifying the Haymana Basin as an accretionary forearc basin providing the depositional history. Moreover, Koçyiğit (1991) proposed that other two Upper Cretaceous-lower Tertiary sedimentary basins (Orhaniye and Alcı) were, too, linked with the Haymana Basin, forming north-northwestern margin of the Haymana accretionary forearc basin. Rojay and Süzen (1997) studied in the Alcı area, and proposed that Upper Cretaceous-Paleogene sequences (Haymana, Polatlı and Tuzgölü) developed on a dynamic ophiolitic mélangé prism, transforming from arc-trench basins (Cenomanian-Turonian) to forearc basins (Maastrichtian-Paleocene) moving northward, away from the trench. Okay et al. (2001) studied the Haymana Basin in the framework of Upper Cretaceous-lower Eocene sedimentary basins of the western Turkey, and claimed the initiation of continent-continent collision being reflected as the Paleocene uplift they observed in the eastern Central Sakarya and the northwestern Haymana Basins, while in the southern parts of Haymana sedimentation continued until middle Eocene, constraining the continental

collision to Paleocene-early Eocene interval. Nairn et al. (2012) worked on the central Anatolian basins including the Haymana Basin, hypothesizing a diachronic closure of the İzmir-Ankara-Erzincan Ocean starting by the collision of the Niğde-Kırşehir Massif and Pontide active margin during Late Cretaceous, while the oceanic crust still remained to the west and the east and continued subducting during late Paleocene-early Eocene until finalizing by late Eocene. Okay and Altner (2016) added that the Haymana Basin was a site of deep marine carbonate sedimentation during Cretaceous, an extensional active margin ridge of volcanic detritus that trapped in the intra-arc basins.

1.5 Regional Geology

The Haymana Basin is an accretionary forearc basin situated on the northern part of the İzmir-Ankara-Erzincan suture, with the Kırşehir Block to the east, the Taurides to the south, and the Sakarya Continent to the west, north-west (Koçyiğit, 1991). The basin formed during the closure of the northern branch of Neo-Tethys, subducting beneath the Rhodope-Pontide-Sakarya continental fragments (Şengör & Yılmaz, 1981; Rojay, 2013). Earlier depressions were filled with carbonate sedimentations of Early Cretaceous age upon Late Jurassic aged deposits of the Pontide carbonate platform (Okay & Altner, 2016). The overlying Upper Cretaceous to middle Eocene fill of the basin is mostly composed of carbonate and clastic deposits (Ünalın et al., 1976). The deformation of the area continued until late Pliocene after the closure of the northern branch Neo-Tethys (Koçyiğit, 1991). Several lithostratigraphical units were described from the area of interest by many researchers (e.g. Sirel, 1975; Gökçen 1976a, see section 1.4; Figure 5), in this thesis, the work of Ünalın et al. (1976) has been taken as the base for this study who distinguished 11 formations from Upper Cretaceous-middle Eocene succession (Figure 6 and Figure 7).

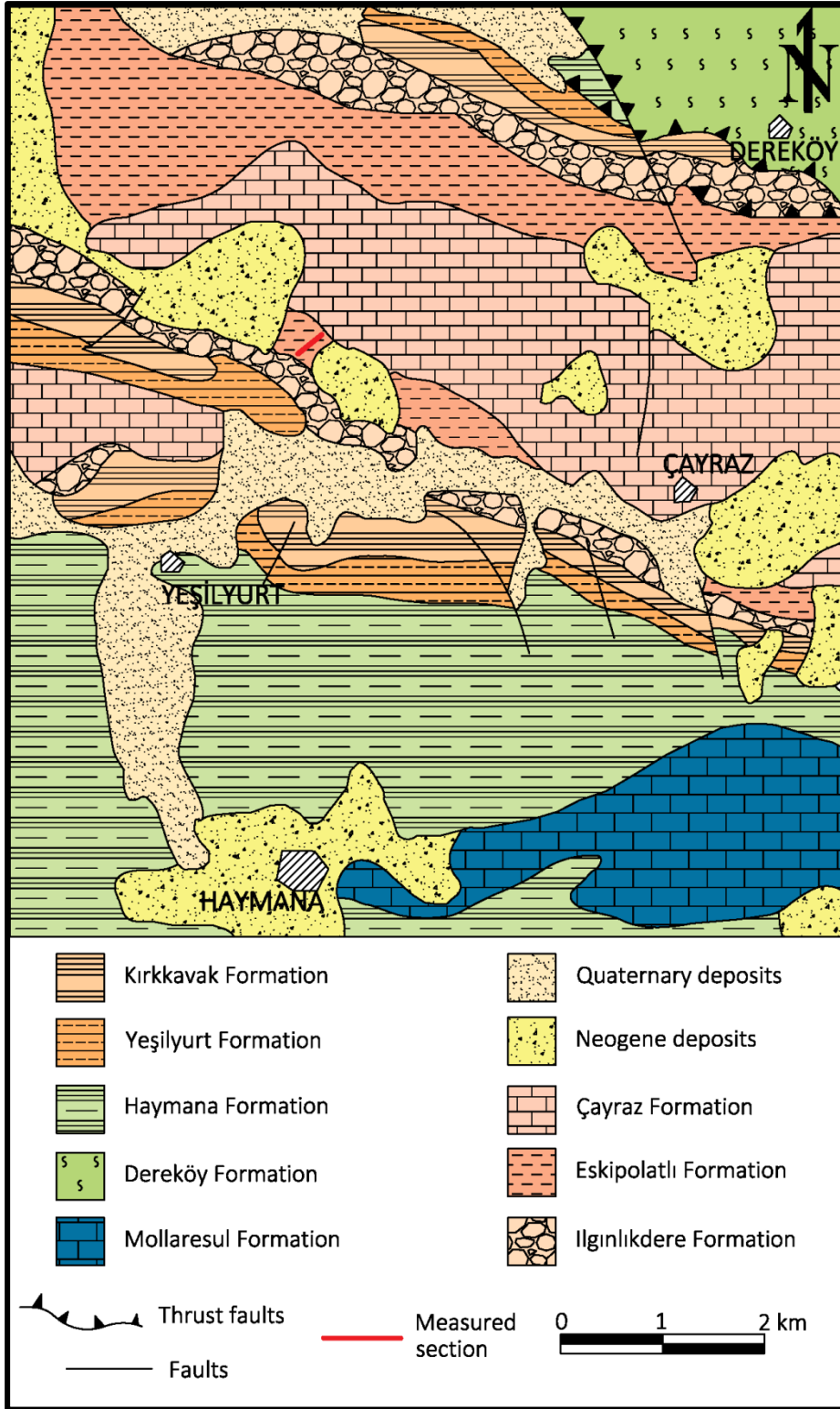


Figure 6: Geological map of the study area taken from Çiner et al. (1996a). Red line indicates the measured section.

System	Series	Stage	Lithology	Description	
QUATERNARY				Alluvium	
NEOGENE				Volcanoclastics, continental and lacustrine deposits	
PALEOGENE	EOCENE	Lutetian		A. BELDEDE FM. Red conglomerate, sandstone, marl	
				B. ÇAYRAZ FM. Yellow-beige nummulitic sandy limestone, marl	
				C. YAMAK FM. Grey conglomerate, sandstone, marl	
		Ypresian		ESKİPOLATLI FM. Grey shale; sandstone, marl, limestone banded upwards	
	PALEOCENE	Thanetian			ILGINLIKDERE FM. Grey conglomerate and sandstone
					KIRKKAVAK FM. Algal limestone, grey marl
		Danian-Selandian			A. KARTAL FM. Red conglomerate, sandstone, marl
					B. ÇALDAĞ FM. Algal limestone
				C. YEŞİLYURT FM. Marl with limestone blocks	
	CRETACEOUS	UPPER	Maastrichtian		A. BEYOBASI FM. Sandstone, conglomerate
				B. HAYMANA FM. Marl with sandstone and conglomerate lenses	
				DEREKÖY FM. Ophiolitic mélange	
JURASSIC				MOLLARESUL FM. Beige, locally massive limestone	
TRIASSIC				TEMİRÖZÜ FM. Limestone blocky metagreywacke	

Figure 7: Generalized columnar section of the Haymana Basin, modified from Ünalın et al. (1976). Red line indicates the measured section

Pre-Upper Cretaceous rocks that do outcrop in the vicinity of Haymana are metamorphics of Triassic age (Temirözü Formation of Ünalın et al., 1976), Upper Jurassic-Lower Cretaceous carbonates (Mollaresul Formation of Ünalın et al., 1976; Bilecik, Soğukçam, Akkaya and Kocatepe Formations of Okay and Altner, 2016) and Upper Cretaceous aged ophiolitic mélangé (Dereköy Formation of Ünalın et al., 1976).

Upper Cretaceous (Maastrichtian) Haymana Formation is mainly a mudrock unit with several conglomerate and sandstone lenses representing turbiditic flyschoidal sedimentation of deep marine systems. The Beyobası Formation, which passes into the Haymana Formation vertically and laterally, represents a much shallower environment (Figure 8) and is composed of sandstones, conglomerates, conglomeratic limestones and sandy marls.

Lower Paleocene is composed of three formations that pass into each other laterally and vertically (Figure 8). The Kartal Formation is the one with most landward setting, comprising of red clastics; the Çaldağ Formation is an algal limestone of shallow marine environment; and the Yeşilyurt Formation represents the deeper marine setting with marl deposition including limestone blocks probably transported from the Çaldağ Formation. Facies map prepared by Ünalın et al. (1976; Figure 9) shows the setting during which these formations deposited; forming an arc shaped shelf deepening southeastward.

The Kırkkavak Formation is composed of algal limestones and grey marls, of Thanetian age, with conformable lower boundaries with all lower Paleocene formations in the study area. The Iğnıkdere Formation covers the Kırkkavak Formation, and is composed of conglomerates and sandstones with thin shale intercalations. The Iğnıkdere Formation is given as of Ilerdian age. Shales of the Iğnıkdere Formation increase in thickness and abundance while conglomerates and sandstones cease to exist to the top the formation, eventually becoming a more or less monotonous shale succession of the Eskipolatlı Formation of Ilerdian to Cuisian age. The shales also include some limestone bands toward the top, and grade into the sandy, Nummulitic limestones of the Çayraz Formation.

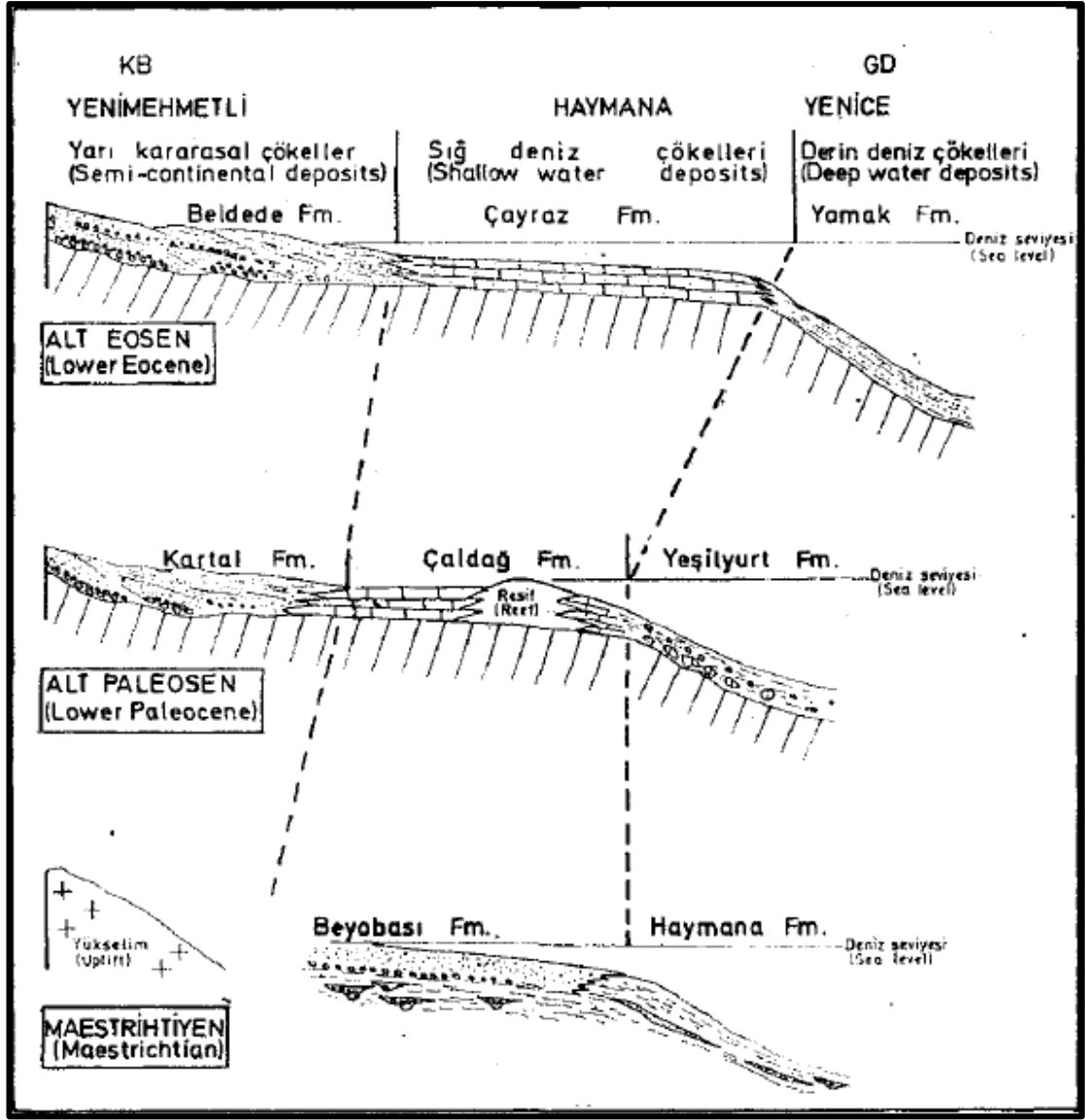


Figure 8: Paleogeographical sketch cross sections of the area (Ünalán et al., 1976).

The Beldede, Çayraz and Yamak Formations of middle Eocene age are very similar to the Kartal, Çaldağ, Yamak triplets of lower Paleocene, representing different depositional depths (Figure 8). The Beldede Formation is the shallowest with red clastics, the Çayraz Formation represents a high energy depositional setting of shallow depths, and the Yamak Formation is composed of coarse to fine grained clastics with turbiditic character. The paleogeographical configuration is similar to that of Kartal, Çaldağ and Yamak Formations, deepening in the southeast direction.

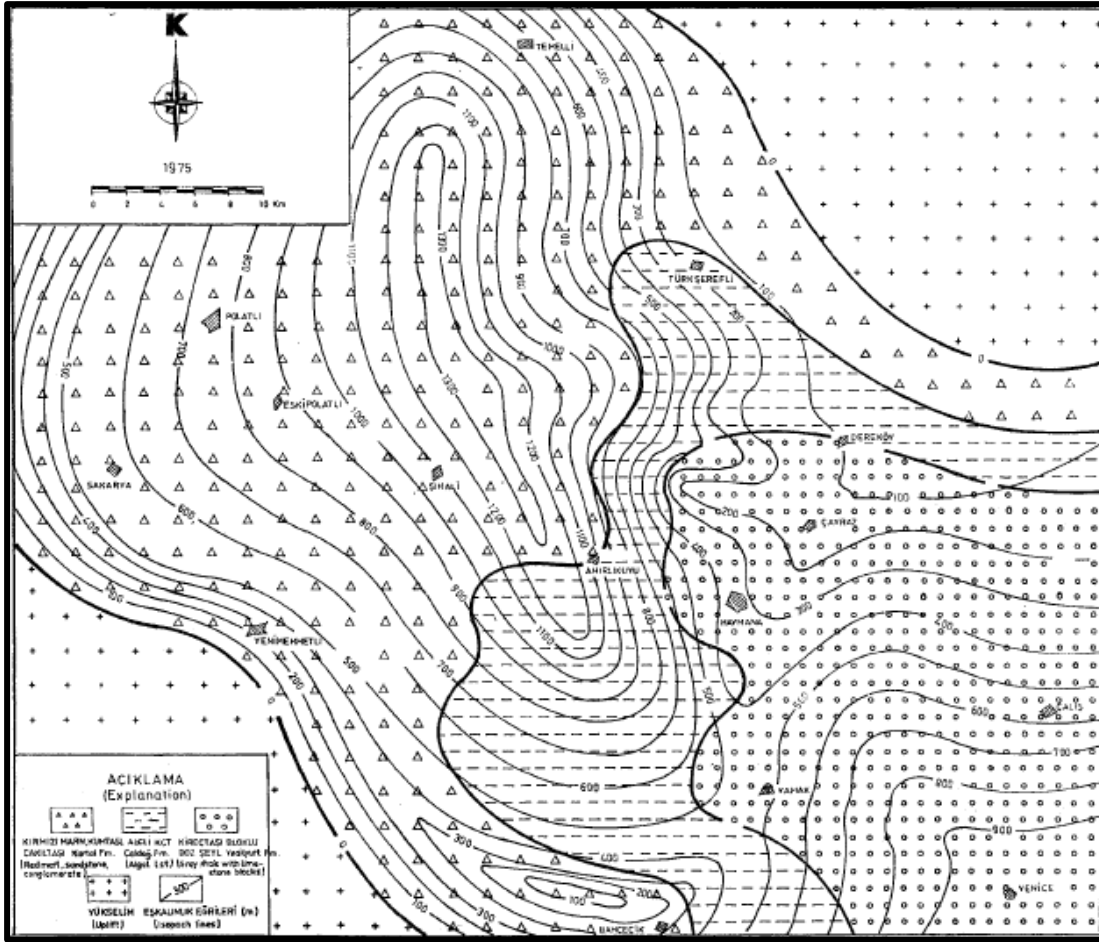


Figure 9: Facies map of Kartal, Çaldağ, Yeşilyurt Formations (Ünalın et al. 1976)

These units are covered unconformably with continental and volcanic rocks of Neogene age, and Quaternary alluvium.

The lateral and vertical relationships of the above mentioned formations led up Ünalın et al. (1976) to a paleogeographic interpretation (Figure 8). The area is thought as an arc shaped shelf deepening to southeastward direction; hence around Haymana settlement being the deeper, northwestern side (Polatlı-Temelli) being the shallower parts (e.g. Figure 9). The work by Gökçen (1976a, 1976b, 1977; southern Haymana) further develops a model of ellipsoidal basin with long axis about ENE-WSW direction which also puts Haymana settlement to deeper parts as in Ünalın et al. (1976). Gökçen (1976b and 1977) also studied the paleocurrents from coarse

grained turbiditic deposits, and pointed out the material transport from four directions.

CHAPTER 2

STRATIGRAPHY

2.1 Lithostratigraphy

The Haymana Basin comprises Cretaceous to Early Cenozoic sedimentary successions of which this study focuses on the Eskipolatlı Formation (Figure 7). The Eskipolatlı Formation was defined by Rigo de Righi and Cortesini (1959) as the grey shales with occasional thin sandstone and limestone bands; and the name was used by several authors for similar successions (e.g. Sirel, 1975; Ünalán et al., 1976, Figure 5). Its type location is 2 kilometers west of Eskipolatlı village. The formation is conformable with the İlginlıkdere Formation below, and the Yamak, Çayraz and Beldede Formations above. In different localities changes in the definitions occur, for example, the İlginlıkdere and Eskipolatlı Formations are not always disassociated from each other; such as in the work of Sirel (1975, Polatlı), the Eskipolatlı Formation starts with a conglomerate and sand alternation above an unconformity, then goes on with a shale dominated system. However, the conglomerate and sandstone alternation is defined as the İlginlıkdere Formation by Ünalán et al. (1976, Haymana).

According to Çetin et al. (1986) the Eskipolatlı Formation is composed of shales (for 80-85%) with small amount of thinly bedded sandstones; the formation was deposited by low energy turbidity currents.

Other lithologically similar units were reported from the southern parts of Haymana, and are named as Saridere and Bahçecik Formations by Gökçen (1976a), which roughly correspond to the Iğnıkdere and Eskipolatlı Formations of Ünalın et al. (1976). These units are also interpreted to be flyschoidal – hemipelagic deposits (Gökçen, 1977).

The boundary of the Iğnıkdere and Eskipolatlı Formations, as well as the Eskipolatlı and Çayraz Formations are not solid in Ünalın et al. (1976). The Eskipolatlı Formation includes sandstone and limestone intercalations in lower and upper parts of the package, respectively; and shale intercalations in upper parts of the Iğnıkdere and lower parts of the Çayraz Formations are also mentioned in the text with boundaries being somewhat arbitrary (Figure 7). In this study, the author defines these boundaries of the Eskipolatlı Formation as follows: lower boundary is the last sandstone bed's upper limit; upper boundary is the base of the first prominent thick limestone layer (Figure 11 and Figure 10).

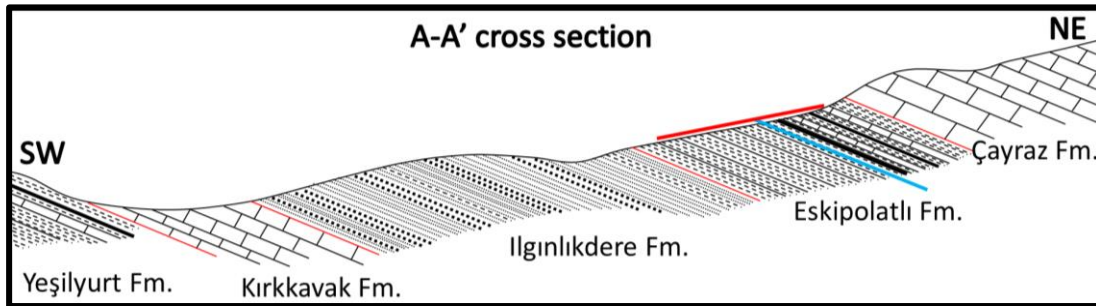


Figure 10: Sketch cross section along A-A' profile in Figure 11. Thick red line indicates the approximate position of the measured section. Blue line indicates the approximate location of P/E boundary.



Figure 11: Close up view of study area taken from Google Earth with formation boundaries and measured section (red line) indicated.

Bedding attitude of the İlginlıkdere and Çayraz Formations which provide the higher relief cliffs in the study area are similar; but, the Eskipolatlı Formation, due to its finer grained texture, does not give outcrops and is covered by a soil layer of variant thickness. No disruption is seen in this relatively low-lying area of the Eskipolatlı Formation, and hence is assumed to be continuous and conformable (Figure 3).

The lithology examined in this work is mainly shale (Figure 10, Figure 12). Throughout the measured section the color of the shale is dark green to dark brown (see Figure 13, color of sample GT-17.625 is the generally observed color; Figure 15), except for the brown - light brown colored small interval (~25cm) about half a meter below the boundary (Figure 14). The rock readily breaks into thin pieces with surfaces parallel / subparallel to bedding plane (Figure 15).



Figure 13: Field photograph from the second field work. Sampling points indicated on the figure

The samples are studied by washing method and thin sections (as explained in section 1.3) Via the washing method, the residues of several sieve sizes were obtained and weighted revealing the grain size as fine dominated (clay and silt, <63 μm), with very few sand size particles (Figure 16 and Table 5, bear in mind that

maximum amount of sand size particles is 3.21 grams per 100 gram of rock in GT-26). Thin section observations (Figure 17) also agree with this mudstone facies, although show that amounts of sand and silt size sediments differs among samples; however, this difference is so minimal that eventually no distinction can be made based on this criterion.



Figure 14: Photographs belonging to sampling pits of samples GT-17.125 and 17.25. Note the color difference



Figure 15: Photograph belonging to GT-24 sample pit showing the lamination and color of the rock

Table 5: Grain size distribution of the measured section: weight of different size intervals for 100 g dry sample

Sample #	>63 μm (g)	>125 μm (g)	>250 μm (g)	Sand size (g)	Mud size (g)
GT- 26	2.04	0.68	0.49	3.21	96.79
GT- 25	0.39	0.17	0.14	0.70	99.30
GT- 24	0.78	0.12	0.13	1.03	98.97
GT- 23	0.32	0.20	0.17	0.69	99.31
GT- 22	0.66	0.17	0.21	1.04	98.96
GT- 21	0.60	0.24	0.15	0.99	99.01
GT- 20	0.66	0.25	0.18	1.09	98.91
GT- 19	0.35	0.21	0.24	0.80	99.20
GT- 18	0.92	0.18	0.19	1.29	98.71
GT- 17	1.12	0.40	0.24	1.76	98.24
GT- 16	0.28	0.00	0.00	0.28	99.72
GT- 15	1.26	0.28	0.15	1.69	98.31
GT- 14	0.90	0.35	0.17	1.42	98.58
GT- 13	1.37	0.41	0.13	1.91	98.09
GT- 12	2.00	0.37	0.10	2.47	97.53
GT- 11	1.04	0.16	0.19	1.39	98.61
GT- 10	2.17	0.22	0.38	2.77	97.23
GT- 9	0.84	0.18	0.21	1.23	98.77
GT- 8	0.92	0.29	0.17	1.38	98.62
GT- 7	1.32	0.24	0.58	2.14	97.86
GT- 6	0.70	0.14	0.10	0.94	99.06
GT- 5	0.63	0.17	0.13	0.93	99.07
GT- 4	1.59	0.28	0.17	2.04	97.96
GT- 3	0.74	0.06	0.08	0.88	99.12
GT- 2	0.91	0.33	0.29	1.53	98.47
GT- 1	1.61	0.18	0.34	2.13	97.87

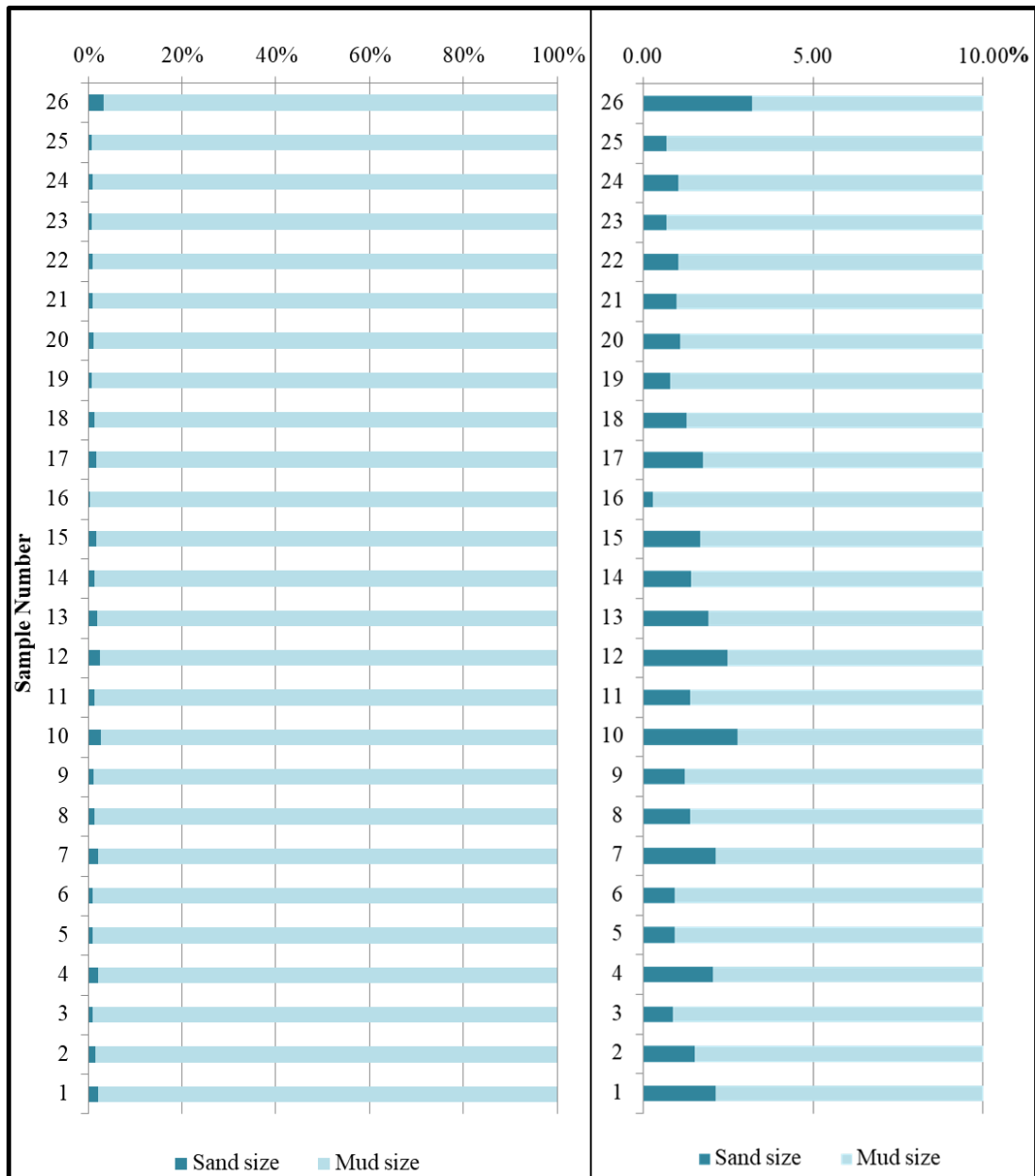


Figure 16: Grain size distribution of initial samples. Sand size refers to the weight of residue over 63 μm sieve after washing, out of 100 g dry sample. Right-hand side graph is enlarged image of the first 10% of the left-hand side graph for better visualization of the changes in sand size fraction

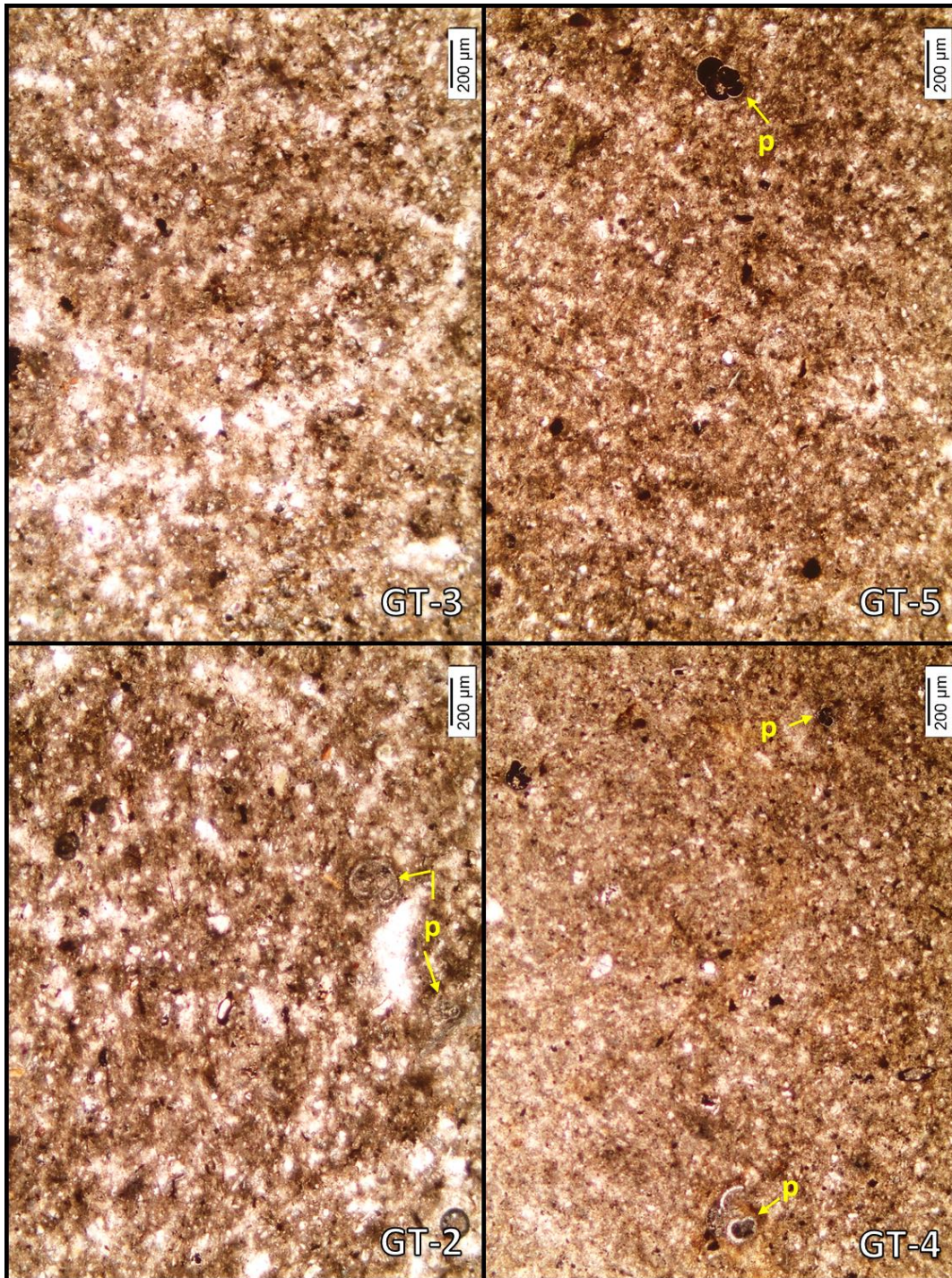


Figure 17: Thin section microphotographs of several samples. p: planktonic foraminifera, b: benthic foraminifera. Sample numbers indicated at the right bottom corner of the microphotographs, along with scale.

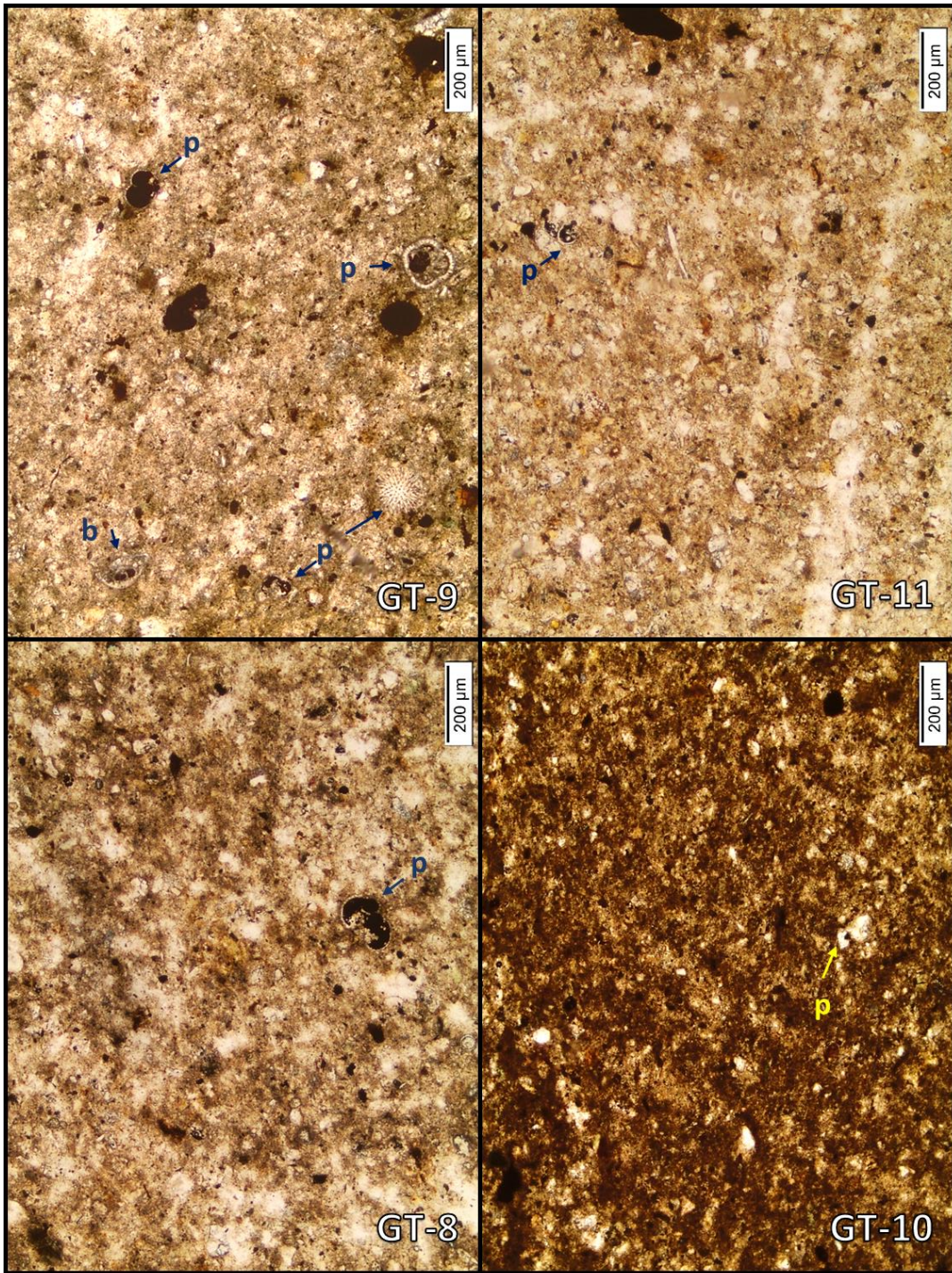


Figure 17 (Continued)

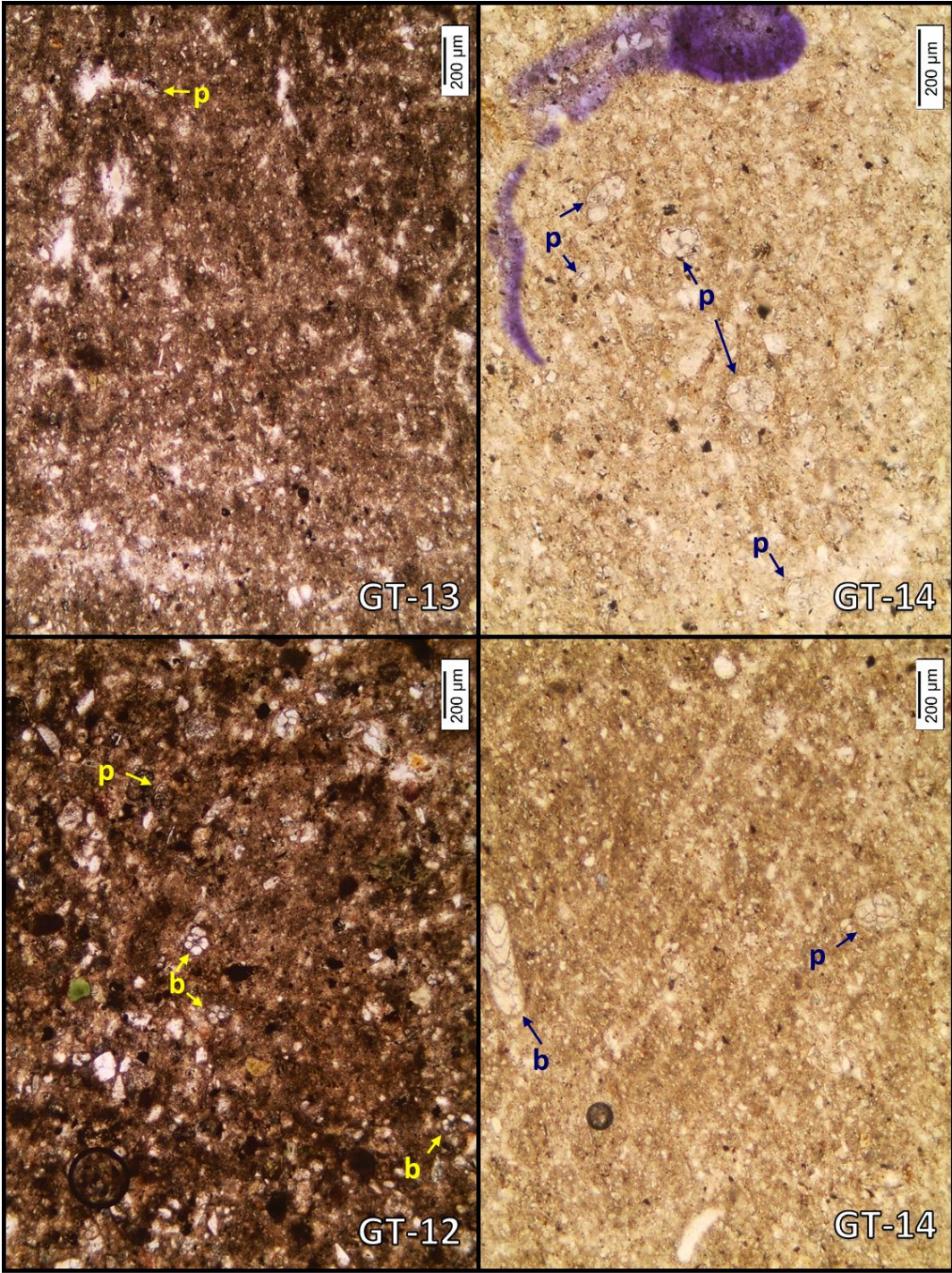


Figure 17 (Continued)

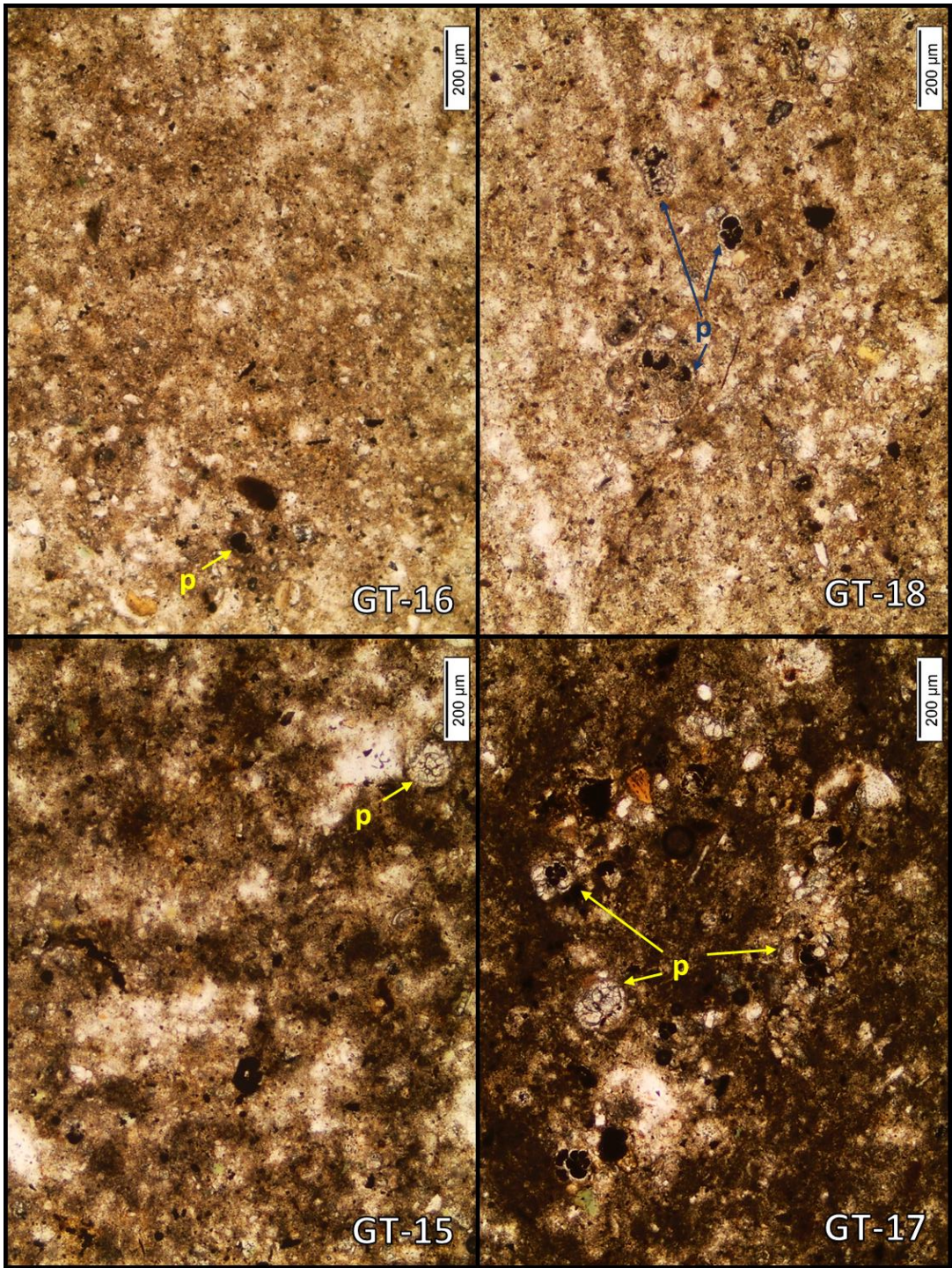


Figure 17 (Continued)

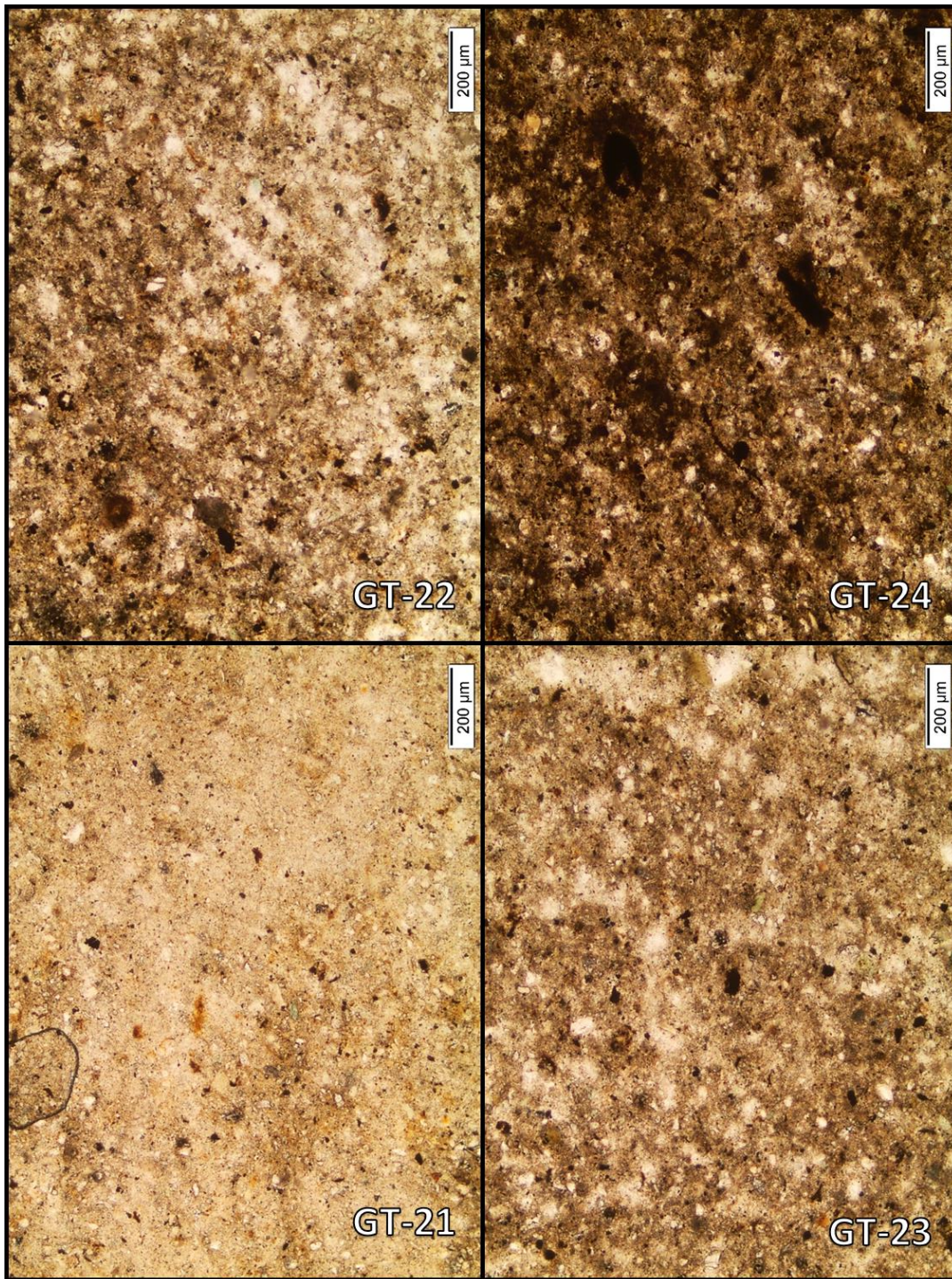


Figure 17 (Continued)

The sand sized particles ($>63 \mu\text{m}$) are the studied fraction in this study. A vast variety of grains are encountered during the studies (Figure 18, Figure 19, Figure 20, Figure 23, Figure 21). The majority of these sand sized grains are biogenic elements and a great amount of non-biogenic elements were also recovered.

The biogenic contents of the samples are mostly planktonic foraminifera (Figure 18-F), followed by benthic foraminifera (Figure 18-D), ostracods (Figure 18-E), micromollusca (Figure 18-B), echinoid spines (Figure 18-A) and biogenic contents of unknown origin.

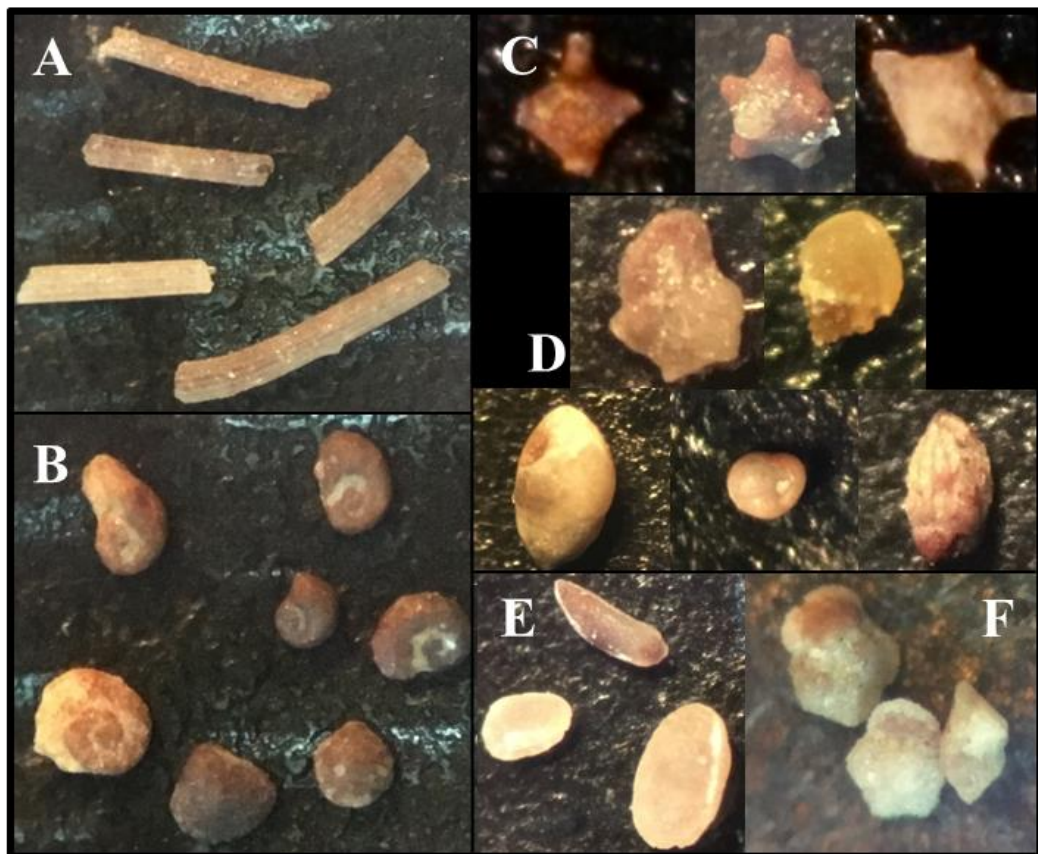


Figure 18: Microphotographs of samples of several biogenic elements recovered from various samples; A: Echinoid spines, B: Micromollusca, C: Unknown elements, D: Benthic foraminifera, E: Ostracoda, F: Planktonic foraminifera

The relative amount of planktonic foraminifera of a certain sieve size is varying between samples; however, majority of the planktonic foraminifera is found to be smaller than 106 μm . A similar condition is observed also for benthic foraminifera. As obvious in Figure 17, the thin section examinations also show sparse and small planktonic foraminifera.

Especially two sets of supposedly biogenic elements are curious: the milky white spheres and amber colored globular grains. Due to their globular-spherical nature these grains were further investigated via SEM imaging and EDS analysis, evaluating the possibility of glass spherules near the boundary similar to those found in Schaller et al. (2016) as impact ejecta. The milky white spheres (Figure 19) show

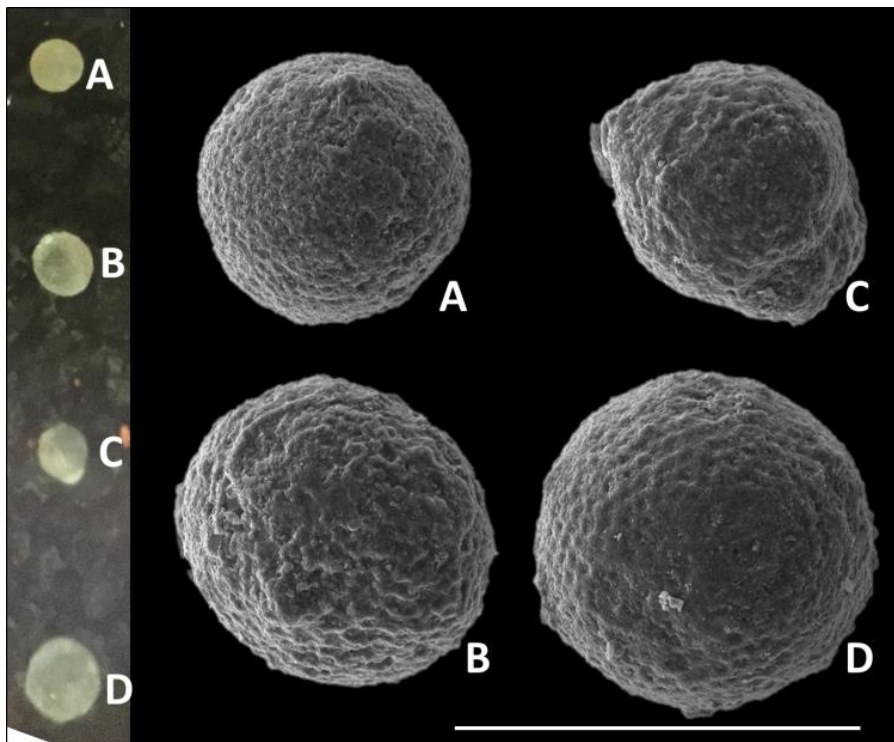


Figure 19: Milky white spheres from the samples GT-16 (A) and GT-4 (B, C, and D). Left-hand side: binocular light microscope microphotograph; right-hand side: SEM images with scale bar representing 200 μm . EDS analysis results can be found in Appendix D:Figure 48, Figure 49

an organized surface textural feature, which is not expected on an inorganic glass spherule, but is expected of tests of living organisms. Although the EDS analysis of these spheres resulted that they are silicate in composition (Appendix D: Figure 48 and Figure 49), their sporadic occurrence in the samples and the surface textural features indicate these are probably biogenic elements. The amber colored globular grains (Figure 20) are transparent to translucent, have smooth surface, and almost always found with a tail attached. The EDS analysis practiced on these grains (Appendix D: Figure 50, Figure 51) show that they are richer in calcium and carbon. Although these grains are found in a much restricted interval then the milky white spheres, they are obviously not silicate, and hence are not the impact related spherules either. Instead, these grains are probably biogenic in origin as well.

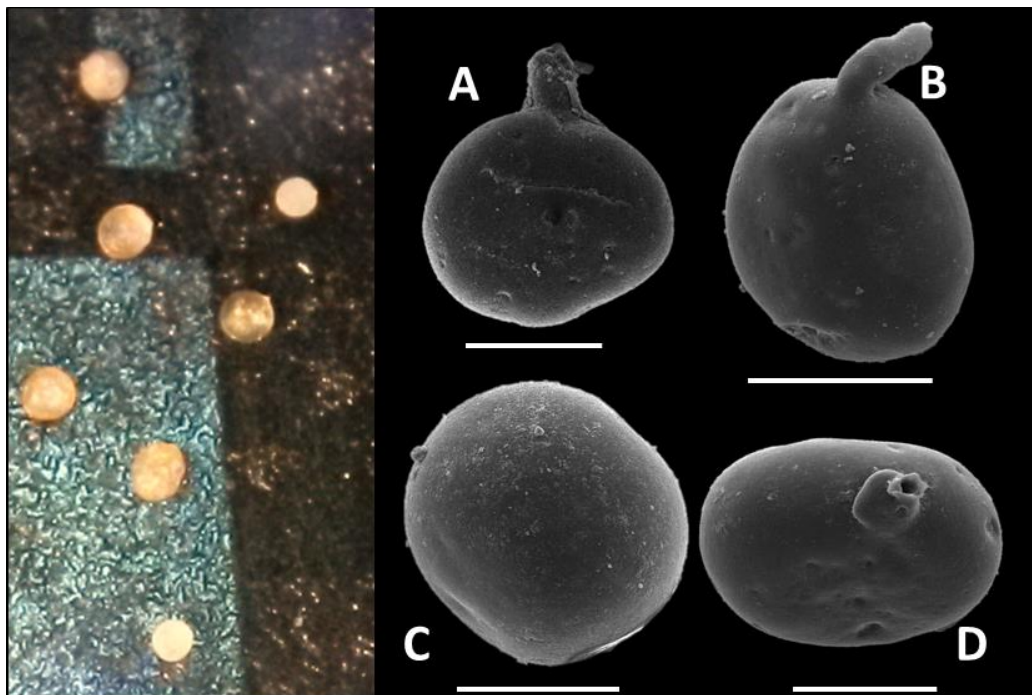


Figure 20: Amber colored globular grains: tailed cysts. Left- hand side: binocular light microscope microphotograph from the sample GT-16; right-hand side: SEM images with scale bar representing 100 μm : A, B and D from GT-15.5, and C from GT-16. EDS analysis results can be found in Appendix D: Figure 50 and Figure 51

The non-biogenic contents of the samples are also very diverse, but main components are calcitic and siliceous grains (Figure 21; Appendix D: Figure 52, Figure 53, Figure 54, Figure 55). A portion of these calcitic grains are thought to be infilling cement of the foraminiferal tests because of their globular shapes. The other portion of calcitic material and the siliceous material are thought to be the main components of the sedimentary influx.

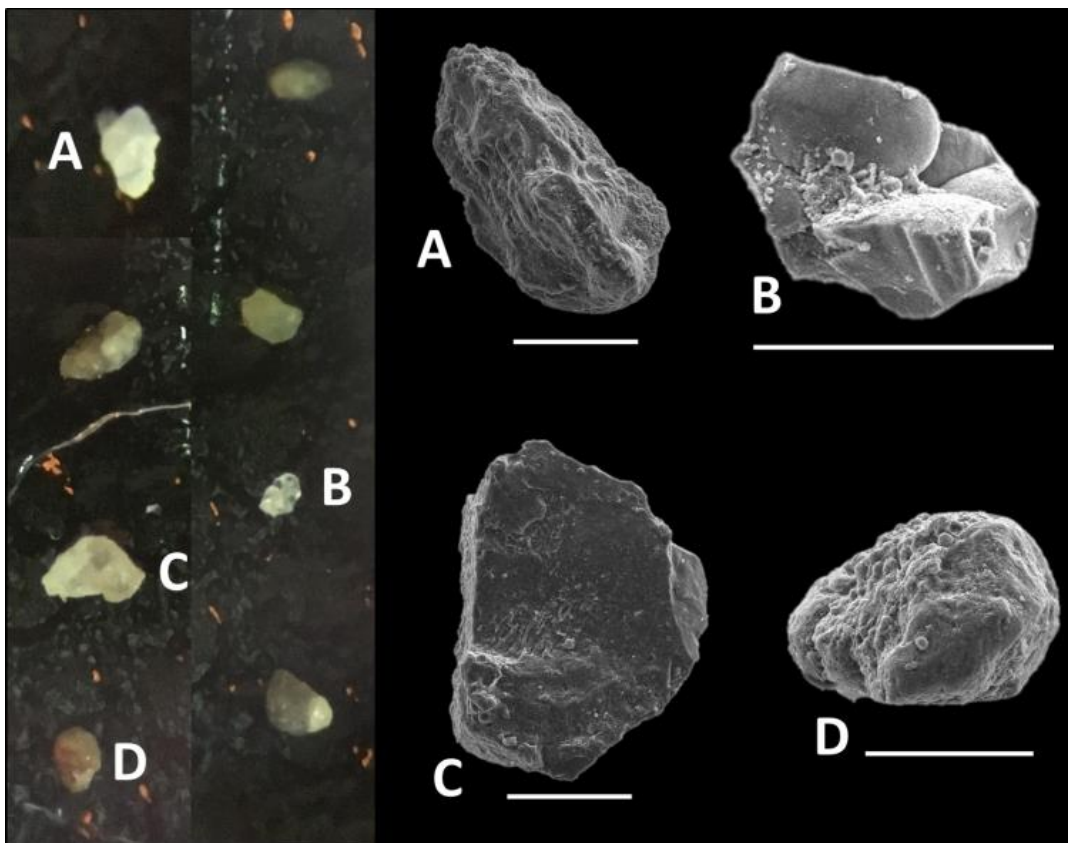


Figure 21: Several calcitic (A and B) and siliceous (C and D) grains from the sample GT-16. Left-hand side: binocular light microscope microphotograph; right-hand side: SEM images with scale bar representing 100 μm . EDS analysis results can be found in Appendix D: Figure 52, Figure 53, Figure 54, Figure 55

Other non-biogenic components are mica, mineral aggregates (Figure 22), and octahedral iron oxide crystals (Figure 23, Appendix D: Figure 47). The mineral aggregates in Figure 22 are probably filling material of borings and burrows at the time of deposition. The shapes of the crystals in Figure 22-B resembles those of pyrite framboids, however, no chemical analysis was carried out on these grains. These mineral aggregates are found in almost every sample of the measured section, increasing in abundance at some levels. The octahedral iron oxide crystals, on the other hand, are only found in the samples near the P/E boundary (e.g. GT-17.75 and GT-18).



Figure 22: A: Several mineral aggregate grains of unknown origin probably iron oxide in composition. B: Close-up view of the grain in white rectangle; note the reddish crystals

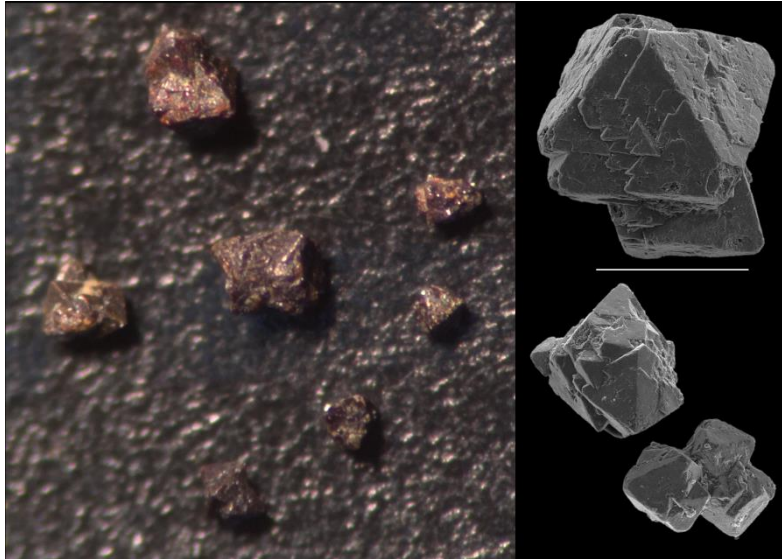


Figure 23: Octahedral iron oxide crystals from the sample GT-18. Left-hand side: binocular light microscope microphotograph; right-hand side: SEM images with scale bar representing 200 μm . EDS analysis results can be found in Appendix D: Figure 47

The amount of sand sized non-biogenic particles is slightly different in each sample, and this is interpreted as the amount of sedimentary influx. In samples with higher sedimentary influx, higher number of larger ($>106 \mu\text{m}$) reworked/transported planktonic foraminifera are encountered (for example GT-11).

The last sample of the measured section (GT-27) is a limestone, taken from the first prominent limestone tongue (Figure 24). This sample was not studied via washing method. It is a grainstone composed of mainly larger benthic foraminifera with minor amount of planktonic foraminifera (Figure 25).

Petrographical examinations of the samples do not yield any differences that can be used in order to present a kind of environmental, depositional, or climatic interpretations. The slight change in grain size may be due to different phases of turbiditic deposition and pelagic deposition, but the sampling resolution is probably too large for such evaluations.

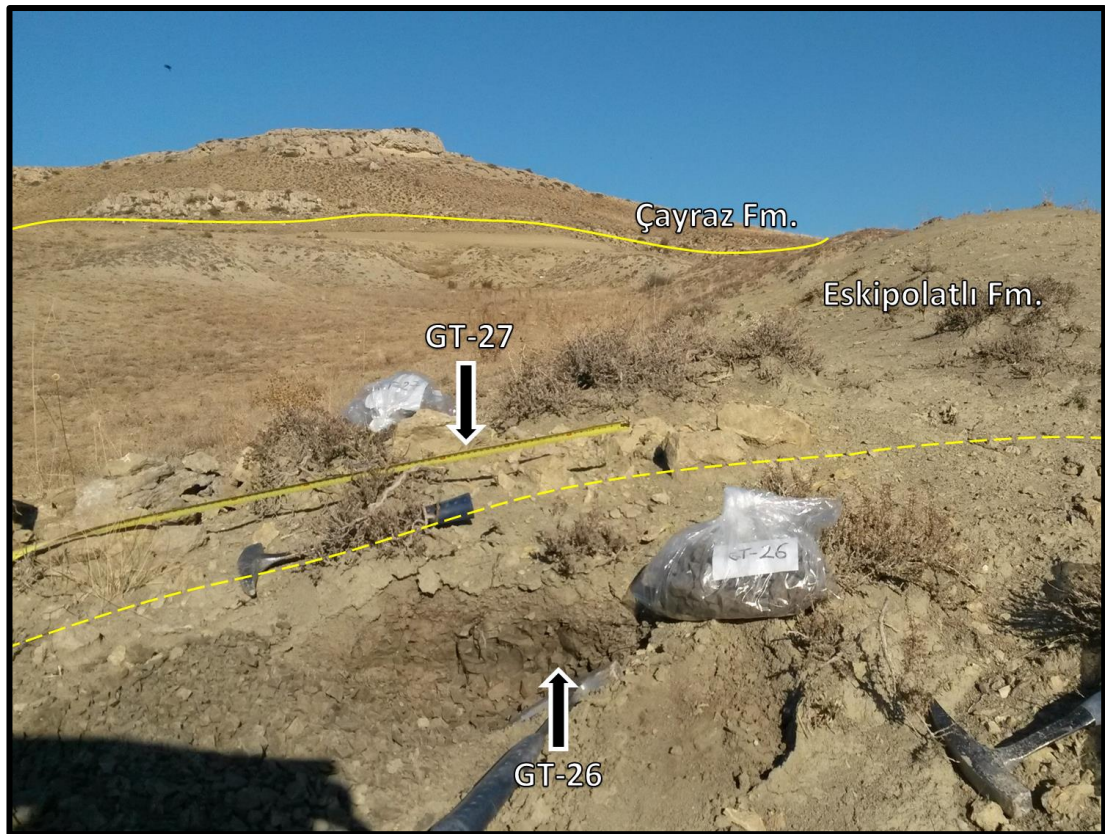


Figure 24: Field photo of the last two samples GT-26 (shale) and GT-27 (limestone). Uppermost limit of the Eskipolatlı Formation and the lowermost beds of the Çayraz Formation are also seen. Dashed line showing the position of the limestone tongue that the sample GT-27 was taken from.

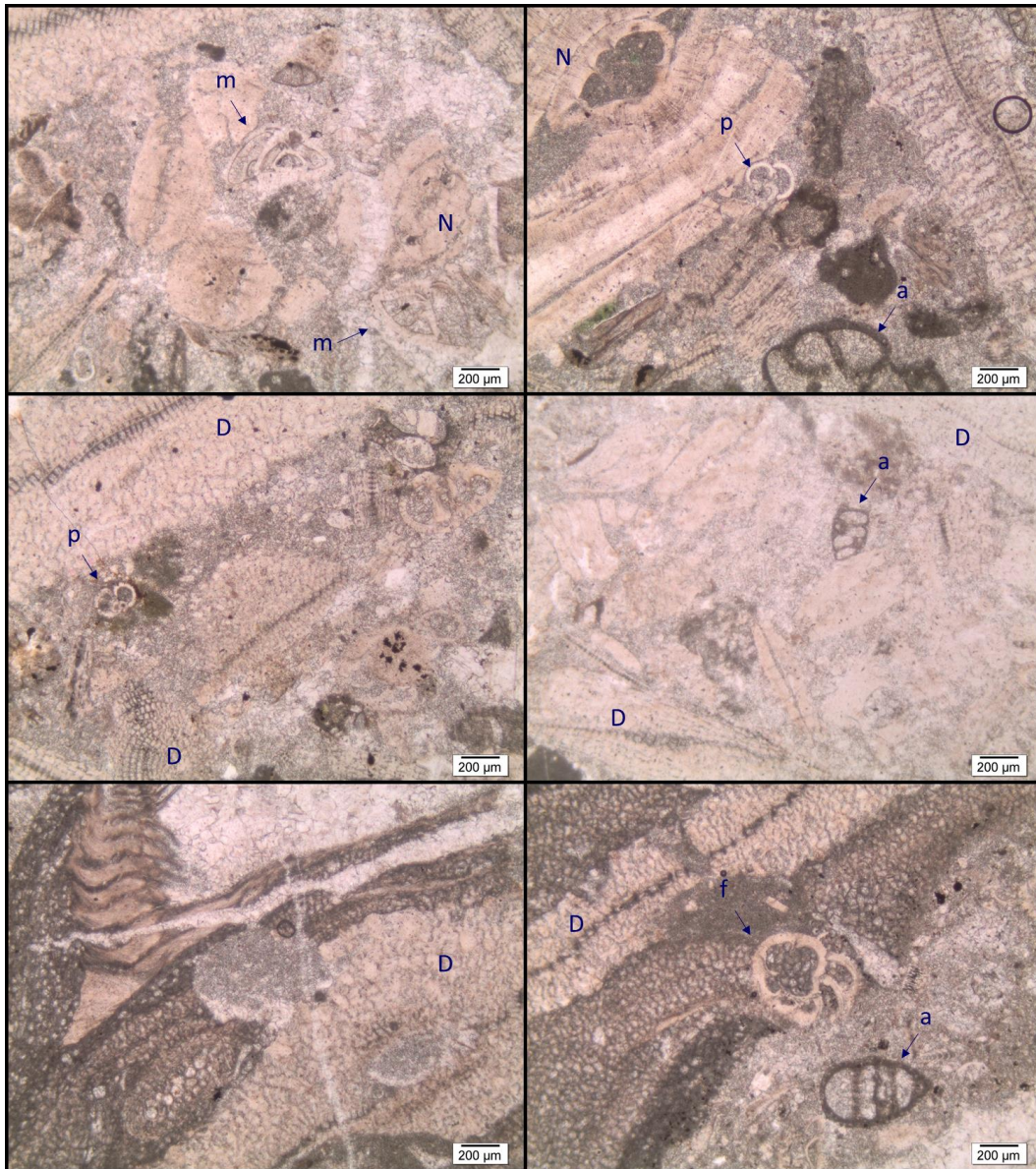


Figure 25: Thin section microphotographs of the sample GT-27. p: planktonic foraminifera, m: Morozovellid, a: agglutinated foraminifera, f: foraminifera of undetermined type, D: Discocylinidae, N: Nummulitidae

2.2 Biostratigraphy

2.2.1 Planktonic foraminiferal biostratigraphy of late Paleocene-early Eocene in literature

Planktonic foraminifera are widely utilized as index fossils for several reasons:

1. Free of substrate: independent of facies
2. Geographically widespread
3. High rate of diversification: short stratigraphic ranges

Cretaceous, Paleogene and Neogene have been being studied extensively in terms of planktonic foraminifera which provide a standardized biozonation and a means of correlation worldwide for aforementioned reasons. Late Paleocene-early Eocene planktonic foraminifera also have been being studied in detail, especially for the P/E boundary and the PETM. Many works have been published trying to put together the taxonomy and biostratigraphic significance of different planktonic foraminiferal taxa. Figure 26 is a summary of several works' zonation schemes for tropical-subtropical regions for the time interval in interest; the column on the left-hand side is from the work by Berggren and Pearson (2005) which makes up the base for this study. Among these schemes the following taxa were used as index very commonly: *Globanomalina pseudomenardii*, *Morozovella velascoensis* and *Morozovella formosa*; which is due to the distinctive morphological properties of these taxa.

Several schemes had been proposed for this time interval, of which one of the oldest ones is by Bolli (1957a) where the zonation scheme is based on first and last occurrences of several species of genera *Globorotalia** (*G.*) and *Globigerina** (*Gg.*).

* *Globorotalia* and *Globigerina* are the historical generic names used for assemblages of taxa now known to be polyphyletic. See Chapter 5 (101) for details concerning the evolution of generic and specific names, as well as taxonomical progress.

		Berggren & Pearson, 2005		Datum events	Supporting events	
PALEOCENE	GLOBANOMALINA <i>Globanomalina pseudomenardii</i>	P4	P4a	<i>G. pseudomenardii</i> - <i>A. subsphaerica</i>	<i>Globorotalia pseudomenardii</i>	Boll, 1957a
			P4b	<i>A. subsphaerica</i> - <i>A. soldadoensis</i>		
			P4c	<i>A. soldadoensis</i> - <i>G. pseudomenardii</i>		
		P5	<i>M. subbotinae</i> - <i>I. albeari</i>			
			<i>M. marginodentata</i> - <i>M. gracilis</i>			
	MOROZOVELLA <i>Morozovella velascoensis</i>	P5	<i>S. sibaiaensis</i> - <i>S. triangularis</i> - <i>I. lodoensis</i>	<i>Morozovella velascoensis</i>	Blow, 1979	
			<i>A. sibaiaensis</i> - <i>A. wilcoxensis</i> - <i>S. triangularis</i> - <i>I. lodoensis</i>			
		P6	<i>M. marginodentata</i> - <i>M. gracilis</i>			
			<i>G.(M) subbotinae</i> - <i>G.(M) subbotinae/ subbotinae/ velascoensis</i> - <i>G.(M) velascoensis acuta</i>			
			<i>G.(A) wilcoxensis berggreni</i>			
EOCENE	ACARININA <i>Acarinina sibaiaensis</i>	E1	<i>A. sibaiaensis</i> - <i>A. wilcoxensis</i> - <i>S. triangularis</i> - <i>I. lodoensis</i>	<i>Globorotalia velascoensis</i>	Blow, 1979	
			<i>P. wilcoxensis</i>			
			<i>M. velascoensis</i>			
	MOROZOVELLA <i>Morozovella velascoensis</i>	E2	<i>M. velascoensis</i>	<i>Morozovella velascoensis</i>	Blow, 1979	
			<i>P. wilcoxensis</i>			
	MARGINODENTATA <i>M. marginodentata</i>	E3	<i>M. marginodentata</i> - <i>M. edgari</i> - <i>A. quetza</i>	<i>Morozovella velascoensis</i>	Blow, 1979	
			<i>M. edgari</i> - <i>A. quetza</i>			
	FORMOSA <i>M. formosa</i>	E4	<i>M. formosa</i> - <i>M. lensiformis</i>	<i>Morozovella velascoensis</i>	Blow, 1979	
			<i>M. formosa</i> - <i>M. lensiformis</i>			
	PALEOCENE	GLOBOROTALIA <i>Globorotalia pseudomenardii</i>	P4	<i>G. pseudomenardii</i> - <i>A. subsphaerica</i>	<i>Globorotalia pseudomenardii</i>	Blow, 1979
<i>A. subsphaerica</i> - <i>A. soldadoensis</i>						
<i>A. soldadoensis</i> - <i>G. pseudomenardii</i>						
P5			<i>M. subbotinae</i> - <i>I. albeari</i>			
			<i>M. marginodentata</i> - <i>M. gracilis</i>			
MOROZOVELLA <i>Morozovella velascoensis</i>		P4	<i>G. pseudomenardii</i> - <i>A. subsphaerica</i>	<i>Morozovella velascoensis</i>	Blow, 1979	
			<i>A. subsphaerica</i> - <i>A. soldadoensis</i>			
		<i>A. soldadoensis</i> - <i>G. pseudomenardii</i>				
		P5	<i>M. subbotinae</i> - <i>I. albeari</i>			
			<i>M. marginodentata</i> - <i>M. gracilis</i>			
EOCENE	MOROZOVELLA <i>Morozovella velascoensis</i>	E1	<i>A. sibaiaensis</i> - <i>A. wilcoxensis</i> - <i>S. triangularis</i> - <i>I. lodoensis</i>	<i>Morozovella velascoensis</i>	Blow, 1979	
			<i>P. wilcoxensis</i>			
			<i>M. velascoensis</i>			
	MARGINODENTATA <i>M. marginodentata</i>	E2	<i>M. marginodentata</i> - <i>M. edgari</i> - <i>A. quetza</i>	<i>Morozovella velascoensis</i>	Blow, 1979	
			<i>M. edgari</i> - <i>A. quetza</i>			
	FORMOSA <i>M. formosa</i>	E3	<i>M. formosa</i> - <i>M. lensiformis</i>	<i>Morozovella velascoensis</i>	Blow, 1979	
			<i>M. formosa</i> - <i>M. lensiformis</i>			
	MOROZOVELLA <i>Morozovella velascoensis</i>	E4	<i>M. formosa</i> - <i>M. lensiformis</i>	<i>Morozovella velascoensis</i>	Blow, 1979	
			<i>M. formosa</i> - <i>M. lensiformis</i>			
	PALEOCENE	GLOBOROTALIA <i>Globorotalia pseudomenardii</i>	P4	<i>G. pseudomenardii</i> - <i>A. subsphaerica</i>	<i>Globorotalia pseudomenardii</i>	Blow, 1979
<i>A. subsphaerica</i> - <i>A. soldadoensis</i>						
<i>A. soldadoensis</i> - <i>G. pseudomenardii</i>						
P5			<i>M. subbotinae</i> - <i>I. albeari</i>			
			<i>M. marginodentata</i> - <i>M. gracilis</i>			
MOROZOVELLA <i>Morozovella velascoensis</i>		P4	<i>G. pseudomenardii</i> - <i>A. subsphaerica</i>	<i>Morozovella velascoensis</i>	Blow, 1979	
			<i>A. subsphaerica</i> - <i>A. soldadoensis</i>			
		<i>A. soldadoensis</i> - <i>G. pseudomenardii</i>				
		P5	<i>M. subbotinae</i> - <i>I. albeari</i>			
			<i>M. marginodentata</i> - <i>M. gracilis</i>			
EOCENE	MOROZOVELLA <i>Morozovella velascoensis</i>	E1	<i>A. sibaiaensis</i> - <i>A. wilcoxensis</i> - <i>S. triangularis</i> - <i>I. lodoensis</i>	<i>Morozovella velascoensis</i>	Blow, 1979	
			<i>P. wilcoxensis</i>			
			<i>M. velascoensis</i>			
	MARGINODENTATA <i>M. marginodentata</i>	E2	<i>M. marginodentata</i> - <i>M. edgari</i> - <i>A. quetza</i>	<i>Morozovella velascoensis</i>	Blow, 1979	
			<i>M. edgari</i> - <i>A. quetza</i>			
	FORMOSA <i>M. formosa</i>	E3	<i>M. formosa</i> - <i>M. lensiformis</i>	<i>Morozovella velascoensis</i>	Blow, 1979	
			<i>M. formosa</i> - <i>M. lensiformis</i>			
	MOROZOVELLA <i>Morozovella velascoensis</i>	E4	<i>M. formosa</i> - <i>M. lensiformis</i>	<i>Morozovella velascoensis</i>	Blow, 1979	
			<i>M. formosa</i> - <i>M. lensiformis</i>			

Figure 26: Comparison of several planktonic foraminiferal zonation schemes of upper Paleocene (P) and part of lower Eocene (E) interval with respect to zonation scheme and stratigraphic ranges by Berggren & Pearson (2005).

Bolli divided the interval this thesis focuses on into 4 biozones (Figure 26): *Globorotalia pseudomenardii* (total range of *G. pseudomenardii*), *G. velascoensis* (between highest occurrence (HO) of *G. pseudomenardii* and HO of *G. velascoensis*), *G. rex** (between HO of *G. velascoensis* and lowest occurrence (LO) of *G. formosa*), and *G. formosa*; with the P/E boundary at the upper boundary of *G. velascoensis* Zone: at the highest occurrence datum (HOD) of *Globorotalia velascoensis*.

Blow (1979), on the other hand, used different set of criteria for their zonation scheme (Figure 26): Zone P5 initiates with LO of *Muricoglobigerina soldadoensis soldadoensis*, lower boundary of P6 is marked with LO of *Globorotalia (Morozovella) subbotinae subbotinae*, and lower boundary of P7 is marked with LO of *G.(Acarinina) wilcoxensis berggreni*. The topmost zone (P8) is the same with that of Bolli (1957a). The P/E boundary is positioned at the P7/P8 boundary and is marked with LO of *G.(A) wilcoxensis berggreni*.

Toumarkine and Luterbacher (1985) proposed a scheme with the same upper Paleocene zonation with Bolli (1957a) (Figure 26). For the lowest Eocene they proposed *Morozovella. edgari* (between HO of *M. velascoensis* and HO of *M. edgari*) and *M. subbotinae* (between HO of *M. edgari* and LO of *M. aragonensis*) Zones instead of Bolli's *M. rex* and *M. formosa* Zones. The boundary, like in Bolli's work, is positioned at the HO of *M. velascoensis*.

Berggren and Miller (1988) also used HO of *M. velascoensis* as the P/E boundary criteria which is positioned in their *Morozovella. subbotinae* Zone (P6). Their Zone P4 is correlative to Bolli's (1957) *Globanomalina. pseudomenardii* Zone, above which a P5* (*M. velascoensis*) Zone was defined as the interval between HO of *G. pseudomenardii* and LO of *M. subbotinae*. They further divided the Zone P6 into

* According to Bolli, *G. rex*, presented here as a junior synonym of *M. subbotinae*, spans a short interval with LO in *G. rex* Zone (at the base) and HO in *G. formosa* Zone. See section 5.2.1 for discussion on stratigraphic range of *M. subbotinae*.

subzones as follows: P6a (*M. subbotinae*/*M. velascoensis* Zone, between LO of *M. subbotinae* and HO of *M. velascoensis*), P6b (*M. subbotinae*-*P. wilcoxensis* Zone, between HO of *M. velascoensis* and LO of *M. formosa*), and P6c (*M. formosa*-*M. lensiformis* Zone, between LO of *M. formosa* and LO of *M. aragonensis*) (Figure 26).

Berggren et al. (1995) proposed a subzonation scheme for the Zone P4 of Berggren and Miller (1988) (Figure 26), which further increases resolution for the late Paleocene: P4a (*Globanomalina pseudomenardii*-*Acarinina subsphaerica* Zone, between LO of *G. pseudomenardii* and HO of *A. subsphaerica*), P4b (*A. subsphaerica*-*A. soldadoensis* Zone, between HO of *A. subsphaerica* and LO of *A. soldadoensis*), and P4c (*A. soldadoensis*-*G. pseudomenardii* Zone, between LO of *A. soldadoensis* and HO of *G. pseudomenardii*). Zone P4 is followed by Zone P5 (*Morozovella velascoensis*) whose upper boundary is marked by HO of *M. velascoensis* and marks P/E boundary; this zone includes Subzone P6a of Berggren and Miller (1988). Subzones P6b and P6c of Berggren and Miller (1988) are rearranged as Subzones P6a (*M. velascoensis*-*M. formosa*/*M. lensiformis* Subzone, between HO of *M. velascoensis* and LO of *M. formosa*/*M. lensiformis*) and P6b (*M. formosa*/*M. lensiformis*-*M. aragonensis* Subzone, between LO of *M. formosa*/*M. lensiformis* and LO of *M. aragonensis*) respectively under Zone P6 (*M. subbotinae* Zone).

Arenillas and Molina (1996) presented a similar zonation scheme to that of Bolli (1957) (Figure 26), but used an additional zone for lower part of *G. velascoensis* Zone of Bolli: *Igorina laevigata* Zone defined by the interval between HO of *G. pseudomenardii* and HO of *I. laevigata***.

* Zone P5 of Berggren and Miller (1988) is not applicable here due to differences in stratigraphic range of *M. subbotinae* (see section 5.2.1).

** *I. laevigata* here used as a junior synonym of *I. albeari*; see section 5.2.3.

Molina et al. (1999) presented much detail for formerly wide *G. (M.) velascoensis* Zone of several authors (Figure 26). They proposed five following subzones: *Morozovella aequa* (between HO of *Luterbacteria** *pseudomenardii* and LO of *M. gracilis*), *M. gracilis* (between LO of *M. gracilis* and LO of *Acarinina berggreni*), *A. berggreni* (between LO of *A. berggreni* and LO of *A. sibaiaensis*), *A. sibaiaensis* (between LO of *A. sibaiaensis* and LO of *Pseudohastigerina wilcoxensis*), *P. wilcoxensis* (between LO of *P. wilcoxensis* and HO of *M. velascoensis*). Above this highly detailed *M. velascoensis* Zone they defined a *M. subbotinae* Zone with three subzones: *M. edgari* (between HO of *M. velascoensis* and HO of *M. edgari*), *M. subbotinae* (between HO of *M. edgari* and LO of *M. formosa*) and *M. formosa* (with LO of *M. formosa* as lower boundary). The P/E boundary was correlated with benthic foraminifera extinction event (BFE) and placed in *A. berggreni* Subzone.

Pardo et al. (1999) proposed a scheme similar to that of Berggren et al. (1995) and Arenillas and Molina (1996) (Figure 26), and divided Zone P5 into two subzones named *Luterbacteria pseudomenardii*-*A. sibaiaensis* Subzone (between HO of *L. pseudomenardii* and LO of *A. sibaiaensis*) and *A. sibaiaensis*/*A. africana*-*M. velascoensis* Subzone (between LO of *A. sibaiaensis*/*A. africana* and HO of *M. velascoensis*). They give the boundary interval as the *A. sibaiaensis*/*A. africana*-*M. velascoensis* Subzone and correlate the BFE to the lower boundary of it.

Speijer et al. (2000) used the zonation of Berggren et al (1995), and proposed the following subzonation of Zone P5 (Figure 26): P5a (between HO of *G. pseudomenardii* and LO of *M. allisonensis*), P5b (total range of *M. allisonensis*) and P5c (between HO of *M. allisonensis* and HO of *M. velascoensis*). They argue that

* *Luterbacteria*, *Planorotalites* and *Globanomalina* generic names are interchangeably used in the literature for the same several species such as *Globanomalina chapmani*, *G. ehrenbergi*, *G. pseudomenardii*. Currently all are listed under genus *Globanomalina*, while the name *Planorotalites* is used for another pinched peripheried group with different wall texture. Name *Luterbacteria* is no longer in use.

formerly proposed index taxa (*A. sibaiaensis* and *A. africana*) for the lowest Eocene biozone are not restricted to such interval, but *M. allisonensis* is.

E zones for Eocene were introduced by Berggren and Pearson (2005) which provided a more detailed zonation of what formerly known as uppermost Paleocene Zone P5 (of Berggren et al., 1995; Figure 26). Zone P5 of Berggren and Pearson (2005) (*M. velascoensis* Zone, between HO of *G. pseudomenardii* and LO of *A. sibaiaensis*) correlates with lowermost part of Zone P5 of Berggren et al. (1995) while Zone E1 (*A. sibaiaensis* Zone, between LO of *A. sibaiaensis* and LO of *P. wilcoxensis*) represents the mid part of Zone P5 of Berggren et al. (1995), and Zone E2 (*P. wilcoxensis*-*M. velascoensis* Zone, between LO of *P. wilcoxensis* and HO of *M. velascoensis*), which is the uppermost part of Zone P5 of Berggren et al. (1995). The boundary is positioned at the lower boundary of Zone E1. Throughout this thesis any given numeric biozone names are of Berggren and Pearson (2005) unless specified otherwise.

2.2.2 Planktonic foraminiferal events throughout the Paleocene and the Eocene

The Paleocene and the Eocene Epochs are divided into several informal partitions with respect to planktonic foraminiferal assemblages (Figure 27).

Earliest Paleocene (P0 and P α) represents the interval of initial recovery after the extinction at the K/T boundary. Forms started to evolve and resettle into the recently vacated niches during the early Paleocene: *Hedbergella*, *Guembelitra*, *Parvularugoglobigerina*, *Praemurica*, *Globoconusa*, *Eoglobigerina* are the characterizing genera and they later cease to exist latest in Zone P3.

The gradual turnover can be observed through P2 and P3 biozones (Figure 27) where early Paleocene taxa diminish one by one, while *Parasubbotina*, *Subbotina* and *Globanomalina* diversify and late Paleocene muricate taxa, namely *Morozovella*, *Acarinina* and *Igorina*, initiate. When late Paleocene (P3-P5 Zonal interval) is

PALEOCENE					EOCENE																	
EARLY		LATE			EARLY				MIDDLE					LATE								
Danian		Selandian	Thanetian		Ypresian				Lutetian			Bartonian		Priabonian								
P α	P0	P1	P2	P3	P4	P5	E2	E3	E4	E5	E7	E8	E9	E10	E11	E12	E13	E14	E15	E16		
							E1				E6											
K/Pg survivors and first Paleocene genera		extinction of several early Paleocene genera, initiation of late Paleocene muricate genera			Gradual turnover in Acarininids from rounded type to angular type				Demise of box-Morozovellids				Acarininid and Subbotinid turnover, initiation of middle Eocene genera			Globigerinathekid initiation, Chiloguembelinid and Acarininid turnover, Morozovellid extinction					<i>Dentaglobigerinella</i> and <i>Tenuitella</i>	

Figure 27: Summary of the Paleocene-Eocene major planktonic foraminiferal events with respect to biozonation scheme of Berggren and Pearson (2005)

examined, it is evident that the morphologies, along with wall structures got more complex with muricate walls and conical chamber shapes. In this interval keeled and decorated Morozovellids (especially peripherally ornamented Morozovellids; page 121 for details) and rounded and highly pustulose Acarininids are distinctive.

Early Eocene is very similar to late Paleocene in general assemblage and morphological characteristics (Figure 27). One evident change is in Acarininid groups where instead of rounded and highly pustulose groups, there are quadrate and less ornamented taxa. Another change is in the dominant Morozovellid morphology: peripherally ornamented Morozovellids are diminished by the end of E2, while full body ornamented Morozovellids are unaffected.

Middle Eocene, on the other hand, is represented by prominent change in morphology by production of several different types: e.g. tubulospinose chambers (Hantkeninids, evolved as early as E7) and spherical tests (Globigerinathekids, evolved during E9). Later on, during Zone E13 and up, *Tenuitella* and *Dentaglobigerina* genera evolved (Figure 27).

Since this thesis is interested in the late Paleocene and earliest Eocene planktonic foraminifera, main characteristics of P4c-E2 zones will be elaborated. The zones P4 and P5 have most of their contents the same, with the only difference being demise

of the keeled, smooth walled species *Globanomalina pseudomenardii* and gradual rise and increase of highly and full body ornamented Morozovellid species (e.g. *Morozovella aequa* and *Morozovella subbotinae*). These changes are succeeded by origination of quadrate Acarininids (e.g. *Acarinina wilcoxensis* and *Acarinina pseudotopilensis*) at the uppermost P5. The earliest Eocene is marked with this assemblage and with a gradual and indistinct change from slightly asymmetrical aperture of *Globanomalina luxorensis* into a symmetrical aperture of *Pseudohastigerina wilcoxensis* the end of Zone E1 is marked. Zone E1 is also the interval during which the PETM happened, and the so-called excursion taxa (*Acarinina sibiyaensis*, *Acarinina africana* and *Morozovella allisonensis*) lived. *Morozovella velascoensis*, which is the index species of *M. velascoensis* (P5) zone of Berggren (1995), and much other zonations due to its distinct morphology, makes an exit at the end of E2.

This interval (between Zones P4c-E2) is what this study focuses on, and is quite different from lower or upper assemblages in terms of several characteristics:

1. *Praemurica* genus is absent which is a marker for early Paleocene
2. Full body ornamented Morozovellids are present
3. Rounded Acarininids are present along with quadrate Acarininids with former gradually diminishing while the latter concurrently increase
5. Hantkeninids, Globigerinathekids and *Turborotalia*, which mark the mid-Eocene, are absent

2.2.3 Planktonic foraminiferal biostratigraphy of the measured section

In the samples examined from the measured section, the markers of middle Eocene are all absent, along with early Paleocene indicators. Instead, the samples are very rich in *Subbotina*, *Acarinina* and *Morozovella* genera, along with minor amounts of *Parasubbotina*, *Igorina* and *Globanomalina*. This assemblage is characteristic for the late Paleocene-early Eocene interval, and is studied in detail for higher resolution biostratigraphy (Figure 29). The measured section is divided into four biozones (Figure 28) as explained in the following subheadings, and the P/E boundary is placed at the lower boundary of *A. sibaiaensis* Zone.

2.2.3.1 *Globanomalina pseudomenardii* Zone

Definition: From bottom of the measured section, up to HOD of *Globanomalina pseudomenardii*.

Author: *Globanomalina pseudomenardii* Zone was first defined by Bolli (1957) as the total range zone of *G. pseudomenardii*.

Remarks: The lowest 10 samples are of this biozone where *Globanomalina pseudomenardii* is the index fossil. The zone's upper limit is drawn by *Globanomalina pseudomenardii* disappearance. This biozone is comparable and correlatable to top part of *G. pseudomenardii* Zone of Bolli (1957), *P. pseudomenardii* Zone of Toumarkine and Luterbacher (1985), Berggren and Miller (1988), and Arenillas and Molina (1996), and *L. pseudomenardii* Zone of Pardo et al. (2000); is the same with Zone P5 of Blow (1979), Subzone P4c of Berggren et al. (1995), *M. soldadoensis* Subzone of Molina et al. (1999) and Subzone P4c of Berggren & Pearson (2005) (Figure 28).

Apart from *G. pseudomenardii*, samples contain *Acarinina soldadoensis*, *A. nitida*, *A. subsphaerica*, *A. esnaensis*, *Morozovella aequa*, *M. acuta*, *Subbotina velascoensis*, and *S. triangularis* as major components.

Series	PALEOCENE		EOCENE	
Biozones	<i>G. pseudomenardi</i>		<i>M. subbotinae</i>	<i>A. sib.</i>
Thickness (m)	0		2	4
Lithology	[Patterned]		[Patterned]	[Patterned]
Sample #	-GT-1 -GT-2 -GT-3 -GT-4 -GT-5 -GT-6 -GT-7 -GT-8 -GT-9 -GT-10 -GT-11 -GT-12 -GT-13 -GT-14 -GT-15 -GT-16 -GT-17 -GT-18 -GT-19 -GT-20 -GT-21 -GT-22 -GT-23 -GT-24 -GT-25 -GT-26 -GT-27			
Datum events	<i>G. pseudomenardi</i> <i>M. subbotinae</i> <i>I. albeeri</i>		<i>G. imitata</i> <i>M. gracilis</i> <i>M. marginodentata</i> <i>I. ladaensis</i> <i>A. wilcoxensis</i> <i>M. edgari</i>	<i>P. wilcoxensis</i> <i>A. sibiyaensis</i>
Supporting events	Glabromalina pseudomenardi		Morzovelia subbotinae	Acarinina sibiyaensis
This Study	Pseudohostigera wilcoxensis		Glabrotia velascoensis	
Boll 1957	P5		P6	
Blow 1979	P4		P7	
Tourkine & Luterbacher 1985	Planrotalites pseudomenardi		Morzovelia velascoensis	
Berggren & Miller 1988	P4		P6a	
Berggren et al. 1995	P4c		P5	
Arenillas & Molina 1996	Planrotalites pseudomenardi		Morzovelia velascoensis	
Molina et al. 1999	Murcojabigera soldoensis		Pseudohostigera wilcoxensis	
Pardo et al. 1999	P4		P5a	
Speijer et al. 2000	P4		P5b	
Berggren and Pearson 2005	P4c		E2	

Figure 28: Summary of the biostratigraphic schemes and their correlation with this study

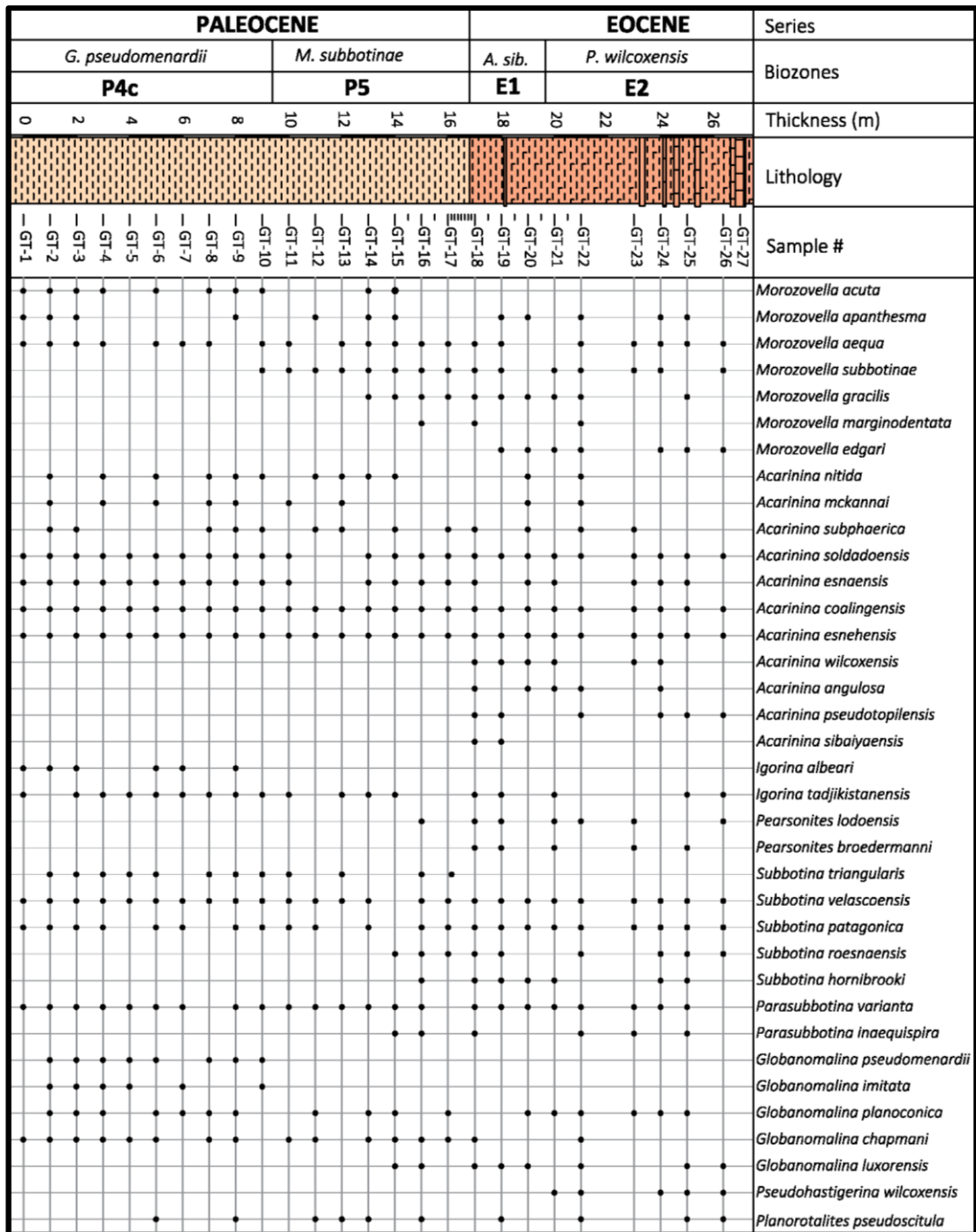


Figure 29: Stratigraphical distribution of the planktonic foraminifera in the measured section

The abundant transportation/reworking problem throughout the measured section were the biggest problem in defining biostratigraphic zones by the highest occurrences. *G. pseudomenardii*, an unmistakably definable species with distinct morphological features, is found in higher levels sporadically and below 1% in amount. Occurrence of this species in stratigraphically higher levels is reported by Blow (1979), Lu et al. (1998) puts *P. cf. pseudomenardii* in upper Zone P4 up in the early Eocene zones in the Alamedilla and Ben Gurion sections, and a species homeomorphic to *G. pseudomenardii* is described from Pakistan from higher levels of lower Eocene (Warraich et al., 2000); however, our findings of this species above this zone are most probably due to transportation/reworking. In the younger samples *G. imitata* and *I. albeari* are also found along with *G. pseudomenardii*, all sporadically and in small numbers, and are suspected to be transported/reworked/resedimented as well. These two species are widely reported to have their HOD near that of *G. pseudomenardii*, and are minor but consistent components of *G. pseudomenardii* Zone.

The presence of the index taxon, along with the two taxa mentioned in the previous paragraph in the lowest 10 samples is clear and there are no *G. pseudomenardii* in sample GT-11 which is the first sample of the next biozone. Furthermore, appearance of *M. subbotinae* in GT-10 signals the approach of HOD for *G. pseudomenardii* (see discussion on stratigraphic distribution of *M. subbotinae* on page 133).

Stratigraphic distribution: From the sample GT-1 to GT-10

Age: 56.5–55.9Ma (Berggren & Pearson, 2005); late Thanetian (late Paleocene)

2.2.3.2 *Morozovella subbotinae* Zone

Definition: This is a third taxon interval zone defined by the interval between HOD of *G. pseudomenardii* and the LOD of *A. sibiyaensis*; *M. subbotinae* is the index fossil for the zone.

Author: Defined for the first time in this study.

Remarks: This zone is prominent as the uppermost biozone of Paleocene. This zone is correlatable with lower part of Zone *G. velascoensis* of Bolli (1957), Zone *M. velascoensis* of Toumarkine and Luterbacher (1985), P5 and P6a of Berggren & Miller (1988), lower part of *M. aequa* Zone of Canudo and Molina (1992), Zone P5 of Berggren et al. (1995); similar to Zone P5 of Blow (1979) and *I. laevigata* Zone of Arenillas and Molina (1996); equivalent to the sum of *M. aequa*, *M. marginodentata* and *M. berggreni* Subzones; and the same with Zone P5a of Pardo et al. (1999) and Speijer et al. (2000), and Subzone P5 of Berggren & Pearson (2005) (Figure 28).

The major components of this zone are *A. soldadoensis*, *A. nitida*, *A. esnaensis*, *M. aequa*, *M. subbotinae*, *M. acuta*, *I. tadjikistanensis*, *S. velascoensis*, *S. patagonica* and *S. triangularis*.

The latest Paleocene is characterized by peripherally ornamented Morozovellids in the tropical regions, especially *M. velascoensis* is a distinctive species and widely used as index (see Figure 26). However, the material from Haymana yielded no peripherally ornamented Morozovellids, which is not an uncommon phenomenon according to Toumarkine and Luterbacher (1985) even for rich assemblages from tropical and subtropical regions; in such a case they propose recognition of their *Morozovella velascoensis* Zone (between HO of *G. pseudomenardii* and HO of *M. velascoensis*; correlative to *M. subbotinae*, *A. sibaiaensis* and *P. wilcoxensis* Zones of this work) based on co-occurrence of *M. acuta* and *A. soldadoensis*. The two taxa are prominent elements of the zone. Moreover, Canudo and Molina (1992) also stress the rarity of *M. velascoensis* in their study area (Zumaya, northern Spain) and in similar latitudes, and choose *M. aequa* as their index fossil for the interval between HO of *P. pseudomenardii* and LO of *P. wilcoxensis*.

In the absence of *M. velascoensis*, the author chooses to name this biozone via one of the dominant Morozovellid species: *M. subbotinae*, which also has a LOD just below the lower boundary of related biozone.

Stratigraphic distribution: From GT-11 to GT-17.675

Age: 55.9–55.5 Ma (Berggren & Pearson, 2005); latest Thanetian (latest Paleocene)

2.2.3.3 *Acarinina sibiyaensis* Zone

Definition: This is a lowest occurrence zone defined by the interval between LOD of *A. sibiyaensis* and LOD of *Pseudohastigerina wilcoxensis*.

Author: Molina et al. (1999)

Remarks: This zone was first described by Molina et al. (1999) with the same name, as the interval between LO of *A. sibiyaensis* and LO of *P. wilcoxensis*. It is correlatable with middle part of *G. velascoensis* Zone of Bolli (1957), *M. velascoensis* Zone of Toumarkine and Luterbacher (1985), P6a of Berggren and Miller (1988), P5 of Berggren et al. 1995; and bottom part of *M. velascoensis* Zone Arenillas and Molina (1996) and P5b of Pardo et al. (1999); and is the same with Zone P5b of Speijer (2000) and Zone E1 by Berggren & Pearson (2005) (Figure 28).

Planktonic foraminiferal assemblage that dominates this zone is very similar to that of the previous ones, with quadrate Acarininids (*A. wilcoxensis*, *A. pseudotopilensis*) in higher amounts than that of rounded ones. The important point is in the changing relative abundances of different groups: Acarininids increase in number (up to 55%) and Subbotinids decrease (down to 15%), which is an expected artifact at the initiation of the PETM (see section 3.2 for changes in relative abundance).

This biozone was proved stratigraphically important and started to be used only recently although two of the so-called excursion taxa were already defined in 1966 (El Naggar, 1966). In 1996, Kelly et al. introduced *M. allisonensis* (formal description in Kelly et al., 1998) from CIE of Allison Guyot (ODP in Pacific) for the first time. With the discovery of short ranged foraminifera existed during the PETM, this zone became important and started to be used as a P/E boundary criterion. The debate among researchers on which species to be accepted as the index remains unsolved while more short ranging species are being reported around the globe: e.g. *A. multicamerata* (Guasti & Speijer, 2008) and *M. rajasthanensis* (Warraich et al., 2000)).

The position of the BFE and the initiation of CIE relative to these planktonic foraminiferal bioevents are also being investigated with high resolution.

Stratigraphic distribution: From GT-17.75 to GT-20.5

Age: 55.5–55.35 Ma (Berggren & Pearson, 2005); earliest Ypresian (earliest Eocene)

2.2.3.4 *Pseudohastigerina wilcoxensis* Zone

Definition: This is a lowest occurrence zone defined by the interval from the LOD of *P. wilcoxensis* and top of measured section.

Author: Molina et al. (1999)

Remarks: This zone was first described by Molina et al. (1999) with the same name, as the interval between LO of *P. wilcoxensis* and HO of *M. velascoensis*. It is correlatable with, mid part of *G. (A) wilcoxensis berggreni* Zone of Blow (1979); top part of *G. velascoensis* Zone of Bolli (1957), *M. velascoensis* Zones of Toumarkine and Luterbacher (1985) and Arenillas and Molina (1996), P6a of Berggren and Miller (1988), P5 of Berggren et al. (1995), P5b of Pardo et al. (1999); and is the same interval with P5c of Speijer et al. (2000) and Zone E2 of Berggren and Pearson (2005) (Figure 28).

Upper boundary of these correlative zones are mostly drawn by HO of *M. velascoensis*, which is then followed by an upper biozone (for example E3 of Berggren and Pearson, 2005) ranging up to LO of *M. formosa*. In this study, in the absence of *M. velascoensis*, the upper boundary of this zone can only be drawn with species with HOs close to that of *M. velascoensis*, such as *M. passionensis*, *M. apantesma*, *M. occlusa*, *M. acuta* and *S. velascoensis*. While *M. passionensis* is a species that was non-existent, and *M. apantesma*, *M. occlusa*, *M. acuta* were significantly rare, *S. velascoensis* was consistently found in the studied samples. Hence, the upper limit of the studied measured section is decided to remain in the *P. wilcoxensis* Zone.

Identification of *P. wilcoxensis* has been problematic not only for the studied samples, but also in literature as well. As Speijer and Samir (1997) indicated the differentiation between *G. luxorensis* (as the ancestor of *P. wilcoxensis*) and *P. wilcoxensis* is rather difficult especially in the stratigraphically lower levels of range of *P. wilcoxensis*. The two taxa are differentiated based on their apertural characteristics: former being very low trochospiral with slightly asymmetrical aperture, and the latter being planispiral with symmetrical aperture that also opens on the spiral side. Speijer and Samir (1997a) argue that in the lower levels the smaller specimens (pre-adult) of *P. wilcoxensis* show a *luxorensis*-type aperture, hence the difference can only be observed in the later stages of ontogenetic development.

Another problem in identification of *P. wilcoxensis* is due to preservation conditions. The *Globanomalina* and *Pseudohastigerina* genera possess a smooth, normal perforate wall texture which may be more prone to dissolution than that of e.g. highly pustulose Acarininids. The specimens of these genera are generally found with a certain amount of sediment covering the umbilicus and the apertural area, or with a dissolved/peeled/broken wall that creates problems in observation of the aperture. For this purpose, all specimens of *G. luxorensis* and *P. wilcoxensis* from the counted aliquot were monitored with SEM imagery for healthier diagnostics.

Stratigraphic distribution: From GT-21 up to GT-26, the topmost sample.

Age: 55.35–54.5 Ma (Berggren & Pearson, 2005); earliest Ypresian (early Eocene)

CHAPTER 3

QUANTITATIVE ANALYSIS

For evaluation of abundance of taxa, a quantitative approach is essential. The process is simple enough as counting of a certain number of individuals from a known amount to give ratios of that taxon to all assemblage. The general practice in foraminiferal studies by washing method is counting of more than 300 specimens from adequate splits.

Buzas (1990) showed that for a taxon of more than 10% abundance in population, the error margin of abundance in a sample is similar to that of in the population, given the sample size is large enough, there calculated as 300 individuals. However, the taxa with <1% abundance in a population would only give realistic proportions in a much larger sample size. Hence, in this study approximately 300 individuals of planktonic foraminifera were collected from aliquot in order to understand the generic distribution and relative abundances.

3.1 Size Fraction

Quantitative analysis was performed by many researchers on upper Paleocene-lower Eocene units from several sieve sizes (Table 6). The size fractions used in these studies are as follows: minimum 38 μm , 63 μm , 106 μm , and 125 μm .

Table 6: Reference table for recent quantitative planktonic foraminiferal analyses on Paleocene-Eocene units. Size: sieve size studied; S/G: counted taxonomical rank, Species or Genus

Reference	Total specimens counted	Size (μm)	S/G
Lu&Keller, 1995	~300	>106	S
Lu et al., 1998	~300	>106	S
Molina et al., 1999	>300	>63	G
Warraich&Nishi, 2003	200-300	>63	S
Petrizzo, 2007	300-400	>125	S
	300-400	>38	S
Luciani et al., 2007	~300	>63	S
Molina, 2015	>300	>63	S
Orabi&Hassan, 2015	~300	>63	G
El-Dawy et al., 2016	~300	>63	G

Petrizzo (2007) studied two nearby ODP cores from two different size fractions (>125 and >38 μm) in order to evaluate the role of size fraction in relative abundance, and concluded that >125 μm fraction counts, although avoid juveniles as intended, underestimate the abundance of smaller species.

The majority of the studies appear to have been conducted from a minimum 63 μm sieve size (Table 6) (Molina et al., 1999; Warraich & Nishi, 2003; Luciani et al., 2007; Molina, 2015; Orabi & Hassan, 2015; El-Dawy et al., 2016), which is why the first attempt on quantitative analysis was also conducted from a minimum 63 μm fraction. The investigation of >63 μm fraction, although not impossible, was not an

easy task due to high number of pre-adult and reworked/transported forms. Hence, a second counting study with the $>106\ \mu\text{m}$ was conducted for healthier results.

$>106\ \mu\text{m}$ fraction was the choice of Lu and Keller (1995) and Lu et al. (1998). They preferred this size fraction because it included the maximum number of species within the confidence limits provided by the sample size of 300. The abundance of the small sized species was found to be smaller than 1% with a $>150\ \mu\text{m}$ fraction, and the abundance of the large sized species was found to be smaller than 1% with a $63\ \mu\text{m}$ fraction. The author agrees with this view due to observations made on the $63\ \mu\text{m}$ and $106\ \mu\text{m}$ fractions, large specimens were very few in number. The calculation in Table 7 shows the estimated number of planktonic foraminifer individuals in 1 gr of unwashed rock in >63 and $>106\ \mu\text{m}$ fractions, and the ratio. This number represents the number of planktonic foraminifera individuals that would be collected from a 1 g rock sample; calculated by direct proportion to the studied aliquots. This calculation includes the division of the number of individuals (e.g. 334 for GT-26- $>106\ \mu\text{m}$) with the split ratio (e.g. 1/64 for the same sample) which makes up the number of planktonic foraminifera individuals in the total 100 g of rock which was washed (e.g. 21376); divided by 100, the number of planktonic foraminifera in 1 g of rock is acquired (213.8). On average, the $>106\ \mu\text{m}$ fraction withholds only the 15% of the whole assemblage above $63\ \mu\text{m}$.

In the $>63\ \mu\text{m}$ fraction the majority of the planktonic foraminiferal specimens are small sized ($<106\ \mu\text{m}$) and many of them are too small to correctly assign to a species. Most of these small individuals are thought as pre-adult forms since pre-adult morphologies are not consistent with the adult equivalents (Brummer et al., 1986). During the life of planktonic foraminifera, they grow in several phases, for example Globigerinidae goes through proloculus, juvenile, neanic, adult and terminal stages, all with remarkably different morphological characteristics (Brummer et al., 1987). Caromel et al. (2015) provided series of figures obtained by Synchrotron radiation X-ray tomographic microscopy (SRXTM), belonging to extant planktonic

Table 7: Estimated number of planktonic foraminifera individuals in 1 gr of rock.

Sample #	#individuals in 1 gr of rock		106/63 ratio
	>63 μm	>106 μm	
GT- 26	1505.3	213.8	0.14
GT- 25	267.5	26.8	0.10
GT- 24	957.4	186.9	0.20
GT- 23	519.7	67.8	0.13
GT- 22	942.1	81.0	0.09
GT- 21	1408.0	172.8	0.12
GT- 20	1397.8	150.4	0.11
GT- 19	791.0	91.2	0.12
GT- 18	1666.6	219.5	0.13
GT- 17	2667.5	325.1	0.12
GT- 16	478.7	26.2	0.05
GT- 15	1648.6	259.2	0.16
GT- 14	1564.2	276.5	0.18
GT- 13	2109.4	439.0	0.21
GT- 12	1525.8	112.0	0.07
GT- 11	1029.1	71.4	0.07
GT- 10	1792.0	167.7	0.09
GT- 9	965.1	41.9	0.04
GT- 8	1525.8	184.3	0.12
GT- 7	1438.7	117.8	0.08
GT- 6	100.2	61.0	0.61
GT- 5	634.9	79.8	0.13
GT- 4	205.4	122.9	0.60
GT- 3	1213.4	108.5	0.09
GT- 2	1149.4	134.4	0.12
GT- 1	1285.1	118.7	0.09
Average:	1184.2	148.3	0.15

foraminiferal species. Chamber by chamber the specimen was modeled in order to develop an ontogenic continuation; it is clear that the juvenile and neanic stages of specimens are quite different from the adult phase. The difference is interpreted as different ecological and metabolic constraints during growth.

An example of this morphological change is given by Brummer et al. (1986) in Figure 30 in three species. *Globigerinoides ruber* (Figure 30-1), a spinose species; *Neogloboquadrina dutertrei* (Figure 30-2), a non-spinose, cancellate species; and *Globigerinita juvenilis* (Figure 30-3), a non-spinose, pustulose species, all show marked differences between pre-adult and adult phases such as wall texture, position of aperture, shape and number of chambers.

Species are defined and limited by adult morphological properties. In the studied samples of the Haymana Basin, a large ratio of the planktonic foraminifera in >63 μm fraction is small and does not have species' characteristics, therefore, they are labeled as pre-adult, and when possible, they are assigned to a genus according to wall type and other gross morphological features of the genus. As stated above, through the development of the test, the morphology changes remarkably, which makes these generic assignments inherently unreliable with high error margin.

The number of foraminifera assigned as pre-adult changes from about ~50-80% in >63 μm fraction (Figure 31), and about 20% of these are left undefined, not assigned to a genus. Similar pre-adult forms were encountered in >106 μm fraction as well; yet, in very small numbers (under 1%), making the larger fraction a more reliable medium to study.

The >63 μm fraction is preferred vastly in the literature for elimination of underestimation of species that are generally found to be in minute size, such as serial group and several Globanomaliniids. The difference of abundance in serial group between two fractions is evident, in average 12% in smaller fraction (Figure 31) to 1 % in larger fraction (Figure 32, Figure 33). Globanomaliniids also show a

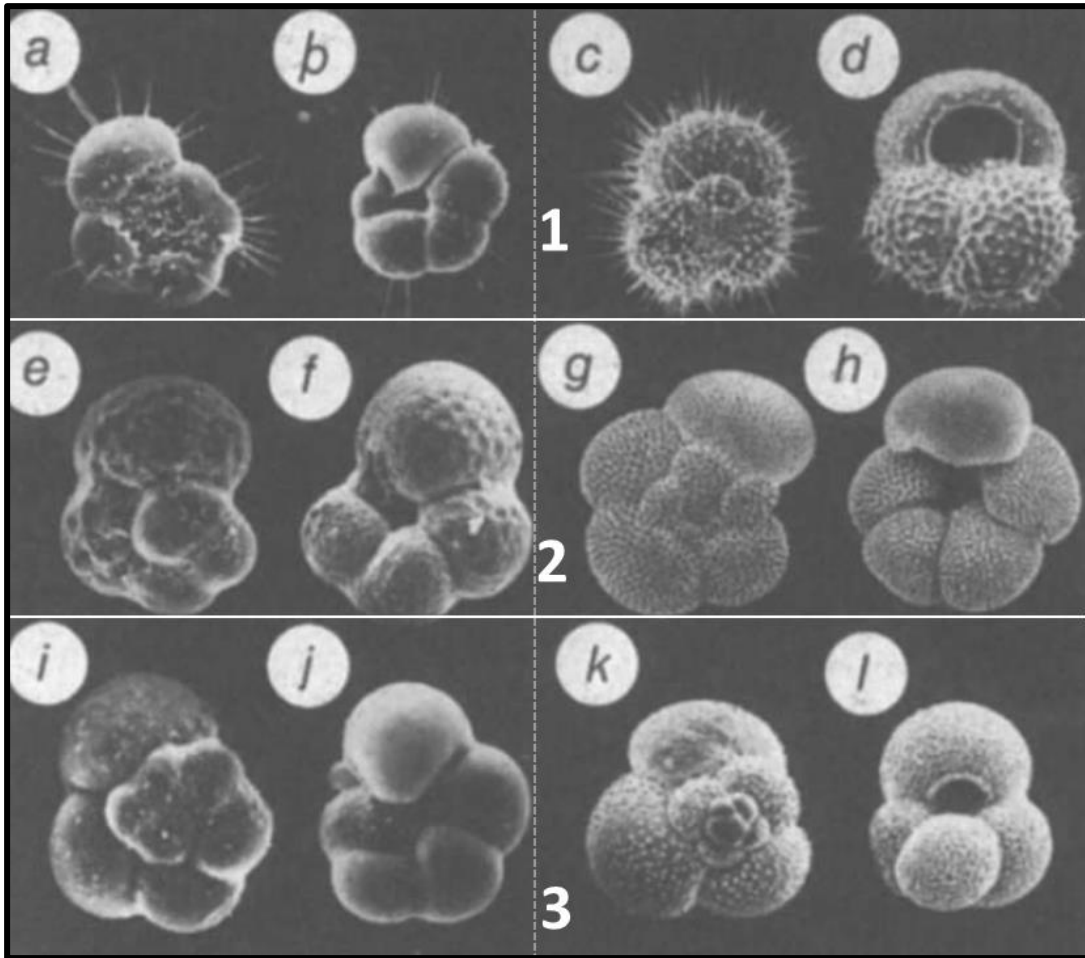


Figure 30: SEM images of pre-adult (left-hand side) and adult (right-hand side) specimens of 1. *Globigerinoides ruber* (magnification: a: x449, b: x469, c: x120, d: x147), 2. *Neogloboquadrina dutertrei* (e: x290, f: x304, g: x74, h: x62), 3. *Globigerininita juvenilis* (i: x653, j: x805, k: x143, l: x136) (taken from Brummer et al., 1986)

distinct abundance difference: in average 10 % in smaller fraction (Figure 31), 5% in larger fraction (Figure 32, Figure 33). However, in this case, elimination of large number of unreliably defined pre-adult forms at the expense of minute groups is favored.

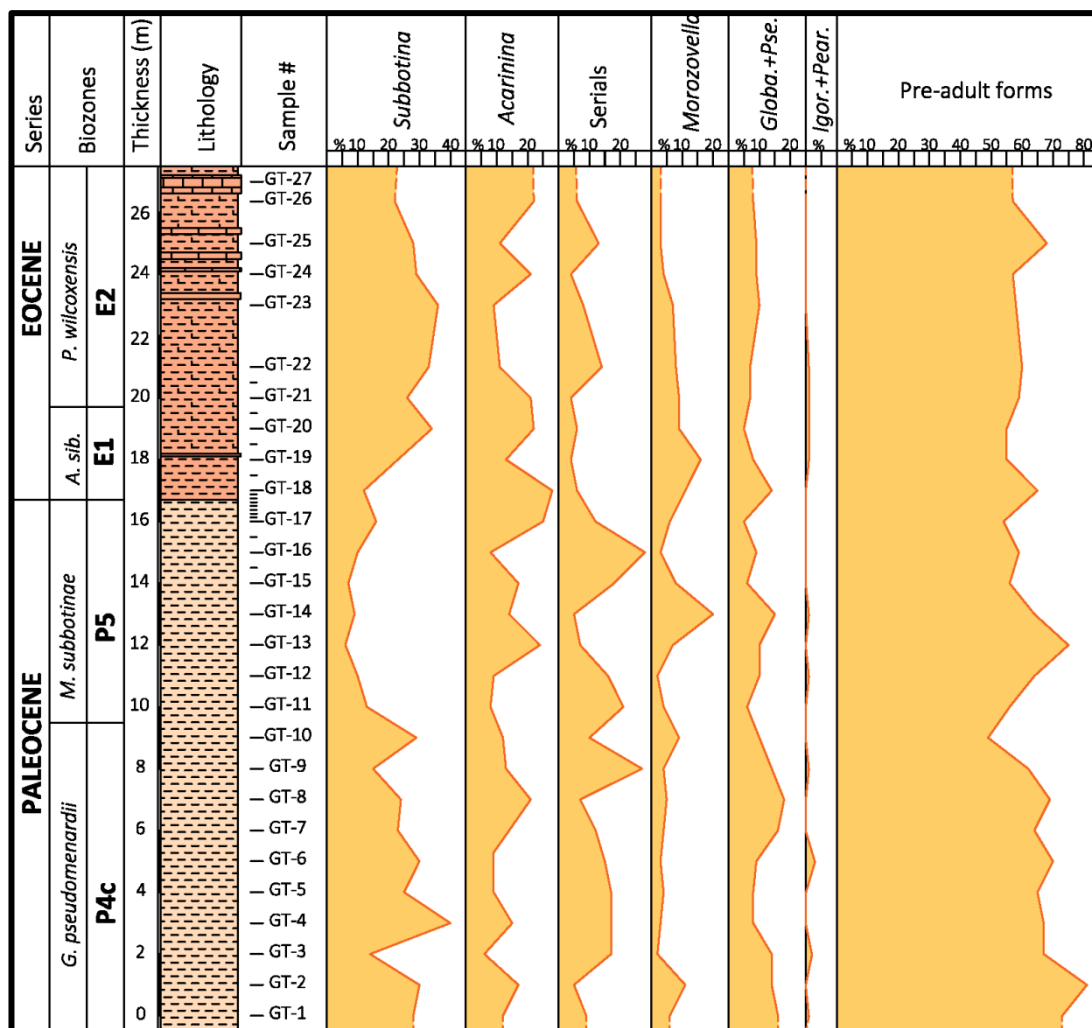


Figure 31: Relative abundance of genera and groups for >63 μm fraction. *Globa.*: *Globanomalina*, *Pse.*: *Pseudohastigerina*, *Igor.*: *Igorina*, *Pear.*: *Pearsonites*

Figure 33 provides a means of comparison of two studied size fractions. The trends are similar in general with remarkably higher numbers achieved in >106 μm fraction for *Acarinina* (in average 40% in larger fraction, 15% in smaller fraction), and a small but observable difference for *Morozovella* as well (in average 12% in larger fraction, 7% in smaller fraction). These two genera are generally found to be in larger sizes in literature, and here, their higher abundance in the larger fraction is

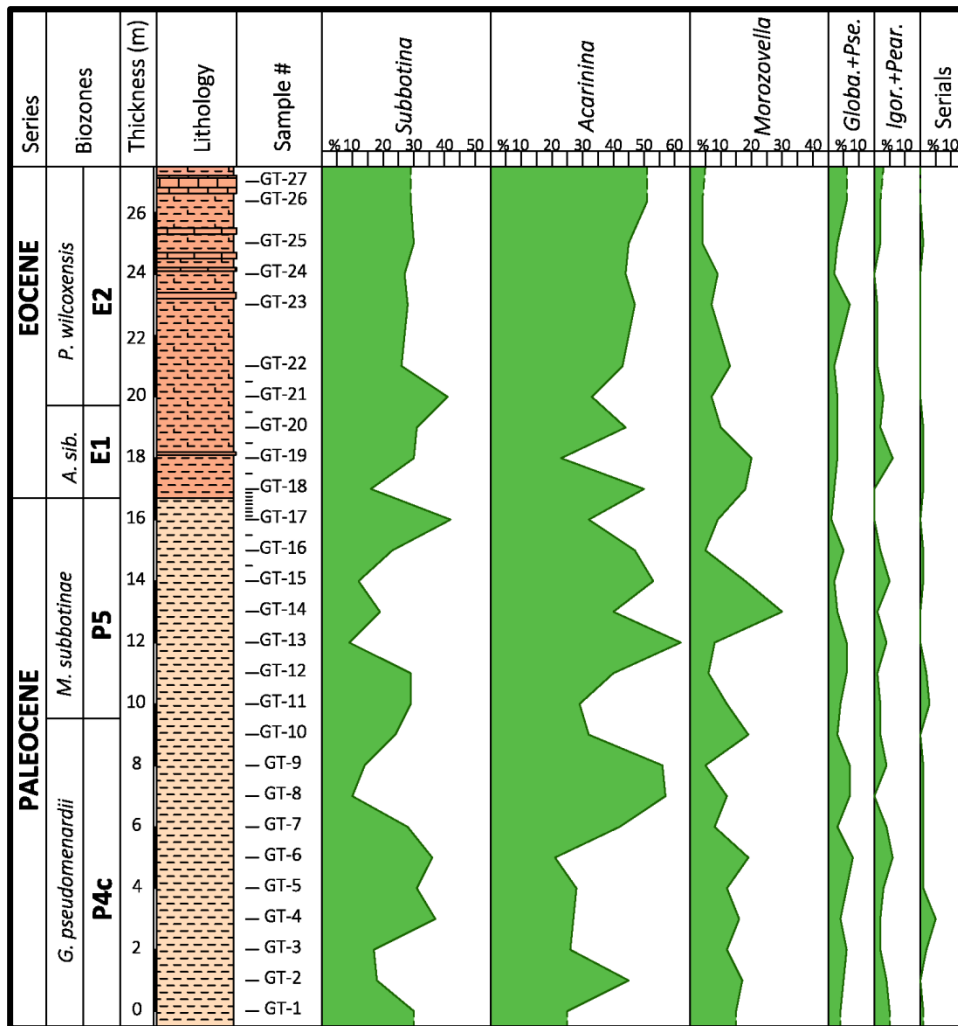


Figure 32: Relative abundance of genera and groups for >106 μm fraction, abbreviations as in Figure 31

expected and understandable. Moreover, a part of the number of undetermined specimens in >63 μm fraction can be attributed to these genera, and are maybe pre-adult forms of them.

A certain amount of the undetermined specimens in >63 μm fraction comes from the reworked/transported minute specimens of Cretaceous and lower Paleocene. The distinction of these forms from *in situ* specimens was not possible by means of their preservational states or kind of infill material. In >106 μm fraction the undetermined

specimens are significantly less, the large reworked/transported material are easier to detect and cast out, which is one of the reasons why undetermined specimen number is less. It appears reworking/transportation process brought a significant number of fossils into continuing deposition, in all sizes, but more of smaller than larger fraction.

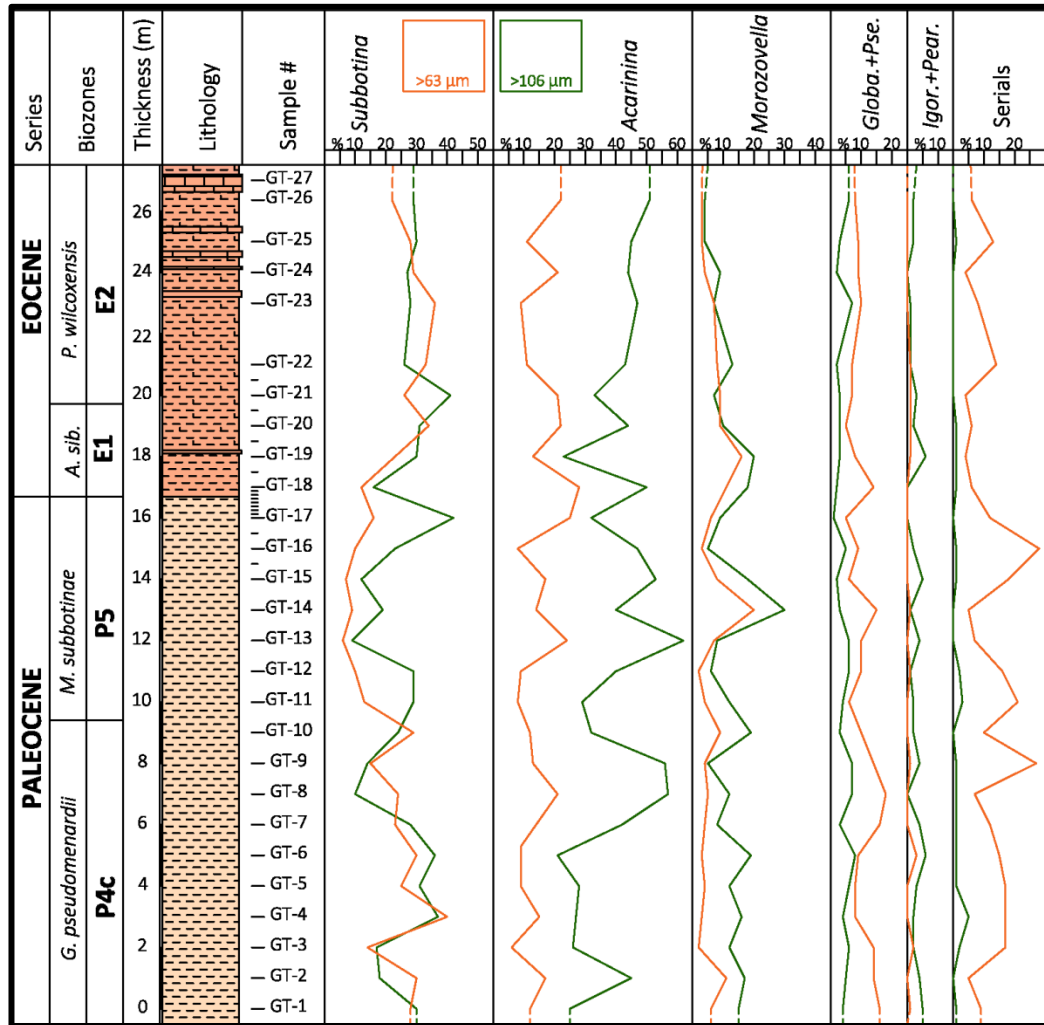


Figure 33: Comparison of relative abundance of genera and groups for >63 μm, and >106 μm fraction, abbreviations as in Figure 31

3.2 Relative Abundance

According to Berggren and Ouda (2003a) the relative abundances of groups interchange during the PETM in Dababiya, with decreasing *Morozovella*, and increasing *Acarinina* and *Subbotina* abundances. Tropical-subtropical Mv group Morozovellids (*Morozovella velascoensis* group: *M. velascoensis*, *M. passionensis*, *M. acuta*) and temperate-subtropical Ms group Morozovellids (*Morozovella subbotinae* group: *M. aequa*, *M. apantesma*, *M. gracilis*, *M. subbotinae*) also show different abundances throughout the CIE. Mv/Ms ratio is higher than pre-CIE assemblages in the lower part of CIE, increasing steadily, then decreases towards the top to the pre-CIE values. The change in dominant Morozovellid group could not be observed in the Haymana Basin, since Mv group is absent, apart from *M. acuta* which is only present in Paleocene assemblages and for a small amount.

Guasti and Speijer (2007) present planktonic foraminiferal relative abundances through several sections in Egypt and Jordan, where most abundant genera are *Subbotina*, *Acarinina* and *Morozovella*. A decrease in *Morozovella* and *Subbotina*, and increase in *Acarinina* is evident in all sections during the PETM (Zone P5b).

Zili (2013) reported that in Tunisia *Acarinina* abundance show two peaks in the Zone E1, oldest being associated with increase in agglutinated benthic foraminifera and LO of *A. sibaiyaensis*.

In Zumaya (Spain) Morozovellids are reported to be the dominant group, yet they decrease in abundance while Acarininids increase during the CIE (Zili et al., 2009; Molina et al., 1999). Alamedilla (Spain) and Possagno (Italy) show a similar trend with high dominance of Morozovellids except for the PETM (Molina et al., 1999).

The Possagno section shows a rather different lower Eocene, though. The Morozovellid turnover is not as complete in this section, as in the Spain sections, it does not reach the pre-PETM values (>40% pre-PETM, <20% post-PETM) (Molina et al., 1999). A later study on nearby Forada section by Luciani et al. (2007) shows a rather more equally shared abundance between genera *Morozovella* and *Acarinina* pre-PETM, a sharp increase in Acarininid abundance with CIE accompanied with a

sharp decrease in Subbotinids and Morozovellids, a rapid comeback and stabilization of Morozovellids but a gradual increase in Subbotinids while a gradual decrease in Acarininids (Figure 34).

In contrast to western and southern Tethyan sites, Kaurtakapy section in Kazakhstan shows very little abundance of Morozovellids, while *Acarinina* and *Subbotina* are in much higher numbers (Figure 35) (Pardo, Keller, & Oberhansli, 1999). Similar to Kaurtakapy, in the western and central Black Sea Region the abundance of Subbotinids and very limited number of Morozovellids are reported from the P/E sections (Güray, 2014).

To summarize, it is evident that genera *Acarinina*, *Morozovella* and *Subbotina* are the dominant groups of late Paleocene-early Eocene assemblages. Acarininids are of similar abundance in all sites; however, Morozovellids dominate the lower latitude sites while Subbotinids dominate the higher latitude sites. In all latitudes Igorinids, Globanomalinids and serial groups hold a much lower percentage of the assemblage.

Morozovella, *Acarinina* and *Subbotina* genera are the dominant ones in the Haymana Basin, too (Figure 31, Figure 32, and Figure 33). The >106 µm fraction counts show that *Acarinina* (40%) is the most abundant genus of all, followed by *Subbotina* (25%), and *Morozovella* (12% in average). Although all groups show fluctuations, Subbotinids seem to maintain the same average along the measured section, while Morozovellids decrease, and Acarininids increase in abundance (Figure 32).

During the PETM (here estimated by lowest occurrence of *Acarinina sibaiyaensis*) a decrease in Subbotinids are observed, coupled with increase in Acarininids and Morozovellids (Figure 31, Figure 32, and Figure 33). The increase in *Acarinina* is reported from all around Tethys (e.g. Pardo et al., 1999; Molina et al., 1999; Luciani et al., 2007; Zili et al., 2009), correlated with occurrence of excursion taxa (Figure 34, Figure 35). The species diversity is also increased during the PETM (such as Figure 35), due to evolution of Eocene species, including excursion taxa. Apart from PFET, several Acarininids and Morozovellids first occur in upper Zone P5, increasing the number of species until the end of Zone E2, when several Morozovellids went extinct.

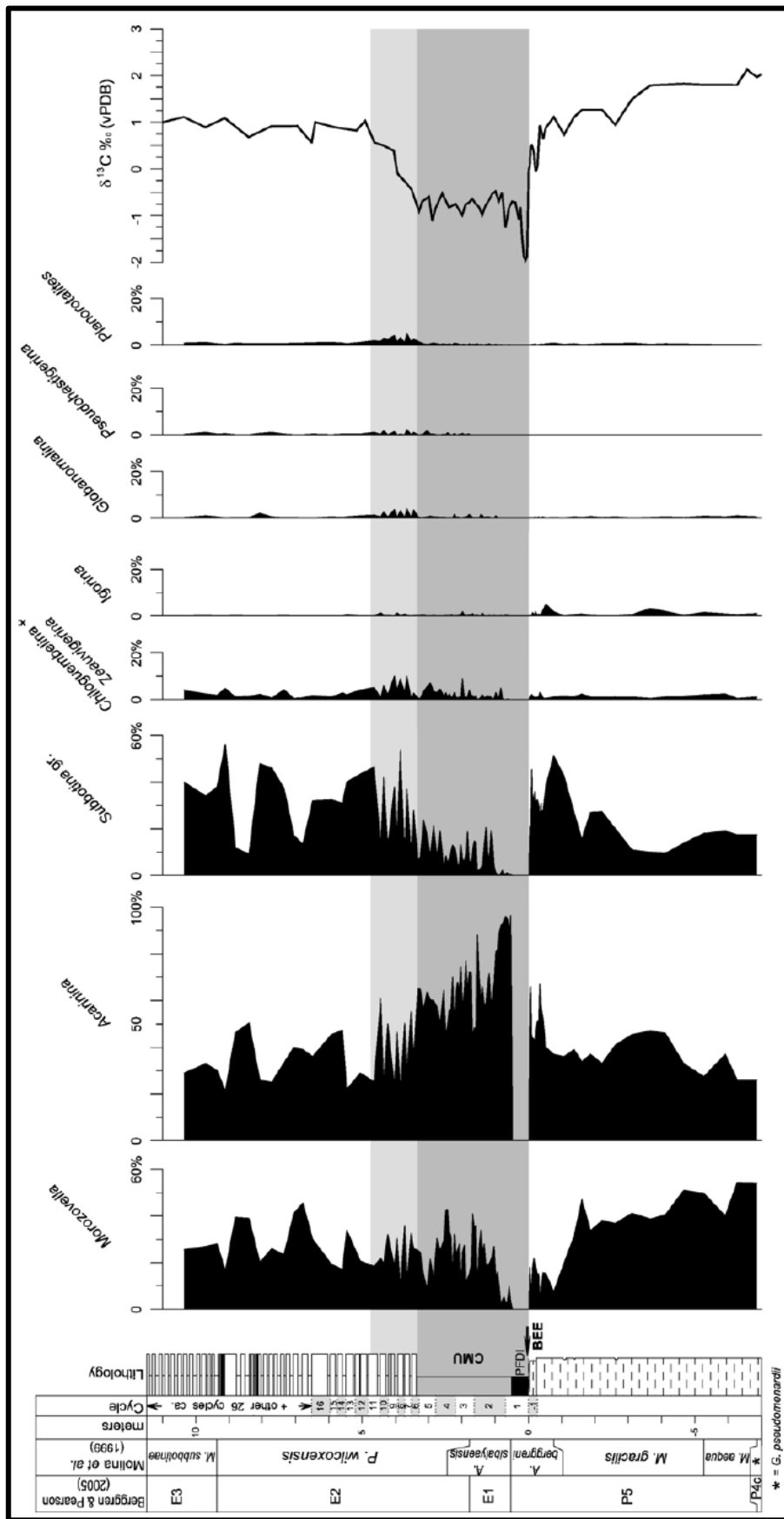


Figure 34: Relative abundances of planktonic foraminifera groups and carbon isotope plotted against lithology and biostratigraphy. *Subbotina* gr. stands for genera *Subbotina*, *Parasubbotina* and *Globorotaloides* of similar habitat. (Luciani et al., 2007)

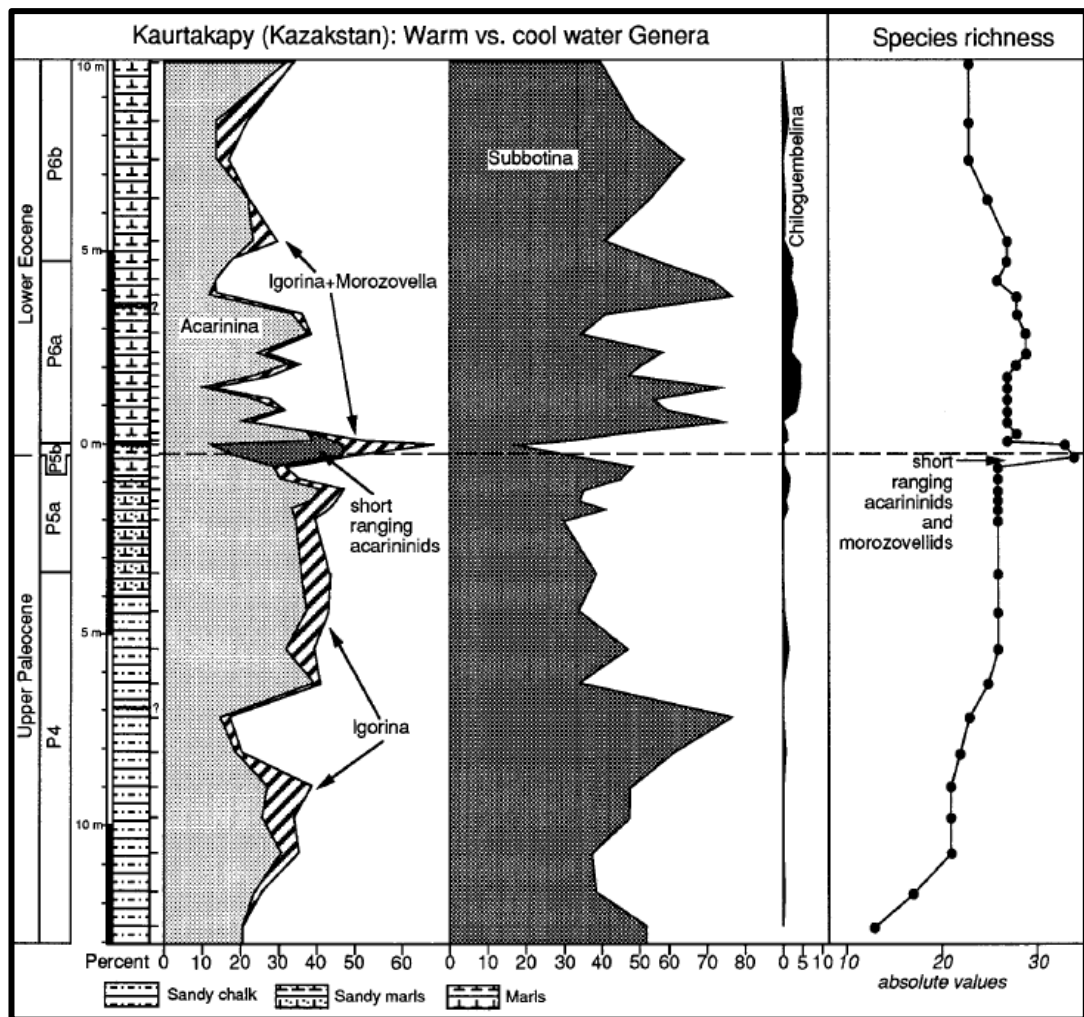


Figure 35: Relative abundances and diversity in Kaurtakapy section (Kazakstan) (Pardo et al., 1999)

3.3 Paleoenvironmental Interpretations

Planktonic foraminifera adapt to different habitats with respect to several characteristics. Employing symbiotic algae, for example, obliges the life in photic zone. Those that employ the algae are mostly muricate forms like *Acarinina* and *Morozovella*, which live in the surface waters, where subsequent amount of light penetrates the water. *Subbotina*, and many other Globigerinidae, and the smooth-walled groups prefer a deeper, cooler habitat, they live in the thermocline

layer. Microperforate group (mainly the serials) prefer eutrophic, near shelf settings (Figure 36, Figure 37) (BouDagher-Fadel, 2015; Luciani et al., 2010; Pearson et al., 2006).

The relative abundances of these groups reflect the paleoenvironmental settings. For example, along the tropical, near equatorial settings, the muricate group flourishes and sustains a high abundance, while thermocline dwellers stay in small numbers (such as in southern Tethyan sites (Zili et al., 2009; Molina et al., 1999). In contrast, in temperate regions, thermocline dwellers are more dominant than those need the high angle sunlight (Pardo et al., 1999; Güray, 2014).

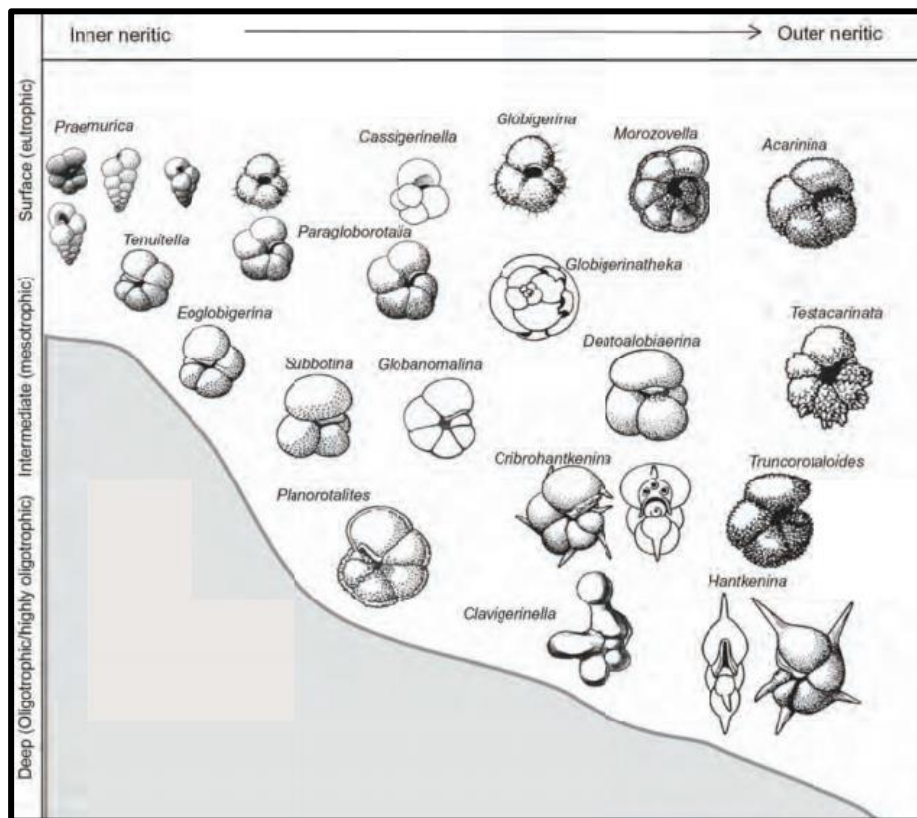


Figure 36: Distribution of the Paleogene planktonic foraminifera in the neritic environment (BouDagher-Fadel, 2015)

The stable isotopic studies of surface water dweller genera reflect their photosymbiotic nature, and even the earliest representatives share this isotopic signal pointing that the photosymbiotic character is inherited from a common ancestor (Quillévéré et al., 2001). Moreover, even morphologically different groups of species of same genus show different isotopic values facilitating the idea of layered inhabitancy of the mixed layer, for example earlier low trochospiral Acarininids show a lower position in the mixed layer (Guasti & Speijer, 2007). These differences are attributed to employment of different symbionts by different groups (Guasti & Speijer, 2007). Photosymbiotic groups (*Acarinina*, *Morozovella*, and *Igorina*) responded differently throughout the PETM, the common aspect from all around Tethys is the rapid increase in Acarininid abundance. According to Guasti and Speijer (2007) the Acarininid excursion species preferred deeper, cooler parts of the mixed layer like their early low trochospiral counterparts, as well as *M. subbotinae* lineage. The other groups may have been diminished due to incompatible algae with the rapidly introduced warming.

The studied samples from the Haymana basin show similar trends. When the >106 µm fraction is examined it is obvious that the majority of the assemblage belongs to the muricate, surface dwelling group (Figure 32), dominant one being the *Acarinina* (40%). *Subbotina* (25%) is also in high abundance. BouDagher-Fadel's paleogeographic reconstruction puts the study area in the temperate region (Figure 38) along with other northern Tethyan sites such as Kaurtakapy and Forada, where the *Subbotina* abundance is also high.

The low-oxygen tolerant, meso- to eutrophic serial taxa are reported to be slightly increased in abundance in the upper parts and after the PETM and linked with high nutrient (high influx), low-oxygen conditions after the PETM (e.g. Pardo et al., 1999; Luciani et al., 2007; D'Haenens et al., 2012). Such a trend is not observed in the studied samples. Serial groups are low in abundance in >106 µm fraction (average 1%; however significantly higher in >63 µm fraction with average 12%, probably due to high amount of reworked/transported, and pre-adult serial taxa).

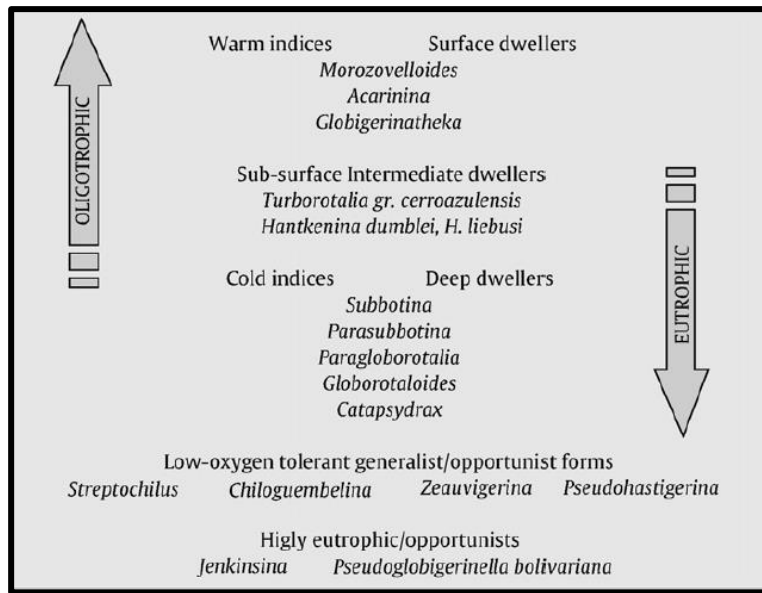


Figure 37: Simplified scheme showing the inferred life strategies and depth ranking of middle Eocene planktonic foraminifera (Luciani, et al., 2010)

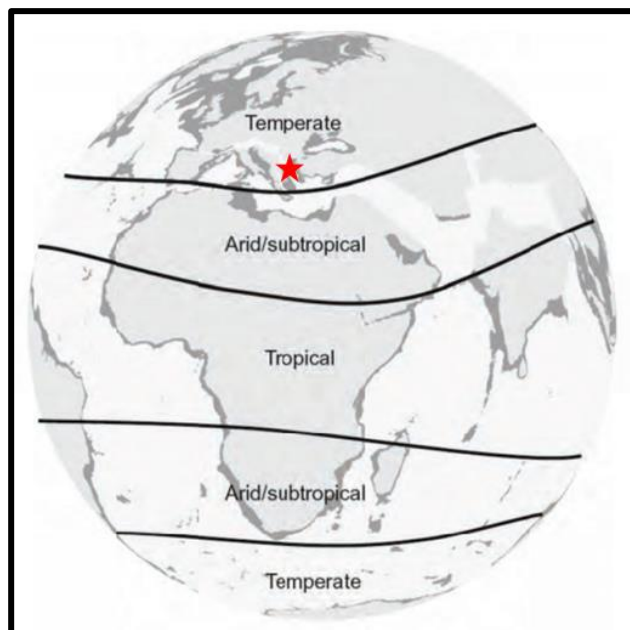


Figure 38: Climate zones in Paleogene (BouDagher-Fadel, 2015), red star indicates the estimated position of the measured section

It is evident that the signals of warm indices (*Acarinina* and *Morozovella* according to Luciani et al., 2010) are somewhat parallel to each other, while *Subbotina* (cold index) works opposite to the former (Figure 32). Not at only the boundary, also at other levels this alternation of signals is observed. Throughout the section the relative abundances are not stable, and dominance is interchanged between warm indices and cold indices, and the controlling factor may be not only the temperature changes, but also tectonic activities, weathering rates, sediment influx and nutrient availability. A higher sediment influx paralleled by high nutrient availability may be the key to increased Subbotinid numbers while hampering the survival of light dependent forms by blurring the water. A flyschoidal turbiditic deposit, such as the studied Eskipolath Formation, may have provided such an environment with alternating phases of pelagic and distal-turbiditic deposits.

There are three distinct poorly preserved intervals in the samples and they coincide with the Subbotinid dominance intervals: GT-4-6, 10-12, 15-16. In these intervals also match with high amount of serials (in $>63 \mu\text{m}$) and more reworked large individuals (in $>106 \mu\text{m}$), and fewer estimated number of planktonic foraminifera individuals in 1 gr of rock (Table 7). These intervals may be thought as high sedimentary influx, and nutrient rich turbiditic deposits, while the intervening phases, rich in warm indices, could be the quieter, pelagic sedimentation.

CHAPTER 4

THE PALEOCENE/EOCENE BOUNDARY AND THE PALEOCENE-EOCENE THERMAL MAXIMUM

Paleocene/Eocene boundary (ca. 56Ma) is marked with a global warming event, called Paleocene-Eocene Thermal Maximum (PETM) with effects recorded both on marine and on terrestrial biota and sediments. This warming event, which is relatively short lived (~200ky), is the largest in the last 65 million years. The warming is associated with a negative shift in carbon isotopic composition, which in turn decreased the depth of lysocline and produced a carbon dissolution interval in deep marine settings, proven by thin clayey layers. Despite all the works, still there is no consensus on the driving mechanism of the event, but some hypotheses are produced.

Great importance is put on the research of Paleocene-Eocene Thermal Maximum (PETM) due to its similarity to today's global climate change. Studies focus on its isotopic record, duration, tempo, biotic record, possible triggers and mechanisms, and aftermath in order to interpret the ongoing climate change. Below, some of these topics are briefly summarized, with a focus on planktonic foraminiferal studies.

4.1 Stable Oxygen and Carbon Isotopic Record

Stable isotopes are used for paleoenvironmental interpretations, especially the temperature change. Although also affected by other factors like salinity, to translate oxygen isotope readings into temperature change is done widely.

One of the first stable isotopic measurements were done from Deep Sea Drilling Project (DSDP) sites to investigate the temperature changes during Cenozoic; however, the sampling interval was too large to obtain a detailed signal, only a general trend in oxygen and carbon isotope was observed (Shackleton & Kennett, 1975; Shackleton et al., 1984). Later on, studies started to focus on the P/E boundary and correlation of the oxygen isotopic signal with the BFE showing a rapid temperature increase in both surface (tested by planktonic foraminifera) and bottom (tested by benthic foraminifera) waters (e.g. Kennett and Stott, 1991). With monospecific analyses, a more precise and a more complete record of the water column during the PETM were produced (e.g. Bornemann et al., 2014). Figure 39 shows the four species' oxygen isotopic compositions for three selected depth zones: *Nutellides truempyi* for bottom waters, *Subbotina patagonica* for thermocline waters and *Morozovella subbotinae* and *Acaranina soldadoensis* for surface waters. All show the same negative shift at P/E boundary (yellow line), towards a lower isotopic composition, translated to ~4°C increase.

The primary studies on carbon isotopes (Shackleton & Kennett, 1975; Shackleton et al., 1984) were done along with oxygen studies, for paleotemperature estimations. Although a negative excursion in carbon isotopes were recorded, not much importance were assigned until a significant negative carbon isotope excursion in foraminifera is first identified (and correlated with many previous works) by Stott et al. (1990a) in an ocean drilling project. The two planktonic foraminifera genera used for analysis (*Acaranina* and *Subbotina*) gave parallel signals with a negative excursion at the vicinity of the Paleocene/Eocene boundary, which is also correlated with the BFE by the authors. In Figure 39, the work by Bornemann et al. (2014) shows a good example of the CIE, and the parallel signals (~2‰ decrease) produced by different species of foraminifera, from different depth zones. Later on, the carbon

isotopic signal was studied in many other sites (in on-land marine successions, deep sea drilling projects and in terrestrial successions) and it was seen that it is a global signal which is also correlative with many biotic events; the signal then was chosen to be the P/E boundary criteria, and the base of Ypresian stage (Aubry, 2000; Aubry, 2002; Aubry et al., 2007).

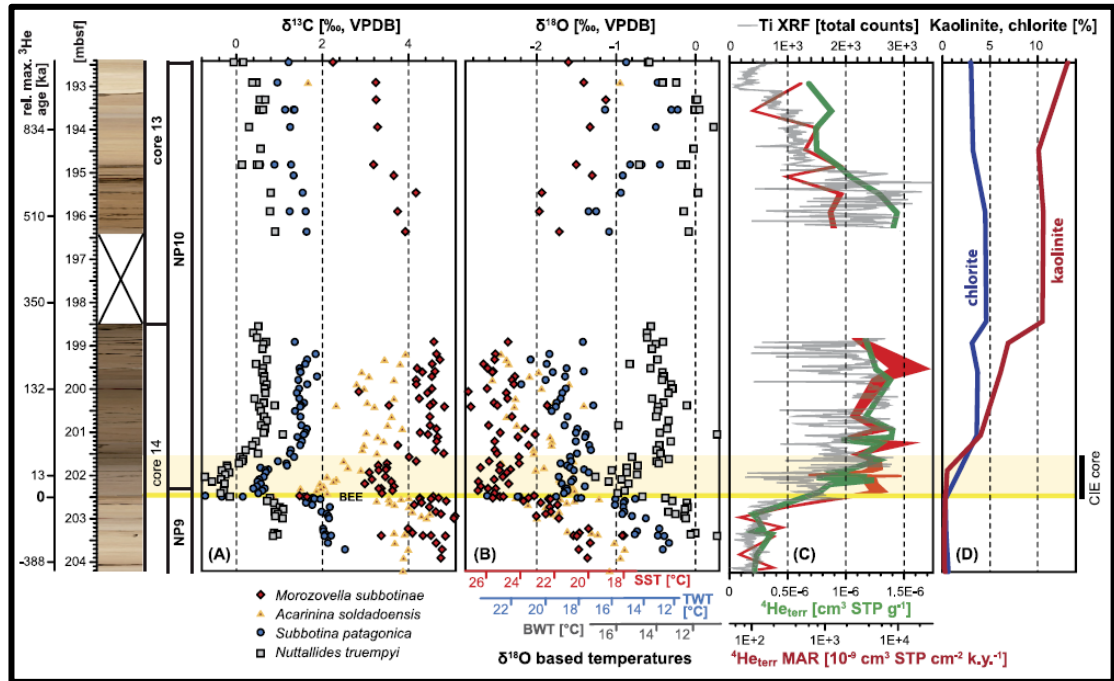


Figure 39: Geochemical data from DSDP Site 401 from Bay of Biscay, North Atlantic. Isotopic studies conducted on benthic foraminifera species *Nuttallides truempyi* (for bottom water conditions), and planktonic foraminifera species *Subbotina patagonica* (for thermocline waters), *Morozovella subbotinae* and *Acarinina soldadoensis* (for surface water conditions) (Bornemann et al. 2014)

The negative CIE is the record of decreased ratio of heavy carbon isotope (^{13}C), occurring due to increased addition of isotopically light carbon (^{12}C) into the ocean atmosphere system. Added carbon results in large concentrations of CO_2 in the oceans, increasing acidity (Zachos et al., 2005). With increased acidity, lysocline, the

depth after which carbonate dissolution rate increases drastically, moves to a shallower level, which leaves a larger surface area on the ocean floor open to carbonate dissolution. Reported in many deep marine sections worldwide, the dissolution interval creates a hiatus, a clay rich layer or a layer barren of calcareous fossils, for example in Dababiya the CIE is recorded in a noncalcareous shale unit (Aubry et al., 2007).

The stable isotope analyses are done on either the bulk rock, or individual fossil samples, and are reliable given that no secondary processes took place like recrystallization or cement fill of the foraminifera. All of the specimens from the Haymana Basin were filled with probably secondary material, which makes them difficult to study in this respect.

4.2 Hypotheses

A globally correlated CIE is of much importance with respect to time equivalence and linkage between terrestrial and marine environments. However, the cause for such a drop in ^{13}C concentrations, meaning the injection of a great amount of isotopically light carbon (^{12}C rich), is still being evaluated. The experienced warming being the result of added carbon has already been refuted by several studies (e.g. Bornemann et al. 2014 and Slujis et al. 2007), yet the reason behind the warming and the source of light carbon injection is still being debated.

Higgins and Schrag (2006) evaluated some theories related to the carbon source without taking into account that warming begun prior to CIE, trying to link the carbon to the warmth. According to their calculations (neglecting the effects of carbon speciation and CaCO_3 dissolution) in order to reach the excursion amount of approximately 2.5 ‰ drop in $\delta^{13}\text{C}$ in modern oceans requires the addition of “40,000 Gt of carbon from the mantle ($\delta^{13}\text{C}=-5\text{‰}$), 4,500 Gt of carbon as organic carbon ($\delta^{13}\text{C}=-25\text{‰}$), or 1,700 Gt of carbon as methane ($\delta^{13}\text{C}=-60\text{‰}$). the majority of the studies (e.g. Slujis et al. 2007) emphasize the methane release from the sea floor

sediments as the most probable carbon source because it the minimum mass required, yet according to Higgins and Schrag (2006) “even the total collapse of the hydrate reservoir at the Paleocene/Eocene boundary would be insufficient to explain the carbon isotope excursion” due to the prediction of small global methane hydrate reservoir in the Paleocene (<2,000Gt C, Buffett and Archer, 2004). Moreover, the warming (if was due to carbon addition) due to methane would not last more than 1000 years, which means the warming of PETM assumed to last between 50 to 200 ky was mostly due to elevated CO₂ levels in the atmosphere rather than methane (Higgins and Schrag, 2006).

The organic carbon hypothesis requires the addition of 4,500 Gt of carbon which would result in a 6°C increase in global temperature which is approximated for the PETM. One hypothesis is the emplacement of North Atlantic igneous province which releases thermogenic methane from organic-rich sediments while metamorphosing the strata. However, there has been no record of large depletion in organic carbon in the metamorphosed zone, neither the oxidation of organic carbon is expected to happen and end in the brief time window of the PETM. (Higgins and Schrag, 2006)

Another organic carbon hypothesis is the wild-fires allowed by a drier climate near Paleocene/Eocene boundary that oxidizes extensive Paleocene peatlands (“warm climates and large epicontinental seaways favored the development of extensive peatlands in the Paleocene”). However, this theory requires an increase in the aridity at all latitudes, involving all peatlands that were geographically separated, prior to the the PETM (Higgins and Schrag, 2006).

Epicontinental seaways with restricted circulation withhold another large carbon source potential in which organic carbon was deposited under suboxic or anoxic conditions during the Mesozoic and early Cenozoic. According to Buffett and Archer (2004), drying up of such water bodies resulting in their desiccation and exposure to well oxygenated meteoric waters is the most likely alternative of all mentioned before. “Assuming that N90% of the sedimentary organic carbon is oxidized, we calculate that the desiccation of the upper 30 m of a $\sim 3 \times 10^6$ km² epicontinental sea

with 5 wt.% organic carbon would add 5000 Gt C to the ocean–atmosphere system.” Moreover, the time frame of the carbon release is also fitting to the PETM CIE peak duration (taken as 10-30 ky) if the soil respiration rates are comparable to the modern rates. (Higgins and Schrag, 2006).

A case of comet impact as a triggering mechanism for the warming was evaluated by Kent et al. (2003) and was reinforced by Schaller et al. (2016) by discovery of impact ejecta (glass spherules and shocked quartz) at the P/E boundary on the Atlantic margin. No glass spherules or shocked quartz were recovered from the examined samples in this study.

4.3 Marine Micropaleontological Record

In the shallow marine setting the Thanetian-Ilerdian boundary is coincident with a turnover (Larger Foraminifera Turnover-LTF), which is temporally equivalent with the PETM, synchronizing larger foraminiferal stage Ilerdian with base of standardized earliest Eocene stage Ypresian (Pujalte, et al., 2009). The P/E boundary is coincident with SBZ4/5 boundary (Figure 40).

In the deep marine setting the P/E boundary is marked by

- Calcareous nannofossil *Rhombaster – Discoaster araneus* (RD) assemblage
- Acme of dinoflagellate *Apectodinium*
- Benthic Foraminifera Extinction Event (BFE)
- Planktonic Foraminifera Excursion Taxa (PFET)

A transient diversification marks the calcareous nannofossil assemblages, a so called *Rhombaster – Discoaster araneus* (RD) assemblage develops abundantly with the PETM, a group comprising several short-range taxa with unusual structure (Aubry, 1996, 1998a). The NP9/10 boundary coincides with the P/E boundary (Figure 40).

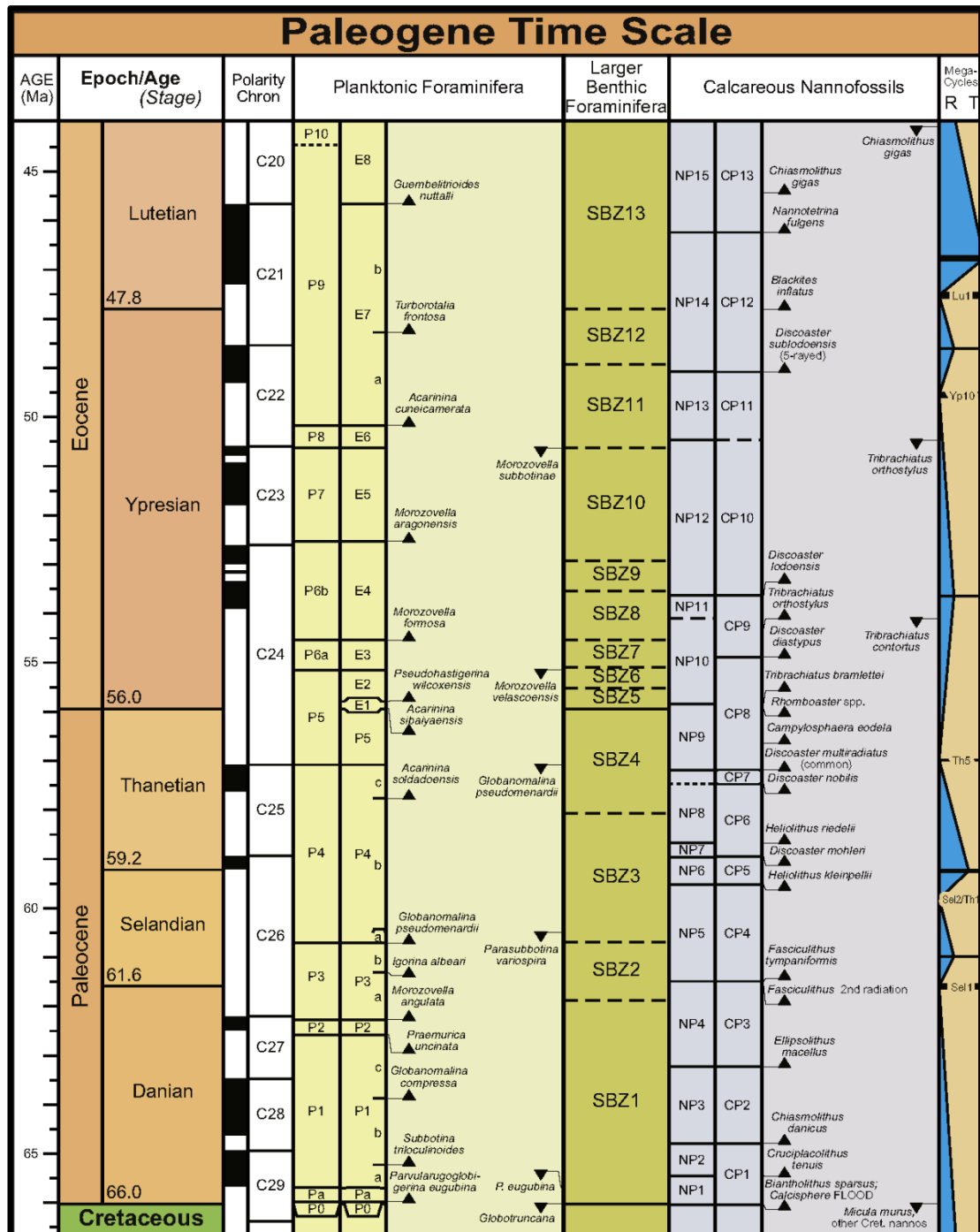


Figure 40: Correlation of planktonic foraminiferal, shallow benthic foraminiferal, and calcareous nannofossil biostratigraphy along Paleocene and lower Eocene (Vandenberghe et al., 2012)

One of the several *Apectodinium* acmes, a low diversity assemblage with abundant *Apectodinium* spp. coincide with the CIE, with *A. augustum* occurring near the P/E (Bujak and Brinkhuis, 1998; Crouch et al., 2003) (Figure 41).

Benthic foraminifera of deep water habitats experienced an extinction event that wiped out about 50% of this group while favoring *Nuttallides*-dominated assemblage and diminishing *Stensioeina*-dominated assemblage. Different depth zones show different characteristics in assemblage: down to the upper bathyal, the assemblage called Midway-type fauna is more abundant, however, from upper bathyal to deeper settings a Velasco-type fauna is dominant. Different depth zones were apparently affected differently from the PETM. Both experienced the extinction yet the shallower zone losing less than the deeper zone. Main extinction taxa are: *Stensioeina beccariiformis*, *Angulogavelinella avnimelechi*, *Coryphostoma midwayensis*, *Aragonia velascoensis*, *A. ouzzanensis*, *Gavelinella hyphalus*, *G. rubiginosus* (= *G. danica*), *G. velascoensis*, *Neoflabellina jarvis*, *N. semireticulata*, *Neoeponides hillebrandti*, *Osangularia velascoensis*, *Pullenia coryelli*, *Tritaxia midwayensis*, *Anomalinoides praeacutus* and *Cibicidoides succedens*. (Aubry et al., 2007).

Planktonic foraminifera experienced a diversification among genera *Acarinina* and *Morozovella* and produced a number of short range taxa that existed only during the warmth period (Kelly et al., 1996; Kelly et al., 1998). The P/E boundary coincides with the P5/E1 zonal boundary where these short ranged taxa first appear (Pearson et al., 2006) (Figure 40).

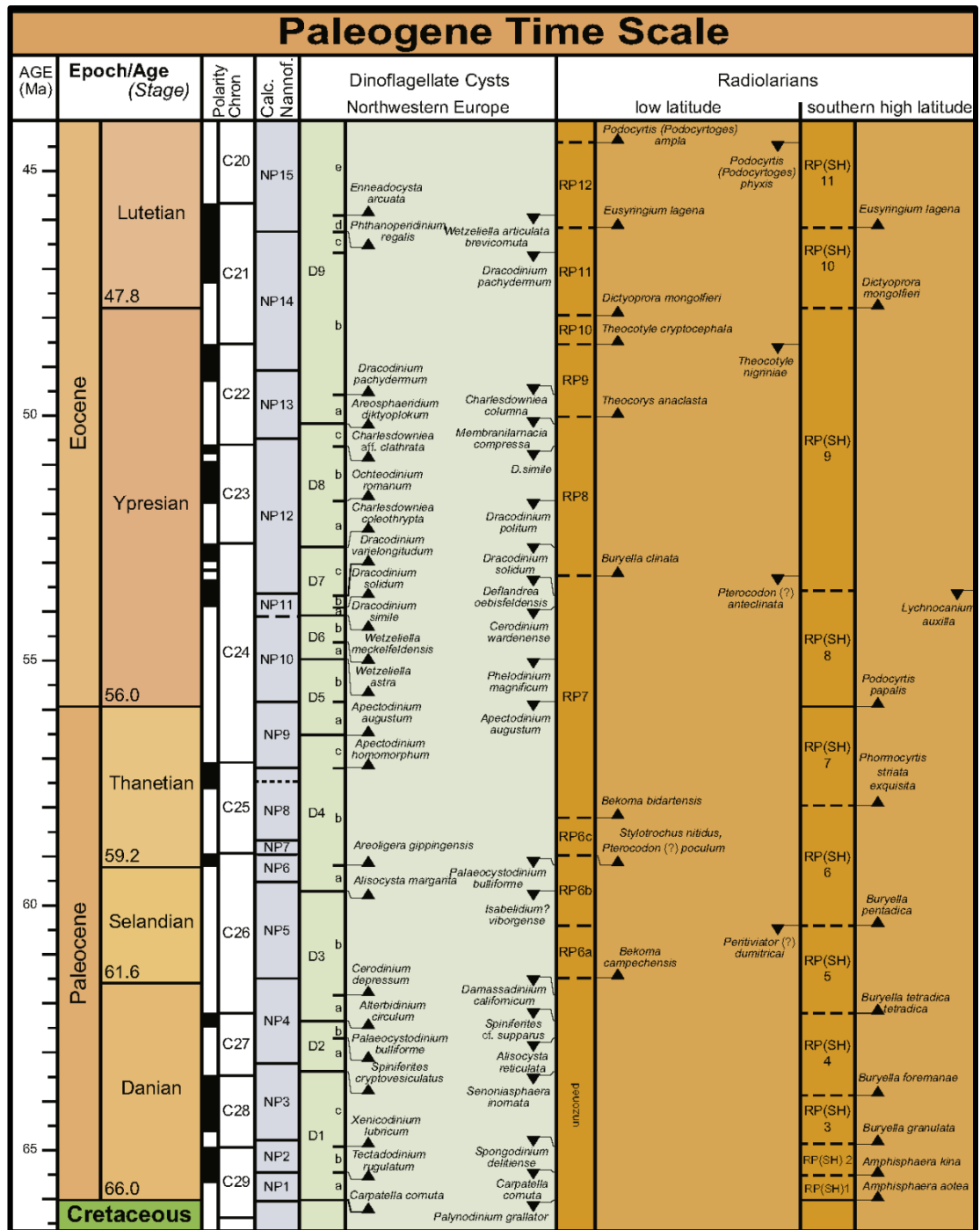


Figure 41: Dinoflagellate cysts and radiolarian biostratigraphy along Paleocene and lower Eocene (Vandenberghé et al., 2012)

4.5 Planktonic Foraminiferal Studies on the P/E Boundary and the PETM

The PETM is recorded in many marine outcrop and well sections around the globe, as compiled in McInerney and Wing (2011) as in Figure 43. The frequently studied Tethyan sites in terms of planktonic foraminifera are mapped in Figure 42, along with several ocean drilling locations. Here, several of these studies will be summarized.

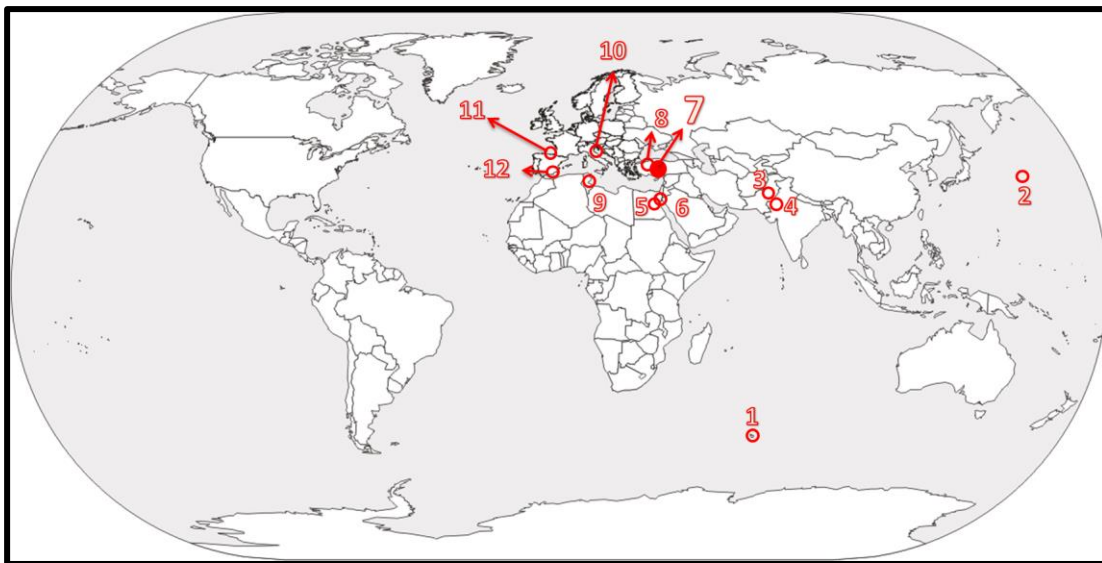


Figure 42: Several P/E planktonic foraminiferal investigation sites including the study area. ODP sites: 1. Kerguelen Island, 2. Shatsky Rise (Central Pacific). Tethyan sites: 3. Pakistan, 4. India, 5. Dababiya (Egypt), 6. Sinai (Egypt), 7. Haymana, Central Anatolia (Turkey), 8. Western Black Sea Region (Turkey), 9. Tunisia, 10. Forada, Possagno (Italy), 11. Zumaya (Spain), 12. Alamedilla, Caravaca (Spain), 13: Kaurtakapy (Kazakhstan)

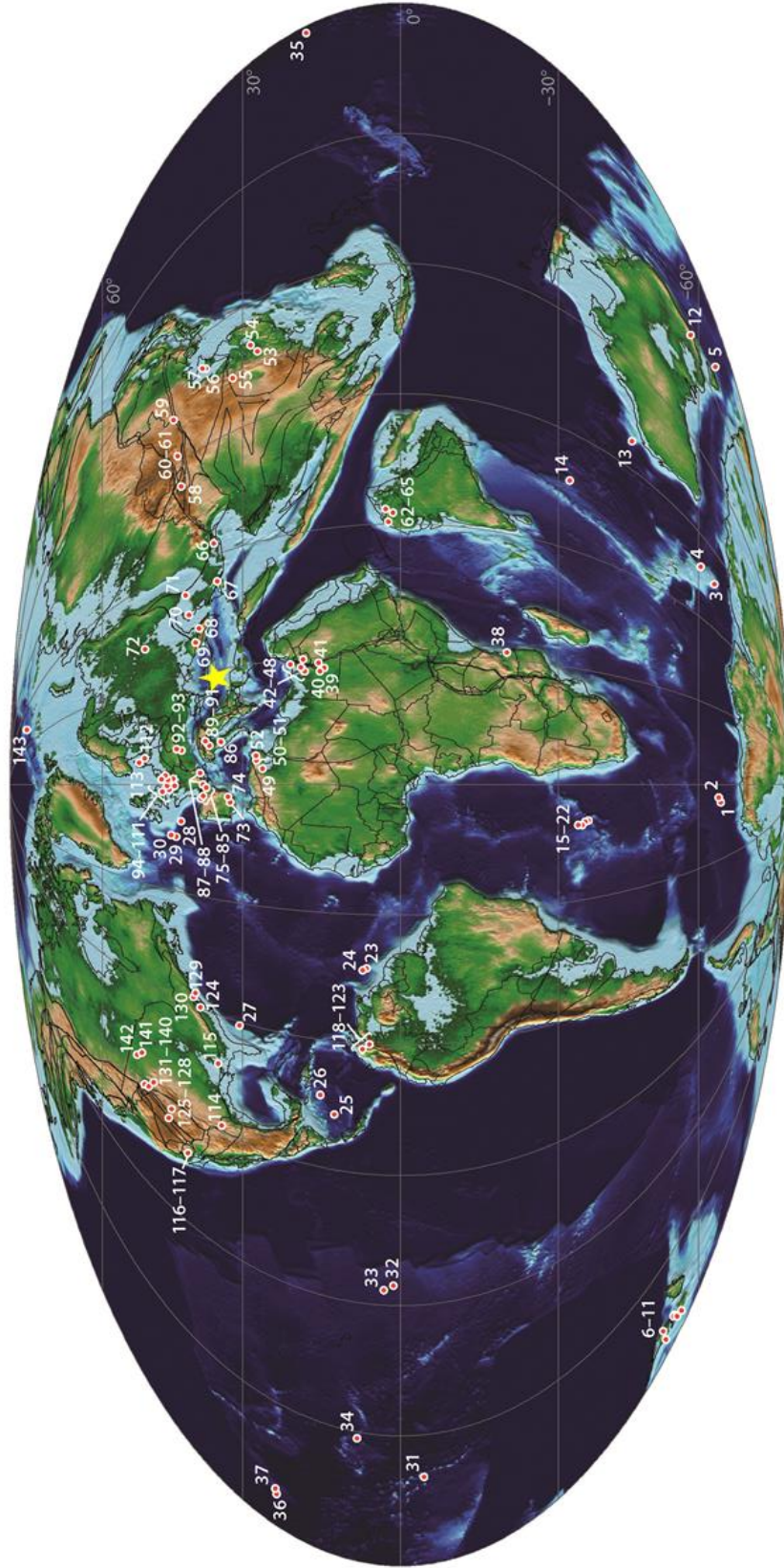


Figure 43: Paleogeographic map for 56 Ma with marine and continental sites of studied P/E boundary interval indicated with red circles, as compiled by McInerney and Wing (2011) (site numbers are keyed in Supplemental Table 1 of McInerney and Wing, 2011). Yellow star indicates approximate position of study area.

Ocean drilling programs such as ODP and DSDP provided a vast amount of data into the P/E planktonic foraminiferal studies, especially by testing the geographic distribution of taxa. One of these sites is the Kerguelen Plateau (Figure 42-1) in the southern hemisphere higher latitudes. Berggren (1992) placed the P/E boundary at the HO of *M. velascoensis*. One other site is Shatsky Rise in Pacific, a low latitudinal site, studied by Petrizzo et al. (2007) showing the intersection *A. sibaiaensis* stratigraphic range and CIE peak interval, with BFE at the bottom. Zone E1 is about 15 cm in this condensed deep marine core.

The Dababiya Quarry Section in Egypt (Figure 42-5; Figure 44, Aubry et al., 2007) is the GSSP for the base of Ypresian, where the boundary is fixed at the bottom boundary of the Dababiya Quarry Member of Esna Formation, overlying the El Hanadi Member (light grey, massive, compact calcareous shale). The member starts with a noncalcareous shale unit (Bed 1) which is barren of planktonic foraminifera, continues with two phosphatic shale layers of different coprolites and phosphatic inclusion amounts (Beds 2 and 3), covered by a grey calcareous shale unit (Bed 4) and marly calcarenitic limestone (Bed 5), which is then overlain by the El-Mahmiya Member which is composed of monotonous, dark, clayey shale. Benthic foraminiferal extinction is given as a range from the base of Bed 1, up to in Bed 3 (Aubry et al., 2007). All three planktonic foraminifera excursion taxa (PFET: *A. sibaiaensis*, *A. africana*, *M. allisonensis*) are found in the Beds 2 to 5, hence putting LOD of *A. sibaiaensis* (base criterion of Zone E1) a 0.8 meters above the CIE. The total thickness of the Zone E1 in this succession of deep marine shales is about 2.2 meters. The entrance of *P. wilcoxensis* roughly corresponds to the end of CIE in Dababiya.

Many works had been carried out on southern Tethys deposits, around the northern part of Red Sea (Figure 42-5 and 6), several on Egyptian side, and several on Israeli side. A study carried out from many samples around that region is Speijer and Samir (1997), which recognized that benthic foraminiferal extinction (BFE) and CIE were

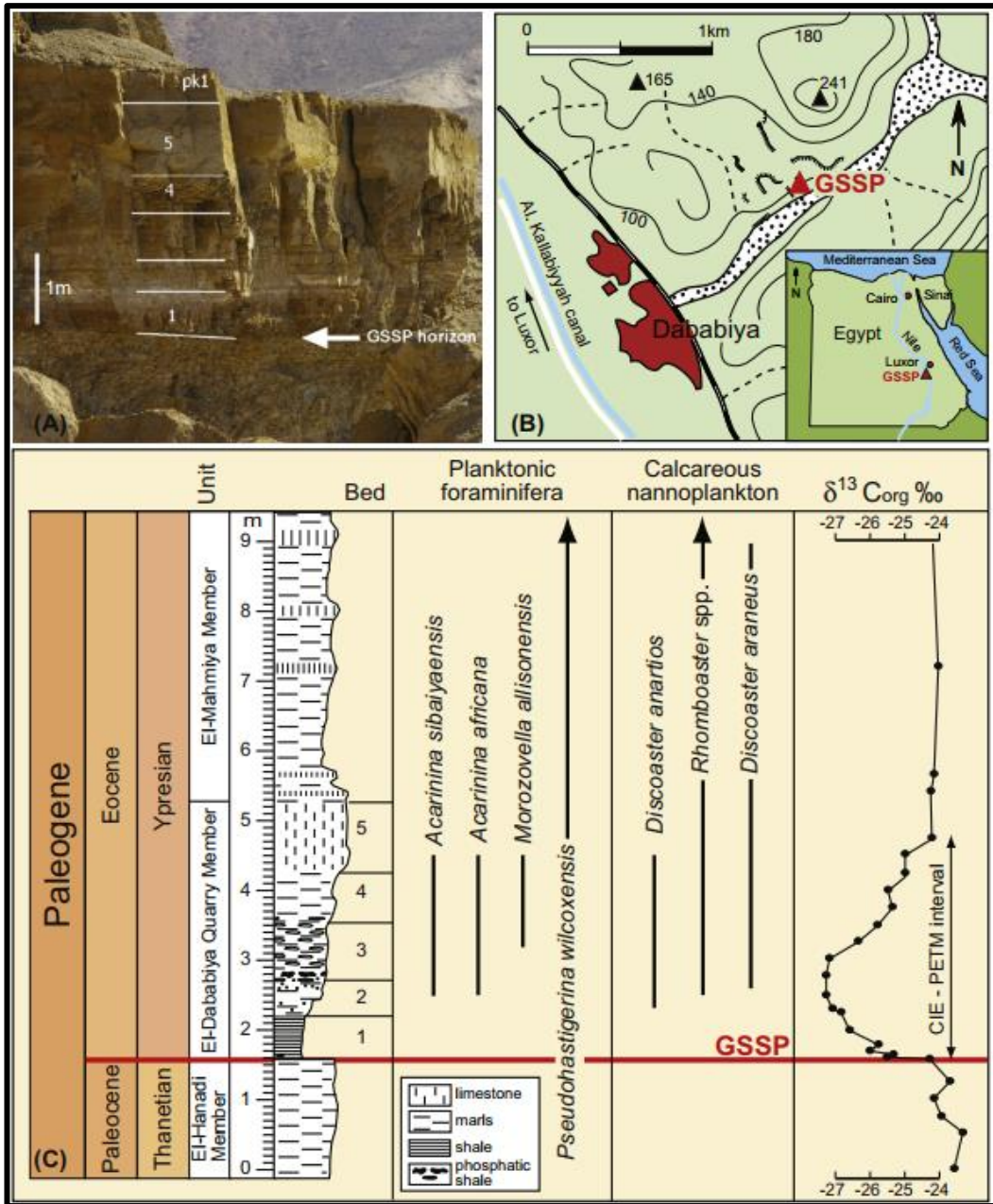


Figure 44: Base of the Ypresian Stage of the Paleogene System at Dababiya, Egypt (Vandenberghe et al., 2012)

close events, and proposed that the boundary should be at that restricted interval. They also found the LOD of *G. luxorensis* was at the same level with BFE, and declared it marker especially for the neritic deposits in which benthic foraminiferal turnover is not so prominent.

Another work in a similar setting is Speijer et al. (2000) and Guasti and Speijer (2007), where they propose a 3-fold zonation of the Zone P5 (of Berggren et al., 1995) with respect to *M. allisonensis*, a species observed at a short interval in the lower part of the CIE, but geographically restricted to lower latitudes. Moreover, they argue presence of excursion Acarininids as scattered in a rather long interval, and these species cannot be used as biostratigraphical markers. *M. allisonensis*, on the other hand, provides a better biostratigraphic resolution, and its absence in low to mid-latitudes should be interpreted as discontinuous sections.

Berggren and Ouda (2003a) provided a detailed study of Dababiya section where they provided an *A. sibaiaensis* biozone (Zone P5b) into a 3-fold zonation of Zone P5 of Berggren et al. (1995) (Figure 45). They acknowledged the three PFET and appointed their sporadic existence to preservational bias in phosphatic sediments. The temperature change throughout the CIE interval is further proven by the changes in relative abundances of several groups; increase in Acarininids at the initiation of the PETM showing the warming, and the increase in Subbotinids and decrease in Morozovellids through the top of the PETM, marking the cooling. Work of Berggren and Ouda (2003b) in a nearby section (Qreiya) shows similar results. The thickness of Zone P5b is given as 2.4 meters in Qreiya. The CIE interval roughly corresponds to the P5b Zone. This zonation scheme was renewed via a study of a corehole (Ouda et al., 2012) where Zone E1 was defined instead of P5b, with ~2,3 meters thickness.

Works in Darb Gaga and Gebel El Aguz (Kharga Oasis, Egypt, Figure 42-5) were carried out by Ouda et al. (2016a; 2016b). While in Darb Gaga the presence of excursion taxa is found within Bed 1 (barren in Dababiya section), the Gebel El Aguz section includes a hiatus corresponding to Bed 1, 2, and 3. Another work in Kharga Oasis is at Naqb Assiut section where the oldest three units of Eocene are also missing (El-Dawy et al., 2016).

Epoch	Rock unit	Lithology	Sample no. DBH	Biozone	Paleoecology	Paleontology	No of individuals 100gr.dr.	P/T%	Ac/Tp%	S/Tp%	M/Tp%	Mv/M%	Ms/M%	Bioevents	
Earliest Eocene	Esna 2 Dababiya Quarry Beds	[Lithology column]	5.5 5.0 4.75 4.5 4.25 4.0 3.75 3.5 3.25 3.0 2.75 2.5 2.25 2.0 1.75 1.5 1.25 1.0 0.75 0.5 0.25 0.0	P5c NP9b P5b	Post CIE interval Decreasing temperature Younger, low-oxygen, highly fossiliferous, calcareous phase Calcareous part Marly part Planktic foraminifera predominate, P/T >95% Abnormal faunal density Normal faunal density	Return to pre PETM faunal density but with higher P/T ratios Ac. wilcoxensis-bearing, subbotinid-rich and with low Mv:Ms ratios	None	393	75	31	42	22	37	63	LCO benthic foraminifera after the BFEE
								74969	95	54	21	24	52	42	
								22380	96	51	27	19	56	43	LO <i>Ps. wilcoxensis</i> Top CIE/PETM
								79740	98	51	12	36	61	35	HO <i>Ac. Sibaiyaensis</i>
								43465	97	56	2	41	70	26	LO foraminiferal flood
								4354	98	56	2	42	75	19	
								1283	97	66	6	27	91	8	
								1367	99	70	4	26	83	14	LO <i>Ac. pseudotopilensis</i> Reappearance of benthic foraminifera after the BFEE
								730	100	61	4	35	79	16	
								none							Only coprolites
								none							<i>Ac. sibaiyaensis</i>
								782	100	96	4	0.0	0.0		
none							LO <i>Ac. sibaiyaensis</i> & <i>D. araneus</i>								
none															
none															
none															
547	41	45	32	22	25	69	Base CIE/PETM=BFEE								
1795	82	26	30	40	45	50	LO <i>Ac. wilcoxensis</i>								
1668	73	29	23	47	47	49	LO <i>Ac. angulosa</i>								
479	51	17	35	38	74	12									
747	57	19	46	33	57	38									
1350	79	23	33	43	49	46	LO <i>Ig. broedermanni</i> & <i>Ac. esnaensis</i>								
2110	88	26	37	35	36	59									
Latest Paleocene	Esna 1	[Lithology column]	0	P5a NP9a	Pre CIE Increasing temperature Older, highly reducing, unfossiliferous clayey phase Maximum warming Middle, reducing, partially fossiliferous phosphatic phase No calcareous benthic foraminifera P/T=100%	calcareous shale of outer shelf environment, showing variable rates of aeration, and temperature fluctuation, with a tendency towards increasing water depth and decreasing oxygen upward (Sub)tropical foraminiferal association with variable P/T values, Mv:Ms ratios, and faunal densities with a tendency towards increasing P/T values upward No calcareous foraminifera only fish remains	547	41	45	32	22	25	69		
							1795	82	26	30	40	45	50		

Figure 45: Details of pre-, within, and post-CIE intervals in Dababiya (DBH section) (Berggren & Ouda, 2003a)

El-Nady (2005) presented a work in Sinai (Egypt) (Figure 42-6) delineating the P/E boundary at the top of *M. velascoensis* biozone, therefore the highest occurrence datum of *M. velascoensis*, along several sections. No isotopic study had been carried out, and the PFET were not recovered, however, the benthic extinction is marked within Zone P5. Another work in Sinai is by Orabi and Hassan (2015) where they presented a 3-fold P5 zonation as in Berggren and Ouda (2003a) and placed the P/E boundary at the LO of *A. sibaiyaensis*.

A section in northern Tunisia (Figure 42-9) is studied by Zili (2013) where upper Paleocene–lower Eocene successions are characterized by grey clays and marls. A ~10 meter E1 interval is marked in this study with the identification of *A. sibaiyaensis* and *M. allisonensis*.

The Indus Basin in Pakistan (Figure 42- 3) is studied in terms of the P/E boundary (Warraich et al., 2012), and due to the absence of excursion taxa, the boundary is estimated with a P5 Zone equivalent to that of Berggren et al. (1995). The boundary in the Indus Basin lays in a siltstone-limestone intercalation.

A study in the Jaisalmer Basin in India (Figure 42- 4) was studied by Kalia and Kinisto (2007), where the boundary was detected at the base of a clayey horizon inside a predominantly carbonate rock formation with occasional shale interlayers. A new excursion taxon was proposed occurring with the PFET: *M. rajasthanensis*.

The Ben Gurion section in Israel is studied by Lu et al. (1998) where the presence of excursion taxa was not detected, probably indicating a hiatus. The lithology in the Ben Gurion section is of clay and marl. In the same study they also covered Alamedilla section in Spain (Figure 42-12), where they detected the boundary in a clay layer in marl deposition, with presence of excursion taxa. Molina et al. (1999) positioned the boundary in the Alamedilla section at the BFE, before the LO of *A. sibiyaensis*.

The Caravaca section (Figure 42-12) was studied by Molina et al. (2001) and the boundary is placed at the base of CIE, which is coincident with a dissolution interval, and probably the *A. berggreni* Subzone. The lithology of the section is composed of marls and sandy limestone intercalations with larger benthic foraminifera.

For the Zumaya section in Spain (Figure 42-11) Molina et al. (1996), produced a planktonic foraminiferal zonation not identifying the excursion taxa and placing the boundary at the bottom boundary of *Morozovella velascoensis* Zone. Later Molina et al. (1999) proposed applied the 5-fold P5 zonation in which the P/E boundary is positioned at the BFE in *A. berggreni* Subzone, before the LO of *A. sibiyaensis*. Years later, Zili et al. (2009) studied the same section and placed the boundary at the LO of *A. berggreni*.

The Possagno section in Italy (Figure 42-10) is composed of marls, and the boundary is placed at the bottom boundary of a clay layer which coincides with BFE and is in

the *A. berggreni* Subzone (Molina et al., 1999). Nearby Forada section withholds a similar litho- and biostratigraphy (Luciani et al., 2007).

In the Kaurtakapy section (Kazakhstan, Figure 42-13) (Pardo et al., 1999) the P/E boundary is located at the LO of *A. sibaiaensis* which occurs along with *A. africana*.

In the western and central Black Sea region (Figure 42-8) Güray (2014) studied several sections and provided the P/E boundary at coinciding LOs of *A. wilcoxensis* and *A. pseudotopilensis*. Excursion taxa were not recorded in any of the sections.

In this study, the P/E boundary was recorded with the occurrence of *A. sibaiaensis* in the sample GT-17.75 in clay rich shale. The uppermost Paleocene is distinguishing by the successive occurrences of the lower Eocene assemblage: *M. gracilis*, *M. marginodentata*, *A. wilcoxensis* and *A. pseudotopilensis*, and the lowermost Eocene is distinguished by *P. wilcoxensis*. Zone E1 (*A. sibaiaensis* Zone) spans for about 3 meters (from GT-17.75 to GT-21), which is similar to those found in other localities. The absence of excursion taxa, apart from *A. sibaiaensis*, may be due to preservational complexities, sampling resolution, or their preferred geographical distribution.

CHAPTER 5

SYSTEMATIC TAXONOMY

“Much of the usefulness of planktonic foraminifers for stratigraphic, ecologic, and evolutionary studies is obscured because their true relationships are not clearly understood.”

Jere H. Lipps, 1966

Above quote still holds after more than 50 years, and is related to the basics of paleontology. As paleontologists we are dealing with the shells, bones, skeletons instead of much important soft parts. The classification scheme of a paleontologist is a bit different than that of a biologist: all we get is little clues and big interpretations. As long as the time machines do not exist, we will not have the chance to truly understand their true relationships.

Yet, our understanding broadens as never ending works are published all around. In time, planktonic foraminifera were studied by many people. Several workers proposed classification schemes for planktonic foraminifera based on slightly different criteria such as coiling characteristics or chamber shape (e.g. Bolli et al., 1957; Banner & Blow, 1959; Parker, 1962; Lipps, 1966). However, gross morphological features proved inadequate in higher level taxonomical grouping due to convergent evolution: these taxa all prefer a planktonic life habit, so, it is expected

to see similar features being used at different lineages, like chamber shape and test shape which provides them means of remaining in suspension. Taxonomy of Cenozoic planktonic foraminifera became more stable after Parker's (1962) classification based on wall textures, more specifically, spinosity. The work by Parker (1962) was carried out on the Pacific Recent foraminifera, and two families were presented by the author: Family Globigerinidae (Carpenter, Parker and Jones, 1862) with spines which are used for increasing buoyancy, and Family Globorotaliidae (Cushman, 1927) with non-spinose wall that is often decorated by ornamentations (there referred to as pseudo-spines). As Pearson et al. (2006a) indicated, with the use of SEM imaging on planktonic foraminifera, especially the well preserved specimens from the Ocean Drilling Programs, proved the importance of wall texture in taxonomy. The latest and widely recognized classification schemes for Paleocene and Eocene are well summarized in two atlases by Olsson et al. (1999) and Pearson et al. (2006). The summary of aforementioned schemes is given in Table 8.

Two main groups are defined based on the wall structures: the normal perforate group (mainly the spiral taxa) and the microperforate group (the serial taxa) (Hemleben et al., 1999; Hemleben & Olsson, 2006). Microperforate group has variants based on surface ornamentation such as number and density of pustules or striations, while normal perforate group is more diverse.

One of the normal perforate group is spinose wall texture. The pores are encircled by slightly elevated margins producing hexagonal patterns (cancellate), and along the corners of the honeycomb pattern spine holes are present. The spines are morphological features of adult forms, and the spines are shed during terminal stage for gametogenesis, and some calcite crusting may take place sealing the spine holes. Further division of spinose wall structure is proposed by Hemleben et al. (2006), however the necessary detail for such distinction was not observed in this study. The other normal perforate group is the non-spinose one, having wide variety of textures from smooth to highly pustulose, and muricate. Muricate wall structure has a cancellate base, not as elevated as spinose type but still pores are encircled by

Table 8: Classification schemes of several authors, the ones marked with asterisk are as compiled in Lipps (1966).

Bolli, Loeblich & Tappan, 1957 *	Banner & Blow, 1959 *	Bermudez, 1961 *	Parker, 1962	Loeblich & Tappan, 1964
Hantkeninidae	Globigerinidae	Globigerinidae	Globigerinidae	Heterohelicidae
Planomaliniinae	Orbulininae	Globigerininae	<i>Globigerina</i>	Guembelitrinae
Hantkeniniinae	<i>Orbulina</i>	<i>Globigerina</i>	<i>Globigerinella</i>	<i>Woodrigina</i>
<i>Schackoia</i>	<i>Biorbulina</i>	<i>Globigerinella</i>	<i>Hastigerina</i>	Heterohelicinae
<i>Hantkenina</i>	<i>Porticulasphaera</i>	<i>Biglobigerinella</i>	<i>Globigerinoides</i>	<i>Bifarina</i>
<i>Cribrohantkenina</i>	<i>Globigerapsis</i>	<i>Globigerinelloides</i>	<i>Orbulina</i>	<i>chiloguembelina</i>
Hastigerininae	Globigerininae	<i>Hastigerina</i>	<i>Pulleniatina</i>	Planomalinidae
<i>Hastigerina</i>	<i>Globigerina</i>	<i>Hastigerinella</i>	<i>Sphaeroidinella</i>	<i>Biglobigerinella</i>
<i>Clavigerinella</i>	<i>Globoquadrina</i>	<i>Hastigerinoides</i>	Globorotaliidae	Shackoinidae
Casigerinellinae	<i>Globigerinoides</i>	<i>Clavigerinella</i>	<i>Globorotalia</i>	Rotaliporidae
<i>Casigerinella</i>	Sphaeroidinellinae	Cassigerinellinae	<i>Globoquadrina</i>	Globotruncanidae
Globorotaliidae	<i>Sphaeroidinellopsis</i>	<i>Cassigerinella</i>		Hantkeninidae
<i>Praeglobotruncana</i>	<i>Sphaeroidinella</i>	Orbulininae		Hastigerininae
<i>Rotalipora</i>	Catapsydracinae	<i>Globigerinoides</i>		<i>Hastigerina</i>
<i>Globorotalia</i>	<i>Catapsydrax</i>	<i>Candorbulina</i>		<i>Bolliella</i>
<i>Truncarotaloides</i>	<i>Tinophodella</i>	<i>Candeina</i>		<i>Clavigerinella</i>
Globotruncanidae	<i>Globigerinita</i>	<i>Globigerapsis</i>		<i>Globanomalina</i>
Orbulinidae	<i>Globigerinoita</i>	<i>Biorbulina</i>		Hantkeniniinae
Globigerininae	<i>Globigerinatheka</i>	<i>Orbulina</i>		<i>Hantkenina</i>
<i>Globigerina</i>	<i>Globigerinatella</i>	Globigerininiinae		<i>Cribrohantkenina</i>
<i>Globoquadrina</i>	Globorotaliinae	<i>Globigerinita</i>		Cassigerinellinae
<i>Hastigerinella</i>	<i>Globorotalia</i>	<i>Globigerinatella</i>		<i>Cassigerinella</i>
<i>Globigerinoides</i>	<i>G. (Globorotalia)</i>	<i>Globigerinoita</i>		Globorotaliidae
<i>Sphaeroidinella</i>	<i>G. (Turborotalia)</i>	<i>Globigerinatheka</i>		Globorotaliinae
<i>Pulleniatina</i>	<i>G. (Hastigerinella)</i>	Sphaeroidinellinae		<i>Globorotalia</i>
Orbulininae	<i>Truncarotaloides</i>	<i>Sphaeroidinella</i>		<i>Turborotalia</i>
<i>Globigerapsis</i>	<i>Pulleniatina</i>	<i>Sphaeroidinellopsis</i>		Truncarotaloidinae
<i>Porticulasphaera</i>	Globorotaloidinae	Globorotaliidae		<i>Truncarotaloides</i>
<i>Candeina</i>	<i>Globorotaloides</i>	<i>Globorotalia</i>		Globigerinidae
<i>Orbulina</i>	Hastigerininae	<i>Globorotaloides</i>		Globigerininiinae
Catapsydracinae	<i>Hastigerina</i>	<i>Globoquadrina</i>		<i>Globigerina</i>
<i>Catapsydrax</i>	<i>H. (Hastigerina)</i>	<i>Turborotalia</i>		<i>Beella</i>
<i>Globigerinita</i>	<i>H. (Bolliella)</i>	<i>Pulleniatina</i>		<i>Globigerinoides</i>
<i>Globigerinoita</i>	Cassigerinellinae	<i>Truncorotalita</i>		<i>Globigerinopsis</i>
<i>Globigerinatheka</i>	<i>Cassigerinella</i>	<i>Pseudogloborotalia</i>		<i>Globoconusa</i>
<i>Globigerinatella</i>	Hantkeninidae	<i>Truncorotaloides</i>		<i>Globoquadrina</i>
	Rotaliporinae	Globotruncanidae		<i>Globorotaloides</i>
	Planomaliniinae			<i>Hastigerinella</i>
	<i>Pseudohastigerina</i>			<i>Pulleniatina</i>
	Hantkeniniinae			<i>Subbotina</i>
	<i>Hantkenina</i>			Sphaeroidinellinae
	<i>H. (Hantkenina)</i>			<i>Sphaeroidinella</i>
	<i>H. (Aragonella)</i>			<i>sphaeroidinellopsis</i>
	<i>Cribrohantkenina</i>			Orbulininae
	<i>Clavigerinella</i>			<i>Orbulina</i>
	Globotruncanide			<i>Candeina</i>
				<i>Globigerapsis</i>
				<i>Porticulasphaera</i>
				Catapsydracinae
				<i>Catapsydrax</i>
				<i>Globigerinatella</i>
				<i>Globigerinatheka</i>
				<i>Globigerinita</i>
				<i>Globigerinoita</i>
				<i>Tinophodella</i>

Table 8 (Continued)

Lipps, 1966	Loeblich & Tappan, 1988	Olsson et al., 1999	Pearson et al., 2006
Globorotaliidae	Guembeltriidae	Globigerinidae	Globigerinidae
Globorotaliinar	<i>Chiloguembeltria</i>	<i>Eoglobigerina</i>	<i>Catapsydrax</i>
<i>Globorotalia</i>	<i>Woodrigina</i>	<i>Parasubbotina</i>	<i>Globorotaloides</i>
Acarinia	Heterohelicidae	<i>Subbotina</i>	<i>Guembeltrioides</i>
<i>Truncarotaloides</i>	Heterohelicinae	Hedbergellidae	<i>Paragloborotalia</i>
<i>Turborotalia</i>	<i>Spiroplecta</i>	<i>Hedbergella</i>	<i>Parasubbotina</i>
Candeininae	<i>Bifarina</i>	<i>Globanomalina</i>	<i>Pseudoglobigerinella</i>
<i>Candeina</i>	Chiloguembelinidae	Truncarotaloididae	<i>Globigerinella</i>
<i>Cassigerinelloita</i>	<i>Chiloguembelina</i>	<i>Acarinina</i>	<i>Globoturborotalia</i>
<i>Eoglobigerina</i>	<i>Laterostomella</i>	<i>Morozovella</i>	<i>Subbotina</i>
<i>Globigerinatella</i>	Eoglobigerinidae	<i>Igorina</i>	<i>Turborotalita</i>
<i>Globigerinita</i>	<i>Eoglobigerina</i>	<i>Praemurica</i>	<i>Globigerinatheka</i>
<i>Globoconusa</i>	<i>Globoconusa</i>	Guembeltriidae	<i>Orbulinoides</i>
<i>Trurbotoralita</i>	<i>Parvularugoglobigerina</i>	<i>Guembeltria</i>	Hantkeninidae
Hantkeninidae	<i>Postrugoglobigerina</i>	<i>Globoconusa</i>	<i>Clavigerinella</i>
Hantkenininae	Globorotaliidae	<i>Parvularugoglobigerina</i>	<i>Cribrorhantkenina</i>
<i>Hantkenina</i>	<i>Astrorotalia</i>	<i>Woodrigina</i>	<i>Hantkenina</i>
<i>Clavigerinella</i>	<i>Igorina</i>	Chiloguembelinidae	Truncarotaloididae
<i>Cribrorhantkenina</i>	<i>Planorotalites</i>	<i>Chiloguembelina</i>	<i>Acarinina</i>
<i>Globanomalina</i>	<i>Turborotalia</i>	Heterohelicidae	<i>Morozovelloides</i>
Cassigerinellinae	Truncarotaloididae	<i>Rectoguembelina</i>	<i>Igorina</i>
<i>Cassigerinella</i>	<i>Acarinina</i>	<i>Zeauvigerina</i>	<i>Morozovella</i>
Catapsydracidae	<i>Globigerapsis</i>		<i>Astrorotalia</i>
<i>Catapsydrax</i>	<i>Morozovella</i>		<i>Planorotalites</i>
<i>Globoquadrina</i>	<i>Muricoglobigerina</i>		Globoquadrinidae
<i>Globorotaloides</i>	<i>Tesacarinata</i>		<i>Dentoglobigerina</i>
<i>Subbotina</i>	<i>Truncarotaloides</i>		Hedbergellidae
Globigerinidae	Candeinidae		<i>Globanomalina</i>
<i>Globigerina</i>	Tenuitellinae		<i>Planoglobanomalina</i>
<i>Candorbulina</i>	<i>Tenuitella</i>		<i>Pseudohastigerina</i>
<i>Globigerapsis</i>	Catapsydracidae		<i>Turborotalia</i>
<i>Globigerinatheka</i>	<i>Cassigerinelloita</i>		Guembeltriidae
<i>Globigerinoides</i>	<i>Catapsydrax</i>		<i>Jenkinsina</i>
<i>Hastigerina</i>	<i>Dentoglobigerina</i>		<i>Cassigerinelloita</i>
<i>Orbulina</i>	<i>Eoclavatorella</i>		Chiloguembelinidae
<i>Porticulasphaera</i>	<i>Globoquadrina</i>		<i>Chiloguembelina</i>
<i>Protella</i>	<i>Globorotaloides</i>		<i>Streptochilus</i>
<i>Pulleniatina</i>	<i>Guembelitroides</i>		Heterohelicidae
<i>Sphaeroidinella</i>	<i>Subbotina</i>		<i>Zeauvigerina</i>
<i>Sphaeroidinellopsis</i>	Globanomalinidae		Cassigerinellidae
	<i>Clavigerinella</i>		<i>Cassigerinella</i>
	<i>Globanomalina</i>		<i>Tenuitella</i>
	<i>Hastigerinella</i>		
	Hantkeninidae		
	<i>Aragonella</i>		
	<i>Cribrorhantkenina</i>		
	<i>Hantkenina</i>		
	Cassigerinellidae		
	<i>Cassigerinella</i>		
	Globigerinidae		
	Globigerininae		
	<i>Globigerina</i>		
	Porticulasphaerinae		
	<i>Globigerinatheka</i>		
	<i>Inordinatosphaera</i>		
	<i>Orbulinoides</i>		
	<i>Porticulasphaera</i>		

cancellate margins, above which pustules of various length and diameter are mounted, even fused together in some (for example muricocarina).

Although wall structures present a good way of classification, depending solely on this feature is not always enough to distinguish different taxa with similar morphologies. In this work the specimens dealt with were collected from a land-section where they have been subjected to many modifying processes other than simple burial and diagenesis; hence, wall textures were not always defined reliably. Moreover, the microscope in use (with x100 magnification maximum) was not adequate for examination of wall texture of smaller specimens. In order to overcome this issue several gross morphological characteristics were put in use for distinguishing of similar taxa.

- Growth rate: The rate of size increase of chambers as added (in the last whorl). A very high growth rate implies a last chamber much bigger in size (as in equal to or greater than twice the size of penultimate one); a very low growth rate means chambers of similar size
- Chamber size & shape: Chamber size are explained by the sizes in three dimensions: tangential, radial and axial. Several shapes are given as reference both for 3-D (such as egg-shape, globular, spherical, conical) and in 2-D (such as trapezoidal, rhombohedral, oval, pie-shaped).
- Spiral sutures: Sutures that were formed due to coiling on the spiral side of a trochospiral form
- Intercameral sutures: Sutures of septa on spiral or umbilical sides. They may be depressed or elevated, and may be of a preferred shape like straight or curved.
- Umbilicus: Umbilicus is the axial space in spiral foraminifera communicating directly through apertures. Here the term is used instead of pseudoumbilicus: the externally visible, extra-axial, narrow or wide, cup-shaped space between infolded distal wall below main cameral aperture and adjacent coil, mimicking an umbilicus.
- Number of chambers: The number of chambers in the last whorl
- Axial outline: The gross shape when a specimen is examined in the edge view: planoconvex, biconvex etc.

- Equatorial outline: The gross shape when a specimen is examined in the spiral/umbilical view: circular, ovate, quadrate and lobulate, nonlobulate etc.

Below, the reader may find brief descriptions of species along with a short synonyms list (for a more comprehensive synonym list one should check the works of Olsson et al. (1999) and Pearson et al. (2006)). Descriptions of the species are given in forms of tables including key features for the groups. These tables (Table 9 - Table 18), rapid recognition charts, are constructed in order to visualize the similarities and differences of all the species of the same genus, independent of the time interval being studied. Several distinguishing features are summarized in order to provide the general variations in the genera, and the main distinction between Paleocene-Eocene species. The data on the tables are based on Olsson et al. (1999) and Pearson et al. (2006) unless specified otherwise.

Main emphasis in this work is on the remarks sections concerning the gross morphological features, similarities with and differences from other taxa; providing a means of key for poorly preserved specimens where the wall texture examination cannot result in satisfactory definitions. Key morphological and wall textural features are noted also for higher taxonomical groups.

The stratigraphic ranges of the taxa are compared to Olsson et al. (1999), Premoli-Silva et al. (2003) and Pearson et al. (2006).

5.1 Family Globigerinidae Carpenter, Parker, and Jones, 1862

This family is composed of groups with normal perforate, cancellate, spinose wall texture, low trochospire, and globular (almost spherical) chambers. This family is referred to in the text as “Subbotinids”, a term uniting *Subbotina* and *Parasubbotina* for their many shared characteristics and similar environmental preferences.

5.1.1 Genus *Parasubbotina* Olsson, Hembleben, Berggren, and Liu, 1992

Type species: *Globigerina pseudobulloides* Plummer, 1926

Remarks: Spinose, cancellate wall texture is seen in this genus, as is the criterion for the family rank. Low trochospiral forms with high chamber growth rate are classified under this genus if the aperture is located at an umbilical-extraumbilical position.

Table 9 is the rapid recognition chart for Paleocene-Eocene *Parasubbotina* species.

Stratigraphic range: Danian – Priabonian (Pearson et al., 2006)

Parasubbotina varianta (Subbotina, 1953)

Plate 3, Figures a-c

- 1953 *Globigerina varianta* Subbotina, p. 63, pl. 3, figs. 5a-c, 6a-7c, 10a-11c, 12a-c; pl. 4, figs. 1a-3c.
- 1962 *Globorotalia (Globorotalia) varianta* (Subbotina) – Hillebrandt, p. 125, pl. 12: figs. 10a-c, 11a, b
- 1979 *Globorotalia (Turborotalia) quadrilocula* – Blow, p. 1109, pl. 87, fig. 7.
- 1992 *Subbotina varianta* (Subbotina) – Berggren, p. 563, pl. 1, fig. 3.
- 1999 *Parasubbotina varianta* (Subbotina) - Olsson et al., p. 26, pl. 9, figs, 16-18; pl. 22, figs. 6-16.
- 2006 *Parasubbotina varianta* (Subbotina) - Pearson et al., p. 104, pl. 5.13, figs. 1-16.

Remarks: As a form of wide morphological range this species was named *varianta*. The chamber growth rate is moderate to high. The aperture is located on the apertural face: an arch at umbilical-extraumbilical position. Aperture is bordered by a lip that is not always preserved and hence not distinguishingly important.

Table 9: Rapid recognition chart for species of genus *Parasubbotina*. * for species identified in this study

Species	Wall	Equatorial Outline	Axial Outline	# of Chambers	Chamber Shape	Chamber Growth Rate	Umbilicus	Sutures
<i>P. eoelava</i>	Large pore pits	Strongly lobulate, loosely coiled; secondary spiral apertures	Periphery rounded, axially compressed test	4-5	Globular, axial size shorter than radial and tangential sizes, last two chambers clavate	Very high	Wide	Straight, depressed
<i>P. griffinae</i>	<i>Clavigerinella</i> - type	Lobulate, circular	Periphery broadly rounded, robust test, very low trochospiral	4-5	Globular, inflated, embracing, strongly appressed	Moderate	Small	Moderately depressed, straight
* <i>P. inaequispira</i>	Symmetrically to asymmetrically cancellate	Strongly lobulate, initial whorl proportionally very small	Periphery rounded, axially compressed test	4-4.5	Globular, axial size shorter than radial and tangential sizes, chambers well separated	High	Moderate	Moderately depressed, straight
<i>P. prebetica</i>	<i>Clavigerinella</i> - type	Highly lobulate	Periphery rounded, axially compressed test	4-4.5	Globular, very well separated	Very low-low	Shallow	Strongly depressed

Table 9 (Continued)

Species	Wall	Equatorial Outline	Axial Outline	# of Chambers	Chamber Shape	Chamber Growth Rate	Umbilicus	Sutures
<i>P. pseudobulloides</i>	Cancellate texture less developed in earlier forms	Lobulate, circular	Rounded periphery	4-5	Globular, ovate, inflated	Low to moderate	Moderately wide	Depressed, straightly
<i>P. pseudowilsoni</i>	<i>Ruber-sacculifer</i> type	Lobulate, circular	Rounded periphery	5	Globular, moderately embracing	Moderate	Narrow	Moderately depressed, straight
* <i>P. varianta</i>	Cancellate	Lobulate, circular	Broadly rounded periphery	4	Globular, ovate, axial size high	High	Small	Moderately depressed, straight
<i>P. variospira</i>	Large pore pits	Lobulate, circular, loosely coiled; occasional secondary spiral apertures	Rounded periphery, moderate to high trochospiral	4-5	Globular with umbilical teeth	Moderate	Wide, covered by umbilical teeth	Depressed

Wall texture is spinose, cancellate. Under stereomicroscope the wall texture is observed as a common Subbotinid wall if preservation is appropriate.

This species is differentiated from any other Subbotinids by its 4 chambers in the last whorl, and the lower trochospiral, more regular coiling type. The chambers are better separated and less embracing than any Subbotinid allowing the umbilicus to be open, yet still closely appressed together so that in umbilical view chambers look more of a quarter circle. The aperture is distinctly shifted to a more extraumbilical position than in Subbotinids.

Chamber shape and size varies largely. For example Olsson et al. (1999) present *P. varianta* with a last chamber that is tangentially longer than radially broad while Pearson et al. (2006) chooses somewhat shorter (tangentially) chambers so that the last chamber is similar to the penultimate one in size. This variety creates a series of overall test shape (from circular to ovate) for this taxon.

Stratigraphic range: According to Pearson et al. (2006) this species is found in Zones P1c up to E10.

Occurrence: In the studied measured section this species occurs in almost every sample (GT-1 – GT-25), although in small numbers (<1% in average).

Parasubbotina inaequispira (Subbotina, 1953)

Plate 3, Figures f, i, l

- 1953 *Globigerina inaequispira* Subbotina, 84, pl.6, figs. 1a-c, 4a-c; pl.6, figs.2a-3c.
- 1979 *Subbotina inaequispira* (Subbotina) - Blow, 1272, pl.151, figs. 5-7; pl. 163, figs. 4-8; pl.180, figs. 1,4-7; pl.191, fig. 7.
- 2001 *Subbotina inaequispira* (Subbotina) - Warraich and Ogasawara, 48, fig.13: 17-19.
- 2004 *Parasubbotina inaequispira* (Subbotina) - Pearson et al., 36, pl. 1, fig. 13.

2006 *Parasubbotina eoclava* (Subbotina) - Pearson et al., p. 101, pl. 5.11, figs. 1-15

Remarks: Chamber growth rate is somewhat irregular in this species; the last chamber is especially large while the other three of the last whorl are relatively similar in size, and the initial whorls are proportionally very small. Chambers are shorter in axial length than radial and tangential dimensions. The coiling is looser than that of *P. varianta*, chambers are well separated with depressed sutures. The aperture is in umbilical-extraumbilical position.

Stratigraphic range: Base of Zone E1 to top of Zone E8 (Pearson et al., 2006).

Occurrence: In this study this species is recorded in most samples in GT-15 – GT-25 interval and up in small numbers (<1% in average).

5.1.2 Genus *Subbotina* Brotzen and Pozaryska, 1961

Type species: *Globigerina triloculinooides* Plummer, 1926

Remarks: Characterized by a cancellate wall structure this group had been placed in Family Catapsydracidae along with many other cancellate genera, later on, with discovery of their spinose wall in adult form, *Subbotina*, along with its sister taxa, are now being classified under Family Globigerinidae. The wall textures of *Subbotina* are divided into three groups by Pearson et al. (2006) due to similarities to extant spinose groups, namely: *sacculifer*-type, *ruber*-type, *ruber/sacculifer*-type, and *clavigerinella*-type. These are noted in Table 10 along with distinctive morphological characters; however, these wall structure details were not observable via light microscope, therefore their application is restricted to SEM imaging.

Main morphological criteria of genus *Subbotina* include cancellate spinose wall, globular chambers, umbilical aperture and tight coiling. The trochospiral coiling of *Subbotina* is mostly described as low, yet some elaboration is needed: due to high-

Table 10: Rapid recognition chart for species of genus *Subbotina*. * for species identified in this study

Species	Wall	Test Shape	# of Chambers	Chamber Shape	Chamber Growth Rate	Sutures	Aperture	Apertural modification
<i>S. angiporooides</i>	<i>sacculifer/ruber</i> - type, often thickened by addition of gametogenetic calcite	Non-umbilicate, spherical, rounded quadrilobate, rounded axial periphery	4	Globular, radially elongated chambers; final chamber strongly embracing and extending over umbilical sutures	Moderate	Weakly depressed, radial to slightly curved	Low, indistinct, interiomarginal slit	Thick lip extending the full width of the chamber face
<i>S. cancellata</i>	Coarsely cancellate	Rounded outline, slightly lobulate	3.5-4	Globular	Low-moderate	Depressed, straight	Umbilically directed aperture	Broad, somewhat irregular lip
<i>S. corpulenta</i>	Cancellate	Lobulate in outline, moderately high trochospiral	4-4.5	Globular; final chamber reduced in size extending over umbilicus, resembling bulla in some specimens	Moderate	Moderately depressed, straight to slightly curved	Umbilical	
<i>S. crociapertura</i>	<i>bulloides</i> -type	Globular test, oval in outline	4	Globular, slightly embracing	High	Moderately depressed, straight	Umbilical high arch	prominent lip that tapers towards the posterior side of the ultimate chamber
<i>S. eoacaena</i>	<i>ruber/sacculifer</i> -type	Globular test, oval in outline	3.5-4	Globular, embracing	High	Moderately depressed, straight	Umbilical to slightly extraumbilical, circular arch	Thin, irregular lip

Table 10 (Continued)

Species	Wall	Test Shape	# of Chambers	Chamber Shape	Chamber Growth Rate	Sutures	Aperture	Apertural modification
<i>S. gortanii</i>	<i>ruber/sacculifer</i> -type	Globular outline, high trochospiral loose coil	4	Globular, slightly embracing	Moderate	Deeply depressed, straight	Umbilical	Thickened, narrow rim
<i>S. hagni</i>	<i>ruber/sacculifer</i> -type	Quadrangle in outline	4	Globular, slightly embracing	Moderate	Moderately depressed, straight	Umbilical to extraumbilical low arch	Thin, irregular lip
* <i>S. hornibrooki</i>	<i>sacculifer</i> -type	Globular, slightly lobulate	3.5-4	Globular, embracing; last chamber reduced in size	High	Slightly depressed and straight	Umbilical	Narrow continuous lip
<i>S. jacksonensis</i>	<i>ruber/sacculifer</i> -type	Globular, ovate	4	Globular, much embracing; final chamber directed over and covering the umbilicus	Moderate	Very slightly depressed, straight	Umbilical	-
<i>S. linaperta</i>	<i>sacculifer</i> -type	Globular, rounded in outline	3-3.5	Globular, embracing; final chamber broader than high	High	Straight to slightly curved, moderately depressed	Umbilical to somewhat extraumbilical low arch	Thin, even lip
* <i>S. patagonica</i>	<i>sacculifer</i> -type	Globular, slightly lobulate outline	3-3.5	Globular, embracing; final chamber make up about half the test size	High	Slightly depressed and straight	Umbilical rounded arch	Thickened lip
* <i>S. roesnaesensis</i>	<i>ruber</i> -type	Tripartite, lobulate in outline	3-4	Globular, ovoid, wider than high, loosely embracing	High	Strongly depressed slightly curved to straight	Umbilical low arch	Narrow lip

Table 10 (Continued)

Species	Wall	Test Shape	# of Chambers	Chamber Shape	Chamber Growth Rate	Sutures	Aperture	Apertural modification
<i>S. senni</i>	<i>sacculifer</i> -type, thick gametogenic calcite	Globular, ovate to circular in outline; moderately elevated initial whorl	4	Globular, slightly embracing, angled to ward the umbilicus	Moderate	Moderately depressed, straight	Umbilical	Thickened rim
* <i>S. triangularis</i>	Asymmetrically cancellate	Broadly rounded axial periphery	3-3.5	Globular; last chamber oval, often smaller than penultimate one	Moderate	Depressed	Umbilical to slightly extraumbilical	Thin, sometimes irregular lip
<i>S. triloculinooides</i>	Cancellate	Lobulate, trilobate	3-3.5	Globular; final chamber make up about half the test size	Moderate	Depressed	Umbilical, slightly asymmetrical to extraumbilical direction	Lip
<i>S. trivialis</i>	Weakly cancellate	-	3.5	Spherical; last chamber equal to or slightly smaller than the penultimate one	Low-Moderate	Depressed	Umbilical	Thin lip

Table 10 (Continued)

Species	Wall	Test Shape	# of Chambers	Chamber Shape	Chamber Growth Rate	Sutures	Aperture	Apertural modification
<i>S. utilisindex</i>	<i>sacculifer/ruber</i> -type	Trilobate, rounded equatorial margin	3	Globular; final chamber comprising less than half of test	Moderate	Radial to slightly curved, moderately depressed	Very low interiomarginal, umbilical-extraumbilical slit	Narrow lip
<i>S. yeguaensis</i>	<i>sacculifer</i> -type	Moderately elevated globular test; lobulate in outline	3.5	Globular, slightly embracing	Moderate	Moderately depressed, straight	Umbilical low rounded opening	Broad lip
* <i>S. velascoensis</i>	Symmetrically cancellate	Subquadrate test	3-3.5	Compressed chambers; final chamber especially radially compressed, axially elongate, overhanging the umbilicus	High	Depressed	Umbilical	Thin elongate lip

very high growth rate and chamber inflation on umbilical side chambers on umbilical side are highly embracing. This generally produces an overall globular form if the chamber separation is small enough (globular Subbotinids, e.g. *S. hornibrooki*). If chambers are better separated and less umbilically inflated with slower growth rate (in axial dimension) than the form becomes more of an oval-cylinder on the side view (straight-standing Subbotinids, e.g. *S. patagonica*). A summary of the characteristic features of the *Subbotina* species is given in Table 10.

Stratigraphic range: Paleocene-Oligocene (Pearson et al., 2006)

Subbotina hornibrooki (Brönnimann, 1952)

Plate 4, Figures f, i

- 1952 *Globigerina hornibrooki* Brönnimann, 15, pl. 2: figs. 4-6.
- 1952 *Globigerina finlayi* Brönnimann, 8, pl. 2: fig. 10a-c.
- 1956 ?*Globigerina bacuana* Khalilov, 235, pl. 3: fig. 4a-c.
- 1979 *Subbotina hornibrooki* (Brönnimann) - Blow, 1269, pl. 124: fig. 8.
- 1979 ?*Subbotina hornibrooki hornibrooki* (Brönnimann) - Blow, (partim), 1269, pl. 101: fig. 7.
- 1995 Not *Subbotina hornibrooki* (Brönnimann) - Poag and Commeau, 144, pl. 3: figs. 25, 26 [= *Subbotina roesnaesensis* n. sp.].
- 206 *Subbotina hornibrooki* (Brönnimann) – Pearson et al., 140, pl. 6: figs. 1-16

Remarks: This is the only globular Subbotinid encountered during the studies. The chambers of the last whorl are stacked close to each other with very shallow intercameral sutures, and the chamber sizes of the last whorl are similar. The chambers are embracing on the umbilical side providing a closed or very shallow umbilicus.

Stratigraphic range: From Zone P5 to E4 (Pearson et al., 2006).

Occurrence: In this study this species is observed sporadically in the GT-16 – GT-25 interval.

Subbotina patagonica (Todd and Kniker, 1952)

Plate 4, Figures a-c

1952 *Globigerina patagonica* Todd and Kniker, 26, pl. 4, figs. 32a-c.

1989 *Globigerina patagonica* (Todd and Kniker) - Murray, Curry, Haynes and King, 530, pl 10.10, figs. 10-12.

1991 *Subbotina patagonica* (Todd and Kniker) - Huber, p. 441, pl. 4, figs. 16, 17.

2006 *Subbotina patagonica* (Todd and Kniker) - Pearson et al., p. 154 pl. 6-15, figs. 1-16.

2014 *Subbotina patagonica* (Todd and Kniker) - Bornemann et al., p. 71, text fig. 2.3.

Remarks: The form is cylindrical with short axial thickness; the last formed chamber is almost spherical. Chamber growth rate is great; the last formed chamber is the size of the rest of the test. An arched umbilical aperture is clearly visible on the umbilical side (Pl. 4, fig. b).

Stratigraphic range: From Zone P4b to Zone E8 (Pearson et al., 2006).

Occurrence: This species is an abundant element of the studied samples throughout the measured section (GT-1 – GT-26).

Subbotina roesnaensis (Olsson and Berggren, 2006)

Plate 3, Figures j, k

- 2006 *Subbotina roesnaensis* Olsson and Berggren, p. 157 pl. 6-16, figs. 1-15.
- 1953 *Globigerina eocaenica* var. *eocaenica* Terquem - Subbotina, p. 80-81, pl. 11, figs.8a-c, 9a-c.
- 1960 *Globigerina yeguaensis* Weinzierl and Applin - Berggren, p. 73-83, pl. 2, figs. 1a-4c; pl. 3, figs. 1a-3c; pl. 4, figs. 1a-2c; pl. 8, figs. 1a-5c.
- 1979 *Subbotina* sp. - Blow, p. 1260, pl. 158, fig. 5.
- 1989 *Globigerina patagonica* Todd and Kniker – Murray et al., p.260, pl. 8.10, figs. 6-8.
- 1991 *Subbotina velascoensis* (Cushman) - Huber, p. 441, pl. 4, figs. 11, 12.
- 1992 *Subbotina patagonica* (Todd and Kniker) - Berggren, p. 563, pl. 2, fig. 16.
- 1995 *Subbotina patagonica* (Todd and Kniker) - Lu and Keller, p. 102, pl. 5, figs. 12-14.
- 2000 *Subbotina patagonica* (Todd and Kniker) – Warraich et al. 299, figs. 18: 4, 5, 11.
- 2001 *Subbotina patagonica* (Todd and Kniker) - Warraich and Ogasawara, p. 48, figs.13: 4, 8, 12

Remarks: This species withholds a similar overall shape with *S. velascoensis* due to chamber compression, but the last formed chamber is less compressed (radially) and less elongate (both axially and tangentially). The aperture is rather visible in umbilical view (Pl. 3, f.g. k) because it is situated on a wall not parallel to the axis but inclined.

Stratigraphic range: From Zone P5 to Zone E10 (Pearson et al., 2006).

Occurrence: This species first occurs in GT-15, and is generally present in the samples until the end of the measured section (GT-26).

Subbotina triangularis (White, 1928)

Plate 4, Figures d-f

- 1928 *Globigerina triangularis* White, p.195, pl. 28, figs. 1a-c.
- 1957a *Globigerina triangularis* (White) - Bolli, p.71, pl. 15, figs. 12-14.
- 1970a *Globigerina triangularis* (White) - Shutskaya, p.104, pl. 3, figs. 5a-c.
- 1970b *Globigerina triangularis* (White) - Shutskaya, p.118, pl. 20, figs. 7a-c; p. 220, pl. 23, figs. 1a-c; p. 224, pl. 25, figs. 1a-c.
- 1979 *Globigerina triangularis triangularis* (White) - Blow, p.1281, pl. 91, figs. 7, 9; pl. 107, figs. 8, 9.
- 1997 *Subbotina triangularis* (White) - Berggren and Norris, p. 81, pl. 5, figs. 1, 5, 9.
- 1999 *Subbotina triangularis* (White) - Olsson et al., p. 30, pl. 26, figs. 1-13.
- 2008 *Subbotina triangularis* (White) - Handley et al., p. 20, text-fig. 2.4.
- 2009 *Subbotina triangularis* (White) - Obaidalla et al., p. 4, pl. 2, fig. 9.

Remarks: The last chamber of the form is tangentially shorter than the rest of the test giving a triangular appearance to the test, and the last formed three chambers are of similar size, though gradually growing. The last chamber hangs over the umbilicus as in *S. velascoensis*.

Stratigraphic range: From Zone P2 to top of Zone P5 (Olsson et al., 1999). This is a minor element of the Paleocene assemblages in the studied samples, occurring in the GT-1 – GT-17 interval.

Occurrence: This is a minor element of the Paleocene assemblages in the studied samples, occurring in the GT-1 – GT-17 interval.

Subbotina velascoensis (Cushman, 1925)

Plate 3, Figures d, e, g, f

- 1925 *Globigerina velascoensis* Cushman, p. 19, pl. 3, figs. 6a-c.
- 1928 *Globigerina velascoensis* Cushman - White, p. 196, pl. 28, figs. 2a-b.144
- 1928 *Globigerina velascoensis* Cushman var. *compressa* - White, p. 196, pl. 28, figs. 3a-b.
- 1957 *Globigerina velascoensis* Cushman - Bolli, p. 71, pl. 15, figs. 9-11.
- 1960 *Globigerina velascoensis* Cushman - Bolli and Cita, p. 374, pl. 34, figs. 8a-c.
- 1962 *Globigerina velascoensis* Cushman - Hillebrandt, p. 120, pl. 11, figs. 4a-b.
- 1963 *Globigerina velascoensis* Cushman - Gohrbandt, p. 47, pl. 2, figs. 1-3.
- 1970a *Globigerina velascoensis* Cushman - Shutskaya, p. 94, pl. 4, figs. 3a-4c, 6a-c
- 1970 *Globigerina nana* Khalilov - Shutskaya, p. 90, pl. 2, figs. 2a-c.
- 1975 *Globigerina velascoensis* Cushman - Stainforth et al., p. 239, 240, text-fig. 96. 1; 96. 2-4.
- 1977 *Subbotina velascoensis* Cushman - Tjalsma, p. 510, pl. 4, fig 1.
- 1979 *Subbotina velascoensis* Cushman - Blow, p. 1292-1294, pl. 98, fig. 9.
- 1983 *Globigerina velascoensis* Cushman - Pujol, p. 645, pl. 2, fig. 9.
- 1985 *Subbotina velascoensis* Cushman - Snyder and Waters, p. 443, pl. 11, figs. 13-15.
- 1991 *Subbotina velascoensis* Cushman - Huber, p. 441, pl. 4, figs. 11, 12.
- 1995 *Subbotina velascoensis* Cushman - Basov, p. 165, pl. 2, figs. 15-17.

- 1997 *Subbotina velascoensis* Cushman - Berggren and Norris, pl. 5, figs. 2, 6,7,11.
- 1999 *Subbotina velascoensis* Cushman - Olsson et al., p. 33, fig. 13; pl. 29, figs. 1-12.
- 2008 *Subbotina velascoensis* Cushman - Handley et al., p. 20, text-figs. 2.1-3.
- 2011 *Subbotina velascoensis* Cushman - Nguyen et al., pl. 2, fig. 5.

Remarks: This form is characterized by radially compressed, axially elongated last formed chamber that hang upon the umbilicus, and the umbilical aperture is situated on a face that is oriented parallel to axis of coiling. Chambers are stacked close to each other with shallow intercameral sutures. Tangential dimension of the last formed chamber is equal to or larger than the rest of the test.

Stratigraphic range: From Zone P3b to Zone E3 (Pearson et al., 2006).

Occurrence: In this study this species is recorded in almost all samples throughout the measured section (GT-1 – GT-26).

5.2 Family Truncorotaloididae Loeblich and Tappan, 1961

This family is composed of non-spinose, muricate genera with various degree and positions of ornamentation. The unornamented parts of the surface have cancellate texture, much like genus *Praemurica*. The forms are low trochospiral and generally have conical chambers.

5.2.1 Genus *Morozovella* McGowran in Luterbacher, 1964

Type species: *Pulvinulina velascoensis* Cushman, 1925

Remarks: Genus *Morozovella* is characterized by a muricate wall structure and peripheral muricocarina. All members of this group show a low arch to slit shaped umbilical-extraumbilical aperture which often reaches periphery; the aperture is

positioned on the apertural face which is mostly recurved hiding the aperture in umbilical and sometimes in axial view. Although almost all Morozovellids are labeled as planoconvex, this definition is more of a relative approximation since Morozovellids show a variety of degree of spiral side convexity from totally flat (*M. velascoensis*) to slightly convex (*M. subbotinae*) to convex (*M. gracilis*); however, convexity is almost always asymmetrical with umbilical side being more convex. The muricocarina thickness and the degree of ornamentation on intercameral sutures are variable between species. Umbilical features also show a great variety from shallow and narrow (*M. aequa*) to wide umbilicus (*M. passionensis*); from decorated umbilical shoulders (*M. velascoensis*) to almost smooth ones (*M. edgari*). Number of chambers in the last whorl and growth rate are distinguishing features, so is the spiral chamber shape. The chambers on the umbilical side are always pie-shaped with varying central angles related to the growth rate and number of chambers in the last whorl. Axial chamber elongation and the angle between the coiling plane and the test sides are other features that are more characteristic in some forms than others. Two ornamentation styles are observed: full body ornamentation of variant degree (e.g. *M. aequa*), and ornamentation only on the periphery as the keel, on the sutures and on umbilical shoulders with smooth sides and spiral chamber walls (peripheral ornamentation, e.g. *M. velascoensis*).

Table 11 is the rapid recognition chart for the *Morozovella* genus.

Stratigraphic range: Danian-Lutetian (Pearson et al., 2006)

Morozovella acuta (Toulmin 1941)

Plate 7, Figures d-e

1941 *Globorotalia wilcoxensis* Cushman and Ponton var. *acuta* Toulmin, p. 608, pl. 82, figs. 6-8.

1957a *Globorotalia acuta* (Toulmin) - Loeblich and Tappan, p. 185, pl. 47, figs. 5a-c; pl. 55, figs. 4a-5c.

- 1964 *Globorotalia acuta* (Toulmin) - Luterbacher, p.686-689, text-figs. 101a-c, 102a- 104c.
- 1970a *Globorotalia velascoensis acuta* (Toulmin) - Shutskaya, p. 119-120, pl. 27, figs. 11a-c; pl. 28, figs. 4a-c; pl. 29, figs. 9a-c.
- 1971 *Globorotalia (Morozovella) acuta* (Toulmin) - Jenkins, p. 106, pl. 9, figs. 205- 207.
- 1985 *Morozovella acuta* (Toulmin) - Toumarkine and Luterbacher, p. 111, text-fig. 14.
- 1991 *Morozovella acuta* (Toulmin) - Van Eijden & Smit, p. 113.
- 1999 *Morozovella acuta* (Toulmin) - Olsson et al., p. 55, pl. 45, figs. 1-14.
- 2009 *Morozovella acuta* (Toulmin) - Obaidalla et al., p. 4, pl. 2, figs. 7-8.

Remarks: This species is characterized by an especially flat spiral side and a distinct carina. Chamber shape is variable from trapezoidal to crescent, generally not more than six in the last whorl, separated with distinctly ornamented sutures on spiral side. Test sides are steep (small angle between test sides and coiling plane). Chambers are elongated in axial dimension, producing a deep umbilicus of variant width. Sutures between umbilical shoulders and on test sides are generally shallowly depressed. This species is included in the peripherally ornamented group.

This species is found sporadically and in small numbers in the Haymana Basin, and the only *M. velascoensis* group representative.

Stratigraphic range: Zone P4b to E2 (Pearson et al., 2006).

Occurrence: This species shows sporadic occurrence between GT-1 – GT-21.5.

Table 11: Rapid recognition chart for species of genus *Morozovella*. * for species identified in this study

Species	Ornamentation	Equatorial Outline	Axial outline	# of chambers	Chamber Growth Rate	Spiral Chamber Shape	Spiral Intercameral Sutures	Umbilical Chamber Height	Umbilicus
* <i>M. acuta</i>	Peripheral ornamentation	Slightly lobulate	Planoconvex	5	Moderate	Semicircular to trapezoidal	Curved, ornamented	High	Deep, variant width
<i>M. acutispira</i>	Full body ornamentation; initial carina thick; initial spire especially ornamented	Lobulate to slightly lobulate, circular	Biconvex, lenticular	4-6	Very low to low	Bean shaped to semicircular	Curved, ornamented	Low	Deep, narrow
* <i>M. aequa</i>	Full body ornamentation	Lobulate to slightly lobulate, oval or subquadrate	Planoconvex to asymmetrically biconvex	4	Very high	Bean shaped to subquadrate	Curved, depressed	High	Shallow, narrow
<i>M. allisonensis</i>	Peripheral ornamentation, especially on initial whorls	Weakly to non-lobulate, circular to ovate	Planoconvex to slightly biconvex	5-9	Low to moderate	Trapezoidal to subquadrate on spiral side	Strongly to weakly curved, varying from raised to slightly depressed	Very low to low	Variant
<i>M. angulata</i>	Full body ornamentation; keel non-distinctive, not sharp	Lobulate, circular to ovate	Planoconvex to asymmetrically biconvex; edge subacute	4-6	Moderate to high	Bean shaped to semicircular	Curved, depressed	Moderate to high	Narrow deep
* <i>M. apantasma</i>	Full body ornamentation, irregular; keel non-distinctive, not sharp	Lobulate to slightly lobulate	Planoconvex, edge subacute to subangular	4-5	Low to moderate	Bean shaped to semicircular	Curved, depressed	High	Narrow, deep

Table 11 (Continued)

Species	Ornamentation	Equatorial Outline	Axial outline	# of chambers	Chamber Growth Rate	Spiral Chamber Shape	Spiral Intercameral Sutures	Umbilical Chamber Height	Umbilicus
<i>M. aragonensis</i>	Full body ornamentation; ornamentation thick and merged producing smooth surfaces on the keel and spiral sutures, and umbilical tips extra ornamented	Circular, weakly to nonlobulate	Planoconvex	5-7	Moderate	Trapezoidal	Slightly raised and thickly ornamented, strongly curved	High	Deep, narrow blunt-tipped muricae scattered over chambers tips
<i>M. caucasica</i>	Peripheral ornamentation	Slightly lobulate to nonlobulate	Planoconvex; strongly muricate and distinct keel	6-8	Low	Trapezoidal to subquadrate	Curved, muricate, elevated	Moderate	Large, deep, circumumbilical chamber tips strongly muricate
<i>M. conitruuncana</i>	Peripheral ornamentation	Circular, weakly to nonlobulate	Planoconvex	5-7	very low	Trapezoidal	Depressed, curved	High	Large, deep
<i>M. crater</i>	Peripheral ornamentation	Weakly lobulate to lobulate, ovate	Planoconvex	4.5-5	Moderate	Bean shaped to trapezoidal	Curved, ornamented	Moderate to high	Deep, wide
* <i>M. edgari</i>	Sparse muricae on the last formed chambers, higher concentration on earlier ones	Weakly lobulate, circular to ovate	Biconvex	5-6	Low to moderate	Trapezoidal	Curved, flush with test	Moderate	Narrow

Table 11 (Continued)

Species	Ornamentation	Equatorial Outline	Axial outline	# of chambers	Chamber Growth Rate	Spiral Chamber Shape	Spiral Intercameral Sutures	Umbilical Chamber Height	Umbilicus
<i>M. formosa</i>	Peripheral ornamentation; keel strongly muricate	Lobulate, subcircular	Planoconvex	6	Low	Trapezoidal to semicircular	Curved, highly ornamented, rised	High	Deep, variant width
* <i>M. grallicis</i>	Peripheral muricae	Weakly lobulate to lobulate	Asymmetrically biconvex	5-6	Low to moderate	Bean shaped to semicircular	Curved, highly ornamented, rised	Moderate to high	Narrow, deep
<i>M. lensiformis</i>	Full body ornamentation; highly developed muricae in some specimens produce a globular test	Subquadrate to subcircular test, weakly lobulate	Asymmetrically biconvex to globular	4-4.5	Moderate to high	Trapezoidal to bean shaped	Depressed	Moderate to high	Narrow, blocked bu muricae in globular specimens
* <i>M. marginodentata</i>	Full body ornamentation; muricocarina dentate	Lobulate, ovate	Biconvex	4-5	Moderate to high	Bean shaped to semicircular	Curved, strongly muricate, raised	Low	Narrow, deep
* <i>M. occlusa</i>	Peripheral ornamentation	Circular, lobulate to slightly lobulate	Biconvex	4-6	Low to moderate	Trapezoidal	Elevated, ornamented, tangentially curved	Low	Narrow, deep
<i>M. pasionensis</i>	Peripheral ornamentation	Circular, lobulate to slightly lobulate	Planoconvex to asymmetrically biconvex	5-7	Very low	Trapezoidal	Elevated, ornamented, curved	Low	Wide, shallow

Table 11 (Continued)

Species	Ornamentation	Equatorial Outline	Axial outline	# of chambers	Chamber Growth Rate	Spiral Chamber Shape	Spiral Intercameral Sutures	Umbilical Chamber Height	Umbilicus
<i>M. praeangulata</i>	Full body ornamentation, no muricocarina	Lobulate	Spiral side slightly convex	5-6	Low to moderate	Crescentic	Curved, depressed	High	Narrow deep
* <i>M. subbotinae</i>	Full body ornamentation, distinctly carinate	Strongly lobulate, ovate	Planoconvex to weakly biconvex	4-5	High	Semicircular to bean shaped	Curved, tangential, partly ornamented	High	Deep, narrow to moderately wide
<i>M. velascoensis</i>	Peripheral ornamentation, keel distinctly thick and muricate	Circular, slightly lobulate	Planoconvex	6-7	Very low to low	Trapezoidal	Raised, ornamented and curved	Low to moderate	Wide, surrounded by fused muricae on umbilical shoulders

Morozovella aequa (Cushman and Renz, 1942)

Plate 5, Figure 1; Plate 6, Figures a-c

- 1942 *Globorotalia crassata* (Cushman) var. *aequa* Cushman and Renz, p. 12, pl. 3, fig. 3a-c.
- 1949 *Globorotalia (Truncorotalia) crassata* (Cushman) var. *aequa* Cushman and Renz.- Cushman and Bermudez, p. 37, pl. 7, figs. 7-9.
- 1957a *Globorotalia aequa* (Cushman and Renz) - Bolli, p. 74, pl. 17, figs. 1-3; pl. 18, figs. 13-15.
- 1957a *Globorotalia aequa* (Cushman and Renz) - Loeblich and Tappan, p. 186, pl. 59, figs. 6a-c; pl. 64, figs. 4a-c.
- 1962 *Globorotalia (Truncorotalia) aequa aequa* (Cushman and Renz) - Hillebrandt, p. 133-134, pl. 13, figs. 1a-c.
- 1975b *Globorotalia aequa* (Cushman and Renz) - Luterbacher, p. 64, pl. 2, figs. 22-24.
- 1985 *Morozovella aequa* (Cushman and Renz) - Snyder and Waters, p. 446, pl. 7, figs. 179 5-7.
- 1985 *Morozovella aequa* (Cushman and Renz) - Toumarkine and Luterbacher, p. 113, figs 15. 1-3.
- 1990 *Morozovella aequa* (Cushman and Renz) - Stott & Kennett, p. 560 pl. 6, figs. 13-15.
- 1995 *Morozovella aequa* (Cushman and Renz) - Lu & Keller, p. 102 pl. 1, figs. 15.
- 1997 *Morozovella aequa* (Cushman and Renz) - Berggren and Norris, p. 103 Plate 16, figures 22-24
- 1999 *Morozovella aequa* (Cushman and Renz) - Olsson et al., p. 57; p. 15, figs. 11, 12, 15; pl. 47, figs. 1-16.

2006 *Morozovella aequa* (Cushman and Renz) - Pearson et al., p. 345, pl. 11-1, figs. 1- 8.

2007 *Morozovella aequa* (Cushman and Renz) - Luciani et al., p. 206, pl. 1, figs. 4, 7, 8.

2011 *Morozovella aequa* (Cushman and Renz) - Nguyen et al., pl. 1, fig. 7.

Remarks: A tightly coiled full body ornamented form with firmly stacked chambers, this form is one of the most abundant in late Paleocene-early Eocene assemblages. The chambers are tangentially elongated and radially compressed, axial length variant. The umbilicus is nearly closed, the aperture not visible. Intercameral sutures on spiral side are depressed shallowly, also are so on umbilical side. About four chambers are in the last formed whorl with great chamber growth rate, the last one being the largest: tangential length of the last chamber equals the rest of the test.

Stratigraphic range: Zone P4c to E5 (Pearson et al., 2006).

Occurrence: This species is a major component of the studied assemblage throughout the measured section (GT-1 – GT-26).

Morozovella apantesma (Loeblich and Tappan 1957)

Plate 5, Figures j-k

1957a *Globorotalia apantesma* Loeblich and Tappan, 187, pl. 48: fig. la-c, pl. 55: fig. la-c, pl. 58: fig. 4a-c (paratype), pl. 59: fig. la-c

1971 *Globorotalia (Morozovella) apantesma* (Loeblich and Tappan) - Jenkins, 102, pl. 8: figs. 186-188

1984 *Globorotalia (Morozovella) apantesma* (Loeblich and Tappan) - Belford, 9, pl. 16: figs. 1-8

1979 ?*Globorotalia (Morozovella) apantesma* (Loeblich and Tappan) –Blow, 988, pl. 251: fig. 2

- 1991b *Acarinina apantesma* (Loeblich and Tappan) - Huber, 446, pl. 4: figs. 1, 2
- 1995 Not *Morozovella apantesma* [sic] Lu and Keller, 102, pl. 1: figs. 18, 19
- 1999 *Morozovella apantesma* (Loeblich and Tappan) – Olsson et al., 59, pl. 17: figs. 1-3, pl. 49: figs. 1-15

Remarks: A rather indistinct species with underdeveloped keel, this species is found in the late Paleocene-early Eocene assemblages of Haymana in small numbers. The spiral side has depressed intercameral sutures between variant shapes of chambers. The umbilical tips of this form are generally rounded.

Stratigraphic range: Zone P4 to E2 (Pearson et al., 2006).

Occurrence: Occurrence of this species is sporadic and in small numbers between GT-1 – GT-25.

Morozovella edgari (Premoli Silva and Bolli, 1973)

Plate 7, Figures a-c

- 1973 *Globorotalia edgari* Premoli Silva and Bolli, p. 526, pl. 7, figs. 10-12; pl. 8, figs. 1-12.
- 1979 *Globorotalia (Morozovella) finchi* Blow, p. 999, pl. 99, figs. 6-11.183
- 1985 *Morozovella edgari* (Premoli Silva and Bolli) – Toumarkine and Luterbacher, p. 114, text-figs. 15.6a-c.
- 2001 *Morozovella edgari* (Premoli Silva and Bolli) – Kelly et al., p. 509, text-fig. 1D-F, 3C
- 2006 *Morozovella edgari* (Premoli Silva and Bolli) – Pearson et al., p. 362, pl. 11.6, figs. 1-16.

Remarks: This species has an indistinct keel, but a nearly nonlobulate equatorial periphery. On spiral side the intercameral sutures are very shallow to shallow, on

umbilical side they are depressed. The chamber growth rate is high, only 5-6 chambers in the last whorl.

Stratigraphic range: Pearson et al. (2006) restricts this species in mid Zone E2-top of Zone E3, however, according to Molina et al. (1996) and Lu et al. (1998), *M edgari* appears in upper Zone P4.

Occurrence: In this study this species is first encountered before the first specimen of *P. wilcoxensis*, in Zone E1, in sample GT-19, and is present in the samples until the end of the measured section (GT-26).

Morozovella gracilis (Bolli, 1957b)

Plate 6, Figures g-i

1957b *Globorotalia formosa gracilis* Bolli, 75-76, pl. 18, figs. 4-6.

1970b *Globorotalia formosa gracilis* (Bolli) - Shutskaya, 118-120, pl. 14, figs. 8a-c.

1971 *Globorotalia (Morozovella) gracilis* (Bolli) - Jenkins, 105, pl. 9, figs. 202-204.

1971b *Morozovella gracilis* (Bolli) - Berggren, 76, pl.5, figs. 7-8.

1985 *Morozovella formosa gracilis* (Bolli) - Snyder and Waters, 446-447, pl. 8, figs. 7-9.

1985 *Morozovella formosa gracilis* (Bolli) - Toumarkine and Luterbacher, 12, text-figs. 15:12a-c.

1991b *Morozovella gracilis* (Bolli) - Huber, 440, pl.4, fig. 8.

1995 *Morozovella gracilis* (Bolli) - Lu and Keller, 102, pl.1, fig. 9.

2006 *Morozovella gracilis* (Bolli) - Pearson et al., p. 366, pl. 11.8, figs. 1-16.

2011 *Morozovella formosa-gracilis* (Bolli) - Nguyen et al., pl. 2, figs. 7-8.

Remarks: A distinct keel, ornamented spiral intercameral sutures and semicircular spiral chambers characterize this species. It is distinguished from *M. subbotinae* by 5-6 chambers in the last whorl instead of 4-4.5, and ornamented spiral sutures instead of depressed. It is different from *M. formosa* with a convex spiral side, instead of flat.

Stratigraphic range: Zone P5 to E4 (Pearson et al., 2006).

Occurrence: In this study this species occurs between GT-14 – GT- 25.

Morozovella marginodentata (Subbotina, 1953)

Plate 6, Figures j-l

- 1953 *Globorotalia marginodentata* Subbotina, 212, pl. 17: figs. 14; pl. 18: figs. 1a-c; pl. 18: figs. 2a-c; pl. 18: figs. 3a-c
- 1962 *Globorotalia (Truncorotalia) aequa marginodentata* (Subbotina) - Hillebrandt, 135, pl. 13: figs. 9a-11
- 1963 *Truncorotalia marginodentata marginodentata* (Subbotina) - Gohrbandt, 1963:62, pl. 6: figs. 4-6
- 1963 *Truncorotalia marginodentata aperta* Gohrbandt, 1963:62, pl. 5: figs. 10-15
- 1964 *Globorotalia marginodentata* (Subbotina) - Luterbacher, 673, text-figs. 75a-76c; 77a-78c; 79a-c; 80a-c; 81a-82c; 83a-c; 84a-c
- 1970 *Globorotalia marginodentata* (Subbotina) - Samanta, 626, pl. 96: figs. 3,4
- 1971 *Globorotalia (Morozovella) aequa marginodentata* (Subbotina) - Jenkins, 101, text-figs. 177-179
- 1971 *Morozovella marginodentata* (Subbotina) - Berggren, 76, pl. 5: fig. 9
- 1975a *Globorotalia marginodentata* (Subbotina) - Luterbacher, 727, pl. 2: figs. 6a-c
- 1975b *Globorotalia marginodentata* (Subbotina) - Luterbacher, 65, pl. 4: figs. 4-6

- 1977 *Morozovella marginodentata* (Subbotina) - Berggren, 241, chart No. 8
- 1979 *Globorotalia (Morozovella) subbotinae* (s.l) forma *marginodentata* (Subbotina) - Blow, 1024-1026, pl. 139: figs. 1-9 and pl. 140: figs.1-3
- 1985 *Morozovella marginodentata* (Subbotina) - Snyder and Waters, 460, pl. 8, figs. 13a-14c
- 2000 *Morozovella marginodentata* (Subbotina) - Warraich, Ogasawara and Nishi, 293, figs. 17. 4,5,10
- 2001 *Morozovella marginodentata* (Subbotina) - Warraich and Ogasawara, 40, fig. 10. 7-9

Remarks: This species is very similar to *M. subbotinae* in many aspects like number of chambers in the last whorl and the umbilical width, and differentiates from it by the lower chamber heights hence lower axial size of test, and a more irregular, dentate carina (Pl. 6, fig. g). In this study the encountered *M. marginodentata* specimens are rather large.

Stratigraphic range: Zone P5 to E5 (Pearson et al., 2006).

Occurrence: Occurs between GT-16 – 22 interval.

Morozovella subbotinae (Morozova, 1939)

Plate 6, Figures d-f

- 1939 *Globorotalia subbotinae* Morozova, 80, pl. 2, figs. 16-17.
- 1943 *Globorotalia rex* Martin, p. 117, pl. 8, figs. 2a-c.
- 1947 *Globorotalia crassata* (Cushman) - Subbotina, p. 119, pl. 5, figs. 31-33.
- 1953 *Globorotalia crassata* (Cushman) - Subbotina, p. 211, 212, pl. 17, figs. 7a-c; pl. 17, figs. 13a-c.

- 1964 *Globorotalia subbotinae* (Morozova) - Luterbacher, p. 676, text-figs. 85, 86, 89, 90.
- 1970a *Globorotalia subbotinae* (Morozova) - Shutskaya, p. 119-120, pl. 13, figs. 6a-c; pl. 14, figs. 6a-c.
- 1971 *Globorotalia (Morozovella) aequa rex* (Martin) - Jenkins, p. 101-102, pl. 7, figs. 180-182.
- 1985 *Morozovella subbotinae* (Morozova) - Synder and Waters, p. 442-443, pl. 9, figs. 10-12.
- 1985 *Morozovella subbotinae* (Morozova) - Toumarkine and Luterbacher, p. 112, textfigs. 15: 9a-c.
- 1993 *Morozovella subbotinae* (Morozova) - Lu and Keller, p. 123, pl. 4, fig. 19.
- 1998 *Morozovella subbotinae* (Morozova) - Lu et al., p. 212, pl. 1, figs. 1-3.
- 1999 *Morozovella subbotinae* (Morozova) – Olsson et al., p. 65, fig. 24; p. 54, figs. 1-12.
- 2001 *Morozovella subbotinae* (Subbotina) - Warraichand Ogasawara, p. 41, figs. 10.16-18.
- 2006 *Morozovella subbotinae* (Morozova) – Pearson et al., p. 370, pl. 11-1, figs. 9-16.
- 2007 *Morozovella subbotinae* (Morozova) – Luciani et al., p. 206, pl. 1, figs. 5, 6.
- 2008 *Morozovella subbotinae* (Morozova) – Handley et al., p. 20, text fig. 2.6, 9.189
- 2011 *Morozovella subbotinae* (Morozova) -Nguyen et al., pl. 1, fig. 2.
- 2014 *Morozovella subbotinae* (Morozova) -Bornemann et al., p. 71, text fig. 2.1.

Remarks: One of the most abundant Morozovellid species studied interval, this species resembles *M. aequa* in wall textural properties and number of chambers in

the last whorl. The surface is covered with short muricae, and the keel is prominent. Chamber tips on the umbilical side are widely separated, providing a wider umbilicus than that of *M. aequa* which is narrow to almost closed. Chamber growth rate is smaller than that of *M. aequa*. Spiral chamber shape is semicircular as in *M. gracilis*, but the intercameral sutures may be depressed or partly ornamented. Equatorial outline is lobulate.

Stratigraphic range: There are three cases for this form's stratigraphic range: 1. It overlaps with *G. pseudomenardii* on a short interval (e.g. Aubry et al., 2007), 2. It is coincident with *G. pseudomenardii*'s highest occurrence (e.g. Berggren and Pearson, 2006; Pearson et al., 2006; and Olsson et al., 1999), 3. It first appears slightly later than highest occurrence of *G. pseudomenardii* (e.g. Canudo and Molina (1992)). In this study first case is observed with *G. pseudomenardii* occurring latest in sample GT-10, while first *M. subbotina* specimens found in samples GT-9 – GT-26 interval.

Occurrence: Occurs between GT-1 and GT-10.

5.2.2 Genus *Acarinina* Subbotina, 1953

Type species: *Acarinina acarinata* Subbotina, 1953

Remarks: Genus *Acarinina* is characterized by muricate wall structure, generally with especially pronounced pustules at umbilical tips of chambers, and cancellate texture beneath the pustules. The degree of ornamentation changes between species. Some forms develop a more delicate surface texture made up of thin and long muricae, while others use fused and thick ornamentations especially on the umbilical tips. Overall morphology is variable from tightly coiled globular forms (e.g. *A. coalingensis*) to quadrate forms (e.g. *A. bullbrooki*). The chamber shape changes from bean shaped to trapezoidal on spiral side, chambers are generally inflated on umbilical side. The crescentic to bean shaped chambers (longer tangential size than radial) is signature of many Acarininids, and is a shared feature with *Igorina*. Other Acarininids have trapezoidal chambers (radial and tangential sizes similar to each other, as in *A. pentacamerata*).

In many, aperture is located in an umbilical-extraumbilical position, on an apertural face generally parallel to coiling axis hence it is not visible in umbilical view; however, the apertural face is distinctly curved. This feature distinguishes Acarininids with 4 chambers in the last whorl from Parasubbotinids, given that the wall structure is not preserved. Several Acarininids, especially globular, compact ones, are equipped with a slit shaped aperture hidden in between the suture of last chamber and the rest of the test, which is the criterion for distinction from Subbotinids (whose aperture are arched and umbilical) in poor wall texture preservation conditions.

4 species span through the PETM, 3 of which are Acarininids: *A. africana*, *A. multicamerata*, and *A. sibiyaensis*. Here, only one of these so called excursion taxa was discovered.

Table 12 is the rapid recognition chart for Paleocene-Eocene *Acarinina* species.

Stratigraphic range: Danian to Rupelian (Pearson et al., 2006)

Acarinina angulosa (Bolli, 1957a)

Plate 1, Figures d, e

1957a *Globigerina soldadoensis angulosa* Bolli, 71, pl. 16: figs. 4-6

1957b *Globigerina soldadoensis angulosa* (Bolli) - Bolli, 1957b:162, pl. 35: figs. 8a-c

1965 *Acarinina soldadoensis angulosa* (Bolli) - Hillebrandt, 345, pl. 5: fig. 11

1974 *Acarinina soldadoensis angulosa* (Bolli) - Fleisher, 1014, pl. 4: fig. 1

1972 *?Turborotalia (Acarinina) soldadoensis angulosa* (Bolli) - Samuel et al., 190, pl. 68, figs. 1a-c

1979 *Muricoglobigerina soldadoensis angulosa* (Bolli) - Blow, 1122, pl. 109: fig. 9, pl. 131: figs. 4-5

Table 12: Rapid recognition chart for species of genus *Acarinina*. * for species identified in this study

Species	Ornamentation	Equatorial Outline	Axial Outline	# of Chambers	Chamber Growth Rate	Chamber Shape	Spiral Intercameral Sutures	Umbilicus
<i>A. africana</i>	Thin pustules cover the surface, especially more on the earlier chambers, at least the last few chambers have muricocarina	Strongly lobulate, ovate	Margin acute with muricocarina, biconvex	4-6	Moderate to high, last chamber especially large	Ovate, semicircular, lensoidal	Gently curved, depressed	Narrow
<i>A. alticonica</i>	Densely muricate, particularly around umbilicus	Weakly lobulate test, circular outline	Biconvex to subspherical	5	Low	Tangentially longer than radially broad, umbilically inflated and embracing, strongly appressed	Weakly curved and indistinct	Narrow, deep umbilicus
* <i>A. angulosa</i>	Pustules especially on umbilical side	Subquadrate, lobulate	Periphery subangular, spiral side flat to weakly convex	4-5	Low	Tangentially longer than radially broad, axially elongate, embracing	Curved, oblique	Moderately wide, open, deep
<i>A. aspensis</i>	Coarse muricae especially concentrated on umbilical side	Lobulate to weakly lobulate	Periphery subrounded, spiral side flat to weakly convex	6-8	Moderate	Trapezoidal on spiral side, triangular/pie-shaped on umbilical side	Weakly curved to radial, depressed	Deep and wide
<i>A. boudreauxi</i>	Heavily calcified, wall with blocky fused muricae	Subquadrate, slightly lobulate to nonlobulate	Planoconvex, subacute periphery	4.5-5	Low to moderate	Tangentially longer than radially broad, axially elongate, embracing	Oblique, slightly depressed to flush	Narrow, deep

Table 12 (Continued)

Species	Ornamentation	Equatorial Outline	Axial Outline	# of Chambers	Chamber Growth Rate	Chamber Shape	Spiral Intercameral Sutures	Umbilicus
<i>A. bullbrooki</i>	Strongly muricate especially on chamber tips	Quadrate, weakly lobulate	Subacute, pseudocarcinate in some specimens, flat spiral side	4	Low to moderate	Tangentially longer than radially broad, axially elongate, embracing	Oblique to radial, slightly depressed	Narrow to moderately wide
* <i>A. coalingensis</i>	Dense, blunt muricae	Subquadrate to rounded	Broadly rounded to subangular periphery	3-4	High	Globular; tangentially longer than radially broad; axially elongate; strongly appressed	Shallow	Very narrow
<i>A. collectea</i>	Densely muricate	Circular, lobulate	Weakly convex to flat spiral side; rounded to subangular peripheral margin	5	Very low-low	Rounded on spiral side, pie-shaped on umbilical side	Curved, depressed	Narrow, deep
<i>A. cuneicamerata</i>	Densely muricate	Circular, lobulate	Flat spiral side; rounded to subangular peripheral margin	5-6	Low	Wedge shaped-trapezoidal on spiral side; pie-shaped on umbilical side	Straight to weakly curved	Wide, deep
<i>A. echinata</i>	Coarsely muricate	Weakly to moderately lobate	Rounded periphery, biconvex	3.5-4	High	Globular	Radial, weakly depressed to indistinct	Often covered by umbilical bulla

Table 12 (Continued)

Species	Ornamentation	Equatorial Outline	Axial Outline	# of Chambers	Chamber Growth Rate	Chamber Shape	Spiral Intercameral Sutures	Umbilicus
<i>*A. esnaensis</i>	Densely muricate, particularly along periphery	Subquadrate, lobulate	Spiral side flat to slightly curved, periphery subrounded	4-4.5	Moderate to high	Egg-shaped chambers axially elongate	Depressed, straight to slightly curved	Small, open
<i>*A. esnehensis</i>	Muricate, with strong concentration of muricae around umbilicus	Lobulate	Spiral side slightly curved, periphery rounded	5-6	Moderate to high	Trapezoidal on spiral side	Incised, radial to only slightly curved	Open, deep and generally relatively wide
<i>A. interposita</i>	Densely muricate on both sides, particularly along periphery	Lobulate	Planoconvex, rounded periphery	4	Moderate	Globular, embracing, appressed	Radial, straight, only slightly depressed	Narrow and deep
<i>A. mcgowrani</i>	Densely muricate	Rounded, moderately lobulate	Globular test	3-4	Moderate to High	Globular, embracing, appressed	incised, weakly curved	Deep umbilicus, commonly covered by bulla
<i>*A. mckannai</i>	Strongly muricate on the umbilical surface	Rounded, moderately lobulate	Broadly rounded periphery, spiral side slightly convex	4.5-6	Low	Tangentially longer, radially compressed, axially elongate, appressed	Slightly curved, gently depressed	Deep and large

Table 12 (Continued)

Species	Ornamentation	Equatorial Outline	Axial Outline	# of Chambers	Chamber Growth Rate	Chamber Shape	Spiral Intercameral Sutures	Umbilicus
<i>A. medizsai</i>	Finely muricate	Quadrato to subcircular in outline, weakly to moderately lobate	Biconvex, rounded periphery	4-6	Low	Globular	Moderately depressed, radial	Narrow to broad depending on the coiling tightness
* <i>A. nitida</i>	Moderately muricate, particularly on umbilical side	Subcircular to subquadrate, weakly lobulate	Spiral side flat to slightly convex, periphery subangular to subrounded	4	Low	Tangentially longer, radially compressed, axially elongate, appressed	Curved, slightly depressed	Narrow to moderately wide
<i>A. penta-camerata</i>	Densely muricate, concentration of muricae around circumumbilical region	Weakly lobulate test, circular outline	Weakly biconvex, peripheral margin rounded	5	Moderate	Rounded, inflated	Radial, weakly retorse	Moderately wide, deep
<i>A. praetopilensis</i>	strongly muricate	Subquadrate, lobulate	high angulo-conical, subacute margin with concentration of partially fused muricae	4	High	Tangentially longer than radially broad, axially elongate, embracing	Radial to weakly curved	Deep and wide

Table 12 (Continued)

Species	Ornamentation	Equatorial Outline	Axial Outline	# of Chambers	Chamber Growth Rate	Chamber Shape	Spiral Intercameral Sutures	Umbilicus
<i>A. primitiva</i>	Coarsely and bluntly muricate	Subquadrate	Subangular margin	3-4	Moderate	Tangentially longer than broad, embracing, appressed	Slightly depressed, generally obscured by muricate ornamentation	Narrow, deep
<i>A. pseudo-subphaerica</i>	Strongly muricate on the umbilical surface	Slightly lobulate, circular	Compact, subspherical	4-6	Low	moderately inflated, radially compressed	Depressed	Open if not covered by a small, sparsely muricate final chamber
* <i>A. pseudo-topilensis</i>	Densely muricate, concentrated along the peripheral margin	Subquadrate to suboval, weakly lobulate	planoconvex; spiral side slightly elevated; edge angular to subangular	4	Moderate	tangentially longer than radially broad, axially elongated; last chamber markedly rectangular	Oblique to curved, slightly depressed	Small, deep
<i>A. puncto-carinata</i>	Strongly muricate, short blunt muricae concentrated on umbilical shoulders, punctate pseudocarina	Subquadrate to quadrate	Flat spiral side; subacute periphery pseudocarinate	4	Low to moderate	Wedge shaped, distinctly longer axially than radially broad	Radial to slightly curved, distinctly incised	Open, deep and generally relatively wide

Table 12 (Continued)

Species	Ornamentation	Equatorial Outline	Axial Outline	# of Chambers	Chamber Growth Rate	Chamber Shape	Spiral Intercameral Sutures	Umbilicus
<i>A. quetra</i>	Moderately to strongly muricate with concentration of muricae along peripheral margin	Subquadrate to quadrate, lobulate	Planoconvex, periphery muricocarinat discontinuously	4	Low to moderate	Anguloconical chambers tangentially longer than radially broad, axially elongated	Curved, slightly depressed to indistinct	Relatively wide, deep
<i>A. rohri</i>	Densely muricate, slight concentration of muricae around margin	Lobulate, subcircular	Flat spiral site, truncate conical; periphery subrounded to angular	5	Low	Hemispherical to wedge shaped chambers; secondary apertures on spiral side	Straight to weakly recurved, depressed	Narrow and relatively deep
* <i>A. sibaiyaensis</i>	Thin pustules cover the surface, especially more on the earlier chambers	Lobulate, subcircular	Spiral side flat to slightly convex, periphery subrounded to rounded	5	Moderate to high, last chamber especially large	Inflated, subtriangular to rounded	Depressed and radial	
* <i>A. soldadoensis</i>	Moderately to strongly muricate	Lobulate, subcircular to subquadrate	Spiral side flat to moderately convex, periphery subangular to subrounded	4-5	Moderate to high	Radially compressed in variant degrees, axially elongated	Deep and curved and/or tangential	Deep and relatively wide umbilicus

Table 12 (Continued)

Species	Ornamentation	Equatorial Outline	Axial Outline	# of Chambers	Chamber Growth Rate	Chamber Shape	Spiral Intercameral Sutures	Umbilicus
<i>A. strabocella</i>	Weakly pustulose	Lobulate, subcircular	Spiral side slightly convex, periphery broadly rounded to subangular	5-6	Low	Subcircular to trapezoidal, umbilically inflated	Curved to radial, depressed	Broad and open
* <i>A. subphaerica</i>	Pustulose, concentrated on umbilical area	Circular outline	Globular, almost spherical with highly elevated spiral side	5-6	Low	Trapezoidal, radially compressed, umbilically directed, embracing	Oblique, indistinct	Narrow and deep
<i>A. topilensis</i>	Strongly muricate, concentration of muricae along peripheral margin	Subquadrate, lobulate	Spiral side flat, periphery angular to acute	3.5-4.5	Moderate	Trapezoidal, radially broad, axially elongate, disjunct	Curved and depressed	Narrow, deep
* <i>A. wilcoxensis</i>	Densely muricate, slight concentration of muricae around margin	Oval, moderately lobulate	Spiral side flat, periphery angular to subrounded	4	High	Oval in spiral view, umbilically inflated. Last two chambers may be flattened dorsally	Depressed and curved	Narrow, deep

1984 *Muricoglobigerina soldadoensis angulosa* (Bolli) - ?Belford, 30, pl. 22: figs. 9-12

2006 *Acarinina angulosa* Bolli - Pearson et al. 268, pl. 9.3; fig. 11-16

Remarks: A quadrate Acarininid, this species have chambers in the last whorl positioned in such an angle in the umbilical view the intercameral sutures do not meet at the center, they are a bit offset. The chambers are trapezoidal to slightly tangentially longer on the spiral side, axially inflated, 4-5 in the last whorl, all similar in size.

Stratigraphic Range: Zone P5 to E7 (Pearson et al., 2006).

Occurrence: This species is present in small numbers in the GT-17.25 – GT-24 interval.

Acarinina coalingensis (Cushman and Hanna, 1927)

Plate 1, Figures a-c

1927 *Globigerina coalingensis* Cushman and Hanna. p. 219, pl. 14, fig. 4.

1947 *Globoquadrina primitiva* Finlay. p. 291, pl. 8, figs. 129-134.

1953 *Acarinina triplex* Subbotina. p. 230, pl. 23, figs. 1-5.

1969b *Acarinina coalingensis* (Cushman and Hanna) - Berggren, p. 152, pl. 1, figs. 27-29.

1979 *Acarinina triplex* Blow. p. 963, pl. 97, figs. 8, 9.

1991b *Acarinina coalingensis* (Cushman and Hanna) - Huber, p. 439, pl. 3, fig. 2.

1992 *Acarinina coalingensis* (Cushman and Hanna) - Berggren, p. 563, pl. 2, fig. 3.

1993 *Acarinina triplex* (Subbotina) - Pearson et al. pl. 1, figs. 11-12.

- 1995 *Acarinina triplex* (Subbotina) - Lu and Keller. pl. 2, figs. 4-5.
- 1999 *Acarinina coalingensis* (Cushman and Hanna). - Olsson et al., p. 47; pl. 39, figs. 1-16.
- 2006 *Acarinina coalingensis* (Cushman and Hanna) - Pearson et al. p. 276, pl. 9.7, figs. 1-16.
- 2008 *Acarinina coalingensis* (Cushman and Hanna) - Handley et al., p. 20, text fig. 2.8.

Remarks: This species is the only one in late Paleocene-early Eocene interval with 3-3.5 chambers in the last whorl, with great chamber growth rate. The last chamber is embracing and large as in a Subbotinid. The chambers are compressed to each other, the umbilicus is very narrow. The aperture is a slit, hidden at the intercameral suture. The pustulose wall texture is the main criteria to distinguish *A. coalingensis* from Subbotinids; moreover, the umbilical-extraumbilical slit aperture, which is barely seen in umbilical view, instead of an umbilical arch is another difference.

Stratigraphic range: From P4c to E13 (Pearson et al., 2006).

Occurrence: This species is present in GT-1 – GT-26 interval.

Acarinina esnaensis (Leroy, 1953)

Plate 1, Figures f, i, j

- 1953 *Globigerina esnaensis* Leroy. p. 31, pl. 6, figs. 8-10.
- 1956 *Truncorotalia esnaensis* (Leroy) -Said and Kenaway, p. 151, pl. 6, figs. 7a-b.
- 1957 *Globorotalia esnaensis* (Leroy) -Loeblich and Tappan, p. 189, pl. 61, figs. 1a-2c, 9a-c; pl. 57, figs. 7a-c.
- 1959 *Globigerina esnaensis* Leroy. – Nakkady, p. 461, pl. 3, figs. 2a-c.
- 1963 *Globigerina esnaensis* Leroy. – Gohrbandt, p. 49, p. 2, figs. 19-21.

- 1965 *Globigerina esnaensis* Leroy. – McGowran, p. 61, 63, pl. 6, fig. 5, text-fig. 10.
- 1970 *Globorotalia esnaensis* (Leroy) -Samanta, p. 624, pl. 95, figs. 7-8.
- 1971 *Globorotalia (Acarinina) esnaensis* (Leroy) -Jenkins, p. 82, pl. 3, figs. 84-86.
- 1977 *Acarinina esnaensis* (Leroy) -Berggren, p. 249, chart 10.
- 1991 *Acarinina esnaensis* (Leroy) -Huber, p.439, pl. 1, figs. 13-15.
- 2006 *Acarinina esnaensis* (Leroy) -Pearson et al., p. 286, pl. 9.11, figs. 1-12.

Remarks: This species has 4 chambers in the last whorl, and the coiling is loose so that the umbilicus is deep. Chambers are egg shaped, axially elongated, and not umbilically directed, so that the long axis of the chambers runs parallel to the axis of coiling. The chambers are well spaced, not appressed to each other. Different from other 4-chambered-Acarininids, this species retains an oval equatorial outline instead of quadrate.

This is a sparsely ornamented, small species. If the pustules on the umbilical side are not preserved this species resembles a Parasubbotinid. The distinction is made via the apertural features, and the axial elongation of the chambers.

Stratigraphic range: Zone P5 to E6 (Pearson et al., 2006).

Occurrence: This species is present in almost all samples of the measured section in the GT-1 – GT- 25 interval.

Acarinina esnehensis (Nakkady, 1950)

Plate 1, Figures g, j

- 1950 *Globigerina cretacea* d'Orbigny var. *esnehensis* Nakkady. p. 689, pl. 90, figs. 14-16.
- 1979 *Muricoglobigerina esnehensis* (Nakkady) – Blow, p.1127, pl. 109, figs. 1-7.

2006 *Acarinina esnehensis* (Nakkady) – Pearson et al., p 289, pl. 9.12, figs. 1-16.

Remarks: This species is loosely coiled with 4-5 trapezoidal to bean shaped chambers in the last whorl. The umbilicus is wide. The last chamber is misplaced either to more outward or inward position. *A. pentacamerata* is more or less similar in overall shape and chamber number, but is more well-arranged have more regularly growing chambers in contrary to *A. esnehensis*.

Stratigraphic range: Zone P5 to E6 (Pearson et al., 2006).

Occurrence: This species is present in almost all samples of the measured section in the GT-1 – GT- 25 interval.

Acarinina mckannai (White, 1928)

1928 *Globigerina mckannai* White, 194, pl. 27: fig. 16a-c

1957a *Globigerina mckannai* (White) - Loeblich and Tappan, 181, pl. 47: fig. 7a-c
pl. 53: figs. 1a-2c, pl. 57: fig. 8a-c, pl. 62: figs. 5a-6c, pl. 62: fig. 7a-c

1957a *Globorotalia mckannai* (White) - Bolli, 79, pl. 19: figs. 16-18

1960 *Globorotalia mckannai* (White) - Bolli and Cita, 383, pl. 33: fig. 6a-c

1962 *Globorotalia (Acarinina) mckannai* (White) - Hillebrandt, 140, pl. 14: figs.
8a-10c

1971 *Globorotalia (Acarinina) mckannai* (White) - Jenkins, 82, pl. 3: figs. 89-93

1973 *Acarinina mckannai* (White) - Krasheninnikov and Hoskins, 116, pl. 2: figs.
6-8

1985 *Acarinina mckannai* (White) - Toumarkine and Luterbacher, 116, text-fig. 18

1993 *Acarinina mckannai* (White) - Lu and Keller, 118, pl. 2: figs. 14-16

1984 *Muricoglobigerina mckannai* (White) - Belford, 13, pl. 22: fig. 408

1990 *Muricoglobigerina mckannai* (White) - Stott and Kennett, 559, pl. 3: figs. 7, 8

1991b *Acarinina praecursoria* (Morozova) - Huber, 439, pl. 1: figs. 3-5 [Not Morozova, 1957.]

1999 *Acarinina mckannai* (White) – Olsson et al., 48, pl. 40: fig. 1-16

Remarks: Very similar to *A. nitida*, but has higher number of chambers in the last whorl. Chambers are axially more elongated and tangentially less broad than *A. nitida*.

Stratigraphic range: Olsson et al. (1999) assigned the HO of *A. mckannai* in Zone P4c, on the other hand Premoli Silva et al. (2003) elongates the range of this taxon up into Zone E2. In the samples of the Haymana Basin, this species is also observed, although few, above the P/E boundary (in the interval of GT-1 – GT-22). Some sporadic occurrences of *A. mckannai* in small numbers in the lower Eocene rocks (above GT-17.75) may be due to the effective reworking/transportation that also affects many other Cretaceous and lower Paleocene species, however, the distinction of *in situ* and reworked specimens seems impossible in the studied samples.

Occurrence: Occurs in the interval of GT-1 – GT-22.

Acarinina nitida (Martin, 1943)

Plate 1, Figures k, l

1943 *Globigerina nitida* Martin. p. 115, pl. 7, fig. 1a-c.

1953 *Acarinina acarinata* Subbotina. p. 229, pl. 22, figs. 4, 5, 8, 10.

1970b *Acarinina acarinata* (Subbotina) - Shutskaya, p.118, 228, pl. 27, fig. 13a-c.

1973 *Acarinina acarinata* (Subbotina) - Krasheninnikov and Hoskins, p. 116, pl. 1, figs. 1-3.

1979 *Globorotalia (Acarinina) acarinata acarinata* (Subbotina) -Blow. p. 904, fig. 7.

1999 *Acarinina nitida* (Martin) -Olsson et al., p. 48; pl. 12, figs. 1-3; pl. 41, figs. 1-16.

2011 *Acarinina nitida* (Martin) -Nguyen et al., pl. 2, fig. 2.

Remarks: A tightly coiled species of generally 4 chambers in the last whorl, this form has an overall globular appearance due to chambers being highly appressed. The chambers are tangentially elongated (crescentic or bean shaped), and axially elongated. The edge of the form is rounded to subrounded, with a slightly convex spiral side. Umbilicus is shallow and narrow. Some specimens of *A. soldadoensis* may resemble *A. nitida*, but *A. soldadoensis* has a more lobulate outline and chambers that are less compressed to each other.

Stratigraphic Range: This form is recorded by Olsson et al. (1999) to have its HO in Zone P4c, however Premoli-Silva et al. (2003) put its HO higher up in the lower Eocene (E5). In the samples of the Haymana Basin, this species is also observed, although few, until the P/E boundary boundary (in the interval of GT-1 – GT-22). Some sporadic occurrences of *A. nitida* in small numbers in the lower Eocene rocks (above GT-17.75) may be due to the effective reworking/transportation that also affects many other Cretaceous and lower Paleocene species, however, the distinction of *in situ* and reworked specimens seems impossible in the studied samples.

Occurrence: Occurs in the interval of GT-1 – GT-22.

Acarinina pseudotopilensis (Subbotina, 1953)

Plate 2, Figures a, b

1953 *Acarinina pseudotopilensis* Subbotina, p. 227, pl. 21, figs. 8a-c, 9a-c; pl. 22, figs. 1a-3c.

- 1960 *Globorotalia pseudotopilensis* (Subbotina) - Reyment, p. 81, 82, pl. 15, figs. 14a-c, pl. 15, figs. 15-17, pl. 16, fig. 1a, b.
- 1975 *Globorotalia pseudotopilensis* (Subbotina) - Lutherbacher, p. 65, pl.3, figs. 4-9.
- 1993 *Acarinina pseudotopilensis* (Subbotina) - Pearson et al., p. 124, pl.1, figs. 13-15.
- 2006 *Acarinina pseudotopilensis* (Subbotina) - Pearson et al. p. 305, pl. 9.18, figs. 1-16.

Remarks: This species is similar to *A. wilcoxensis*, but withholds a more angular edge, and a higher growth rate. Moreover, chambers are more compressed to each other.

Stratigraphic range: along with *A. wilcoxensis*, these two species are the first to evolve in the upper Zone P5, and become abundant members of the lower Eocene assemblages. Up to Zone E7 (Pearson et al., 2006). In this work *A. pseudotopilensis* occurs near the P/E boundary (GT-17.25) and is present throughout the rest of the measured section (until last sample GT-26).

Occurrence: Occurs between GT-17.25 and GT-26.

Acarinina sibaiaensis (El Naggari 1966)

Plate 2, Figures g, j-l

- 1966 *Globorotalia sibaiaensis* El Naggari, 235, pl. 23: fig. 6a-c
- 1996 *Acarinina sibaiaensis* (El Naggari) - Kelly et al., 424, fig. 2-1a-b
- 1998 *Acarinina sibaiaensis* (El Naggari) - Kelly et al., 159, figs. 5c, 9d-e
- 1999 *Acarinina sibaiaensis* (El Naggari) - Pardo et al., 44, pl. 2: figs. 19-20
- 1999 *Acarinina* aff. *sibaiaensis* (El Naggari) - Pardo et al., 44, pl. 2: figs. 17-18

2007 *Acarinina sibiyaensis* (El Naggar) – Luciani et al. 206, pl. 1: figs. 11, 14, 15, 20

2008 *Acarinina sibiyaensis* (El Naggar) – Guasti and Speijer, 7, pl. 1: figs. 1-3, pl. 2: figs 1-3

2016 *Acarinina sibiyaensis* (El Naggar) – El-Dawy et al. 217, pl 1: figs. 9-10

2016a *Acarinina sibiyaensis* (El Naggar) – Ouda et al. 22, pl. 1: figs. 5-15

Remarks: One of the PFET, this species has distinctly pustulose wall texture. 5 globular chambers in the last whorls are coiled loosely, so that the umbilicus is wide, yet shallow due to low umbilical inflation of the chambers. The chamber growth rate is moderate to high, last chamber is significantly larger than the penultimate chamber. Test edge is rounded to subrounded.

Two sister species of similar range are *A. multicamerata*, which has number of chambers in the last whorl more than that of *A. sibiyaensis*, and *A. africana*, which has a carinate, pinched periphery. These two taxa were not discovered in the studied samples may be due to preservational complexities, sampling resolution, or their preferred geographical distribution.

Stratigraphic Range: Although some discrepancies are recorded about the range of this species and its correlation to the PETM and CIE, in planktonic foraminifera studies it is standardized to represent the P/E boundary with LO of *A. sibiyaensis*.

Occurrence: In this study *A. sibiyaensis* is found in samples GT-17.75, GT-18, GT-19, GT-19.5, and GT-20.5; hence, the P/E boundary is placed in the GT-17.675 – GT-17.75 interval.

Acarinina soldadoensis (Brönnimann, 1952)

Plate 2, Figures f, h, i

1952 *Globigerina soldadoensis* Brönnimann, p. 7, 9, pl. 1, figs. 1-9.

- 1962 *Globorotalia (Acarinina) soldadoensis* (Brönnimann). - Hillebrandt, p.142, pl.14, figs.5-6.
- 1971b *Acarinina soldadoensis* (Brönnimann) -Berggren, p. 76, pl. 5, figs. 1-3.
- 1979 *Muricoglobigerina soldadoensis soldadoensis* (Brönnimann) - Blow, p. 1120, pl.98, figs.1-3; pl. 107, figs. 1-5; pl. 109, fig. 8.
- 1999 *Acarinina soldadoensis* (Brönnimann) - Olsson et al., p. 50; fig. 20; pl. 15, figs. 4, 7, 8; pl. 42, figs. 1-16.
- 2006 *Acarinina soldadoensis* (Brönnimann) - Pearson et al., p. 318; pl. 9.3, figs. 1-10.
- 2007 *Acarinina soldadoensis* (Brönnimann) - Luciani et al., p. 206, pl. 1, figs. 3.
- 2011 *Acarinina soldadoensis* (Brönnimann) - Nguyen et al., pl. 2, figs. 4, 6

Remarks: This species is defined as having 4 subglobular chambers in the last whorl elongated axially, and strongly ornate wall. The author identified two subgroups for this species: one group is more loosely coiled, the other with a tighter coil. Former group resembles first Eocene quadrate Acarininids (*A. wilcoxensis* and *A. pseudotopilensis*) with a more open umbilicus, shorter axial dimension and less radial compression of chambers. the latter group is more similar to late Paleocene compact Acarininids (*A. nitida* and *A. mckannai*) in having radially compressed and axially elongate chambers which are appressed to each other. The two groups are not as distinct from each other to be divided at a subspecies rank, however, may be an evidence to phylogenetic relationships.

Stratigraphic range: From P4c to E7 (Pearson et al., 2006). This species is a major component in the studied assemblage from GT-1 to GT-26.

Occurrence: This species is a major component in the studied assemblage from GT-1 to GT-26.

Acarinina subsphaerica (Subbotina 1947)

Plate 2, Figure c

- 1947 *Globigerina subsphaerica* Subbotina, 108, pl. 5: figs. 26-28, pl. 5: figs. 23-25
- 1953 *Globigerina subsphaerica* Subbotina, 59, pl. 2: fig. 15a-c
- 1965 *Globigerina subsphaerica* (Subbotina) - Shutskaya, 91, pl. 3: fig. 1
- 1956 *Globoconusa quadripartitaformis* Khalilov, 249, pl. 5: fig. 3a-c
- 1957a *Globigerina chascanona* Loeblich and Tappan, 180, pl. 49: fig. 5a-c
- 1957a *Globigerina spiralis* (Bolli) - Loeblich and Tappan, 182, pl. 47: fig. 3a-c, pl. 49: fig. 3a-c, pl. 51: figs. 6a-9c, pl. 53: fig. 3a-c, [Not Bolli, 1957a.]
- 1958 *Acarinina subsphaerica* (Subbotina) - Shutskaya, 89, pl. 2: figs. 12-14, pl. 3: figs. 1-3
- 1960 *Acarinina subsphaerica* (Subbotina) – Shutskaya, 249, pl. 2: fig. 8;
- 1970b *Acarinina subsphaerica* (Subbotina) – Shutskaya, 118-120, pl. 2: fig. 8a-c, pl. 6: fig. 3a-c, pl. 26: fig. 3a-c
- 1964 *Acarinina falsospiralis* Davidzon and Morozova, 26, 28, pl. 1: fig. 5a-c
- 1967 *Acarinina microsphaerica* Morozova in Morozova, Kozhevnikova, and Kuryleva, 195, pl. 6: figs. 3, 4
- 1979 *Globorotalia (Acarinina) subsphaerica* (Subbotina) - Blow, 960, pl. 91: figs. 4-6, pl. 92: figs. 1-3
- 1979 *Muricoglobigerina chascanona* (Loeblich and Tappan) - Blow, 1126, pl. 91: figs. 1, 2, pl. 92: fig. 3, pl. 93: figs. 7-9, pl. 235: figs. 1-3, pl. 101: figs. 5, 6
- 1991b *Acarinina chascanona* (Loeblich and Tappan) - Huber, 439, pl. 2: fig. 3 [Not Loeblich and Tappan, 1957a.]

1999 *Acarinina subsphaerica* (Subbotina) – Olsson et al., 52, pl. 15: figs. 9-10, pl. 44: figs. 1-16

Remarks: This species is the highest trochospiral form of genus *Acarinina* with embracing chambers on the umbilical side. The form is globular to cylindrical in overall shape. Its differences from its homeomorph *A. pseudosphaerica* are a smaller umbilicus and higher degree of appression of the chambers.

Stratigraphic range: Olsson et al. (1999) restricted range of this form in tropical-subtropical regions in Zone P4a (by definition), and put the species until top of Zone E3 in the Austral realm (Pearson et al., 2006). Olsson et al. (1999) also mentions the record of high spired Acarininids in several other localities in higher levels (up in early Eocene) which may be referred to this species. Premoli Silva et al. (2003) draw a longer stratigraphic range, up into P4c and also, *A. aquiensis*, which is treated as a junior synonym to *A. subsphaerica* in this study, is also given a range Zone P4c to E8. The observations of the Haymana Basin samples agree with Premoli-Silva's interpretation, *A. subsphaerica* ss. is found in almost all samples (GT-2 – GT-23), although sporadically and in small numbers in the upper levels along with similar unidentified high spired forms (Section 5.7 High Trochospired Tests). However, this may also be an issue related with the mentioned reworking/transportation problem as in other Paleocene Acarininids.

Occurrence: This species is found in almost all samples (GT-2 – GT-23), although sporadically and in small numbers in the upper levels.

Acarinina wilcoxensis (Cushman & Ponton 1932)

Plate 2, Figures d-e

1932 *Globorotalia wilcoxensis* Cushman and Ponton, p. 71, pl. 9, figs. 10 a-c.

1944 *Globorotalia wilcoxensis* (Cushman and Ponton) - Cushman, p. 15, pl. 2, figs. 14, 15 a, b.

- 1957a *Globorotalia wilcoxensis* (Cushman and Ponton) - Bolli, p. 79, pl. 19, figs. 7-9.
- 1960a *Globorotalia wilcoxensis* (Cushman and Ponton) - Berggren, p. 97-100, pl. 13, figs. 3a-4c.
- 1968 *Truncorotaloides (Acarinina) wilcoxensis* (Cushman and Ponton) - McGowran, pl. 3, fig. 1.
- 1971 *Globorotalia wilcoxensis* (Cushman and Ponton) - Postuma, p. 221.
- 1985 *Morozovella wilcoxensis* (Cushman and Ponton) - Snyder and Waters, p. 446, pl. 10, figs. 3-5.
- 1990 *Acarinina wilcoxensis berggreni* (El Naggari) Stott and Kennett, p. 560, pl. 4, figs. 5, 6.
- 1993 *Acarinina wilcoxensis* (Cushman and Ponton) - Lu and Keller, p. 102, pl. 2, figs. 14, 15.
- 2001 *Acarinina wilcoxensis* (Cushman and Ponton) - Warraich and Ogasawara, p. 33, figs. 8.4-6.
- 2006 *Acarinina wilcoxensis* (Cushman and Ponton) - Pearson et al., p. 320, pl. 9.23, figs. 1-16.

Remarks: This species is close to loosely coiled *A. soldadoensis*. Chamber growth rate is low to moderate in this species, shaped oval on spiral side. Chambers are not axially elongate. The edge may be subangular to rounded.

Stratigraphic range: Zone P5 to E5 (Pearson et al., 2006). *A. wilcoxensis* first occurs close to the P/E boundary (in sample GT-17.125) and is present in the samples until GT-24. Its absence in the last two samples of the section matches with other several species' absence, and is probably linked with paleoenvironmental changes (such as shallowing).

Occurrence: This species is found in the interval GT-17.125 – GT-24.

5.2.3 Genus *Igorina* Davidzon, 1976

Type species: *Acarinina tadjikistanensis* Bykova, 1953

Remarks: *Igorina*, in terms of wall texture, is similar to *Acarinina* and *Praemurica* having a cancellate base, and ornamentations which are short and coalesced. The group is formed by moderately high trochospiral forms; the overall shape of the test is symmetrically or asymmetrically biconvex. 5-7 chambers in the last whorl coiled tightly and compressed to each other. Intercameral sutures are shallow to indistinct on both sides. Umbilicus is either closed or very shallow. Table 13 provides the distinctive properties of the species of this genus.

Stratigraphic range: Danian to Ypresian (Pearson et al., 2006)

Igorina albeari (Cushman and Bermudez 1949)

Plate 4, Figures k, l

- 1949 *Globorotalia albeari* Cushman and Bermudez, 33, pl. 6: figs. 13-15
- 1957a *Globorotalia pusilla laevigata* Bolli, 78, pl. 20: figs. 5-7
- 1957a *Globorotalia pseudoscitula* (Glaessner) - Loeblich and Tappan, 193, pl. 46: fig. 4a-c, pl. 53: fig. 5a-c, pl. 59: fig. 2a-c, pl. 63: fig. 6a-c [Not Glaessner, 1937.]
- 1960 *Globorotalia pusilla laevigata* (Bolli) - Bolli and Cita, 27, pl. 32: fig. 6a-c
- 1962 *Globorotalia pusilla laevigata* (Bolli) - Hillebrandt, 128, 129, pl. 11: fig. 17a-c
- 1965 *Globorotalia pusilla laevigata* (Bolli) - McGowran, 63, pl. 6: fig. 4
- 1977 *Globorotalia albeari* (Cushman and Bermudez) - Cifelli and Belford, 100, pl. 1: figs. 4-6

1979 *Globorotalia (Globorotalia) albeari* (Cushman and Bermudez) - Blow, 883, pl. 92: figs. 4, 8, 9, pl. 93: figs. 1-4

1999 *Igorina albeari* (Cushman and Bermudez) - Olsson et al., 69, pl. 16: figs. 1-6; pl. 56: figs. 1-16

2011 *Igorina albeari* (Cushman and Bermudez) - Soldan et al., 266, fig. 5-1&2

Remarks: With a relatively high trochospire, the spiral side is highly convex, even more than umbilical side in some specimens. The form is keeled with a sharp margin. The umbilicus is closed, umbilical sutures are very shallow to indistinct, making the number of chambers in the last whorl difficult to count. This species is quite similar with *Pl. pseudoscitula*, the distinction is on the spiral side, while latter has a smooth transition of whorls, *I. albeari* has a distinctly elevated initial whorl.

Stratigraphic Range: Zone P3 to P4 (Olsson et al., 1999). This species is found in the upper Paleocene of the measured section, in the GT-1 – GT- 9 interval. Some forms attributable to *I. albeari* were also present in the higher samples, although are assumed to be reworked.

Occurrence: This species is present in the interval GT-1 – GT-9.

Igorina tadjikistanensis (Bykova 1953)

Plate 4, Figures g, h, j

1953 *Globorotalia tadjikistanensis* Bykova, 86, pl. 3: fig. 5a-c

1960 *Globorotalia tadjikistanensis* (Bykova) - Leonov and Alimarina, 53, pl. 7: figs. 1, 2, 7, figs. 3, 4, 7

1964 *Globorotalia tadjikistanensis* (Bykova) - Luterbacher, 52, text-fig. 52a-c

1953 *Globorotalia convexa* Subbotina, 209, pl. 17: fig. 2a-c, fig. 3a-c

Table 13: Rapid recognition chart for species of genera *Igorina* and *Pearsonites*. * for species identified in this study

Species	Equatorial Outline	Axial Outline	# of Chambers	Spiral Chamber Shape	Spiral Sutures	Umbilical Sutures	Umbilicus
* <i>I. albeari</i>	Circular	Strongly biconvex; distinctly carinate	6-8	Trapezoidal	Strongly recurved, showing distinct limbation (thickening)	Radial to weakly recurved	Small, shallow, often closed
<i>I. pusilla</i>	Circular; slightly lobate	Biconvex	5-6	Crescentic	Moderately to strongly curved, depressed/ weakly incised	Radial, depressed	Narrow and shallow
* <i>I. tadjikistanensis</i>	Ovate to subcircular, moderately lobulate test	Subrounded to subacute, noncarinate	5-7	Crescentic	Depressed, strongly recurved, tangential to inner whorl	Curved, depressed	Small, shallow
<i>P. anapetes</i>	Subcircular, weakly lobulate	Planoconvex; rounded to subacute edge	8-9	Trapezoidal, radially elongate	Flush with test, proximally radial, becoming retorse towards junction with peripheral margin	Nearly straight, radial, moderately incised	Relatively broad and deep
* <i>P. broedermanni</i>	Subcircular, weakly lobulate	Planoconvex to weakly biconvex; rounded to subangular edge	6-7	Subquadrate to subrectangular	Curved and retorse at junction with peripheral margin	Depressed, radial	Narrow, deep
* <i>P. lodoensis</i>	Subcircular, lobulate	Equally biconvex; subangular edge	5.5-6	Trapezoidal, radially elongate	Lunate/semicircular, smoothly recurved	Radial, straight, weakly incised	Relatively narrowly open and deep

- 1957a *Globorotalia convexa* (Subbotina) - Loeblich and Tappan, 188, pl. 48: fig. 4a-c, pl. 50: fig. 7a-c, pl. 53: figs. 6a-8c, pl. 57: figs. 5a-6c, pl. 63: fig. 4a-c
- 1983 *Globorotalia convexa* (Subbotina) - Pujol, 644, pl. 3: figs. 1, 2
- 1968 *Truncorotaloides (Morozovella) convexus* (Subbotina) - McGowran, 192, pl. 2: figs. 11-14
- 1971 *Globorotalia (Acarinina) convexa* (Subbotina) - Jenkins, 81, pl. 3: figs. 79-83
- 1979 *Globorotalia (Acarinina) convexa* (Subbotina) - Blow, 920, pl. 85: figs. 2-7, pl. 88: figs. 3, 4, pl. 100: figs. 3, 5-9
- 1979 *Globorotalia (Acarinina) convexa cf. convexa* (Subbotina) - Blow, 921, pl. 100: figs. 1, 2, 4
- 1984 *Globorotalia (Morozovella) tadjikistanensis* (Bykova) - Belford, 10, pl. 18: figs. 18-23
- 1990 *Morozovella convexa* (Subbotina) - Stott and Kennett, 560, pl. 3: figs. 5, 6
- 1999 *Igorina tadjikistanensis* (Cushman and Bermudez) - Olsson et al., 71, pl. 11: figs. 1-9; pl. 58: figs. 1-12
- 2011 *Igorina tadjikistanensis* (Cushman and Bermudez) - Soldan et al., 266, fig. 5-7&8

Remarks: Moderate to high trochospirally coiled form with convex spiral side. The form has a wide range of axial outline, from subangular to widely subrounded. Chambers are compressed to each other showing a crescentic to trapezoidal shape in spiral view with low growth rate. Intercameral sutures are shallow on both sides.

In literature lower trochospiral specimens are often attributed to *I. convexa*, which here is taken as synonymous to *I. tadjikistanensis*.

Stratigraphic Range: Zone P3b to E3 (Pearson et al., 2006).

Occurrence: This species is found in almost all the samples of the measured section (GT-1 – GT-26).

5.2.4 Genus *Pearsonites* Soldan, Petrizzo & Premoli Silva, 2014

Type species: *Globorotalia (Truncorotalia) broedermanni* Cushman & Bermudez, 1949

Remarks: Similar to genus *Igorina* (and making up the group Igorinids with it) this group withholds a wall texture of praemuricate (cancellate) base, and Acarininid ornamentations; the pustules are longer and not fused together, producing a different texture than that of *Igorina*. Low trochospiral forms with flat to slightly convex spiral side are in this group. Last whorl is composed of 5-8 compressed chambers, trapezoidal on spiral, pie shaped on umbilical side. The Intercameral sutures are more distinct than in *Igorina*, also, umbilicus is open and generally deep. Table 13 provides the distinctive properties of the species of this genus.

Stratigraphic range: Zone P5 to E9 (Soldan et al., 2014)

Pearsonites broedermanni (Cushman & Bermudez, 1949)

Plate 5, Figures g-h

1949 *Globorotalia (Truncorotalia) broedermanni* Cushman and Bermudez, 40, pl.7, figs. 22-24.

1957a *Globorotalia broedermanni* (Cushman and Bermudez) - Bolli., p. 167, pl. 37, figs. 13a-c.

1957b *Globorotalia broedermanni* (Cushman and Bermudez) - Bolli, p. 80, pl. 19, figs. 13-15.

1961 *Pseudogloborotalia broedermanni* (Cushman and Bermudez) - Bermudez, p.1340, pl. 16, fig. 7.

- 1979 *Globorotalia (Acarinina) broedermanni broedermanni* (Cushman and Bermudez) - Blow, p. 911, pl. 130, figs. 7-9; pl. 135, fig. 4; pl. 142, figs. 1-3; pl. 153, figs. 7, 8; pl. 179, figs. 3-5.
- 1985 *Acarinina broedermanni* (Cushman and Bermudez) - Synder and Waters, p. 446, pl. 6, figs. 1-3.
- 1993 *Morozovella broedermanni* (Cushman and Bermudez) - Pearson et al., p. 125, pl.1, fig. 21.
- 1995 *Igorina broedermanni* (Cushman and Bermudez) - Lu and Keller, p. 102, pl. 4, fig. 16.
- 2000 *Igorina broedermanni* (Cushman and Bermudez) - Warraich et al., p. 293, pl.18, figs. 18-20.
- 2001 *Igorina broedermanni* (Cushman and Bermudez) – Warraich and Ogasawara, p.17, figs. 4.1-3.
- 2004 *Igorina broedermanni* (Cushman and Bermudez) - Pearson et al., p. 37, pl. 2, fig. 2.
- 2006 *Igorina broedermanni* (Cushman and Bermudez) - Pearson et al., p. 384, pl. 12-2, figs. 1-12.
- 2011 *Igorina broedermanni* (Cushman and Bermudez) - Nguyen et al., pl. 1, fig. 5.
- 2011 *Igorina broedermanni* (Cushman and Bermudez) - Soldan et al., p. 265, figs. 4, 6.
- 2014 *Pearsonites broedermanni* (Mallory) - Soldan et al., p. 21-23, figs. 5-2, 7-1

Remarks: Trapezoidal to crescentic chambers divided by depressed sutures (shallower than *P. lodoensis*). Coiling tighter than *P. lodoensis*, umbilicus smaller.

Stratigraphic range: Zone P5 to E9 (Pearson et al., 2006). This species is present in the measured section starting with GT-17.125.

Occurrence: This species is present in the measured section in the interval GT-17.125 – GT-26.

Pearsonites lodoensis (Mallory, 1959)

Plate 5, Figures d-e, i

1959 *Globorotalia broedermanni* Cushman and Bermudez var. *lodoensis* Mallory, 253, pl.23, figs. 3 a-c.

1957b *Globorotalia broedermanni* Cushman and Bermudez, 1949 - Bolli, p. 80, pl. 19, figs. 13-15.

1962 *Globorotalia caylaensis* Gartner and Hay, p. 561, pl. 1, figs. 2a-c.

1979 *Globorotalia (Acarinina) lodoensis* (Mallory) - Blow, p. 933-935, pl. 117, figs. 1-6.

1998 *Igorina lodoensis* (Mallory) - Lu et al., p. 212, pl. 1, figs. 10-11.

2006 *Igorina lodoensis* (Mallory) - Pearson et al., p. 388, pl. 12-3, figs. 1-16.

2011 *Igorina lodoensis* (Mallory) - Soldan et al., p. 265, figs. 3, 5.

2014 *Pearsonites lodoensis* (Mallory) - Soldan et al., p. 22-23, figs. 6-1, 7-1

Remarks: Trapezoidal chambers, generally radially longer than tangentially broad. Intercameral sutures are depressed on both sides. Subangular to subrounded axial outline.

Stratigraphic range: Zone P5 to E6 (Pearson et al., 2006). This species is present in the measured section starting with GT-16.

Occurrence: This species is present in the measured section in the interval GT-16 – GT-26.

5.2.5 Genus *Planorotalites* Morozova, 1957

Type species: *Globorotalia pseudoscitula* Glaessner, 1937

Remarks: Biconvex genus with subacute to acute axial outline, and moderate to low trochospire. This group withholds a wall texture with short pustules on cancellate base like in Igorinids. Morphologically this group resembles biconvex Morozovellids in being carinated and has spiral intercameral sutures similar to that of *Igorina*. In Table 14 reader may find the properties of the two species of this genus.

Stratigraphic range: Tanetian to Priabonian (Pearson et al., 2006)

Planorotalites pseudoscitula (Glaessner, 1937)

Plate 5, Figures a-c

- 1937 *Globorotalia pseudoscitula* Glaessner, 32, text- figs. 3a-c.
- 1947 *Globorotalia pseudoscitula* (Glaessner) - Subbotina, p. 121-122, pl. 9, figs. 18-20.
- 1953 *Globorotalia pseudoscitula* (Glaessner) - Subbotina, p. 208, pl. 16, figs. 17a-c, 18a-c; pl. 17, figs. 1a-c.
- 1972 *Globorotalia pseudoscitula* (Glaessner) - Samuel, p. 193-194, pl. 51, figs. 2a-4c.
- 1973 *Globorotalia pseudoscitula* (Glaessner) - Schmidt and Raju, p. 181-182, pl. 1, figs. 3a-c, 4.
- 1976 *Planorotalites pseudoscitula* (Glaessner) - Hillebrandt, p. 345, pl. 4, figs. 14.
- 1977 *Planorotalites pseudoscitula* (Glaessner) - Berggren, p. 244, chart no. 3.
- 1979 *Globorotalia (Globorotalia) pseudoscitula* Glaessner (sensu lato) - Blow, 897, pl. 116, figs. 8-10; pl. 173, figs. 1-8.

Table 14: Rapid recognition chart for species of genera *Planorotalites*. * for species identified in this study

Species	Equatorial Outline	Axial Outline	Spiral Intercameral Sutures	# of Chambers	Chamber Shape	Umbilicus	Aperture
<i>P. capdevilensis</i>	Subcircular, very weakly lobulate	Biconvex	Flush with test, distinctly curved and limbate	6-8 chambers	Trapezoidal	Narrow, shallow	Low, umbilical - extraumbilical arch with distinct lip
<i>P. pseudoscitula</i> *	Oval to subcircular, weakly lobulate	Biconvex	Flush with test, distinctly curved	6-8 chambers	Trapezoidal	Narrow, shallow	Low, umbilical - extraumbilical arch with distinct lip which extends to the periphery

- 1985 *Planorotalites pseudoscitula* (Glaessner) - Toumarkine and Luterbacher, p. 118, figs. 20.5-10.
- 1988 *Planorotalites pseudoscitula* (Glaessner) - Loeblich and Tappan, p. 477, pl. 518, figs. 6-8.
- 1993 *Planorotalites pseudoscitula* (Glaessner) - Lu and Keller, p. 114, pl. 5, figs. 5-7.
- 1995 *Planorotalites pseudoscitula* (Glaessner) - Lu and Keller, p. 100, pl. 6, figs. 15-17.
- 2006 *Planorotalites pseudoscitula* (Glaessner) - Pearson et al., p. 393, pl. 12-5, figs. 1-16

Remarks: A biconvex, carinate species with weakly lobulate equatorial outline. This species resembles *M. edgari*, and can be distinguished from it by less incised umbilical sutures, and less lobulate outline. *P. pseudoscitula* can be distinguished from *P. capdevilensis* by more ornamented several last chambers and clear extension of keel on spiral sutures.

Stratigraphic range: Zone P5 to E7 (Pearson et al., 2006). This species is shows two sporadic occurrences in the measured section in *G. pseudomenardii* Zone, in the samples GT-6 and GT-9, however, is very scarce. Its prominent presence is recorded starting with GT-12, and it is present until the end of the measured section (GT-26).

Occurrence: This species is identified in samples GT-6, 9, and between samples GT-12 and GT-26.

5.3 Family Hedbergellidae Loeblich and Tappan, 1961

This family includes smooth walled genera with very low trochospiral to planispiral coiling.

5.3.1 Genus *Globanomalina* Haque, 1956

Type species: *Globanomalina ovalis* Haque, 1956

Remarks: This genus is characterized by low to very low trochospiral coiling. Aperture is mostly in an umbilical to extraumbilical position, generally not reaching the periphery. The group has evolute spiral sides, though, the degree of involuteness on umbilical side varies between species. Chamber shape is variable between species (Figure 46), sometimes even between individuals. Intercameral sutures are generally incised. Axial test shape changes from asymmetrically biconvex to almost symmetrically biumbilicate if the chambers are inflated on the spiral side. Occasional pustules are present on test, especially on spiral side. Characteristic features of the species of this genus are summarized in Table 15.

Over the time several generic names were used that now seen are synonyms: *Globorotalia*, *Luterbacheria* and *Planorotalites*.

Stratigraphic range: Danian to Priabonian (Pearson et al., 2006)

Globanomalina chapmani (Parr, 1938)

Plate 8, Figures e-d

- 1938 *Globanomalina chapmani* Parr. Holotype: pl.3, figs. 9a, b; topotype: pl. 3, fig 8.
- 1953 *Globorotalia membranacea* Subbotina, p. 205, pl. 16, figs. 12 a-c.
- 1967 *Globanomalina chapmani* (Parr) -Berggren, Olsson and Reyment. p. 277, textfigs. 1, 3, nos. 1a-c, 4, pl. 1, figs. 1-6.
- 1987 *Globanomalina chapmani* (Parr) - Nederbragt and Van Hinte p. 586 pl. 2, figs. 3-10; pl. 3, figs. 4-6.

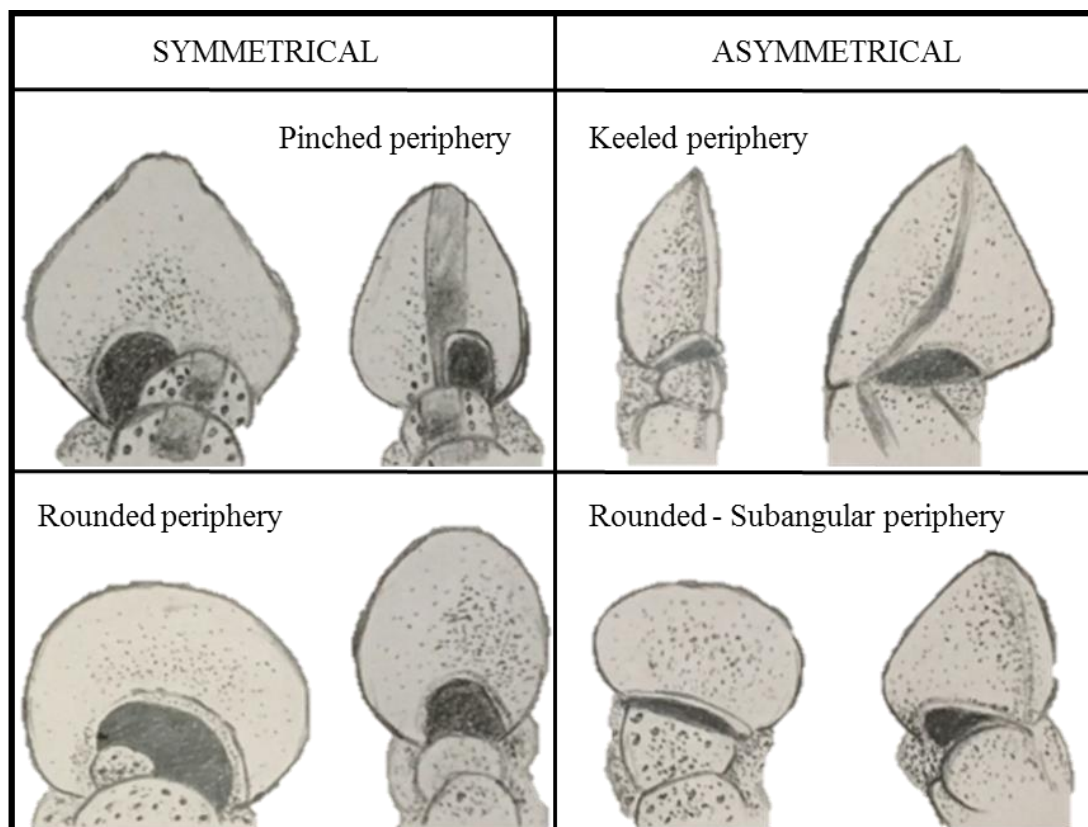


Figure 46: Hand sketched figure showing chamber shape, apertural position, and peripheral geometry variety in genus *Globabanomalina*

1991 *Globanomalina chapmani* (Parr) -Huber, p. 440, pl. 6, figs. 19-20.

1999 *Globanomalina chapmani* (Parr) -Olsson et al., p. 39; pl. 34, figs. 1-7.

2013 *Globanomalina chapmani* (Parr) -Sarı, p. 2, figs. 2-3.

Remarks: One of the symmetrical pinched peripheried types, chambers of this species are rhombohedral in edge view with an imperforate band at the periphery. The axial thickness of the chambers on the spiral side produces a pseudobiumbilicate appearance in some specimens. Others, with a convex spiral side, resemble *G. pseudomenardii*, and is distinguished from it by the absence of keel (instead *G. chapmani* withholds an imperforate peripheral band), and the lobate appearance of

Table 15: Rapid recognition chart for species of genus *Globanomalina*. * for species identified in this study

Species	Wall	Equatorial Outline	Axial Outline	# of Chambers	Chamber Shape	Growth Rate	Umbilicus	Umbilical Intercameral Sutures	Spiral Intercameral Sutures
<i>G. archeo-compressa</i>	Imperforate periphery	Moderately lobulate	Spiral side flat to slightly convex; subrounded periphery	5-6	Compressed oval-conical	Low	Shallow, broad	Radial, straight, depressed	Oblique to radial, depressed
* <i>G. australiformis</i>	Imperforate periphery; earlier chambers covered by short pustules	Lobulate	Subacute periphery; spiral side slightly convex	4	Low conical	High	Narrow, shallow	Radial, straight, depressed	Recurved, depressed
* <i>G. chapmani</i>	Thickened imperforate periphery	Lobulate	Pinched periphery; pseudobiumbilicate	5-6	Rhombohedral	High	Wide	Gently curved, depressed	Gently curved, depressed
<i>G. compressa</i>	Smooth	Lobulate	Slightly pinched to subrounded; spiral side slightly convex	5	Rhombohedral	Moderate	Wide	Radial, straight, depressed	Radial to curved, depressed
<i>G. eherenbergi</i>	Smooth	Lobulate	Pinched periphery; spiral side convex	5-5.5	Rhombohedral	Moderate	Wide	Radial, straight, depressed	Slightly curved, depressed

Table 15 (Continued)

Species	Wall	Equatorial Outline	Axial Outline	# of Chambers	Chamber Shape	Growth Rate	Umbilicus	Umbilical Intercameral Sutures	Spiral Intercameral Sutures
* <i>G. imitata</i>	Fine scattered to dense pustules on earlier chambers	Lobulate	Subangular to rounded periphery, spiral side flat to convex	4-5	Bean shaped	High	Wide, shallow	Radial, straight, depressed	Slightly curved, depressed
* <i>G. luxorensis</i>	Smooth, perforate periphery	Slightly lobulate, ovate	Rounded - subrounded periphery, compressed	6-7	Inflated, globular	High	Small	Straight to slightly curved, moderately depressed	Straight to slightly curved, moderately depressed
<i>G. ovalis</i>	Smooth	Lobulate	Widely rounded periphery, biumbilicate	5-6	Inflated, globular	High	Small	Depressed, slightly curved	Depressed, slightly curved
<i>G. plano-compressa</i>	Imperforate periphery	Lobulate	Rounded periphery	5	Inflated, globular to ovoid	Moderate	Small	Straight to slightly curved, moderately depressed	Straight to slightly curved, moderately depressed
* <i>G. planoconica</i>	Imperforate periphery	Slightly to moderately lobulate	Pinched periphery, planoconvex	5-6	Angular rhomboid to asymmetrical conical	Moderate to high	Moderate	Straight, depressed	Curved, depressed
* <i>G. pseudomenardii</i>	Smooth	Slightly to moderately lobulate	Pinched periphery, distinctly carinate, biconvex	5-6	Angular rhomboid	High	Narrow	Straight, depressed	Strongly curved, slightly depressed to flush

the spiral side in edge view due to depressed spiral intercameral sutures (*G. pseudomenardii* has a smooth, nonlobate spiral side due to flush sutures).

One Globanomalinid lineage is *G. chapmani*-*G. luxorensis*-*P. wilcoxensis*, and all three of this lineage show similar varieties that may make the distinction difficult. The chamber shapes, Intercameral suture shapes, chamber growth rate and most other morphological characters are similar in these species, distinction being the aperture. In *G. chapmani*, aperture is umbilical-extraumbilical, and does not cross the midline of the imperforate band, while in *G. luxorensis* the aperture crosses the midline, and in *P. wilcoxensis*, the aperture is umbilical-extraumbilical-umbilical reaching to the spiral side. Moreover, according to Speijer and Samir (1997) these three taxa intergrade into each other, such as the earlier juvenile *P. wilcoxensis* with *G. luxorensis* apertural characteristics

Stratigraphic Range: Zone P3 to E3 (Pearson et al., 2006). This species is a minor component in the studied samples from GT-1 to GT-22. Its absence in the highest samples may be due to preservational complexities, paleoenvironmental changes (shallowing) or just the species' rarity.

Occurrence: GT-1 to GT-22

Globanomalina imitata (Subbotina, 1953)

Plate 8, Figures a-c

1953 *Globorotalia imitata* Subbotina. p. 259, pl. 16, figs. 14a-c, 15a-c, 16a-c.

1957a *Globorotalia imitata* Subbotina - Loeblich and Tappan, pl. 54, figs. 8a-c; pl. 59, figs. 5a-c; p. 63, figs. 3a-c.

1960 *Globorotalia imitata* Subbotina - Olsson, p. 46, pl. 9, figs. 7-9.

1999 *Globanomalina imitata* (Subbotina) - Olsson et al., p. 42, pl. 10, figs. 12-14; pl. 12, figs. 10-12; pl. 36, figs. 7-12, 16.

2013 *Globanomalina imitata* (Subbotina) - Arenillas and Arz, p. 241, text-figs. 4G-J.

Remarks: The chambers are bean shaped on spiral side, in edge view they may be oval (with axial inflation) or trapezoidal (with subrounded edges). Last whorl is made up of 4 chambers.

Stratigraphic Range: Zone P1c to P4c (Olsson et al., 1999). This species is found in samples GT-2 – GT-10, and it acts as a reinforcement to *G. pseudomenardii*'s stratigraphic distribution. Although some specimens were found in the higher samples, they are assumed reworked.

Occurrence: GT-2 to GT-10

Globanomalina luxorensis (Nakkady 1951)

Plate 8, Figures f, h, i

- 1950 *Anomalina luxorensis* Nakkady, 691, pl. 90: figs. 39-41
- 1959 *Anomalina luxorensis* (Nakkady) - Nakkady, 465, pl. 5: fig. 1a-c
- 1967 *Pseudohastigerina wilcoxensis* (Cushman and Ponton) - Berggren, Olsson, and Reyment, 1967:278 (partim), text-fig. 2: d-f, m-r
- 1975 *Pseudohastigerina wilcoxensis* (Cushman and Ponton) - Stainforth et al., 243, fig. 99: 6a-c
- 1976 *Globorotalia (Turborotalia) sp.* Blow, 1061, pl. 111: fig. 5
- 1979 *Globorotalia (Turborotalia) chapmani* (Parr) - Blow, 1059 (partim, not pl. 116: fig. 2), pl. 116: figs. 1, 3-5
- 1990 *Pseudohastigerina wilcoxensis* (Cushman and Ponton) - Stott and Kennett, 560, pl. 5: figs. 5, 6

1997 *Globanomalina luxorensis* (Nakkady) - Speijer and Samir, 53 (partim, not pl. 1: fig. 6a-c), pl. 1: figs. 4a-5c; pl. 2: figs. 1a-4c

Remarks: *G. luxorensis* is a marker for uppermost Paleocene and lowermost Eocene, a nearly planispiral form ancestral to true planispiral *P. wilcoxensis*. The form may have rounded to oval chambers (in edge view) as in *G. chapmani*. Chamber growth rate is high, producing an especially large last chamber, and an overall oval equatorial outline.

Stratigraphic Range: Zone P5 to E3 (Pearson et al., 2006). *G. luxorensis* in the measured section first occurs in *M. subbotinae* Zone, in the sample GT-15, and is present until the last sample of the section (GT-26).

Occurrence: GT-15 to GT-26

Globanomalina planoconica (Subbotina, 1953)

Plate 7, Figures f-i

1953 *Globorotalia planoconica* Subbotina. p. 263 holotype: pl. 17, figs. 4a-c; paratypes, figs. 5a-c, 6a-c.

1999 *Globanomalina planoconica* (Subbotina) - Olsson et al., p. 44., pl. 10, figs. 15-17; pl. 34, figs. 8-17.

2006 *Globanomalina planoconica* (Subbotina) - Pearson et al. p. 418.

Remarks: Very similar to *G. pseudomenardii* this form is made up of angular rhomboid to conical chambers with a distinctly acute, carinated periphery. The spiral side is flat and spiral intercameral sutures are depressed to slightly depressed unlike *G. pseudomenardii*. Umbilical side of the chambers from the keel may be rounded to conical.

Stratigraphic Range: Zone P4 to E4 (Pearson et al., 2006).

Occurrence: This form is found in almost all samples of the section (GT-1 – GT-25).

Globanomalina pseudomenardii (Bolli, 1957a)

Plate 7, Figures j-l

- 1957 *Globorotalia pseudomenardii* Bolli. p. 77, pl. 20, figs. 14-17
- 1960 *Globorotalia pseudomenardii* (Bolli) - Bolli and Cita, p. 26, pl. 33, figs. 2a-c.
- 1979 *Globorotalia (Globorotalia) pseudomenardii* (Bolli) - Blow, p. 892, pl. 89, figs. 1- 5; pl. 94, figs. 1-5; pl. 108, figs. 4-7, pl. 111, figs. 1-4; pl. 112, figs. 2, 3, 9, 10.
- 1987 *Planorotalites pseudomenardii* (Bolli) - Nederbraght and Van Hinte, p. 587, pl. 1, figs. 1-16.
- 1991 *Planorotalites pseudomenardii* (Bolli) - Nocchi et al., p. 269, pl. 1, figs. 7-9.
- 1999 *Globanomalina pseudomenardii* (Bolli) - Olsson et al., p. 45.; fig 18; pl. 14, figs. 5-7; pl. 38, figs. 1-16.
- 2009 *Globanomalina pseudomenardii* (Bolli) - Obaidalla et al., p. 4, pl. 2, fig. 6.
- 2012 *Globanomalina pseudomenardii* (Bolli) - Robertson et al., p. 273, fig. 6 l, m

Remarks: *G. pseudomenardii* is the index species for Zone P4, and has a crucial place in Paleocene biostratigraphy. It has a true keel along the acutely angled periphery and angular rhomboid chambers. The spiral side of the test is convex and not distinctly divided (nonlobate) in edge view due to slightly depressed to flush spiral intercameral sutures. Umbilical sides of the chambers from the keel are conical with rounded tips. Spiral intercameral suture curvature is not a major feature but generally strongly curved especially in last two, however, there are specimens with gentler curved sutures.

Stratigraphic Range: By definition, *G. pseudomenardii* spans the Zone P4 (Pearson et al., 2006). However, according to Lu et al. (1998), *P. cf. pseudomenardii* appears in upper Zone P4, and overlaps with *P. pseudomenardii*, and is present up in the early Eocene zones in the Alamedilla and Ben Gurion sections. Blow (1979)

recorded the *G. pseudomenardii* higher in lower Eocene samples, which may be due to a wider species definition. Moreover, *G. rakhiensis* was defined as a lower Eocene *G. pseudomenardii* homeomorph from Pakistan (Warraich et al., 2000; Warraich & Nishi, 2003). In the studied samples of the Haymana Basin, we found consistent presence of *G. pseudomenardii* in the samples GT-2 – GT-10, and forms attributable to *G. pseudomenardii* in the higher levels (in Zones E1, E2, and sporadically in P5). The presence of other Cretaceous and lower Paleocene specimens in the samples due to reworking/transportation led us to conclude that the forms in the upper levels are transported/reworked rather than a delayed HO, a variant or a different species.

Occurrence: GT-2 to GT-10

5.3.2 Genus *Pseudohastigerina* Banner and Blow, 1959

Type species: *Nonion micrus* Cole, 1927

Remarks: This genus is characterized by planispiral coiling, a symmetrical, umbilical-extraumbilical-umbilical aperture which is sometimes bipartite, and smooth wall texture with occasional pustules. Table 16 provides the characteristic features of the species of this genus.

Stratigraphic range: Ypresian to Rupelian (Pearson et al., 2006)

Pseudohastigerina wilcoxensis (Cushman & Ponton 1932)

Plate 8, Figures g, j, k

1932 *Nonion wilcoxensis* Cushman and Ponton, 64, pl. 8, fig. 11.

1967 *Pseudohastigerina wilcoxensis* (Cushman and Ponton) - Berggren, Olsson and Reymont, p. 278, text-figs. 2: s-v, 3: 2a-5c, 4: 2a-5c, 6: 1a-6c.

1967 *Globanomalina wilcoxensis globulosa* Gohrbandt, p. 321, pl. 1, figs. 16, 17.

- 1975 *Pseudohastigerina wilcoxensis* (Cushman and Ponton) - Stainforth et al., p. 243, text-figs. 99: 1-5.
- 1985 *Pseudohastigerina wilcoxensis* (Cushman and Ponton) - Toumarkine and Bolli, p. 108, figs. 12: 9a-c, 10a-c, 11a-b, 12a-c.
- 1995 *Pseudohastigerina wilcoxensis* (Cushman and Ponton) - Lu and Keller, p. 102, pl. 6, figs. 7, 8.
- 1997 *Pseudohastigerina wilcoxensis* (Cushman and Ponton) - Speijer and Samir, p. 54, pl. 2, figs. 5a-c.
- 2001 *Pseudohastigerina wilcoxensis* (Cushman and Ponton) - Orue-Etxebarra et al., p. 57, pl. 1, figs. 6-7.
- 2006 *Pseudohastigerina wilcoxensis* (Cushman and Ponton) - Pearson et al., p. 429, pl. 14.4, figs. 1-8.
- 2007 *Pseudohastigerina wilcoxensis* (Cushman and Ponton) - Luciani et al., p. 206, pl. 1, figs. 12-13.

Remarks: Apart from occasional pustules, this species has a distinct symmetrical aperture which is the primary criterion to distinguish it from its ancestor, *G. luxorensis*. Moreover, the chamber growth rate is lower, and the sutures are more depressed.

In the studied samples the distinction of this form is made on the basis of aperture location, with the aid of SEM imaging.

Stratigraphic range: Zone E2 to E10 (Pearson P. N., Olsson, Huber, Hembleben, & Berggren, 2006).

Occurrence: In the studied samples this species is found in the samples in and above GT-21. This species is in low abundance, and the distinction from *G. luxorensis* was not possible with light microscope, therefore it is packed with *Globanomalina* for quantitative analysis.

Table 16: Rapid recognition chart for species of genus *Pseudohastigerina*. * for species identified in this study

Species	Equatorial Outline	Axial Outline	# of Chambers	Chamber Shape	Chamber Growth Rate	Sutures	Aperture
<i>P. micra</i>	Circular to oval	Compressed; circular to slightly acute periphery	6-7	Globular	Low	Slightly depressed, straight	Equatorial, symmetric, circular high arch; sometimes bipartite; narrow lip
<i>P. naguewichiensis</i>	circular to oval; slightly lobulate	compressed; rounded periphery	6-8	Globular	Low	Slightly depressed, straight to slightly curved	Moderately high arch with thickened prominent lip
<i>P. sharkriverensis</i>	oval to quadrate; slightly lobulate	compressed; rounded periphery	6	Globular, inflated	Rapidly	Moderately depressed, straight to slightly curved	Oval, low arch; commonly bipartite; narrow lip
* <i>P. wilcoxensis</i>	oval; lobulate	compressed; rounded periphery	6-7	Globular, inflated	Rapidly	Slightly depressed, straight to slightly curved	Equatorial, symmetric to slightly asymmetric, circular high arch; sometimes bipartite; narrow lip

5.4 Family Chiloguembelinidae Reiss, 1963

This family contains the biserial groups.

5.4.1 Genus *Chiloguembelina* Loeblich and Tappan, 1956

Type species: *Guembelina midwayensis* Cushman, 1940

Remarks: A biserial group with globular/ovate chambers and moderate to high growth rate. Chambers are generally elongated laterally than axially. Aperture is an arch at the base of the final chamber. Wall may be smooth or finely pustulose, or striate (in one species). Characteristics of this group are summarized in Table 17.

Serial forms make up the maximum of 3% of planktonic assemblage in the samples, in >106 μm fraction. Forms attributable to *C. wilcoxensis* and *C. trinitatensis* were encountered in the samples.

In >63 μm fraction the biserial numbers are much higher; and morphologies are much diverse. Via SEM imaging, though, much of these biserials are found to be reworked Cretaceous forms. The distinction is based on surface characteristics, like striations; and gross morphological features, such as initial planispiral portion which is not found in the Paleocene-Eocene biserials. However, as also the case with other reworked/transported taxa, the preservation or the infill type do not give a direct idea, therefore many features need higher detail investigations (e.g. SEM).

Stratigraphic range: Danian to Rupelian (Pearson et al., 2006)

Chiloguembelina trinitatensis (Cushman and Renz 1942)

1942 *Guembelina trinitatensis* Cushman and Renz, 8, pl. 2: fig. 8

1957 *Chiloguembelina trinitatensis* (Cushman and Renz) - Beckmann, 91, pl. 21: fig. 7, text-fig. 15 (43-45)

Table 17: Rapid recognition chart for species of genus *Chiloguembelina*. * for species identified in this study

Species	Wall	Test Shape	Chamber Shape	Growth Rate	Sutures	Aperture	Apertural Modifications
<i>C. crinita</i>	Last chambers finely hispid	Axis may be deformed	Subglobular chambers	High	Distinct and depressed	Asymmetrical half rounded arch	Narrow asymmetrical lip
<i>C. cubensis</i>	Finely pustulose on youngest chambers, later becoming faintly but distinctly costate	Elongate, subtriangular in outline, moderately expanding, periphery rounded rather than compressed	Globular	Moderate	Depressed, perpendicular to slightly oblique to growth axis	Low, symmetrical arch centered or slightly off-center	Narrow asymmetrical collar
<i>C. midwayensis</i>	Finely pustulose	Rapidly flaring, periphery compressed	Elliptical, laterally longer than axial	Moderate	Distinct, depressed, very slightly curved	High, arched	One distinct lateral flange
<i>C. morsei</i>	Finely pustulose	Slender, about twice as long as broad	Globular chambers, lateral dimension slightly longer	Low to moderate	Earlier sutures sub-horizontal, later ones oblique	High, arched	One distinct lateral flange
<i>C. ototara</i>	Uniformly finely pustulose	Subtriangular, moderately expanding, periphery rounded	Globular	Moderate	Depressed, perpendicular to slightly oblique to growth axis	Slightly asymmetrical arch	Asymmetrical lip

Table 17 (Continued)

Species	Wall	Test Shape	Chamber Shape	Growth Rate	Sutures	Aperture	Apertural Modifications
<i>C. paralella</i>	Finely pustulose	Short, rapidly tapering, periphery rounded	Globular	Moderate to high	Moderately depressed, slightly oblique toward apical axis	High, narrow and symmetrical arch	Two parallel lateral flanges
<i>C. sub-triangularis</i>	Finely pustulose	Rapidly tapering, subangular periphery	Slightly inflated	Chambers increasing nearly twice as rapidly in breadth than in height	Depressed and nearly straight	Low, asymmetrical	Asymmetrical lip
* <i>C. trinitatis</i>	Finely pustulose	Moderately tapering, periphery broadly rounded	Globular, nearly spherical	Moderate	Depressed	Symmetrical	Narrow equidimensional lip
* <i>C. wilcoxensis</i>	Distinctly papillate	Rapidly flaring, then regular in last two sets, broadly rounded periphery	Inflated	Very high	Distinct and depressed	Symmetrical low arch	Equidimensional lip

1999 *Chiloguembelina trinitatensis* (Cushman and Renz) - Olsson et al, 92, pl. 13: figs. 11, 16, pl. 70: figs. 8-10, 14

Remarks: Chamber gradually growing, almost spherical in contrast to *C. crinata* which withholds more elliptical chambers (laterally broader). Aperture is symmetrical, may be bipartite.

Stratigraphic Range: Zone P5 to E3 (Pearson et al., 2006).

Occurrence: This form was encountered in the samples GT-16 and GT-25.

Chiloguembelina wilcoxensis (Cushman and Ponton 1932)

Plate 8, Figure 1

1932 *Guembelina wilcoxensis* Cushman and Ponton, 66, pl. 8: figs. 16, 17

1957 *Chiloguembelina wilcoxensis* (Cushman and Ponton) – Beckmann, 92, pl. 21: figs. 10, 12-13, text-fig. 15 (49-58)

1999 *Chiloguembelina wilcoxensis* (Cushman and Ponton) - Olsson et al., 92-93, pl. 13: figs. 19-20, pl. 70: figs. 11-13, 15-18

Remarks: Equally large chambers for the last two sets make up more like a square outline rather than triangular. Earlier chamber distinctly smaller and very few.

Stratigraphic Range: Zone P4 to E3 (Pearson et al., 2006).

Occurrence: This form was encountered in the samples GT-4, GT-10 and GT-16.

5.5 Family Heterohelicidae Cushman, 1927

This family contains the biserial groups.

5.5.1 Genus *Zeauvigerina* Finlay, 1939

Type species: *Zeauvigerina zelandica* Finlay, 1939

Remarks: A small biserial group of uniserial tendency at later ontogenic stages, with globular chambers and low growth rate. The sutures are shallowly depressed, and the aperture is either areal/terminal or produced on a short neck. This form tends to produce parallel sides as opposed to distinctly flaring in *Chiloguembelina*. Table 18 is the summary of distinct features of the species of this genus.

Serial forms make up the maximum of 3% of planktonic assemblage in the samples, in >106 µm fraction. Apart from several *C. wilcoxensis* and *C. trinitatensis*, forms attributable to *Z. aegyptiaca* were encountered in the samples.

In >63 µm fraction the numbers of biserial forms are much higher; and morphologies are much diverse. Via SEM imaging, though, much of these biserials are found to be reworked Cretaceous forms. The distinction is based on surface characteristics, like striations; and gross morphological features, such as initial planispiral portion which is not found in the Paleocene-Eocene biserials. However, as also the case with other reworked/transported taxa, the preservation or the infill type do not give a direct idea, therefore many features need higher detail investigations (e.g. SEM).

Stratigraphic range: Maastrichtian to Upper Eocene (Pearson et al., 2006)

Zeauvigerina aegyptiaca (Said and Kenaway 1956)

1956 *Zeauvigerina aegyptiaca* Said and Kenaway, 141, pl. 4: fig. 1

1994 *Zeauvigerina aegyptiaca* (Said and Kenaway) - Huber and Boersma, 271-273, text-figs. 6a, 7a-j, pl. 2: figs. 6-8

1999 *Zeauvigerina aegyptiaca* (Said and Kenaway) - Olsson et al., 1999:95, text-fig. 36a, pl. 71: figs. 19-20

Table 18: Rapid recognition chart for species of genus *Zeuvingerina*. * for species identified in this study

Species	Wall	Test Shape	Chamber Shape	Growth Rate	Sutures	Aperture
* <i>Z. aegyptica</i>	-	Outline elliptical, last chamber uniserial	Broader than high	Low	Indistinct	Rounded, terminal, at the end of a short but distinct neck with surrounding rim
<i>Z. Iodoensis</i>	Finely pustulose	Elongate, periphery rounded	Early chambers slightly compressed, later becoming increasingly globular	Moderate	Depressed, nearly perpendicular to the growth axis	Nearly terminal on a very short neck and raised from the base of the final chamber face
<i>Z. parri</i>	Smooth to finely pustulose	Elongate, parallel sided, elliptical in cross-section	Slightly inflated	Moderate	Slightly depressed, nearly perpendicular to growth axis	Terminal elliptical opening
<i>Z. teuria</i>	Very finely and densely roughened	Outline elliptical, last chamber uniserial	Globular	Low	Indistinct	At the end of a short, thick, central, tubular neck with distinct rim
"Z": <i>virgata</i>	Covered with row of pores	Elongate	Spherical	Low	Depressed, slightly curved	Interiomarginal with an equidimensional thickened rim or lip
<i>Z. waiparae nsis</i>	Finely pustulose	Moderately tapered, last chamber has tendency to become uniserial	Subglobular	Irregular	Subparallel in side view, slightly depressed, distinct	Terminal, oval with equidimensional narrow lip partially surrounding and folding into the aperture
<i>Z. zelandica</i>	Finely pustulose	Small, elongate, moderately tapering	Initially compressed, later globular	Moderate	Distinct, moderately depressed, nearly perpendicular to the growth axis	Terminal on a variably produced neck

Remarks: The test has an ovate overall shape with gradually increasing chamber size for a few chambers, then stabilizing, and finishing with last several chambers successively smaller laterally. The uniserial tendency is strong in this form with addition of last uniserial chamber. The last chamber is rather centered on the top, with a neck at the highest point.

Stratigraphic Range: Zone P5 to E3 (Pearson et al., 2006).

Occurrence: This form was encountered in the samples GT-1 and GT-11.

5.6 Triserial Tests

A number of triserial tests were encountered in the smaller fraction ($>63\ \mu\text{m}$), with almost spherical chambers, and arched aperture (Plate 9, Figures n and o). The forms are probably too small and altered for recognition and need further study, though, they resemble lower Paleocene *Guembelitra*, or Lower Eocene *Jenkinsina*. In the larger fraction ($>106\ \mu\text{m}$) no triserial forms have been observed.

5.7 High Trochospired Tests

A number of high trochospiral tests with 4-5 chambers in the last whorl are encountered in $>106\ \mu\text{m}$ fraction and they make up an average of 4% of the whole population. Coiling-wise they resemble the compact Acarininids, however, a solid deduction could not be made; therefore, they are left out in the quantitative analysis.

5.8. Reworked Tests

A high amount of reworked individuals were found in the samples, representing Cretaceous, early Paleocene and late Paleocene intervals. Majority of the biserial

groups encountered in the samples were later discovered to be Cretaceous forms with striations and irregular chamber arrangements (Plate 9, Figures j-m). The triserial forms, which are small (<106 μm), remained unidentified (Plate 9, Figures n, o). Many planispiral taxa attributable to Cretaceous genus *Globigerinelloides* (Plate 9, Figures g-i) are recovered from the samples, along with medium to low trochospiral forms attributable to early Paleocene genus *Praemurica* (Plate 9, Figures d-f). Globanomalinid (Plate 9, Figure c) and Igorinid species are also recovered out of their stratigraphic range, e.g. *G. pseudomenardii* is found in the higher levels (Plate 9, Figures a, b, specimens from GT-23).

CHAPTER 6

DISCUSSION AND CONCLUSIONS

A measured section of 33 m of shale in the middle part of the Eskipolatlı Formation in the Haymana Basin was sampled with a total of 41 samples examined with the purpose of detecting the P/E boundary and the planktonic foraminiferal record of the PETM in the Haymana Basin. A detailed taxonomical study on planktonic foraminifera was carried out, in total 40 species of 11 genera were identified. 4 biozones were distinguished, namely *G. pseudomenardii* Zone, *M. subbotinae* Zone, *A. sibaiyaensis* Zone, and *P. wilcoxensis* Zone. 26 of the samples were studied in terms of quantitative analysis for investigation of state of generic relative abundances throughout the measured section.

The Haymana Basin, a forearc basin formed during the closure of northern Neo-Tethys, is situated at higher latitudes compared to most of the Tethyan P/E sites such as Egypt and southern Spain. Difference in the relative abundances of genera between northern (Haymana, western and central Black Sea Region, Kazakhstan, Italy) and southern Tethyan sites (Egypt, Jordan, Tunisia, Spain) is the dominant group: *Subbotina*, *Acarinina*, or *Morozovella*. While the lower latitudes are dominated by *Morozovella*, in higher latitudes *Subbotina* has the highest abundance. The Haymana Basin, shows a higher Subbotinid abundance than that of lower latitudes, but not as high as western and central Black Sea Region. The average abundances of the dominant groups are as follows: *Acarinina* 40%, *Subbotina* 25%, and *Morozovella* 12%.

Almost all P/E sections show a rapid increase in abundance of *Acarinina* at the onset of PETM. This increase in Acarininid abundance stems from the evolution of new quadrate Acarininid species just prior to, and the excursion taxa (PFET) at the P/E boundary (by definition). A similar trend was also observed in the Haymana Basin with a sharp increase in *Acarinina*, a smaller increase in *Morozovella*, and a drop in *Subbotina* at the P/E boundary which is delineated by the lowest occurrence of *Acarinina sibaiaensis*, the only PFET found in the Haymana Basin. The absence of other excursion taxa may be due to preservational complexities, sampling resolution, or their preferred geographical distribution.

Almost all examined samples had individuals that stood out, which were interpreted as reworked/transported. For example, members of Globotruncanid, Globigerinellid, Heterohelicid groups from Cretaceous, genus *Praemurica* from lower Paleocene, and several Globanomalinids and Igorinids were found along with much younger species. However, no means of distinction of the reworked/transported from *in situ* specimens could be developed since no difference in preservation or infill material was observed.

All the tests of encountered planktonic foraminifera were filled. There were two types of infill materials: calcite and iron oxide. If a specimen were to be found filled with a different material than all the other specimens in a sample, it being transported from somewhere else would be the reasonable deduction. However, in the examined samples, both infill materials existed in the individuals, even of the same species, and the preservation state of these specimens was similar. Independent of the infill material, the preservation state could have clued reworking, but there were Cretaceous foraminifera preserved just as well as the youngest species in the assemblage.

This created problems with establishing the biostratigraphy. The Cretaceous foraminifera, and the lowest Paleocene taxa were easier to detect and cast out of the assemblage, however the upper Paleocene taxa mixed up in just a few meters above their stratigraphic range were confusing. The solution was to trust the LO's instead of HO's. In the interval of the measured section, there are two zonal boundaries

depending on HO's of taxa: P4/P5 boundary and E2/E3 boundary, former being the HO of *G. pseudomenardii*, and the latter being the HO of *M. velascoensis*; one is found in the upper levels among younger taxa, the other non-existent in the samples.

The P4/P5 boundary is placed at the HO of *G. pseudomenardii*, and is reinforced by 3 other events occurring near that datum: LO of *M. subbotinae*, and HO of *G. imitata* and *I. albeari*. Although HO of *G. imitata* and *I. albeari* are also subjected to doubt due to their reworked/transported occurrences in the upper levels, LO of *M. subbotinae* provided a datum for the boundary.

The E2/E3 boundary was not detected due to absence of the index taxon, and the secondary elements. The secondary elements for the boundary are the other Morozovellids with peripheral ornamentation (*M. passionensis*, *M. occlusa*, *M. acuta*; page 121 for Morozovellid group explanations) which are absent or significantly rare in the studied samples. One other mark is the HO of *S. velascoensis* and it is consistently found in the samples; however, this may also be an apparent HO, and the specimens may be reworked/transported. Yet, *M. formosa*, whose LO defines the E3/E4 boundary, and other late early Eocene taxa have not been found in the samples; therefore, even if the *S. velascoensis* specimens were reworked/transported, it is evident that the last sample of the measured section is within E2-E4 interval.

As specimens of many timelines were found together in the samples as reworked/transported two possible hypothesis arise: there must be a mechanism that eroded and redeposited sediment over and over again, or erosion of a large packet of rock must have occurred in a very short time interval, and get repeated several times.

One scenario begins with the erosion of already exposed Cretaceous rocks, transportation of those sediments via canyons digging in Paleocene rocks or sediments, dumping of coarser fraction in upper fan, depositing finer fraction in distal fan setting. Higher the influx, further the larger pieces' reach. This should require major uplift in a previously marine area in a short time (~10 Ma from K/Pg to P/E) which may be not so impossible since it is an active convergent margin.

With a slower but continuous uplift the fan deposits may have become unstable and redeposited over and over again, every time mixing the older sediment with the younger deposition, providing an almost continuous record in one layer.

The higher amounts of reworked taxa are found within the worst preserved samples, namely the GT-4-6, 10-12, 15-16 intervals, along with higher *Subbotina* abundance. These intervals may represent a time of higher erosion on the land, hence higher sedimentary influx into the marine setting. The warm water indices (*Morozovella* and *Acarinina*) may be suppressed during these intervals either by higher reproduction rates of *Subbotina* due to higher nutrient availability (may be a result of higher influx), or decreased water clarity affecting the light conditions that *Morozovella* and *Acarinina* need for their photosymbionts.

For the whole span of measured section the relative abundances of genera interchanged constantly. Although the temperature change had a large impact at the P/E boundary, all the changes cannot be attributable to that. Phases of distal turbiditic deposition interlayered with pelagic sedimentation is one hypothesis for this record as explained above.

Two size fractions were studied from the same samples, namely the larger (>106 μm) and smaller fraction (>63 μm). Smaller fraction studies were difficult for two reasons: first being simply their small size obscuring the fine details needed for species identification, second being the high amount of pre-adult specimens. Pre-adult individuals withhold great differences from their adult counterparts, and since the species definitions are based on adult morphologies their identification is not reliable even if possible. This is why in this study the >106 μm fraction was chosen as the main quantitative method. It is better understood when the *Acarinina* abundance difference in between the two fractions is examined: its abundance in the smaller fraction is considerably lower mostly because the Acarininid species are generally larger in size, also the pre-adult specimens probably are distinctly different to be recognized into the genus.

To conclude, with this study the position of the P/E boundary and the planktonic foraminiferal record of the PETM were detected in the Haymana Basin, in middle

part of the Eskipolatlı Formation. The boundary is placed at the lowest occurrence datum of *A. sibiyaensis*, identified in Turkey the first time with this study, a so called excursion taxon that ranges only the PETM. The chronostratigraphically important biozone E1 (*A. sibiyaensis* Zone: between LO of *A. sibiyaensis* and LO of *P. wilcoxensis*) was found to span about 3 m, a similar thickness to that of other sites (e.g. Dababiya: 2.2 m, Darb Gaga: 2.5 m, Qreiya: 2.4 m).

REFERENCES

- Akarsu, İ. (1971). *II. Bölge AR/TPO/747 nolu sahanın terk raporu*. Ankara: Pet. İş. Gen. Müd. (Unpublished).
- Amirov, E. (2008). *Planktonic foraminiferal biostratigraphy, sequence stratigraphy and foraminiferal response to sedimentary cyclicity in the Upper Cretaceous-Paleocene of the Haymana Basin (Central Anatolia, Turkey)*. Ankara: MSc. Thesis, Middle East Technical University.
- Arenillas, I., & Arz, J. (2013). New evidence on the origin of non-spinose pitted-cancellate species of the early Danian planktonic foraminifera. *Geologica Carpathica*, 64, pp. 237-251.
- Arenillas, I., & Molina, E. (1996). Bioestratigrafía y evolución de las asociaciones de foraminíferos planctónicos del tránsito Paleoceno- Eoceno en Alamedilla (Cordilleras Béticas). *Revista Espanola de Micropaleontologia*, v. 18, pp. 75-96.
- Aubry, M. P. (1996). Towards an Upper Paleocene-Lower Eocene high resolution stratigraphy based on calcareous nannofossil stratigraphy. *Israel Journal of Earth Sciences*, 44, pp. 239-253.
- Aubry, M. P. (1998). The upper Paleocene-lower Eocene stratigraphic puzzle. *Strata*, 6, pp. 7-9.
- Aubry, M. P. (2000). Where should the Global Stratotype Section and Point (GSSP) for the Paleocene/Eocene boundary be located? *Bulletin de la Societe Geologique de France*, t. 171, no. 4, pp. 461-476.

- Aubry, M. P. (2002). The Paleocene/Eocene boundary Global Standard Stratotype-section and Point (GSSP): Criteria for Characterisation and Correlation. *Tertiary Research*, 21, (1-4), pp. 57-70.
- Aubry, M. P., Ouda, K., Dupuis, C., Berggren, W. A., & Van Couvering, J. A. (2007). The Global Standard Stratotype-section and Point (GSSP) for the base of the Eocene Series in the Dababiya section (Egypt). *Episodes*, 30/4, pp. 271-286.
- Banner, F. T., & Blow, W. H. (1959). The classification and stratigraphical distribution of the Globigerinaceae. *Palaeontology*, v. 2, pt. 1, pp.1-27.
- Bayhan, E., & Gökçen, S. L. (1990). "Ankara Vigrasyonu" Üst Kretase-Alt Tersiyer havzalarının petrolojik karşılaştırılması. *MTA Dergisi*, 111, pp. 101-110.
- Beckmann, J. (1957). Chiloguembelina Loeblich and Tappan and Related Foraminifera from the Lower Tertiary. In J. a. A.R. Loeblich, *Studies in Foraminifera*, 215 (pp. 83-95). Bulletin of the United States National Museum.
- Belford, D. (1984). Tertiary Foraminifera and Age of Sediments, Ok Tedi-Wabag, Papua, New Guinea. *Bulletin, Bureau of Mineral Resources, Geology, and Geophysics, Australia*, 216, pp. 1-52.
- Berggren, W. A. (1960). Paleogene biostratigraphy and planktonic Foraminifera of SW Soviet Union: an analysis of recent Soviet investigations. *Stockholm Contributions in Geology*, v. 6, no. 5, pp. 63-125.
- Berggren, W. A. (1969). Paleogene Biostratigraphy and Planktonic Foraminifera of Northwestern Europe. *Proceedings of the First International Conference on Planktonic Microfossils 1* (P. Brönnimann and H.H. Renz, editors), (pp. pp. 121-160).
- Berggren, W. A. (1971). Paleogene Planktonic Foraminiferal Faunas on Legs I-IV (Atlantic Ocean), JOIDES Deep Sea Drilling Program-a Synthesis. In e. A.

Farinacci, *Proceedings of the II Planktonic Conference, 1* (pp. 57-77). Rome: Edizioni Tecnoscienza.

Berggren, W. A. (1977). Atlas of Palaeogene Planktonic Foraminifera: Some Species of the Genera Subbotina, Planorotalites, Morozovella, Acarinina and Truncorotaloides. In e. A.T.S. Ramsay, *Oceanic Micropaleontology* (pp. 205-300). London: Academic Press.

Berggren, W. A. (1992). 31. Paleogene planktonic foraminifer magnetobiostratigraphy of the southern Kerguelen Plateau (Sites 747-749). In S. W. Wise, & R. e. Schlich, *Proceedings of the Ocean Drilling Program, Scientific Results, Vol. 120* (pp. 551-568). Texas: Ocean Drilling Program.

Berggren, W. A., & Miller, K. G. (1988). Paleogene tropical planktonic foraminiferal biostratigraphy and magnetobiochronology. *Micropaleontology*, vol. 34, no. 4, pp. 362-380.

Berggren, W. A., & Norris, R. D. (1997). Taxonomy and Biostratigraphy of (Sub)tropical Paleocene Planktonic Foraminifera. *Micropaleontology, Supplement 1*, 43, pp. 1-116.

Berggren, W. A., & Ouda, K. (2003a). Upper Paleocene-lower Eocene planktonic foraminiferal biostratigraphy of the Dababiya section, Upper Nile Valley (Egypt). *Micropaleontology*, vol. 49, pp. 61-92.

Berggren, W. A., & Ouda, K. (2003b). Upper Paleocene-lower Eocene planktonic foraminiferal biostratigraphy of the Qreiya (Gebel Abu Had) section, Upper Nile Valley (Egypt). *Micropaleontology*, vol. 49, pp. 105-122.

Berggren, W. A., & Pearson, P. N. (2005). A revised tropical to subtropical Paleogene planktonic foraminiferal Zonation. *Journal of Foraminiferal Research*, v. 35, no. 4, p. 279-298.

Berggren, W. A., Kent, D. V., Swisher, C. C., & Aubry, M. -P. (1995). A revised Cenozoic geochronology and chronostratigraphy. In W. A. Berggren, D. V. Kent, M. -P. Aubry, & J. Hardenbol, *Geochronology, Time Scales and Global*

- Stratigraphic Correlation* (pp. 129-212). SEPM Society for Sedimentary Geology, SEPM Special Publication no. 54.
- Berggren, W., Olsson, R., & Reymont, R. (1967). Origin and Development of the Foraminiferal Genus *Pseudohastigerina* Banner and Blow, 1959. *Micropaleontology*, 13, pp. 265-288.
- Bermudez, P. (1961). Contribución al estudio de las Globigerinidea de la region Caribe-Antillana (Paleocene-Reciente). *Boletín de Geología {Venezuela}, Publicación Especial, 3 (Congres Geología Venezolano, 3d, Caracas, 1959, Mem. 3, 1119-1393.*
- Birch, H. S., Coxall, H. K., & Pearson, P. N. (2012). Evolutionary ecology of Early Paleocene planktonic foraminifera: size, depth habitat and symbiosis. *Paleobiology*, 38(3), pp. 374–390.
- Blow, W. H. (1979). *The Cainozoic Globigerinida*. The Netherlands: E. J. Brill.
- Bolli, H. (1957b). Planktonic Foraminifera from the Eocene Navet and San Fernando Formations of Trinidad, B.W.I. In J. a. A.R. Loeblich, *Studies in Foraminifera*, 215 (pp. 155-172). Bulletin of the United States National Museum.
- Bolli, H. M. (1957a). The genera *Globigerina* and *Globorotalia* in the Paleocene - lower Eocene Lizard Springs Formation of Trinidad, B.W.I. *Bulletin United States National Museum*, 215, pp. 51-81.
- Bolli, H. M., Loeblich, A. R., & Tappan, H. (1957). Planktonic foraminiferal families Hantkeninidae, Orbulinidae, Globorotaliidae, and Globotruncanidae. *U. S. Natural Museum Bulletin*, 215, pp. 3-50.
- Bolli, H., & M.B., C. (1960). Globigerine e Globorotalie del Paleocene di Pademo d'Adda (Italia). *Rivista Italiana di Paleontologia e Stratigrafia*, 66, pp. 361-408.

- Bornemann, A., Norris, R. D., Lyman, J. A., D'haenens, S., Groeneveld, J., Röhl, U., et al. (2014). Persistent environmental change after the Paleocene-Eocene Thermal Maximum in the eastern North Atlantic. *Earth and Planetary Science Letters*, vol. 394, pp. 70-81.
- BouDagher-Fadel, M. K. (2015). *Biostratigraphic and Geological Significance of Planktonic Foraminifera, Updated 2nd Ed.* London: UCL Press.
- Brönnimann, P. (1952). Trinidad Paleocene and Lower Eocene Globigerinidae. *Bulletins of American Paleontology*, 34: 34.
- Brummer, G. A., Hembleben, C., & Spindler, M. (1986). Planktonic foraminiferal ontogeny and new perspectives for micropaleontology. *Nature*, vol. 319, pp. 50-52.
- Brummer, G. A., Hembleben, C., & Spindler, M. (1987). Ontogeny of extant spinose planktonic foraminifera (Globigerinidae): a concept exemplified by *Globigerinoides sacculifer* (Brady) and *G. ruber* (d'Orbigny). *Marine Micropaleontology*, 12, pp. 357-381.
- Buffet, B., & Archer, D. (2004). Global inventory of methane clathrate: sensitivity to changes in the deep ocean. *Earth and Planetary Science Letters*, 227, pp. 185-199.
- Buzas, M. A. (1990). Another look at confidence limits for species proportions. *Journal of Paleontology*, 64, pp. 842-843.
- Bykova, N. (1953). Foraminifery suzaskogo yarusy Tadzhijskoi depressii [Foraminifera of the Suzakh Stage of the Tadjik Depression]. *Trudy Vsesoyuznogo Neftyanogo Nauchno-Issledovat'skogo GeologoRazvedochnogo Instituta (VNIGRT), Mikrofauna SSSR, Sbornik*, 6, pp. 5-103.
- Canudo, J. I., & Molina, E. (1992). Planktic foraminiferal faunal turnover and bio-chronostratigraphy of the Paleocene-Eocene boundary at Zumaya, northern Spain. *Revista de la Sociedad Geológica de España*, 5, (1-2), pp. 145-157.

- Caromel, A. G., Schmidt, D. N., Fletcher, I., & Rayfield, E. J. (2015). Morphological change during the ontogeny of the planktic foraminifera. *Journal of Micropaleontology* 2014-017, Vol. 35, 2-19.
- Cushman, J. A. (1925). Some New Foraminifera from the Velasco Shale of Mexico. *Contributions from the Cushman Laboratory for Foraminiferal Research*, 1, pp. 18-23.
- Cushman, J. A. (1944). A Foraminiferal Fauna of the Wilcox Eocene, Bashi Formation, from near Yellow Bluff, Alabama. *American Journal of Science*, 242:7-18.
- Cushman, J. A., & Ponton, G. M. (1932). An Eocene Foraminiferal Fauna of Wilcox Age from Alabama. *Contributions from the Cushman Laboratory for Foraminiferal Research*, 8, pp. 51-72.
- Cushman, J., & Bermúdez, P. (1949). Some Cuban Species of Globorotalia. *Contributions from the Cushman Laboratory for Foraminiferal Research*, 25, pp. 26-45.
- Cushman, J., & Hanna, G. (1927). Foraminifera from the Eocene near San Diego, California. *Transactions of the San Diego Society of Natural History*, 5, pp. 45-64.
- Cushman, J., & Renz, H. (1942). Eocene, Midway, Foraminifera from Soldado Rock, Trinidad. *Contributions from the Cushman Laboratory for Foraminiferal Research*, 18, pp. 1-14.
- Çetin, H., Demirel, İ. H., & Gökçen, S. L. (1986). Haymana (SW Ankara) doğusu ve batısındaki Üst Kretase - Alt Tersiyer istifinin sedimantolojik ve sedimenter petrolojik incelenmesi. *Türkiye Jeoloji Kurumu Bülteni*, c. 29, pp. 21-33.
- Çiner, A. (1996). Distribution of small scale sedimentary cycles throughout several selected basins. *Turkish Journal of Earth Sciences*, 5, pp. 25-37.

- Çiner, A., Deynoux, M., & Kosun, E. (1996b). Cyclicity in the middle Eocene Yamak turbidite complex of the Haymana basin, Central Anatolia, Turkey. *Geol Rundsch*, 85, pp. 669-682.
- Çiner, A., Deynoux, M., Koşun, E., & Gündoğdu, N. (1993a). Beldede Örgülü-Delta Karmaşığı'nın (BÖDK) sekans stratigrafik analizi; Polatlı-Haymana Baseni, (Orta Eosen) Orta Anadolu. *Yerbilimleri*, 16, pp. 61-92.
- Çiner, A., Deynoux, M., Koşun, E., & Gündoğdu, N. (1993b). Yamak Türbidit Karmaşığı'nın (YTK) sekansiyel stratigrafik analizi: Haymana Baseni (Orta Eosen). *Sekans Stratigrafisi*, Sedimantoloji Çalışma Grubu Özel Yayını No. 1, pp. 53-70.
- Çiner, A., Deynoux, M., Ricou, S., & Kosun, E. (1996a). Cyclicity in the Middle Eocene Çayraz Carbonate Formation, Haymana Basin, Central Anatolia, Turkey. *Palaeogeography, Palaeoclimatology, Palaeoecology*, 121, pp. 313-329.
- Çolakoğlu, S., & Özcan, E. (2003). Orthophragminid foraminiferal assemblages from an Ilerdian-early Cuisian reference section (Sakarya section, Haymana-Polatlı Basin, Central Anatolia-Turkey). *Rivista Italiana di Paleontologia e Stratigrafia*, vol. 109, no. 1, ta. 3, pp. 1-17.
- Davidzon, R., & Morozova, V. (1964). Planktonnye i bentosnye izvestkovye foraminifery Bucharshikh sloev (Paleotsen) Tadzhikskoi depressii. *Paleontologicheskiy Zhurnal*, 3, pp. 23-29.
- Deveciler, A. (2008). *Haymana çevresindeki Eosen yaşlı Çayraz Formastonu pelecypoda ve gastropoda faunalarının paleontolojisi*. Ankara: MSc. Tez, Ankara Üni. Fen Bilimleri Ens.
- D'Haenens, S., Bornemann, A., Roose, K., Claeys, P., & Speijer, R. P. (2012). Stable isotope paleoecology (D13C and D18O) of early Eocene *Zeauvigerina aegyptiaca* from the North Atlantic (DSDP Site 401). *Austrian Journal of Earth Sciences*, vol. 105/1, pp. 179-188.

- Dinçer, F. (2016). Eocene benthic foraminiferal assemblages from Central Anatolia (Turkey): biostratigraphy, stable isotope data, paleoenvironmental and paleontological interpretations. *Journal of African Earth Sciences*, 114, pp. 143-157.
- Duru, M., & Gökçen, N. (1990). Polatlı (GB Ankara) güneyi Monsiyen-Küziyen istifinin ostrakod biyostratigrafisi ve ortamsal yorumu. *MTA Bülteni*, 110, pp. 165-174.
- El Naggar, Z. R. (1966). Stratigraphy and planktonic foraminifera of the Upper Cretaceous-Lower Tertiary. *Bulletin of the British Museum (Natural History), Geology*, Supplement 2, 291 p.
- El-Dawy, M. H., Obaidalla, N. A., Mahfouz, K. H., & Wahed, S. A. (2016). Paleocene-Eocene transition at Naqb Assiut Oasis, Western Desert, Egypt: Stratigraphical and paleoenvironmental inferences. *Journal of African Earth Sciences*, 117, pp. 207-222.
- El-Nady, H. (2005). The impact of Paleocene/Eocene (P/E) boundary events in northern Sinai, Egypt: Planktonic foraminiferal biostratigraphy and faunal turnovers. *Revue de Paléobiologie*, 24 (1), pp. 1-16.
- Eser Doğdu, B. (2007). *Haymana güneyi (Ankara) Yamak formasyonu iz fosilleri*. Ankara: MSc. Tez, Ankara Üni. Fen Bilimleri Ens.
- Esmeray, S. (2008). *Cretaceous/Paleogene boundary in the Haymana Basin, Central Anatolia, Turkey: micropaleontological and sequence stratigraphic approach*. Ankara: MSc. Thesis, Middle East Technical University.
- Esmeray-Senlet, S., Özkan-Altner, S., Altner, D., & Miller, K. G. (2015). Planktonic foraminiferal biostratigraphy, microfacies analysis, sequence stratigraphy and sea-level changes across Cretaceous across the Cretaceous-Paleogene boundary in the Haymana Basin, Central Anatolia, Turkey. *Journal of Sedimentary Research*, v. 85, pp. 489-508.

- Finlay, H. J. (1947). New Zealand Foraminifera: Key Species in Stratigraphy, No. 5. *New Zealand Journal of Science and Technology*, 28, pp. 259-292.
- Fleisher, R. (1974). Cenozoic planktonic foraminifera and biostratigraphy, Arabian Sea, Deep Sea Drilling Project, Leg 23A. In R. Whitmarsh, D. O.E.Ross, & editors, *Initial Reports of the Deep Sea Drilling Project Vol. 23* (pp. 1001-1072).
- Gartner, S. J., & Hay, W. (1962). Planktonic Foraminifera from the Type Ilerdian. *Eclogae Geologicae Helvetiae*, 55, pp. 553-575.
- Geyikçiođlu Erbař, B. (2008). *Meter scale cycles in the eocene ayraz Formation (Haymana Basin) and response of foraminifers to cyclicality*. Ankara: MSc. Thesis, Middle East Technical University.
- Glaessner, M. (1937a). Planktonische Foraminiferen aus der Kreide und dem Eozän und ihre stratigraphische Bedeutung. *Studies in Micropaleontology, Publications of the Laboratory of Paleontology, Moscow University*, 1, pp. 27-52.
- Gohrbandt, K. A. (1963). Zur Gliederung der Paläogen im Helvetikum nördlich Salzburg nach planktonischen Foraminiferen, I. Teil: Paleozän und tiefstes Untereozän. *Mitteilungen der Geologischen Gesellschaft in Wien*, 56, pp. 1-116.
- Gökçen, S. L. (1976a). Ankara - Haymana güneyinin sedimantolojik incelenmesi I: stratigrafik birimler ve tektonik. *Hacettepe Üni. Yer Bilimleri Ens. Yayın Organı*, C. 2, No. 2, pp. 161-199.
- Gökçen, S. L. (1976b). Ankara-Haymana güneyinin sedimantolojik incelenmesi II: sedimantoloji ve paleoakıntılar. *Hacettepe Üni. Yer Bilimleri Ens. Yayın Organı*, C. 2, No. 2, pp. 201-235.
- Gökçen, S. L. (1977). Ankara-Haymana güneyinin sedimantolojik incelenmesi III: bölge tortullařma modeli ve paleocođrafya. *Hacettepe Üni. Yer Bilimleri Ens. Yayın Organı*, C. 3, No. 1, 2, pp. 13-23.

- Gökçen, S. L., & Kelling, G. (1983). The Palaeogene Yamak sand-rich submarine-fan complex, Haymana Basin, Turkey. *Sedimentary Geology*, 34, pp. 219-243.
- Görür, N. (1981). Tuzgölü-Haymana havzasının stratigrafik analizi. *TKJ, İç Anadolu'nun Jeolojisi Simpozyumu, Ankara*, pp. 60-66.
- Görür, N., Oktay, F. Y., Seymen, İ., & Şengör, A. C. (1984). Paleotectonic evolution of the Tuzgölü Basin complex, central Turkey: Sedimentary record of the neo-tethyan closure. In J. Dixon, & A. F. Robertson, *The Geological Evolution of the Eastern Mediterranean* (pp. 467-481). London: Geological Society of London, Special Publications, 17.
- Guasti, E., & Speijer, R. P. (2007). The Paleocene-Eocene Thermal Maximum in Egypt and Jordan: An overview of the planktonic foraminiferal record. In S. Monechi, R. Coccioni, & M. Rampino, *Large Ecosystem Perturbations: Causes and Consequences* (pp. pp. 53-67). Geological Society of America Special Paper 424.
- Guasti, E., & Speijer, R. P. (2008). *Acarinina multicamerata* n. sp. (Foraminifera): a new marker for the Paleocene-Eocene thermal maximum. *Journal of Micropaleontology*, 27, pp. 5-12.
- Güngör, A. (1975). Ankara-Haymana bölgesi Eoseninde bulunan *Campanile Bayle* (In Fischer), 1884, cinsine ait türlerin etüdü. *MTA Bülteni*, 84, pp. 30-34.
- Güray, A. (2014). *Planktonic foraminiferal biostratigraphy of the Paleocene-Eocene sequences in the western and central Black Sea Region, Turkey*. Ankara: PhD. Thesis, Middle East Technical University.
- Handley, L., Pearson, P. N., McMillian, I. K., & Pancost, R. D. (2008). Large terrestrial and marine carbon and hydrogen isotope excursions in a new Paleocene/Eocene boundary section from Tanzania. *Earth and Planetary Science Letters*, v. 275, pp. 17-25.

- Hanif, M., Hart, M. B., & Grimes, S. T. (2012). Revised late Paleocene-early Eocene planktonic foraminiferal biostratigraphy of the Indus Basin, Pakistan. *Journal of Nepal Geological Society*, vol. 44, pp. 23-32.
- Hemleben, C., & Olsson, R. K. (2006). Wall textures of Eocene Planktonic Foraminifera. In P. N. Pearson, R. K. Olsson, B. T. Huber, C. Hemleben, & W. A. Berggren, *Atlas of Eocene Planktonic Foraminifera* (pp. 47-66). Fredericksburg, USA: Cushman Foundation for Foraminiferal Research Special Publication, vol. 41, Cushman Foundation for Foraminiferal Research.
- Hemleben, C., Olsson, R. K., Berggren, W. A., & Norris, R. D. (1999). Wall texture, classification and phylogeny. In R. K. Olsson, C. Hemleben, W. A. Berggren, & B. T. Huber, *Atlas of Paleocene Planktonic Foraminifera* (pp. 10-13). Washington, D.C., USA: Smithsonian Contributions to Paleobiology, No 85, Smithsonian Institution Press.
- Higgins, J. A., & Schrag, D. P. (2006). Beyond methane: Towards a theory for the Paleocene–Eocene Thermal Maximum. *Earth and Planetary Science Letters*, 245, pp. 523–537.
- Hillebrandt, A. (1962). *Das Paleozän und seine Foraminiferenfauna im Becken von Reichenhall und Salzburg*. München: Bayerische Akademie der Wissenschaften, 10.
- Hoşgör, İ. (2012). *Haymana-Polatlı Havzası Paleosen mollusklarının taksonomik tanımlanması, paleoekolojisi, paleocoğrafyası ve bentik foraminiferlerle biyostratigrafik denestirilmesi*. Ankara: MSc. Tez, Ankara Üni. Fen Bilimleri Ens.
- Huber, B. T. (1991). Paleocene and Early Neogene Planktonic Foraminifer Biostratigraphy of Sites 738 and 744, Kerguelen Plateau (Southern Indian Ocean). In J. Barron, & B. e. Larsen, *Proceedings of the Ocean Drilling Program, Scientific Results, 119* (pp. 427-449). College Station, Texas: Ocean Drilling Program.

- Huber, B., & Boersma, A. (1994). Cretaceous Origin of Zeauvigerina and Its Relationship to Paleocene Biserial Planktonic Foraminifera. *Journal of Foraminiferal Research*, 24, pp. 268-287.
- Huseynov, A. (2007). *Sedimentary cyclicality in the Upper Cretaceous Successions of the Haymana Basin (Turkey): depositional sequences as response to relative sea-level changes*. Ankara: MSc. Thesis, Middle East Technical University.
- İslamoğlu, Y., Dominici, S., & Kowalke, T. (2011). Early Eocene Caenogastropods (Mollusca, Gastropoda) from Haymana-Polatlı Basin, Central Anatolia (Turkey): taxonomy and palaeoecology. *Geodiversitas*, 33 (2), pp. 303-330.
- Jenkins, D. G. (1971). New Zealand Cenozoic Planktonic Foraminifera. *Palaeontological Bulletin, New Zealand Geological Survey*, 42: 278 pages.
- Kalia, P., & Kintso, R. (2007). Planktonic foraminifera at the Paleocene/Eocene boundary in the Jaisalmer Basin, Rajasthan, India. *Micropaleontology*, vol. 52, no. 6, 521-536.
- Kelly, D. C., Bralower, T. J., & Zachos, J. C. (1998). Evolutionary consequences of the latest Paleocene thermal maximum for tropical planktonic foraminifera. *Palaeogeography, Palaeoclimatology, Palaeoecology*, 141, pp. 139-161.
- Kelly, D. C., Bralower, T. J., & Zachos, J. C. (2001). On the demise of the early Paleogene *Morozovella velascoensis* lineage: terminal progenesis in the planktonic foraminifera. *Palios*, vol. 16, 507-523.
- Kelly, D. C., Bralower, T. J., Zachos, J. C., Premoli Silva, I., & Thomas, E. (1996). Rapid diversification of planktonic foraminifera in the tropical Pacific (ODP Site 865) during the late Paleocene thermal maximum. *Geology*, v. 24, no. 5, 423-426.
- Kennett, J. P., & Stott, L. D. (1991). Abrupt deep-sea warming, palaeoceanographic changes and benthic extinctions at the end of the Paleocene. *Nature*, vol. 353, pp. 225-229.

- Kent, D. V., Cramer, B. S., Lanci, L., Wang, D., Wright, J. D., & Van der Voo, R. (2003). A case for a comet impact trigger for the Paleocene/Eocene thermal maximum and carbon isotope excursion. *Earth and Planetary Science Letters*, 211, pp. 13-26.
- Khalilov, D. M. (1956). O pelagicheskoy faune foraminifer Paleogenovykh otlozheniy Azerbaydzhana [Pelagic Foraminifera of the Paleogene Deposits of the Azerbaizhan SSR]. *Trudy Instituta Geologii, Akademiya Nauk Azerbaidzhanskoi SSR*, 17: 234-255. .
- Koçyiğit, A. (1991). An example of an accretionary forearc basin from northern Central Anatolia and its implications for the history of subduction of Neo-Tethys in Turkey. *Geological Society of America Bulletin*, 103, no. 1, pp. 22-36.
- Koçyiğit, A., Özkan, S., & Rojay, B. F. (1988). Examples from the forearc basin remnants at the active margin of northern Neo-tethys; development and emplacement ages of the Anatolian Nappe, Turkey. *METU Journal of Pure and Applied Sciences*, Vol. 21, No. 1-3, pp. 183-210.
- Krasheninnikov, V., & R.H., H. (1973). Late Cretaceous, Paleogene and Neogene Planktonic Foraminifera. In B. Heezen, & M. I. al., *Initial Reports of the Deep Sea Drilling Project, 20* (pp. 105-203). Washington, D.C.: U.S. Government Printing Office.
- Leonov, G., & Alimarina, V. (1960). Stratigrafiya i planktonnye foraminifery "perekhodnykh" ot mela k paleogeny sloev tsentral'nogo Predkavkazy. *Problema V: Granitsa melovoi i paleogenovoi sistem* (pp. 29-60). Mezhdunarodnyi Geologicheskii Kongress, XXI Sessiya, Doklady Sovetskikh Geologov Izdatelstvo Akademiya Nauk.
- Leroy, L. W. (1953). Biostratigraphy of the Maqfi Section, Egypt. *Geological Society of America, Memoir*, , 54, pp. 1-73.

- Lipps, J. H. (1966). Wall structure, systematics, and phylogeny studies of Cenozoic planktonic foraminifera. *Journal of Paleontology*, Vol. 40, No. 6, pp. 1257-1274.
- Loeblich, A. J., & Tappan, H. (1988). *Foraminiferal Genera and Their Classification*. New York: Van Nostrand and Reinhold Company.
- Loeblich, A. R., & Tappan, H. (1957). Planktonic Foraminifera of Paleocene and Early Eocene Age from the Gulf and Atlantic Coastal Plains. In J. a. A.R. Loeblich, *Studies in Foraminifera*, 215 (pp. pp. 173-198). Bulletin of the United States National Museum.
- Lu, G., & Keller, G. (1993). The Paleocene-Eocene Transition in the Antarctic Indian Ocean: Inference from Planktic Foraminifera. *Marine Micropaleontology*, 21, pp. 101-142.
- Lu, G., & Keller, G. (1995). Planktic foraminiferal faunal turnovers in the subtropical Pacific during the late Paleocene to early Eocene. *Journal of Foraminiferal Research*, v. 25, no. 2, 97-116.
- Lu, G., Keller, G., & Pardo, A. (1998). Stability and change in Tethyan planktic foraminifera across the Paleocene-Eocene transition. *Marine Micropaleontology*, 35, pp. 203-233.
- Luciani, V., Giusberti, L., Agnini, C., Fornaciari, E., Rio, D., Spofforth, D. J., et al. (2010). Ecological and evolutionary response of Tethyan planktonic foraminifera to the middle Eocene climatic optimum (MECO) from the Alano section (NE Italy). *Palaeogeography, Palaeoclimatology, Palaeoecology* 292, 82-95.
- Luciani, V., Giusberti, L., Agnini, C., Backman, J., Fornaciari, E., & Rio, D. (2007). The Paleocene-Eocene Thermal Maximum as recorded by Tethyan planktonic foraminifera in the Forada section (northern Italy). *Marine Micropaleontology*, 64, pp. 189-214.

- Luterbacher, H. (1957). Planktonic Foraminifera of the Paleocene and Early Eocene, Possagno Section. *Schweizerische Paläontologische Abhandlungen*, 97, pp. 57-67, plates 1-4.
- Luterbacher, H. P. (1964). Studies in Some Globorotalia from the Paleocene and Lower Eocene of the Central Apennines. *Eclogae Geologicae Helvetiae*, 57, pp.631-730.
- Mallory, V. (1959). *Lower Tertiary Biostratigraphy of the California Coast Ranges*. Tulsa, Oklahoma: American Association of Petroleum Geologists.
- Martin, L. T. (1943). Eocene Foraminifera from the Type Lodo Formation, Fresno County, California. *Stanford University Publications, Geological Sciences*, 3, pp. 93-125.
- Matsumaru, K. (1997). On Pseudorbitoides Trechmanni Douville (orbitoidal foraminifera) from Turkey. *Revue de Micropaleontologie*, 40, pp. 339-346.
- Matsumaru, K. (1999). Multiple Fission in Alveolina oblonga D'Orbigny in Turkey. *Revue de Micropaleontologie*, vol. 42, no. 3, pp. 245-251.
- McGorwan, B. (1965). Two Paleocene Foraminiferal Faunas from the Wangerrip Group, Pebble Point Coastal Section, Western Australia. *Proceedings of the Royal Society of Victoria*, 79, pp. 9-74.
- McGorwan, B. (1968). Reclassification of Early Tertiary Globorotalia. *Micropaleontology*, 14, pp. 179-198.
- McInerney, F. A., & Wing, S. L. (2011). The Paleocene-Eocene Thermal Maximum: a perturbation of carbon cycle, climate, and biosphere with implications for the future. *Annual Review of Earth and Planetary Sciences*, 39, pp. 489-516.
- Meriç, E., & Görür, N. (1970-80). Haymana-Polatlı havzasındaki Çaldağ kireçtaşının kireçtaşının yaş konağı. *MTA Bülteni*, 93/94, pp. 137-142.

- Molina, E. (2015). Evidence and causes of the main extinction events in the Paleogene based on extinction and survival patterns of foraminifera. *Earth-Science Reviews* 140, 166-181.
- Molina, E., Arenillas, I., & Martín-Ruiz, F. C. (2001). Stop 3: The Paleocene/Eocene Boundary. In F. C. Martínez-Ruiz, E. Molina, & F. J. Rodríguez-Tovar, *Field-trip Guide to the Agost and Caravaca Sections (Betic Cordillera, Spain)* (pp. 54-63). Granada: Impact Markers in the Stratigraphic Record, Granada (Spain), May 19- May 25, 2001.
- Molina, E., Arenillas, I., & Pardo, A. (1999). High resolution planktic foraminiferal biostratigraphy and correlation across the Palaeocene/Eocene boundary in the Tethys. *Bulletin de la Société Géologique de France*, t. 170, no. 4, pp. 521-530.
- Molina, E., Arenillas, I., & Schmitz, B. (1996). Field trip guide to the Paleocene and early Eocene of Zumaya section. *Early Paleogene Stage Boundaries*, (pp. 57-72). Zaragoza.
- Morozova, V. G. (1939). K stratigraphii verchnego mela i paleogena Embenskoj oblasti po faune foraminifer. *Byulleten Moskovskogo Obshchestva Ispytatelei Prirody, Otdel Geologicheskii*, 17, pp. 59-96.
- Morozova, V., Kozhevnikova, G., & Kuryleva, A. (1967). Datsko-Paleotsenovye Raznofatsial'nye otlozheniya Kopet-Daga i metody ikh korrelyatsii po foraminiferam. *Trudy Geologicheskogo Instituta, Akademiya Nauk SSSR*, 157, pp. 1-208.
- Murray, J. W., Curry, D., Haynes, J. R., & King, C. (1989). Chapter 10. Paleogene. In D. G. Jenkins, & J. W. Murray, *Stratigraphical Atlas of Fossil Foraminifera (2nd Ed.)* (pp. 490-536). Chichester: Ellis Horwood (for the British Micropaleontological Society).
- Nairn, S. P., Robertson, A. H., Ünlügenç, U. C., Taşlı, K., & İnan, N. (2012). Tectonostratigraphic evolution of the Upper Cretaceous–Cenozoic central

- Anatolian basins: an integrated study of diachronous ocean basin closure and continental collision. In A. H. Robertson, O. Parlak, & U. C. Ünlügenç, *Geological Development of Anatolia and the Easternmost Mediterranean Region*. London: The Geological Society of London Special Publications, 372.
- Nakkady, S. E. (1950). A new foraminiferal fauna from the Esna shales and Upper Cretaceous chalk of Egypt. *Journal of Paleontology*, Vol. 24 p. 675-692.
- Nakkady, S. E. (1959). Biostratigraphy of the Um Elghanayem section, Egypt. *Micropaleontology*, 5, pp. 453-472.
- Nederbragt, A., & Van Hinte, J. (1987). Biometrie Analysis of Planorotalites pseudomenardii (Upper Paleocene) at Deep Sea Drilling Site 605, Northwestern Atlantic. . In S. W. J.E. Van Hinte, *Initial Reports of the Deep Sea Drilling Project, 93* (pp. 577-592). Washington, D.C.: U.S. Government Printing Office.
- Nguyen, T., Petrizzo, M. R., Stassen, P., & Speijer, R. P. (2011). Dissolution susceptibility of Paleocene–Eocene planktic foraminifera: Implications for palaeoceanographic reconstructions. *Marine Micropaleontology*, 81, pp. 1-21.
- Nocchi, M., Amici, E., & Premoli Silva, I. (1991). Planktonic Foraminiferal Biostratigraphy and Paleoenvironmental Interpretation of Paleocene Faunas from the Subantarctic Transect, Leg 114. In Y. K. P.F. Ciesielski, *Proceedings of the Ocean Drilling Program, Scientific Results, 114* (pp. 233-279). College Station, Texas: Ocean Drilling Program.
- Norman, T., & Rad, M. J. (1971). Çayraz (Haymana) civarındaki Harhor (Eosen) Formasyonunda alttan üste doğru doku parametrelerinde ve ağır mineral bolluk derecelerinde değişmeler. *TJK Bülteni*, 14/2, pp. 205-225.
- Obaidalla, N. A., El-Dawy, M. H., & Kassab, A. S. (2009). Biostratigraphy and paleoenvironment of the Danian/Selandian (D/S) transition in the Southern

- Tethys: A case study from north Eastern Desert, Egypt. *Journal of African Earth Sciences*, 53 (1), pp. 1-15.
- Okan, Y., & Hoşgör, İ. (2008). The ampullinid gastropod *Globularia* (Swainson 1840) from the late Thanetian-early Ilerdian Kırkkavak Formation (Polatlı-Ankara) of the Tethyan Realm. *Turkish Journal of Earth Sciences*, vol. 17, pp. 785-801.
- Okay, A. I., & Altiner, D. (2016). Carbonate sedimentation in an extensional active margin: Cretaceous history of the Haymana region, Pontides. *International Journal of Earth Sciences (Geologische Rundschau)*, 105, pp. 2013-2030.
- Okay, A. I., Tansel, İ., & Tüysüz, O. (2001). Obduction, subduction and collision as reflected in the Upper Cretaceous-lower Eocene sedimentary record of western Turkey. *Geological Magazine*, 138 (2), pp. 117-142.
- Olsson, R. (1960). Foraminifera of Latest Cretaceous and Earliest Tertiary Age in the New Jersey Coastal Plain. *Journal of Paleontology*, 34, pp. 1-58.
- Olsson, R. K., Hembleben, C., Berggren, W. A., & Huber, B. T. (1999). *Atlas of Paleocene Planktonic Foraminifera*. Washington, D.C., USA: Smithsonian Contributions to Paleobiology, No. 85, Smithsonian Institution Press.
- Orabi, O. H., & Hassan, H. F. (2015). Foraminifera from Paleocene-early Eocene rocks of Bir El Markha section (West Central Sinai), Egypt: Paleobathymetric and paleotemperature significance. *Journal of African Earth Sciences*, 111, pp. 202-213.
- Orue-Etxebarria, X., Pujalte, V., Bemaola, G., Apellaniz, E., Baceta, J. I., & Payros, A. (2001). Did the Late Paleocene thermal maximum affect the evolution of larger foraminifera? Evidence from calcareous plankton of the Campo Section (Pyrenees, Spain). *Marine Micropaleontology*, vol. 41, is. 1-2, pp. 45-71.
- Ouda, K., Berggren, W. A., & Sabour, A. A. (2012). Planktonic foraminiferal biostratigraphy of the Paleocene/Eocene boundary interval in the Dababiya

- Quarry Corehole, Dababiya, Upper Nile Valley, Egypt. *Stratigraphy*, vol. 9, nos. 3-4, pp. 213-227.
- Ouda, K., Berggren, W. A., & Sabour, A. A. (2016a). Upper Paleocene-lower Eocene biostratigraphy of Darb Gaga, Southeastern Kharga Oasis Western Desert, Egypt. *Journal of African Earth Sciences*, 118, pp. 12-23.
- Ouda, K., Berggren, W. A., & Sabour, A. A. (2016b). Bistatigraphy of the upper Paleocene-lower Eocene succession of Gebel El Aguz, northeastern Kharga Oasis, Western Desert, Egypt. *Revue de Paléobiologie*, 35 (1), pp. 341-371.
- Özcan, E. (2002). Cuisian orthophragminid assemblages (*Discocyclina*, *Orbitoclypeus* and *Nemkovella*) from the Haymana-Polatlı Basin (Central Turkey): biometry and description of two new taxa. *Eclogae geol. Helv.*, 95, pp. 75-97.
- Özcan, E., & Özkan-Altınır, S. (1997). Late Campanian-Maastrichtian evolution of orbitoid foraminifera in Haymana basin succession (Ankara, Central Turkey). *Revue de Paléobiologie*, 16/1, pp. 271-290.
- Özcan, E., & Özkan-Altınır, S. (1999). The genus *Lepidorbitoides* and *Orbitoides*: Evolution and stratigraphic significance in some Anatolian basins (Turkey). *Geological Journal*, 34/3, pp. 275-286.
- Özcan, E., & Özkan-Altınır, S. (2001). Description of an early ontogenetic evolutionary step in *Lepidorbitoides*: *Lepidorbitoides bisambergensis asymmetrica* subsp. n., Early Maastrichtian (Central Turkey). *Rivista Italiana di Paleontologia e Stratigrafia*, 107, pp. 137-144.
- Özcan, E., Sirel, E., Özkan-Altınır, S., & Çolakoğlu, S. (2001). Late Paleocene Orthophragminae (foraminifera) from the Haymana-Polatlı Basin, Central Turkey) and description of a new taxon, *Orbitoclypeus haymanaensis*. *Micropaleontology*, 47/4, pp. 339-357.
- Özer, S. (1986). İç Anadolu Bölgesi rudist paleontolojisi ve paleobiyocoğrafyası. *Dokuz Eylül Üni. Fen Bilimleri Ens. Araştırma Raporları*, 1-14.

- Özkan-Altner, S., & Özcan, E. (1999). Upper Cretaceous planktonic foraminiferal biostratigraphy from NW Turkey: calibration of the stratigraphic ranges of larger benthonic foraminifera. *Geological Journal*, 34/3, pp. 287-301.
- Pardo, A., Keller, G., & Oberhänsli, H. (1999). Paleoecologic and paleoceanographic evolution of the Tethyan realm during the Paleocene-Eocene transition. *Journal of Foraminiferal Research*, v. 29, no. 1, pp. 37-57.
- Parker, F. L. (1962). Planktonic foraminiferal species in Pacific sediments. *Micropaleontology*, v. 8, no. 2, pp. 219-254.
- Parr, W. (1938). Upper Eocene Foraminifera from Deep Borings in King's Park, Perth, Western Australia. *Journal of the Royal Society of Western Australia*, 24, pp. 69-101.
- Pearson, P. N. (1993). A Lineage Phylogeny for the Paleogene Planktonic Foraminifera. *Micropaleontology*, 39, pp. 193-232.
- Pearson, P. N., Nicholas, C. J., Singano, J. M., Bown, P. R., Coxall, H. K., van Dongen, B. E., et al. (2004). Paleogene and Cretaceous sediment cores from the Kilwa and Lindi areas of coastal Tanzania: Tanzania Drilling Project Sites 1–5. *Journal of African Earth Sciences*, vol. 39- no. 1-2, pp. 25-62.
- Pearson, P. N., Olsson, R. K., Huber, B. T., Hembleben, C., & Berggren, W. A. (2006). *Atlas of Eocene Planktonic Foraminifera*. Fredericksburg, USA: Cushman Foundation for Foraminiferal Research Special Publication, vol. 41, Cushman Foundation for Foraminiferal Research.
- Pearson, P. N., Olsson, R. K., Huber, B. T., Hembleben, C., Berggren, W. A., & Coxall, H. K. (2006a). Overview of Eocene planktonic foraminiferal taxonomy, paleoecology, phylogeny, and biostratigraphy. In P. N. Pearson, R. K. Olsson, B. T. Huber, C. Hembleben, & W. A. Berggren, *Atlas of Eocene Planktonic Foraminifera* (pp. 11-28). Fredericksburg, USA: Cushman Foundation for Foraminiferal Research Special Publication, vol. 41, Cushman Foundation for Foraminiferal Research.

- Pearson, P., Shackleton, N., & Hall, M. (1993). The Stable Isotope Paleocology of Middle Eocene Planktonic Foraminifera and Multi-species integrated Isotope Stratigraphy. *Journal of Foraminiferal Research*, Vol. 23 p. 123-140.
- Petrizzo, M. R. (2007). The onset of the Paleocene-Eocene Thermal Maximum (PETM) at Sites 1209 and 1210 (Shatsky Rise, Pacific Ocean) as recorded by planktonic foraminifera. *Marine Micropaleontology*, 63, pp. 187-200.
- Petrizzo, M. R., Leoni, G., Speijer, R. P., De Bernardi, B., & Feletti, F. (2008). Dissolution susceptibility of some Paleogene planktonic foraminifera from ODP Site 1209 (Shatsky Rise, Pacific Ocean). *Journal of Foraminiferal Research*, v. 38, no. 4, pp. 357-371.
- Poag, C. W., & Commeau, J. A. (1995). Paleocene to middle Miocene planktic foraminifera of the southwestern Salisbury Embayment, Virginia and Maryland; biostratigraphy, allostratigraphy, and sequence stratigraphy. *Journal of Foraminiferal Research*, v. 25, n. 2, pp. 134-155.
- Postuma, J. A. (1971). *Manual of Planktonic Foraminifera*. . Amsterdam: Elsevier Publishing Co.
- Premoli Silva, I., & H.M., B. (1973). Late Cretaceous to Eocene Planktonic Foraminifera and Stratigraphy of Leg 15 Sites in the Caribbean Sea. In J. S. N.T. Edgar, *Initial Reports of the Deep Sea Drilling Project, 15* (pp. 499-547). Washington, D.C.: U.S. Government Printing Office.
- Premoli Silva, I., Rettori, R., & Verga, D. (2003). *Practical Manual of Paleocene and Eocene Planktonic Foraminifera*. Perugia: Dipartimento di Scienze della Terra, University of Perugia, International School on Planktonic Foraminifera.
- Pujalte, V., Schmitz, B., Baceta, J. I., Orue-Extebarria, X., Bernaola, G., Dinarés-Turel, J., et al. (2009). Correlation of the Thanetian-Ilerdian turnover of larger foraminifera and the Paleocene-Eocene thermal maximum: confirming

- evidence from the Campo area (Pyrenees, Spain). *Geologica Acta*, vol. 7, no. 1-2, pp. 161-175.
- Pujol, C. (1983). Cenozoic Planktonic Foraminiferal Biostratigraphy of the Southwestern Atlantic (Rio Grande Rise): Deep Sea Drilling Project Leg 72. In D. J. P.F. Barker, *Initial Reports of the Deep Sea Drilling Project*, 72 (pp. 623-673). Washington, D.C: U.S. Government Printing Office.
- Quillévéré, F., Norris, R. D., Moussa, I., & Berggren, W. A. (2001). Role of photosymbiosis and biogeography in the diversification of early Paleogene acarininids (planktonic foraminifera). *Paleobiology*, 27 (2), pp. 311-326.
- Recamp, J. U., & Özbey, S. (1960). *Petroleum geology of Temelli and Kuştepe structures, Polatlı area*. Ankara (Unpublished): Pet. İş. Gen. Müd.
- Reyment, R. A. (1960). Notes on some Globigerinidae, Globotruncanidae and Globorotaliidae from the upper Cretaceous and lower Tertiary of western Nigeria. *Records of the Geological Survey of Nigeria*, pp. 68-86.
- Rigo de Righi, M., & Cortesini, A. (1959). *Regional studies in central Anatolian basin. Progress Report 1*. Ankara (Unpublished): Turkish Gulf Oil Co., Petrol İş. Gen. Müd.
- Rojay, B. (2013). Tectonic evolution of the Cretaceous Ankara Ophiolitic Mélange during the Late Cretaceous to pre-Miocene interval in Central Anatolia, Turkey. *Journal of Geodynamics*, 65, pp. 66-81.
- Rojay, B., & Süzen, M. L. (1997). Tectonostratigraphic evolution of the cretaceous dynamic basins on accretionary ophiolitic melange prism, SW of Ankara region. *TPJD Bülteni*, c. 9, no. 1, pp. 1-12.
- Said, R., & Kenaway, A. (1956). Upper Cretaceous and Lower Tertiary Foraminifera from Northern Sinai, Egypt. *Micropaleontology*, 2, pp. 105-173.
- Samanta, B. (1970). Planktonic Foraminifera from the Early Tertiary Pondicherry Formation of Madras, South India. *Journal of Paleontology*, 44, pp. 605-641.

- Samuel, O., Borza, K., & Kohler, E. (1972). Microfauna and lithostratigraphy of the Paleogene and adjacent Cretaceous of the Middle Vah Valley (West Carpathian). *Geologicky ustav Dionyza Stura, Bratislava*, 246.
- Schaller, M. F., Fung, M. K., Wright, J. D., Katz, M. E., & Kent, D. V. (2016). Impact ejecta at the Paleocene-Eocene boundary. *Science*, vol. 354, issue 6309, pp. 225-229.
- Schmidt, G. C. (1960). *AR/MEM/365-266-367 sahalarının nihai terk raporu*. Ankara (Unpublished): Pet. İş. Gen. Müd.
- Shackleton, N. J., & Kennett, J. P. (1975). Paleotemperature history of the Cenozoic and the initiation of antarctic glaciation: oxygen and carbon isotope analyses in DSDP sites 277, 279, and 281. In J. P. Kennett, R. E. Houtz, P. B. Andrews, A. R. Edwards, V. A. Gostin, M. Hajos, et al., *Initial Reports of the Deep Sea Drilling Project Vol. 29* (pp. 743-755). Washington: U. S. Government Printing Office.
- Shackleton, N. J., Hall, M. A., & Boersma, A. (1984). Oxygen and carbon isotope data from Leg 74 foraminifers. In T. C. Moore, P. D. Rabinowitz, A. Boersma, P. E. Borella, A. D. Chave, D. Duée, et al., *Initial Reports of the Deep Sea Drilling Project Vol. 74* (pp. 599-612). Washington: U. S. Government Printing Office.
- Shutskaya, E. K. (1958). Izmenchivosti nekotorykh nizhnepaleogenovykh plannktonovykh foraminifer severnogo Kavkaza. *Voprosy Mikropaleontologii, Akademiya Nauk SSSR*, 2, pp. 84-90.
- Shutskaya, E. K. (1960). *Stratigrafiya ifatsii nizhnego paleogena Predkavkazy*. Moscow: Gostoptekhizdat: Vsesoyuznyi Nauchno-Issledovatel'skii Geologorazvedochnyi Neftyanoi Institut (VNIGNI).
- Shutskaya, E. K. (1965). Filogeneticheskie vzaimootnoscheniya vidov gruppy *Globorotalia compressa* Plummer v datskom vekhe i paleotzenovoi epokhe. *Voprosy Mikropaleontologii, Akademiya Nauk SSSR*, 9, pp. 173-188.

- Shutskaya, E. K. (1970a). Morfologicheskie grupirovki vidov rodov Globigerina i Acarinina v nizhnei chasti paleogena Kryma, Predkavkazya i zapada Srednei Azii i ipisanie vidov. In E. K. Shutkaya, *Stratigrafiya i paleontologiya Mezozoiskikh i Paleogenovykh otlozhenii Srednei Azii* (pp. 79-134). Trudy, Vsesoyuznyi Nauchno-Issledovatel'skii Geologorazvedochnyi Neftyanoi Institut (VNIGNI), 69.
- Shutskaya, E. K. (1970b). Stratigrafiya, foraminifery i paleogeografiya nizhnego paleogena Kryma, predkavkaz'ya i zapadnoi chadsti srednei azii. *Trudy, Vsesoyuznyi Nauchno-Issledovadatel 'skii Geologorazvedochnyi Neftyanoi Institut (VNIGNI)*, 70, 265 pages.
- Sirel, E. (1975). Polatlı (GB Ankara) güneyinin stratigrafisi / Stratigraphy of the south of Polatlı (SW Ankara). *Türkiye Jeoloji Kurumu Bülteni / Bulletin of the Geological Society of Turkey*, v. 18, pp. 181-192.
- Sirel, E. (1976a). Polatlı (GB Ankara) güneyinde bulunan Alveolina, Nummulites, Ranikothalia ve Assilina cinslerinin bazı türlerinin sistematik incelemeleri. *TJK Bülteni*, 19/2, pp. 89-103.
- Sirel, E. (1976b). Description of six new species of the Alveolina found in the South of Polatlı (SW Ankara) region. *TJK Bülteni*, 19, pp. 19-22.
- Sirel, E. (1976c). Haymana (G Ankara) yöresi İlerdiyen, Küziyen ve Lütəsiyen'deki Nummulites, Assilina ve Alveolina cinslerinin bazı türlerinin tanımlamaları ve stratigrafik dağılımları. *TJK Bülteni*, 19, pp. 31-44.
- Sirel, E. (1998). *Foraminiferal description and biostratigraphy of the Paleocene-Lower Eocene shallow-water limestones and discussion on the Cretaceous-Tertiary boundary in Turkey*. General Directorate of the Mineral Research and Exploration, Monography Series, 2, 117 p.
- Sirel, E. (1999). Four new genera (Haymanella, Kayseriella, Elazigella and Orduella) and one new species of Hottingerina from the Paleocene of Turkey. *Micropaleontology*, 45/2, pp. 113-137.

- Sirel, E., & Gündüz, H. (1976). Description and stratigraphic distribution of some species the genera Nummulites, Assilina and Alveolina from the Ilerdian, Cuisian and Lutetian of Haymana region. *TJK Bülteni*, 19, pp. 33-44.
- Slujs, A., Brinhuis, H., Schouten, S., Bohaty, S. M., John, C. M., Zachos, J. C., et al. (2007). Environmental precursors to rapid light carbon injection at the Paleocene/Eocene boundary. *Nature*, vol. 450, pp. 1218-1222.
- Snyder, S., & Waters, V. (1985). Cenozoic Planktonic Foraminiferal Biostratigraphy of the Goban Spur Region, Deep Sea Drilling Project Leg 80. In C. P. P.C. de Graciannsky, *Initial Reports of the Deep Sea Drilling Project, 80* (pp. 439-472). Washington, D.C.: U.S. Government Printing Office.
- Soldan, D. M., Petrizzio, M. R., & Premoli Silva, I. (2014). Pearsonites, a new Paleogene planktonic foraminiferal genus for the broedermanni lineage. *Journal of Foraminiferal Research*, v. 44, no. 1, 17-27.
- Soldan, D. M., Petrizzo, M. R., Premoli Silva, I., & Cau, A. (2011). Phylogenetic relationships and evolutionary history of the Paleogene genus Igorina through parsimony analysis. *Journal of Foraminiferal Research*, v. 41, no. 3, 260-284.
- Speijer, R. P., & Samir, A. M. (1997). Globanomalina luxorensis, a Tethyan biostratigraphic marker of latest Paleocene global events. *Micropaleontology*. vol. 43, no. 1, 51-62.
- Speijer, R. P., Schmitz, B., & Luger, P. (2000). Stratigraphy of late Palaeocene events in the Middle East: implications for low- to middle-latitude successions and correlations. *Journal of the Geological Society, London*, vol. 157, pp. 37-47.
- Stainforth, R. M., Lamb, J. L., Luterbacher, H., Beard, J. H., & Jeffords, R. M. (1975). Cenozoic Planktonic Foraminiferal Zonation and Characteristics of Index Forms. *University of Kansas Paleontological Contributions*, Article 62, 425 pages.

- Stott, L. D., Kennet, J. P., Shackleton, N. J., & Corfield, R. M. (1990a). The evolution of Antarctic surface waters during the Paleogene: inferences from the stable isotopic composition of planktonic foraminifers. In P. F. Barker, J. P. Kennett, S. O'Connell, & N. G. Pisias, *Proceedings of the Ocean Drilling Program Scientific Results Vol. 113* (pp. 849-863). College Station, TX: Ocean Drilling Program.
- Stott, L., & Kennett, J. (1990b). Antarctic Paleogene Planktonic Foraminifer Biostratigraphy: ODP Leg 113, Sites 689 and 690. In J. K. P.F. Barker, *Proceedings of the Ocean Drilling Program, Scientific Results, 113* (pp. pp. 549-569). College Station, Texas: Ocean Drilling Program.
- Subbotina, N. N. (1947). Foraminifery datskikh i paleogenovykh otlozhenii severnogo Kavkaza. In *Mikrofauna nefryanykh mestorozhdenii. Trudy, Vsesoyuznyi NauchnoIssledovatel'skii Geologorazvedochnyi Neftyanoi Institut (VNIGNT)*, 39-160.
- Subbotina, N. N. (1953). *Iskopaemye foraminifery SSSR (Globigerinidy, Hantkeninidy i Globorotalüdy) [Fossil Foraminifera of the USSR: Globigerinidae, Hantkeninidae and Globorotalidae]*. Leningrad: Trudy Vsesoyznogo Nauchno-Issle-dovatel'skogo Geologorazvedochnogo Instituta (VNIGRI), v. 76, (translation by E. Lees, 1971, Collet's Ltd., London and Wellingborough).
- Şengör, A., & Yılmaz, Y. (1981). Tethyan evolution of Turkey: a plate tectonic approach. *Tectonophysics*, 75, pp. 181-241.
- Tjalsma, R. C. (1977). Cenozoic Foraminifera from the South Atlantic, DSDP Leg 36. In I. D. P.F. Barker, *Initial Reports of the Deep Sea Drilling Project, 36* (pp. 493-518). Washington, D.C: U.S. Government Printing Office.
- Todd, R., & Knicker, H. T. (1952). An Eocene foraminiferal fauna from the Agua Fresca Shale of Magallenes Province, southernmost Chile. *Cushman Foundation for Foraminiferal Research Special Publications*, 1, 1-28.

- Toker, V. (1975). *Haymana yöresinin (SW Ankara) planktonik foraminifera ve nannoplanktonlarla biyostratigrafik incelenmesi*. Ankara, PhD. Thesis: Ankara Üni. Fen Fak.
- Toker, V. (1977). Haymana ve Kavak formasyonlarındaki planktonik foraminifera ve nannoplanktonlar. *TÜBİTAK VI. Bilim Kongresi Tebliğleri*, pp. 57-70.
- Toker, V. (1979). Haymana yöresi (GB Ankara) Üst Kretase planktonik foraminiferaları ve biyostratigrafi incelemesi. *TJK Bülteni*, 22, pp. 121-132.
- Toker, V. (1980). Haymana yöresi (GB Ankara) nannoplankton biyostratigrafisi. *TJK Bülteni*, 23/2, pp. 165-178.
- Toker, V. (1981). Haymana yöresi (GB Ankara) Tersiyer oluşuklarının planktonik foraminiferlerle biyostratigrafik incelemesi. *KTÜ Yer Bilimleri Dergisi, Jeoloji 1*, 2, pp. 115-126.
- Toulmin, L. D. (1941). Eocene Smaller Foraminifera from the Salt Mountain Limestone of Alabama. *Journal of Paleontology*, 15, pp. 567-611.
- Toumarkine, M., & Luterbacher, H. (1985). Paleocene and Eocene planktic foraminifera. In A. H. Cook, W. B. Harland, N. F. Hughes, A. Putnis, & M. R. Thomson, *Plankton Stratigraphy* (pp. 87-154). New York, USA: Cambridge University Press.
- Ünalın, G., Yüksel, V., Tekeli, T., Gönenç, O., Seyirt, Z., & Hüseyin, S. (1976). Haymana-Polatlı yöresinin (güneybatı Ankara) Üst Kretase-Alt Tersiyer stratigrafisi ve paleocoğrafik evrimi / The stratigraphy and paleogeographical evolution of the Upper Cretaceous-Lower Tertiary sediments in the Haymana-Polatlı region (SW of Ankara). *Türkiye Jeoloji Kurumu Bülteni / Bulletin of the Geological Society of Turkey*, v. 19, pp. 159-176.
- Van Eiden, A., & Smit, J. (1992). Eastern Indian Ocean Cretaceous and Paleogene Quantitative Biostratigraphy. In J. P. J. Weissel, *Proceedings of the Ocean Drilling Program, Scientific Results, 121* (pp. 77-124). College Station, Texas: Ocean Drilling Program.

- Vandenbergh, N., Hilgen, F. J., Speijer, R. P., Ogg, J. G., Gradstein, F. M., Hammer, O., et al. (2012). Chapter 28 - The Paleogene Period. In F. M. Gradstein, J. G. Ogg, M. Schmitz, & G. Ogg, *The Geologic Time Scale 2012* (pp. 855-921). Boston: Elsevier.
- von Hillebrandt, A. (1965). Los foraminiferos planctonicos, nummulitidos y coccolitoforidos de la zona de Globorotalia palmerae del Cuisiense (Eoceno Inferior) en el SE de Espania, (provincias de Murcia y Alicante). *Revista Espanola de Micropaleontologia*, vol. 8 p. 323-394.
- Warrach, M. Y., & Nishi, H. (2003). Eocene planktic foraminiferal biostratigraphy of the Sulaiman Range, Indus Basin, Pakistan. *Journal of Foraminiferal Research*, v. 33, no. 3, 219-236.
- Warrach, M. Y., & Ogasawara, K. (2001). Tethyan Paleocene-Eocene planktic foraminifera from the Rakhi Nala and Zinda Pir land sections of the Sulaiman Range, Pakistan. *Science reports of the Institute of Geoscience, University of Tsukuba. Section B, Geological sciences*, 22, 1-59.
- Warrach, M. Y., Ogasawara, K., & Nishi, H. (2000). Late Paleocene to early Eocene planktonic foraminiferal biostratigraphy of the Dungan Formation, Sulaiman Range, central Pakistan. *Paleontological Research*, vol. 4, no. 4, 275-301.
- White, M. P. (1928). Some Index Foraminifera of the Tampico Embayment of Mexico, Part I and Part II. *Journal of Paleontology*, 2, pp. 177-215, 280-317.
- Yüksel, S. (1970). *Etude geologique de la region d'Haymana (Turquie central)*. France: Thesis, Fac. Sci. Univ. Nancy (Unpublished).
- Zachos, J. C., Lohmann, K. C., Walker, J. G., & Wise, S. W. (1993). Abrupt climate change and transient climates during the Paleogene: a marine perspective. *The Journal of Geology*, vol. 101, pp. 191-213.
- Zachos, J. C., Röhl, U., Schellenberg, S. A., Slujs, A., Hodell, D. A., Kelly, D. C., et al. (2005). Rapid Acidification of the Ocean During the Paleocene-Eocene Thermal Maximum. *Science*, vol. 308, pp. 1611-1615.

- Zachos, J., Pagani, M., Sloan, L., Thomas, E., & Billups, K. (2001). Trends, rhythms, and aberrations in global climate 65 Ma to present. *Science*, vol. 292, pp. 686-693.
- Zili, L. (2013). Biostratigraphic study of the Paleocene-Eocene boundary in Northern Tunisia, North Africa. *Acta Geologica Sinica (English Edition)*, vol. 87, no. 6, pp. 1533-1539.
- Zili, L., Zaghib-Turki, D., Alegret, L., Arenillas, I., & Molina, E. (2009). Foraminiferal turnover across the Paleocene/Eocene boundary at the Zumaya section, Spain: record of a bathyal gradual mass extinction. *Revista Mexicana de Ciencias Geológicas*, vol. 26, num. 3. pp. 729-744.

APPENDICES

APPENDIX A

QUANTITATIVE DATA FOR $>106\mu\text{m}$ AND $>63\mu\text{m}$

Table 19: Quantitative data and percent relative abundances of genera for >106 µm

>106 µm	Subbotina		Parasubbotina		Morozovella		Planorotalites		Acarinina		Igorina		Pearsonites		Glob. + Pseu.		Serials		Others/Unknown		high_sp_sp		TOTAL
	#	%	#	%	#	%	#	%	#	%	#	%	#	%	#	%	#	%	#	%	#	%	
GT-26	94	28.1	4	1.2	11	3.3	3	0.9	169	50.6	4	1.2	3	0.9	19	5.7	1	0.3	26	7.8	0	0.0	334
GT-25	96	28.7	4	1.2	11	3.3	3	0.9	150	44.8	4	1.2	3	0.9	10	3.0	2	0.6	52	15.5	0	0.0	335
GT-24	75	25.8	3	1.0	27	9.3	0	0.0	129	44.3	0	0.0	0	0.0	6	2.1	0	0.0	39	13.4	12	4.1	291
GT-23	119	27.1	5	1.1	29	6.6	0	0.0	208	47.4	0	0.0	4	0.9	22	5.0	0	0.0	52	11.8	0	0.0	439
GT-22	125	24.7	5	1.0	66	13.0	2	0.4	220	43.5	0	0.0	5	1.0	12	2.4	2	0.4	55	10.9	14	2.8	506
GT-21	105	38.9	5	1.9	20	7.4	0	0.0	89	33.0	4	1.5	3	1.1	8	3.0	1	0.4	30	11.1	5	1.9	270
GT-20	141	30.0	7	1.5	48	10.2	0	0.0	205	43.6	8	1.7	0	0.0	12	2.6	2	0.4	42	8.9	5	1.1	470
GT-19	82	29.0	4	1.4	56	19.8	0	0.0	66	23.3	9	3.2	8	2.8	8	2.8	2	0.7	41	14.5	7	2.5	283
GT-18	52	14.9	5	1.4	64	18.4	0	0.0	168	48.3	1	0.3	3	0.9	7	2.0	2	0.6	46	13.2	0	0.0	348
GT-17	100	40.0	5	2.0	23	9.2	0	0.0	81	32.4	0	0.0	0	0.0	3	1.2	0	0.0	28	11.2	10	4.0	250
GT-16	66	20.2	2	0.6	16	4.9	1	0.3	150	45.9	0	0.0	8	2.4	15	4.6	4	1.2	49	15.0	16	4.9	327
GT-15	46	11.4	2	0.5	71	17.5	0	0.0	214	52.8	19	4.7	0	0.0	8	2.0	6	1.5	35	8.6	4	1.0	405
GT-14	78	18.1	3	0.7	129	29.9	2	0.5	173	40.0	4	0.9	0	0.0	12	2.8	1	0.2	23	5.3	7	1.6	432
GT-13	27	7.9	2	0.6	26	7.6	1	0.3	210	61.6	14	4.1	0	0.0	21	6.2	0	0.0	40	11.7	0	0.0	341
GT-12	94	26.9	6	1.7	19	5.4	2	0.6	139	39.7	3	0.9	0	0.0	20	5.7	6	1.7	40	11.4	21	6.0	350
GT-11	122	27.4	8	1.8	53	11.9	0	0.0	131	29.4	10	2.2	0	0.0	18	4.0	14	3.1	54	12.1	36	8.1	446
GT-10	122	23.3	6	1.1	99	18.9	0	0.0	167	31.9	10	1.9	0	0.0	15	2.9	1	0.2	65	12.4	39	7.4	524
GT-9	38	14.7	2	0.8	7	2.7	2	0.8	147	56.8	9	3.5	0	0.0	24	9.3	3	1.2	27	10.4	0	0.0	259
GT-8	28	9.8	2	0.7	35	12.2	0	0.0	159	55.4	5	1.7	0	0.0	20	7.0	2	0.7	34	11.8	2	0.7	287
GT-7	97	26.4	6	1.6	28	7.6	0	0.0	156	42.4	15	4.1	0	0.0	12	3.3	3	0.8	33	9.0	18	4.9	368
GT-6	129	34.0	7	1.8	69	18.2	1	0.3	81	21.4	22	5.8	0	0.0	30	7.9	5	1.3	20	5.3	15	4.0	379
GT-5	109	29.1	7	1.9	46	12.3	0	0.0	106	28.3	10	2.7	0	0.0	23	6.1	2	0.5	33	8.8	38	10.2	374
GT-4	96	34.9	5	1.8	44	16.0	0	0.0	73	26.5	4	1.5	0	0.0	11	4.0	13	4.7	14	5.1	15	5.5	275
GT-3	54	16.4	3	0.9	38	11.5	0	0.0	85	25.8	17	5.2	0	0.0	17	5.2	6	1.8	82	24.8	28	8.5	330
GT-2	72	17.1	2	0.5	72	17.1	0	0.0	179	42.6	16	3.8	0	0.0	20	4.8	2	0.5	32	7.6	25	6.0	420
GT-1	106	28.6	4	1.1	57	15.4	0	0.0	93	25.1	19	5.1	0	0.0	14	3.8	4	1.1	45	12.1	29	7.8	371
Average:		24.4		1.2		11.9		0.2		39.9		2.2		0.4		4.2		0.9		11.2		3.6	362.1

Table 20: Quantitative data and percent relative abundances of genera for >63 μm

>63 μm	Subbotina		Morozovella		Acarinina		Igor.+Pear.		Glob.+P.yeu.		Serials		Others/Unknown+high_sp		Pre-adults		TOTAL
	#	%	#	%	#	%	#	%	#	%	#	%	#	%	#	%	
GT-26	32	22.4	4	2.8	32	22.4	0	0.0	12	8.4	9	6.3	54	37.8	82	57.3	143
GT-25	59	28.4	7	3.4	23	11.1	0	0.0	19	9.1	26	12.5	74	35.6	141	67.8	208
GT-24	53	28.8	8	4.3	39	21.2	0	0.0	17	9.2	8	4.3	59	32.1	104	56.5	184
GT-23	61	35.9	12	7.1	16	9.4	0	0.0	17	10.0	13	7.6	51	30.0	99	58.2	170
GT-22	107	32.6	27	8.2	35	10.7	3	0.9	22	6.7	46	14.0	88	26.8	197	60.1	328
GT-21	66	25.8	24	9.4	55	21.5	3	1.2	18	7.0	10	3.9	80	31.3	151	59.0	256
GT-20	87	34.1	22	8.6	55	21.6	3	1.2	12	4.7	15	5.9	61	23.9	139	54.5	255
GT-19	68	23.4	48	16.5	38	13.1	3	1.0	24	8.2	12	4.1	98	33.7	159	54.6	291
GT-18	59	10.7	59	10.7	155	28.1	0	0.0	77	14.0	31	5.6	170	30.9	360	65.3	551
GT-17	64	15.8	20	5.0	100	24.8	0	0.0	19	4.7	49	12.1	152	37.6	217	53.7	404
GT-16	50	10.0	14	2.8	38	7.6	0	0.0	46	9.2	140	28.0	212	42.4	294	58.8	500
GT-15	22	7.1	26	8.4	52	16.8	0	0.0	18	5.8	57	18.4	134	43.4	173	56.0	309
GT-14	43	9.1	92	19.5	64	13.6	6	1.3	73	15.5	25	5.3	168	35.7	300	63.7	471
GT-13	21	5.6	25	6.6	89	23.7	0	0.0	36	9.6	28	7.4	177	47.1	283	75.3	376
GT-12	35	10.5	6	1.8	30	9.0	2	0.6	34	10.2	52	15.6	175	52.4	215	64.4	334
GT-11	25	12.7	8	4.1	15	7.6	0	0.0	12	6.1	41	20.8	96	48.7	110	55.8	197
GT-10	51	29.0	16	9.1	21	11.9	0	0.0	18	10.2	18	10.2	52	29.5	87	49.4	176
GT-9	50	15.1	12	3.6	42	12.7	3	0.9	47	14.2	91	27.4	87	26.2	206	62.0	332
GT-8	74	24.3	14	4.6	63	20.7	1	0.3	55	18.1	22	7.2	75	24.7	211	69.4	304
GT-7	59	23.0	11	4.3	37	14.4	1	0.4	40	15.6	32	12.5	77	30.0	164	63.8	257
GT-6	82	30.5	8	3.0	23	8.6	7	2.6	23	8.6	41	15.2	85	31.6	187	69.5	269
GT-5	56	25.0	10	4.5	20	8.9	0	0.0	19	8.5	37	16.5	82	36.6	146	65.2	224
GT-4	106	40.0	9	3.4	40	15.1	1	0.4	21	7.9	46	17.4	42	15.8	178	67.2	265
GT-3	26	13.7	4	2.1	12	6.3	3	1.6	27	14.2	33	17.4	85	44.7	127	66.8	190
GT-2	137	29.9	51	11.1	80	17.5	1	0.2	63	13.8	24	5.2	102	22.3	372	81.2	458
GT-1	71	28.1	16	6.3	31	12.3	2	0.8	41	16.2	22	8.7	70	27.7	184	72.7	253
Average:		22.0		6.6		15.0		0.5		10.2		11.9		33.8		62.6	296.3

APPENDIX B

LIST OF PLANKTONIC FORAMINIFERA

Table 21: Page and Plate-Figure addresses of planktonic foraminifera identified in this study

Species	Page	Plate-figure no
<i>Acarinina angulosa</i>	136	1- d, e
<i>Acarinina coalingensis</i>	144	1- a-c
<i>Acarinina esnaensis</i>	145	1- f, h, i
<i>Acarinina esnehensis</i>	146	1- g, j
<i>Acarinina mckannai</i>	147	
<i>Acarinina nitida</i>	148	1- k, l
<i>Acarinina pseudotopilensis</i>	149	2-a, b
<i>Acarinina sibaiyaensis</i>	150	2-g, j-l
<i>Acarinina soldadoensis</i>	151	2-f, h, i
<i>Acarinina subsphaerica</i>	153	2- c
<i>Acarinina wilcoxensis</i>	154	2-d, e

Table 21 (Continued)

Species	Page	Plate-figure no
<i>Chiloguembelina trinitatensis</i>	177	
<i>Chiloguembelina wilcoxensis</i>	180	8- l
<i>Globanomalina chapmani</i>	166	8- d-e
<i>Globanomalina imitata</i>	170	8- a-c
<i>Globanomalina luxorensis</i>	171	8- f, h, i
<i>Globanomalina planoconica</i>	172	7- f-i
<i>Globanomalina pseudomenardii</i>	173	7- j-l
<i>Igorina albeari</i>	156	4- k, l
<i>Igorina tadjikistanensis</i>	157	4- g, h, j
<i>Morozovella acuta</i>	122	7- d-e
<i>Morozovella aequa</i>	128	5- l; 6- a-c
<i>Morozovella apantesma</i>	129	5- j, k
<i>Morozovella edgari</i>	130	7- a-c
<i>Morozovella gracilis</i>	131	6- g-i
<i>Morozovella marginodentata</i>	132	6- j-l
<i>Morozovella subbotinae</i>	133	6- d-f
<i>Parasubbotina inaequispira</i>	110	3- f, i, l
<i>Parasubbotina varianta</i>	107	3- a-c

Table 21 (Continued)

Species	Page	Plate-figure no
<i>Pearsonites broedermanni</i>	160	5- g, h
<i>Pearsonites lodoensis</i>	162	5- d-f, i
<i>Planorotalites pseudoscitula</i>	163	g- a-c
<i>Pseudohastigerina wilcoxensis</i>	174	8- g, j, k
<i>Subbotina hornibrooki</i>	116	4- f, i
<i>Subbotina patagonica</i>	116	4- a-c
<i>Subbotina roesnaesensis</i>	117	3- j, k
<i>Subbotina triangularis</i>	119	4- d, e
<i>Subbotina velascoensis</i>	120	3- d, e, g, h
<i>Zeauvigerina aegyptiaca</i>	181	

APPENDIX C

PLATES AND EXPLANATIONS

PLATE 1

- a. *Acarinina coalingensis*: Umbilical view, GT-2
- b. *Acarinina coalingensis*: Side-oblique view, GT-2
- c. *Acarinina coalingensis*: Umbilical view, GT-22
- d. *Acarinina angulosa*: Spiral view, GT-18
- e. *Acarinina angulosa*: Umbilical view, GT-18
- f. *Acarinina esnaensis*: Side view, GT-19
- g. *Acarinina esnehensis*: Side-oblique view, GT-18
- h. *Acarinina esnaensis*: Side view, GT-18
- i. *Acarinina esnaensis*: Spiral view, GT-18
- j. *Acarinina esnehensis*: Spiral view, GT-19
- k. *Acarinina nitida*: Spiral view, GT-22
- l. *Acarinina nitida*: Side view, GT-22

Plate 1: SEM images of in situ taxa, with scale bar indicating 100 μm

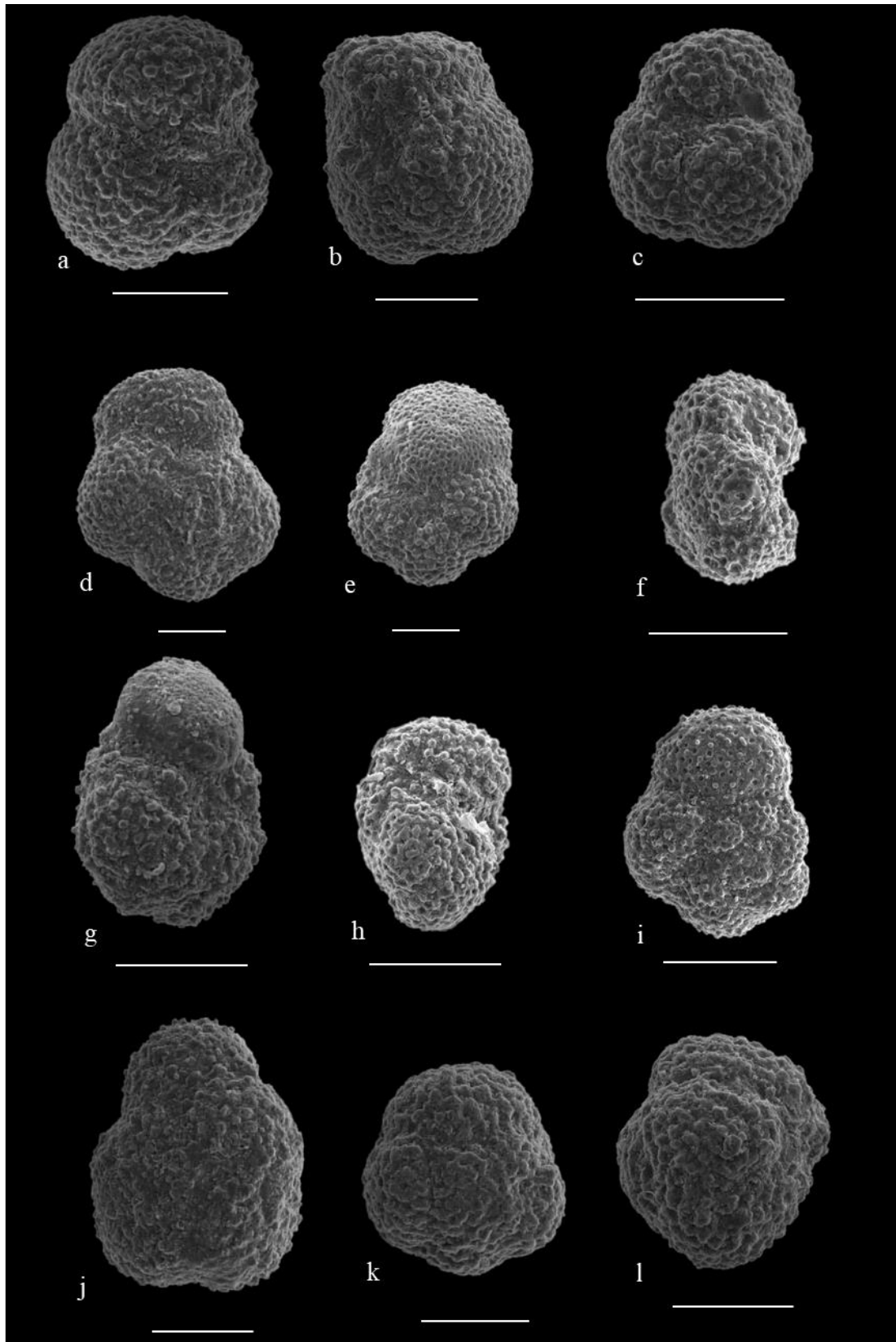


PLATE 2

- a. *Acarinina pseudotopilensis*: Side view, GT-22
- b. *Acarinina pseudotopilensis*: Spiral view, GT-22
- c. *Acarinina subsphaerica*: Side view, GT-4
- d. *Acarinina wilcoxensis*: Spiral view, GT-21
- e. *Acarinina wilcoxensis*: Umbilical view, GT-21
- f. *Acarinina soldadoensis*: Spiral view, GT-22
- g. *Acarinina sibiyaensis*: Side view, GT-18
- h. *Acarinina soldadoensis*: Side view, GT-22
- i. *Acarinina soldadoensis*: Umbilical view, GT-22
- j. *Acarinina sibiyaensis*: Spiral view, GT-18
- k. *Acarinina sibiyaensis*: Umbilical view, GT-20
- l. *Acarinina sibiyaensis*: Umbilical view, GT-19

Plate 2: SEM images of in situ taxa, with scale bar indicating 100 μm

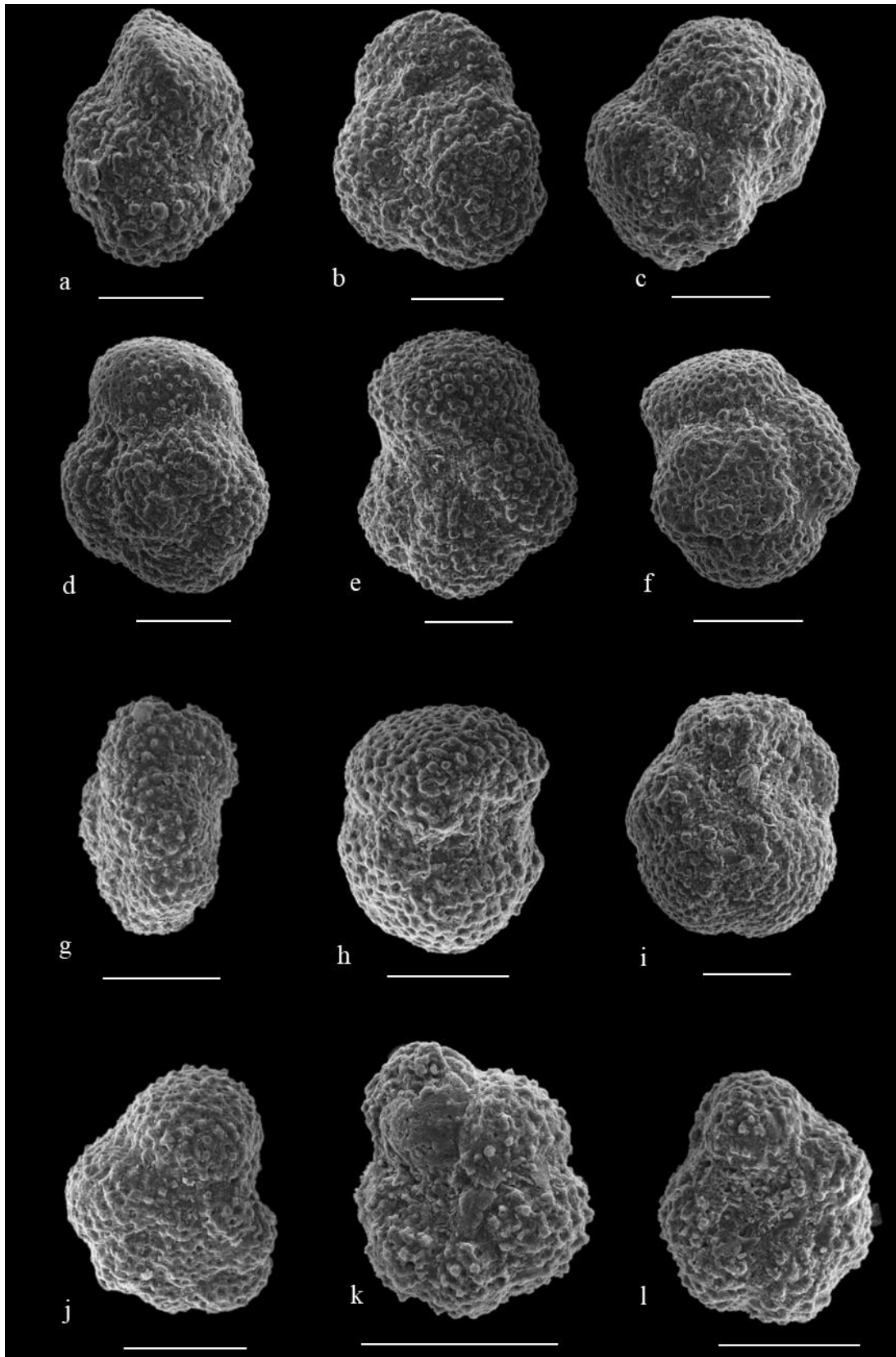


PLATE 3

- a. *Parasubbotina varianta*: Spiral view, GT-18
- b. *Parasubbotina varianta*: Umbilical view; sediment fill in umbilicus, GT-18
- c. *Parasubbotina varianta*: Side view, GT-18
- d. *Subbotina velascoensis*: Umbilical view, GT-20
- e. *Subbotina velascoensis*: Spiral view, GT-20
- f. *Parasubbotina inaequispira*: Spiral view, GT-17.75
- g. *Subbotina velascoensis*: Umbilical view, GT-20
- h. *Subbotina velascoensis*: Side view, GT-20
- i. *Parasubbotina inaequispira*: Spiral-oblique view, GT-18
- j. *Subbotina roesnaesensis*: Side view, GT-20
- k. *Subbotina roesnaesensis*: Umbilical-oblique view, GT-20
- l. *Parasubbotina inaequispira*: Side-oblique view, GT-18

Plate 3: SEM images of in situ taxa, with scale bar indicating 100 μm

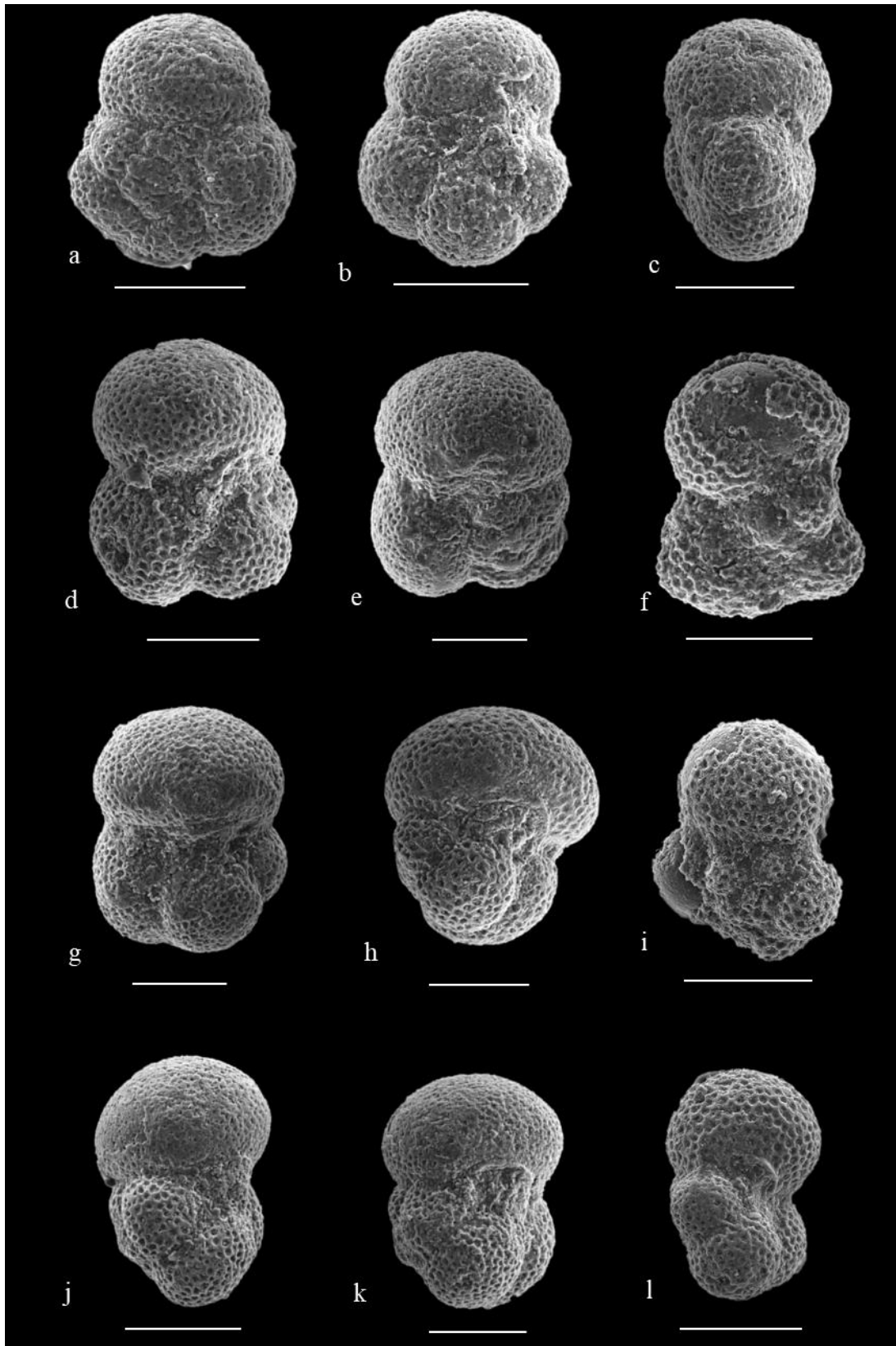


PLATE 4

- a. *Subbotina patagonica*: Spiral view, GT-18
- b. *Subbotina patagonica*: Side view, GT-18
- c. *Subbotina patagonica* : Spiral view,GT-18
- d. *Subbotina triangularis*: Spiral view; last chamber wall stripped, penultimate chamber partly broken, GT-2
- e. *Subbotina triangularis*: Umbilical view; last chamber wall stripped, GT-5
- f. *Subbotina hornibrooki*: Spiral view, GT-20
- g. *Igorina tadjikistanensis*: Umbilical view, GT-17.75
- h. *Igorina tadjikistanensis*: Side view, GT-6
- i. *Subbotina hornibrook*: Umbilical view,*i* GT-20
- j. *Igorina tadjikistanensis*: Spiral view, GT-17.75
- k. *Igorina albeari*: Side view, GT-9
- l. *Igorina albeari*: Spiral view, GT-9

Plate 4: SEM images of in situ taxa, with scale bar indicating 100 μm

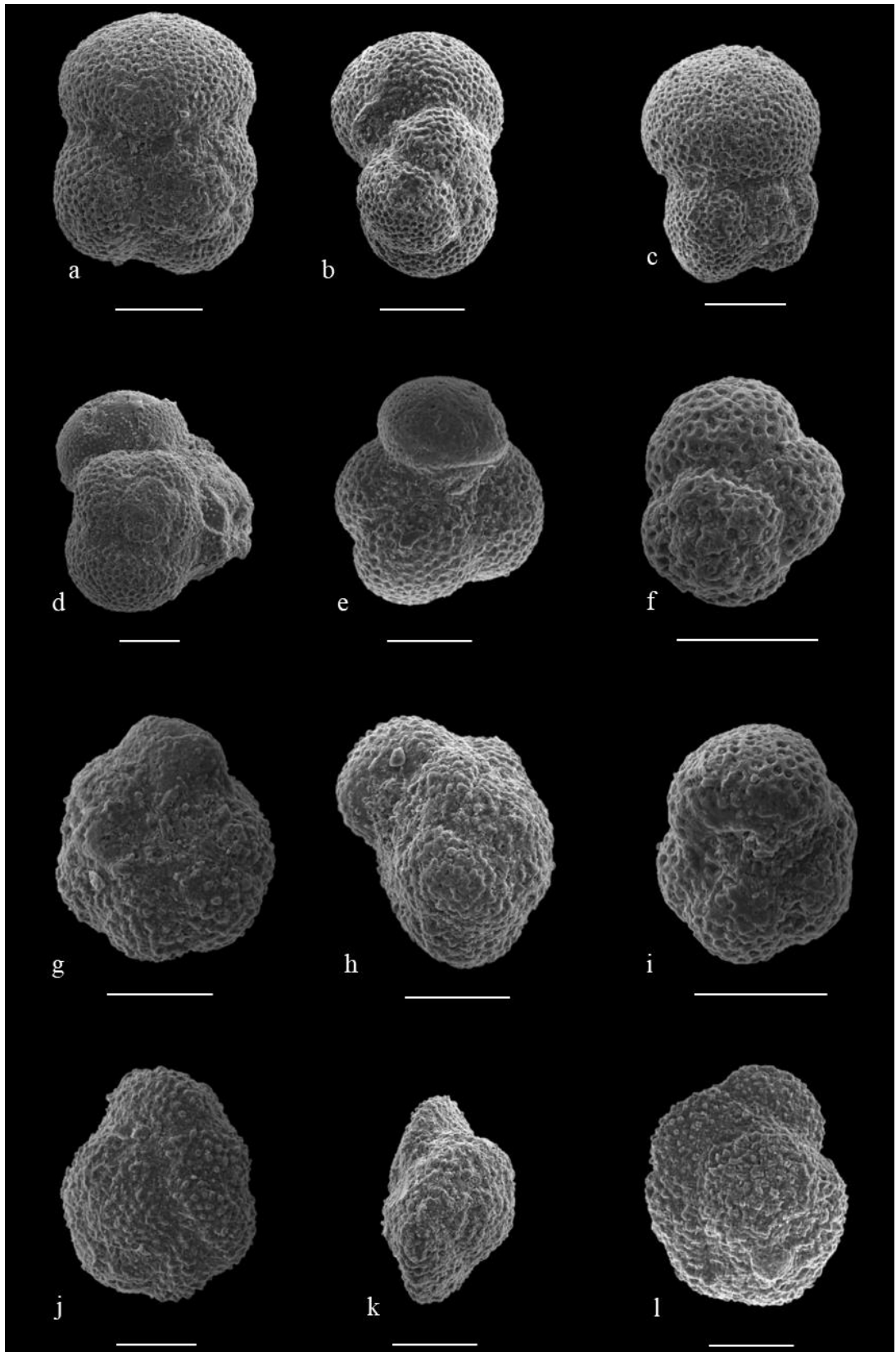


PLATE 5

- a. *Planorotalites pseudoscitula*: Spiral-oblique view, last chamber wall stripped, GT-6
- b. *Planorotalites pseudoscitula*: Spiral view, GT-6
- c. *Planorotalites pseudoscitula*: Umbilical view, GT-6
- d. *Pearsonites lodoensis*: Side view, GT-21
- e. *Pearsonites lodoensis*: Side view, GT-19
- f. *Pearsonites lodoensis*: Umbilical view, GT-19
- g. *Pearsonites broedermann*: Umbilical view, *i* GT-21
- h. *Pearsonites broedermann*: Spiral view, GT-21
- i. *Pearsonites lodoensis*: Spiral view, GT-19
- j. *Morozovella apantesma*: Spiral-oblique view, GT-2
- k. *Morozovella apantesma*: Spiral-oblique view, GT-2
- l. *Morozovella aequa*: Umbilical view, GT-14

Plate 5: SEM images of in situ taxa, with scale bar indicating 100 μm

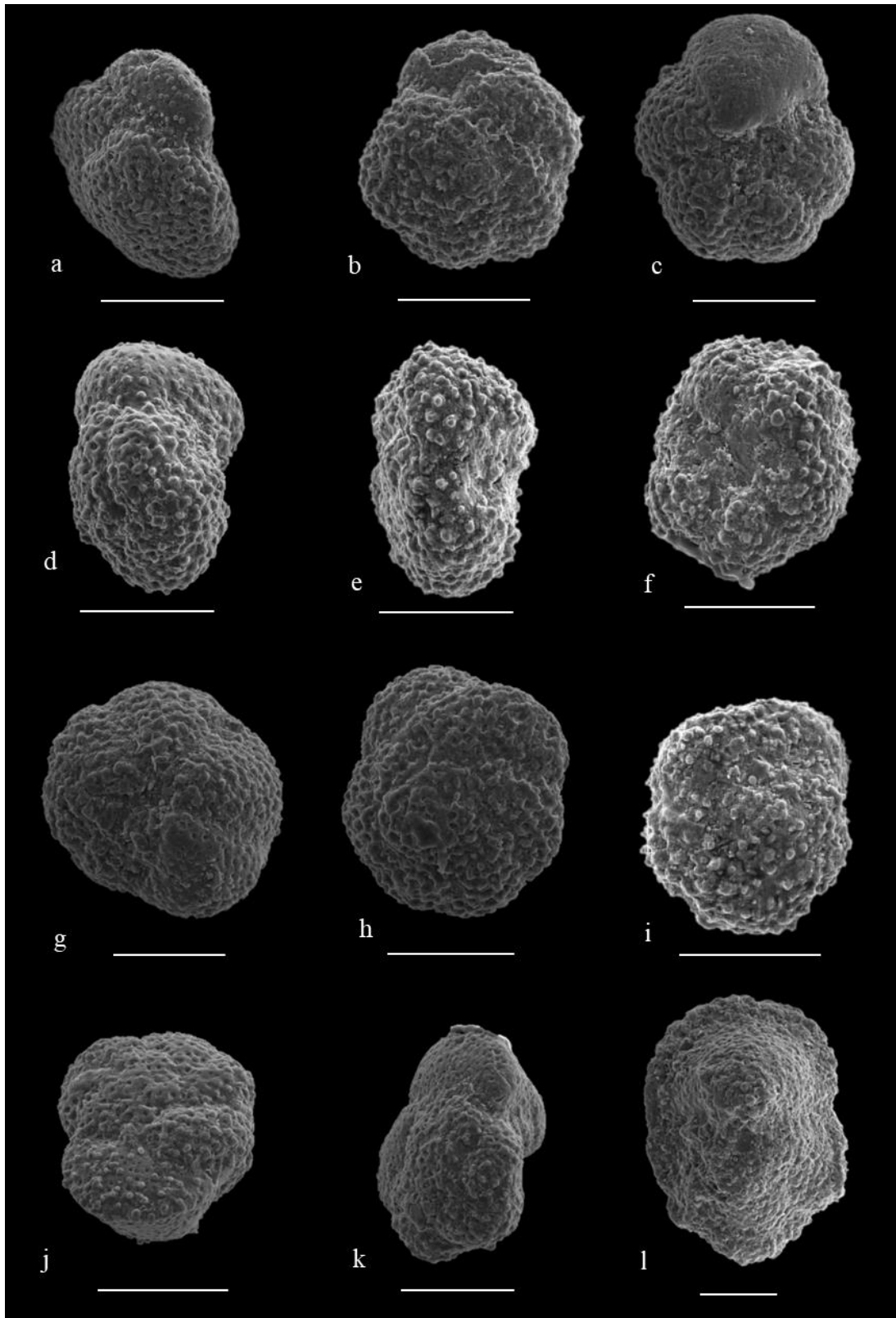


PLATE 6

- a. *Morozovella aequa*: Umbilical view; sediment accumulated in apertural area, GT-14
- b. *Morozovella aequa*: Side view, GT-14
- c. *Morozovella aequa*: Side-oblique view, GT-14
- d. *Morozovella subbotinae*: Umbilical view, GT-14
- e. *Morozovella subbotinae*: Side-oblique view, GT-14
- f. *Morozovella subbotinae*: Spiral-oblique view, GT-14
- g. *Morozovella gracilis*: Spiral-oblique view, GT-19
- h. *Morozovella gracilis*: Umbilical view, GT-19
- i. *Morozovella gracilis*: Side view, GT-22
- j. *Morozovella marginodentata*: Umbilical view, GT-22
- k. *Morozovella marginodentata*: Side view, GT-22
- l. *Morozovella marginodentata*: Spiral view, GT-22

Plate 6: SEM images of in situ taxa, with scale bar indicating 100 μm

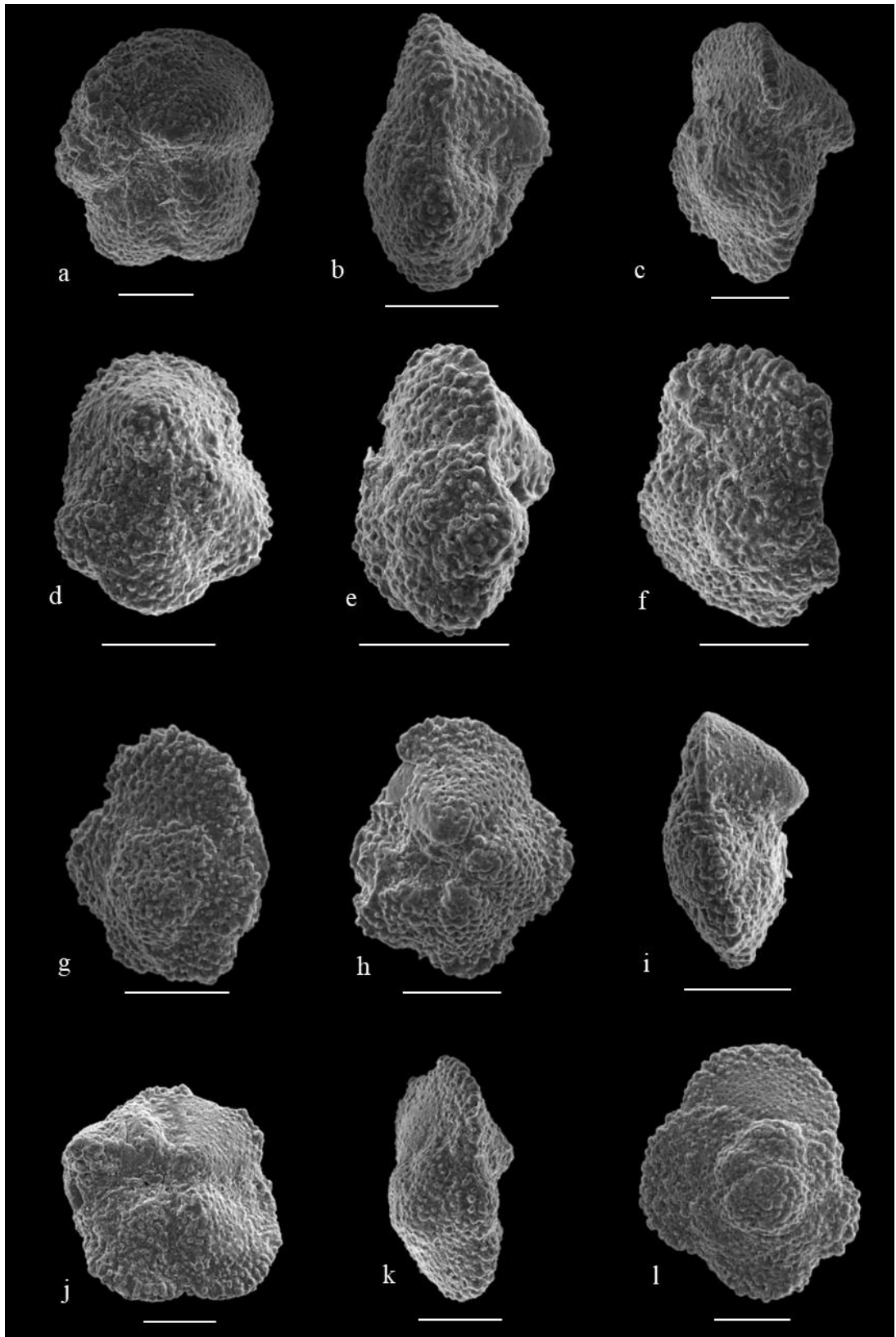


PLATE 7

- a. *Morozovella edgari*: Umbilical view, GT-22
- b. *Morozovella edgari*: Spiral view, GT-22
- c. *Morozovella edgari*: Spiral-oblique view, GT-22
- d. *Morozovella acuta*: Side view, GT-2
- e. *Morozovella acuta*: Spiral-oblique view, GT-2
- f. *Globanomalina planoconica*: Spiral view, GT-6
- g. *Globanomalina planoconica*: Side view, GT-23
- h. *Globanomalina planoconica*: Spiral-oblique view, GT-23
- i. *Globanomalina planoconica*: Umbilical view, GT-9
- j. *Globanomalina pseudomenardii*: Spiral-oblique view, GT-6
- k. *Globanomalina pseudomenardii*: Spiral view, GT-9
- l. *Globanomalina pseudomenardii*: Side-oblique view, GT-9

Plate 7: SEM images of in situ taxa, with scale bar indicating 100 μm

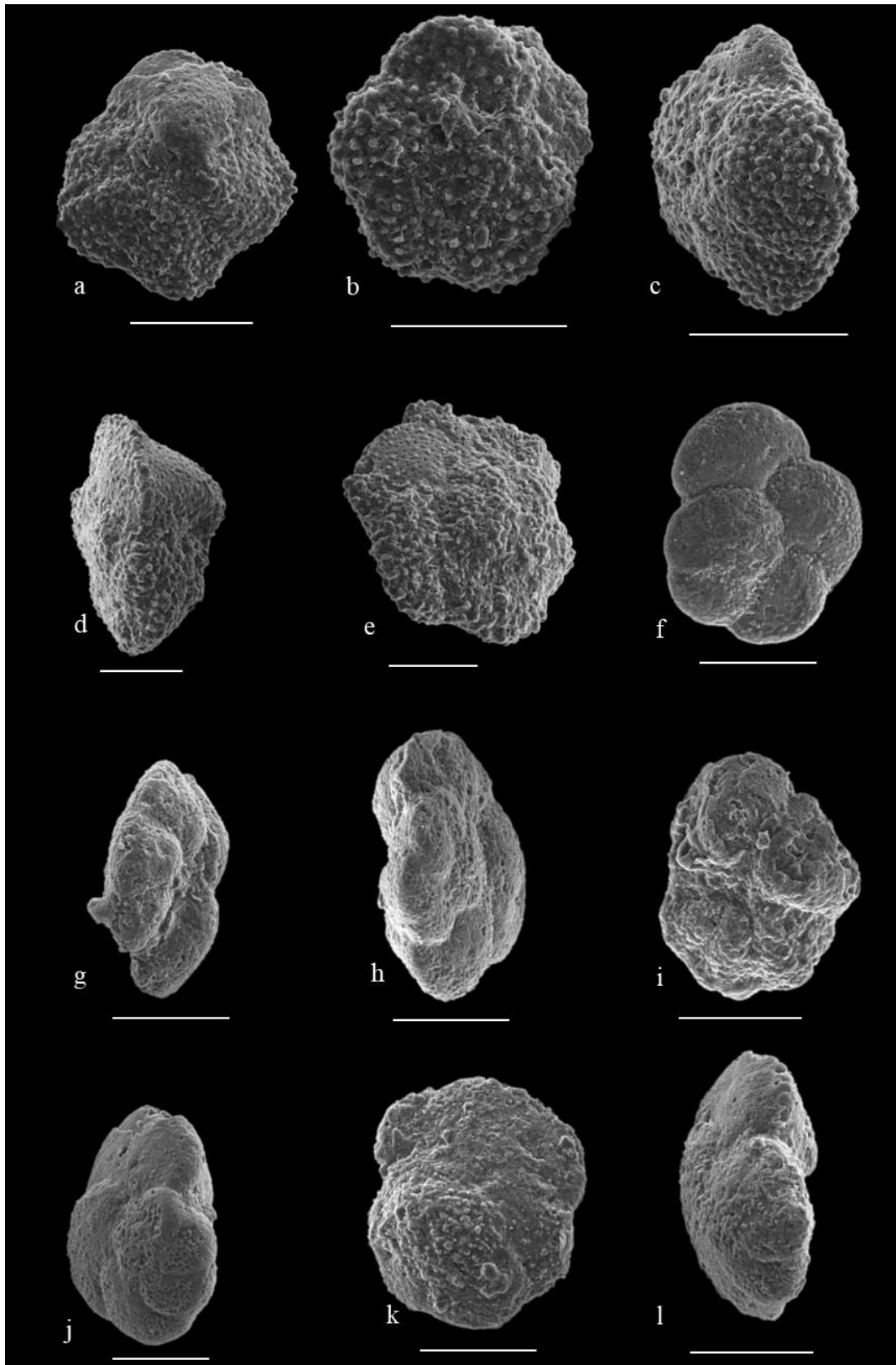


PLATE 8

- a. *Globanomalina imitata*: Side-oblique view, last chamber wall stripped, GT-10
- b. *Globanomalina imitata*: Spiral view, GT-10
- c. *Globanomalina imitata*: Umbilical view, GT-10
- d. *Globanomalina chapmani*: Side view, GT-9
- e. *Globanomalina chapmani*: Spiral view, GT-4
- f. *Globanomalina luxorensis*: Side view, GT-17.5
- g. *Pseudohastigerina wilcoxensis*: Side view, sediment stuck in apertural area, GT-25
- h. *Globanomalina luxorensis*: Side view, GT-20
- i. *Globanomalina luxorensis*: Side view, GT-19
- j. *Pseudohastigerina wilcoxensis*: Equatorial-oblique view, GT-22
- k. *Pseudohastigerina wilcoxensis*: Equatorial view, last chamber broken, GT-22
- l. *Chiloguembelina wilcoxensis* GT-4

Plate 8: SEM images of in situ taxa, with scale bar indicating 100 μm

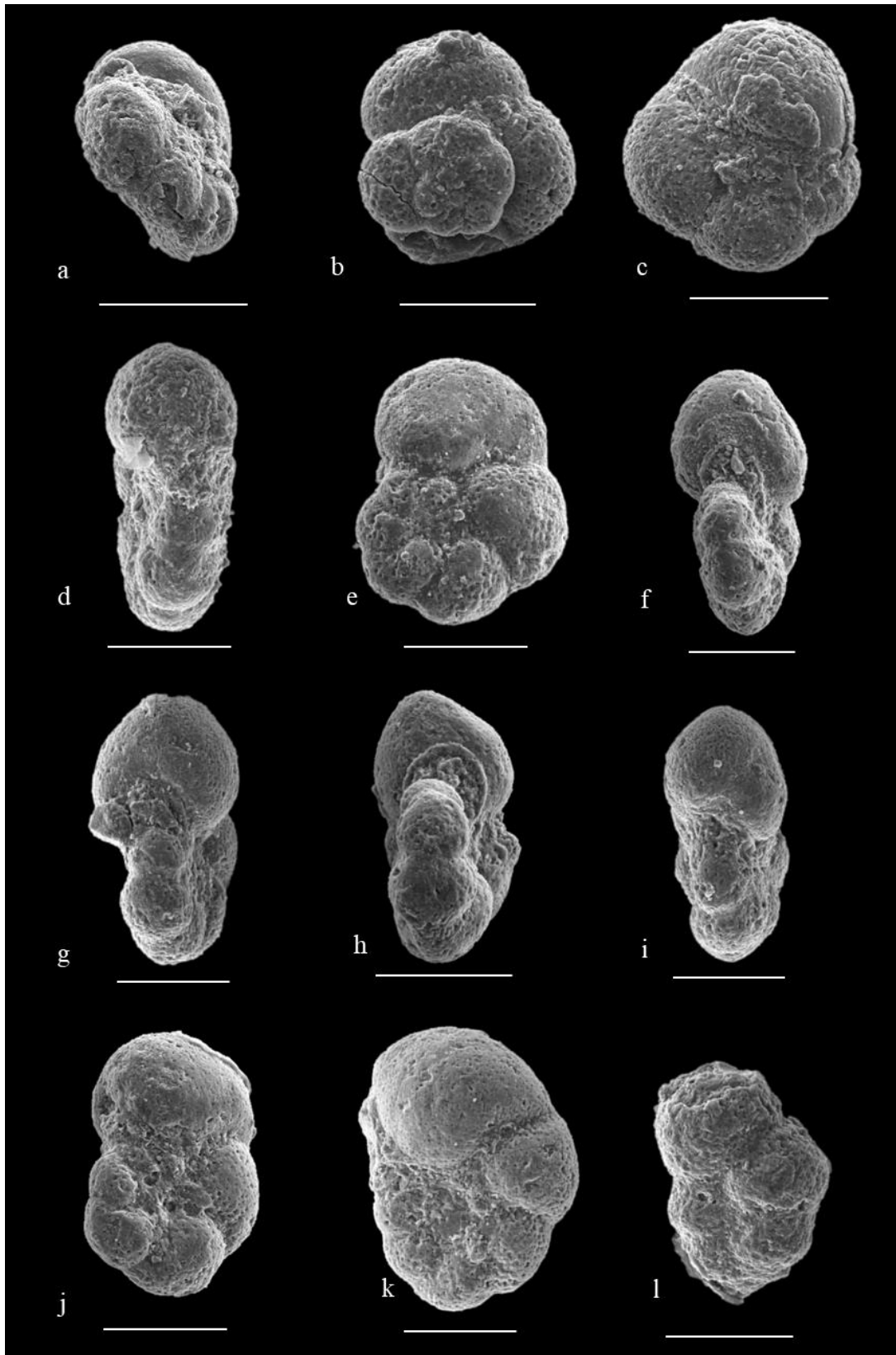
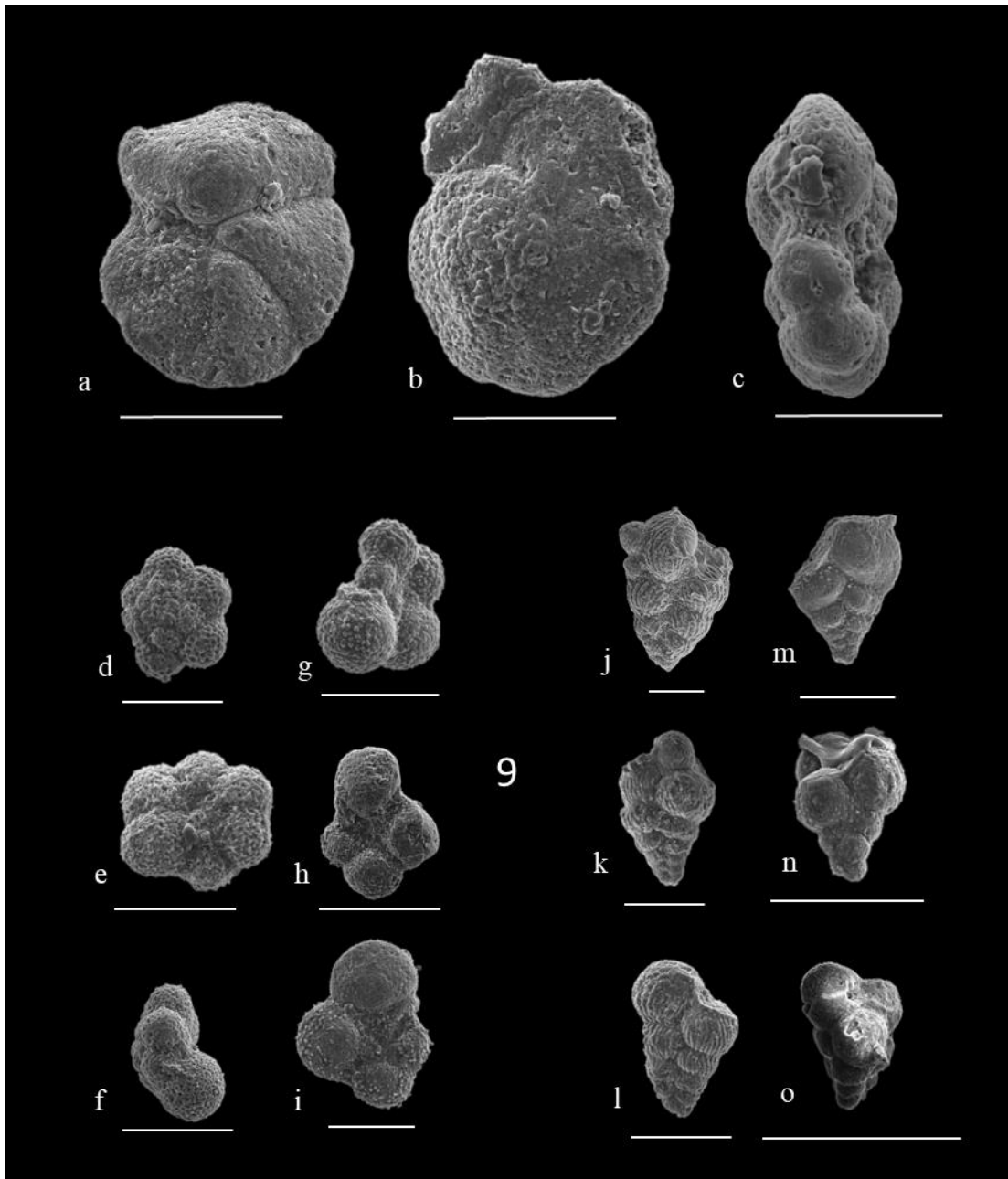


PLATE 9

- a. *Globanomalina pseudomenardii* (Reworked): Umbilical view, GT-23
- b. *Globanomalina pseudomenardii* (Reworked): Spiral view, GT-23
- c. *Globanomalina* sp. (Reworked) : Side view, GT-21
- d. Low trochospiral form (*Praemurica?*, Reworked) : Spiral view, GT-18
- e. Low trochospiral form (*Praemurica?*, Reworked) : Umbilical view, GT-18
- f. Low trochospiral form (*Praemurica?*, Reworked) : Side view, GT-18
- g. Planispiral form (*Globigerinelloides?*, Reworked) : Spiral view, GT-18
- h. Planispiral form (*Globigerinelloides?*, Reworked) : Spiral view, GT-16
- i. Planispiral form (*Globigerinelloides?*, Reworked) : Spiral view, GT-18
- j. Biserial form (Heterohelicidae? Reworked), GT-16
- k. Biserial form (Heterohelicidae? Reworked), GT-18
- l. Biserial form (Heterohelicidae? Reworked), GT-18
- m. Biserial form (Heterohelicidae? Reworked), GT-18
- n. Triserial form (Guembelitreidae? Reworked), GT-16
- o. Triserial form (Guembelitreidae? Reworked), GT-16

Plate 9: SEM images of reworked individuals, with scale bar indicating 100 μ m



APPENDIX D

EDS ANALYSES RESULTS OF SEVERAL GRAINS

1. Octahedral iron oxide crystal from GT-18, Figure 23
2. Milky white sphere from GT-4, Figure 19-B
3. Milky white sphere from GT-16, Figure 19-A
4. Amber colored, translucent globe from GT-16, Figure 20-C
5. Amber colored, translucent globe from GT- 15.5, Figure 20-A
6. Calcitic grain from GT-16, Figure 21-A
7. Calcitic grain from GT-16, Figure 21-B
8. Siliceous grain from GT-16, Figure 21-C
9. Siliceous grain from GT-16, Figure 21-D

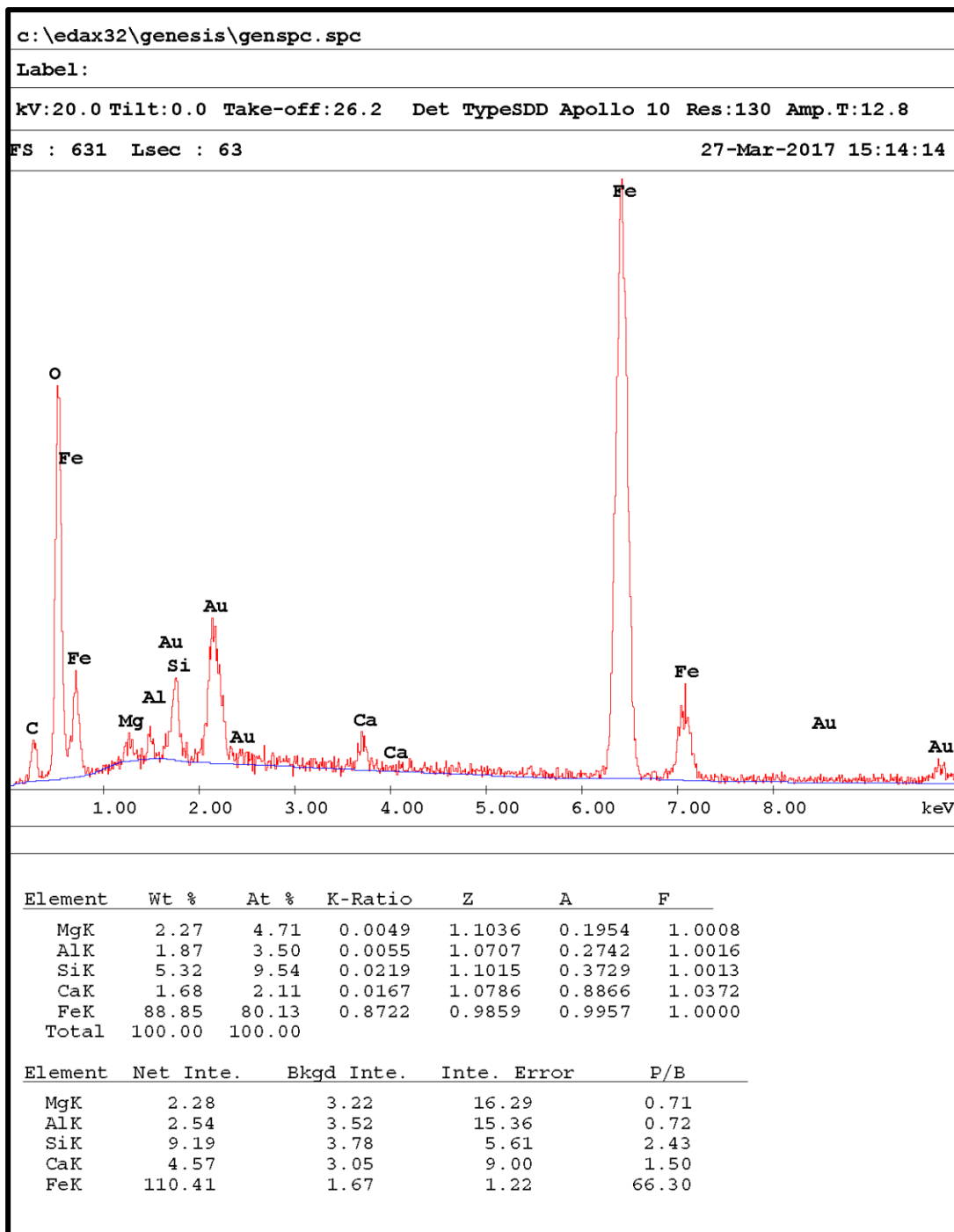


Figure 47: Octahedral iron oxide crystal from GT-18, Figure 23

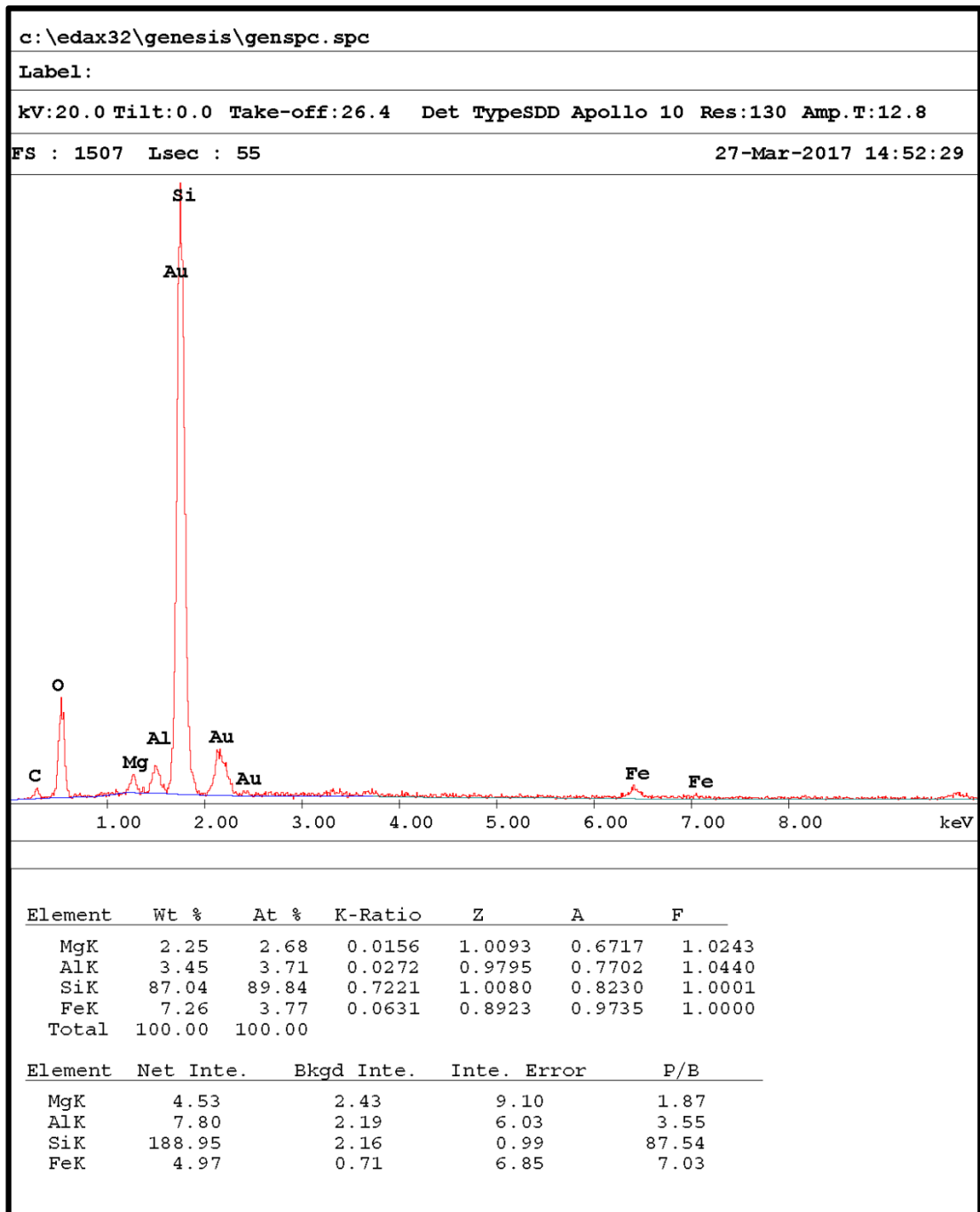


Figure 48: Milky white sphere from GT-4, Figure 19-B

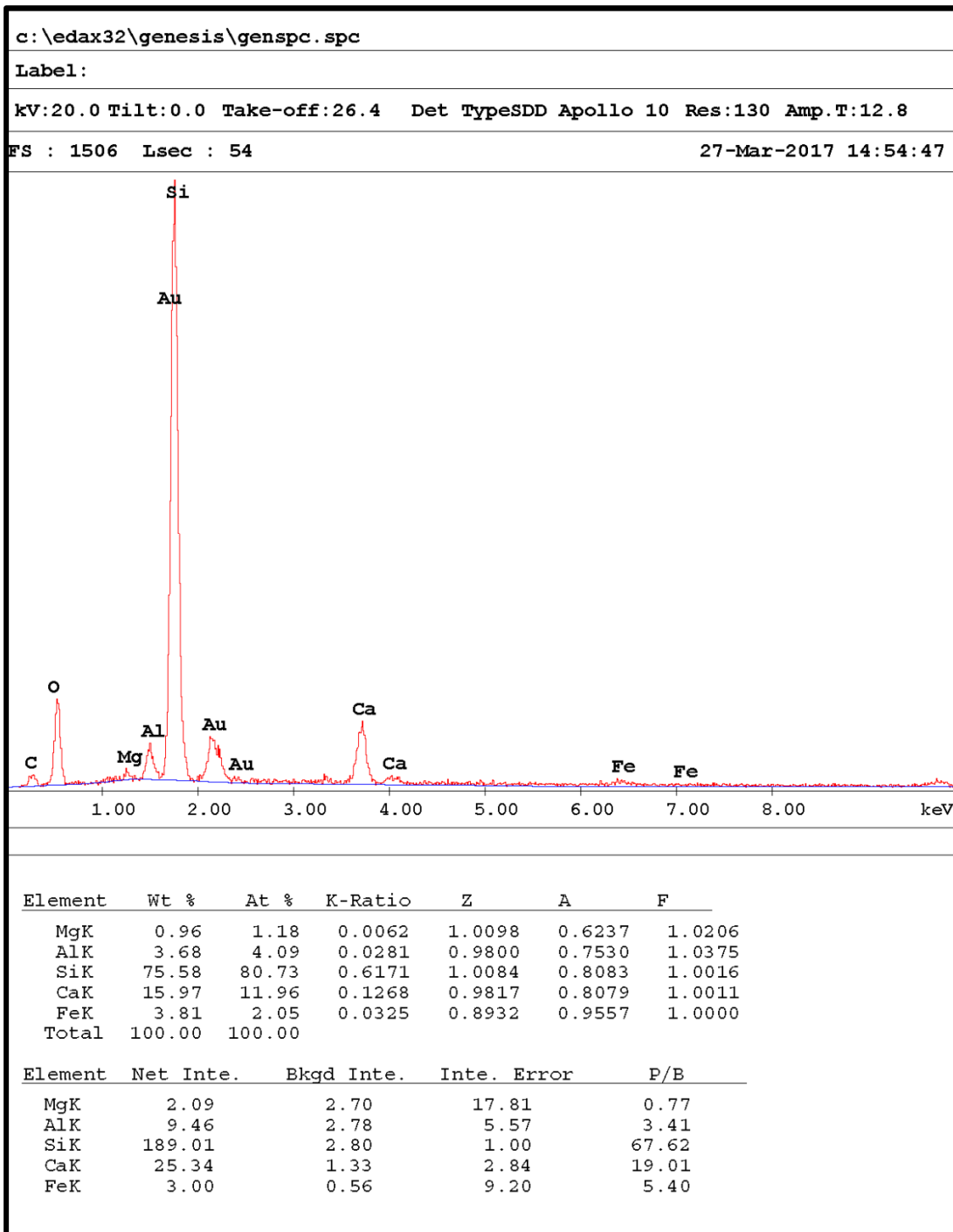


Figure 49: Milky white sphere from GT-16, Figure 19-A

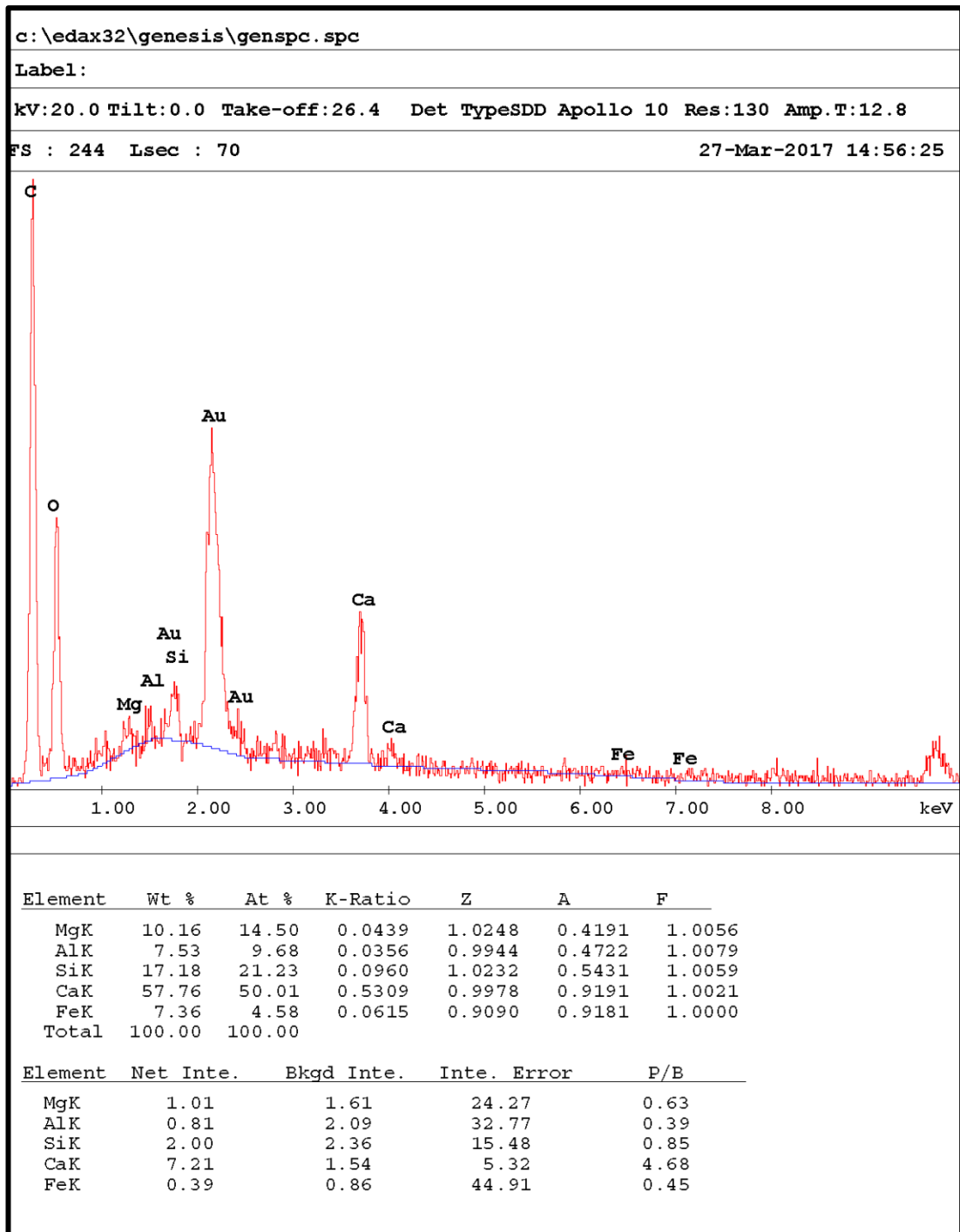


Figure 50: Amber colored globular grain from GT-16, Figure 20-C

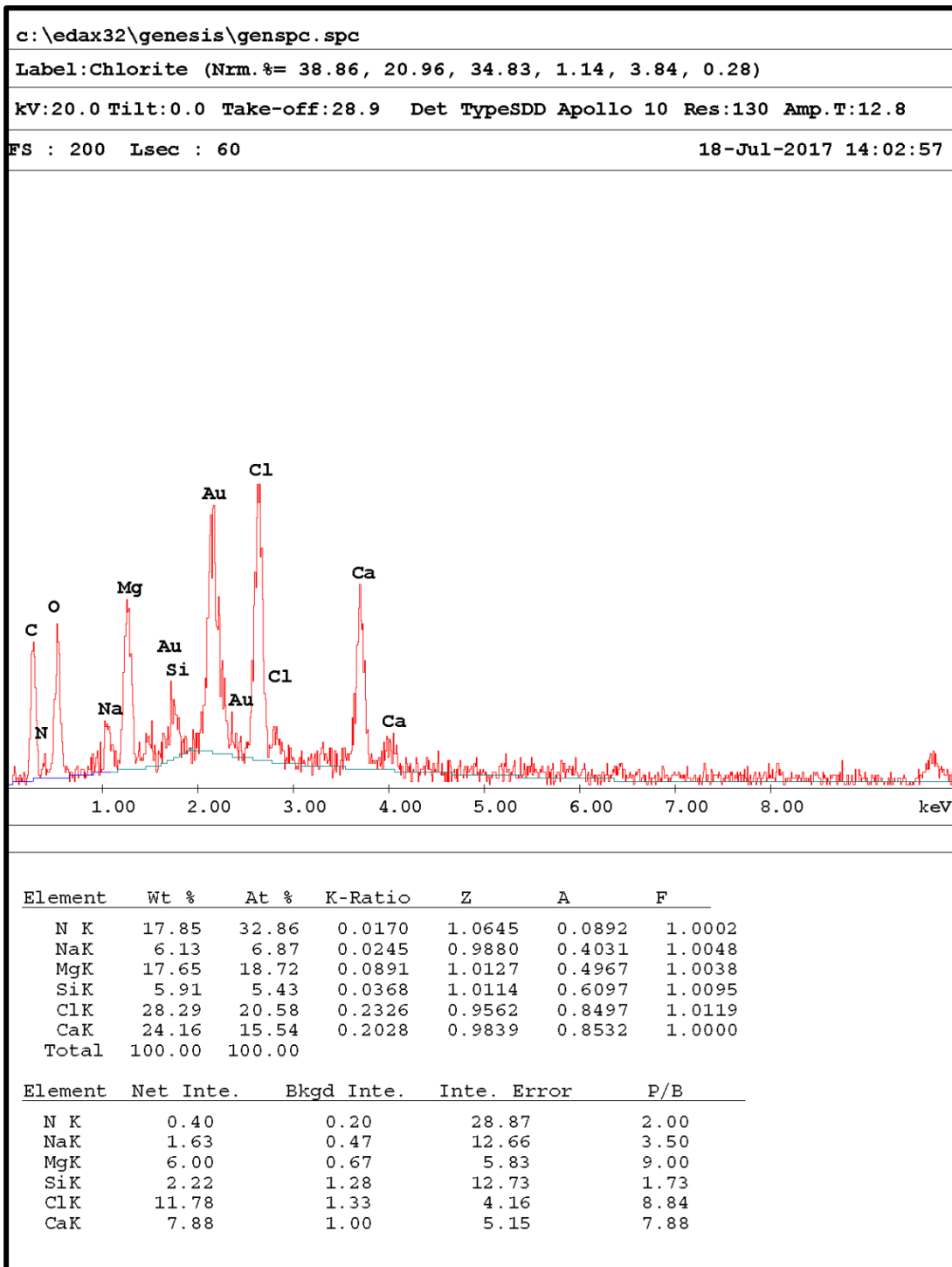


Figure 51: Amber colored globular grain from GT-15.5, Figure 20-A

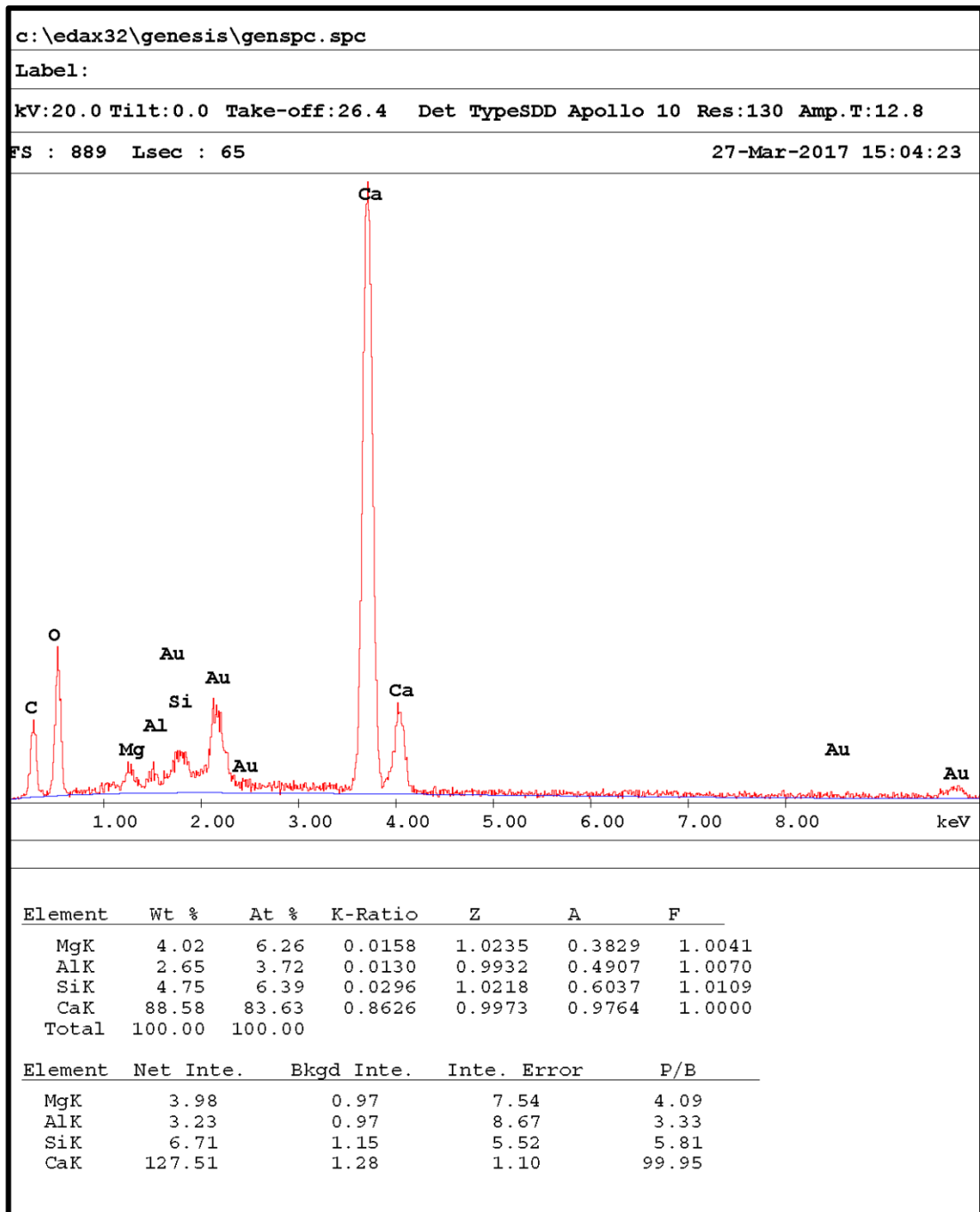


Figure 52: Calcitic grain from GT-16, Figure 21-A

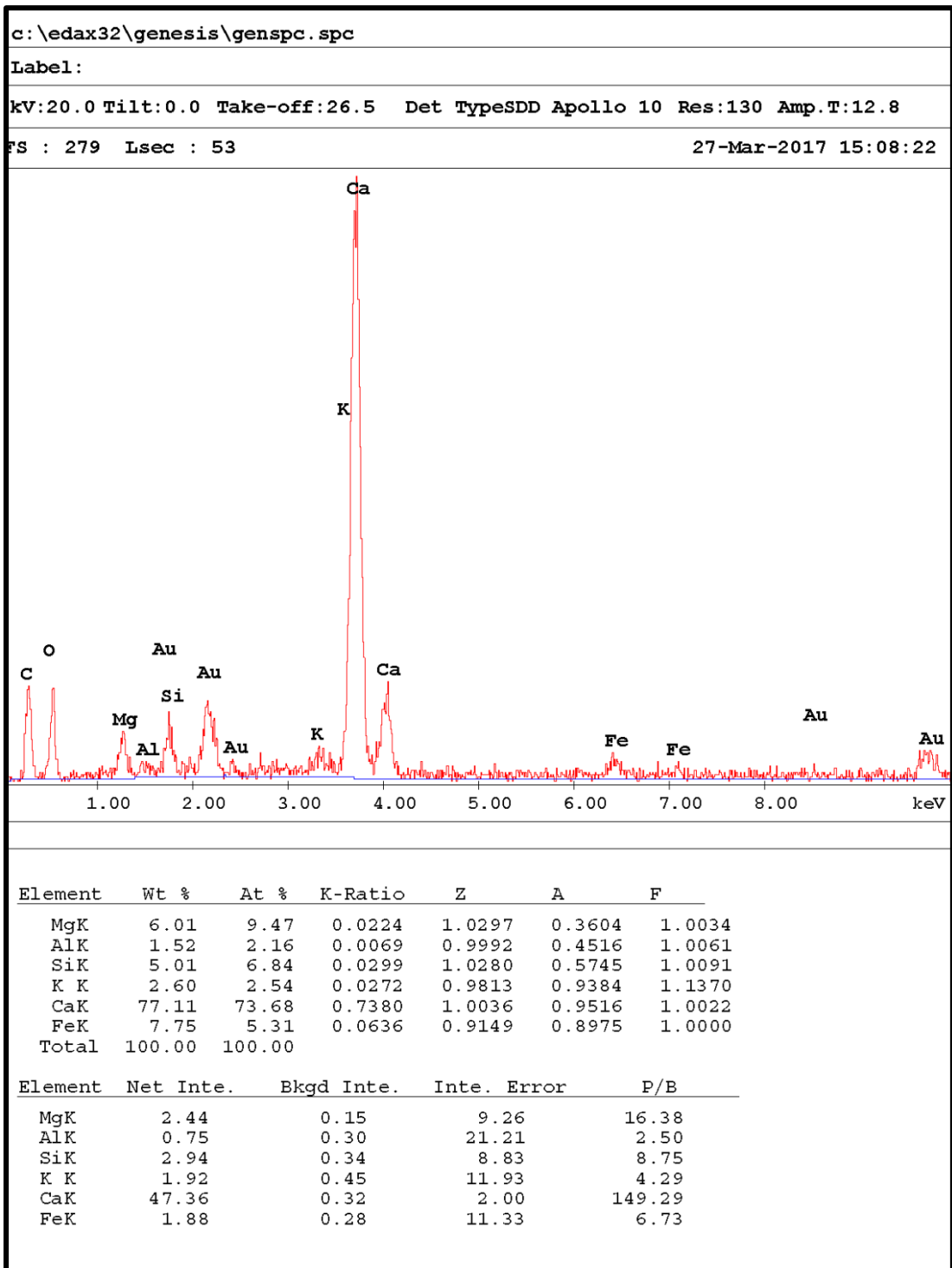


Figure 53: Calcitic grain from GT-16, Figure 21-B

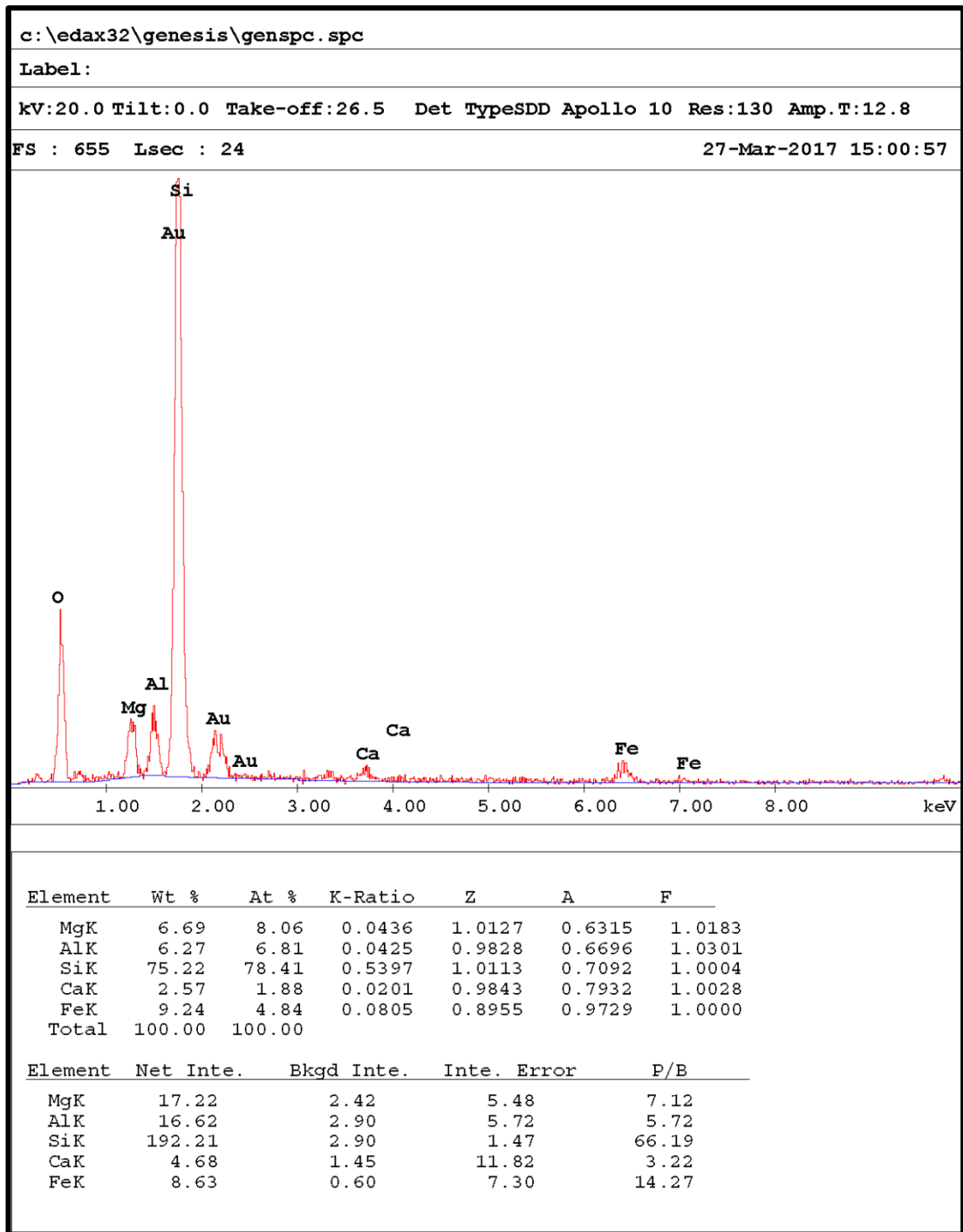


Figure 54: Siliceous grain from GT-16, Figure 21-C

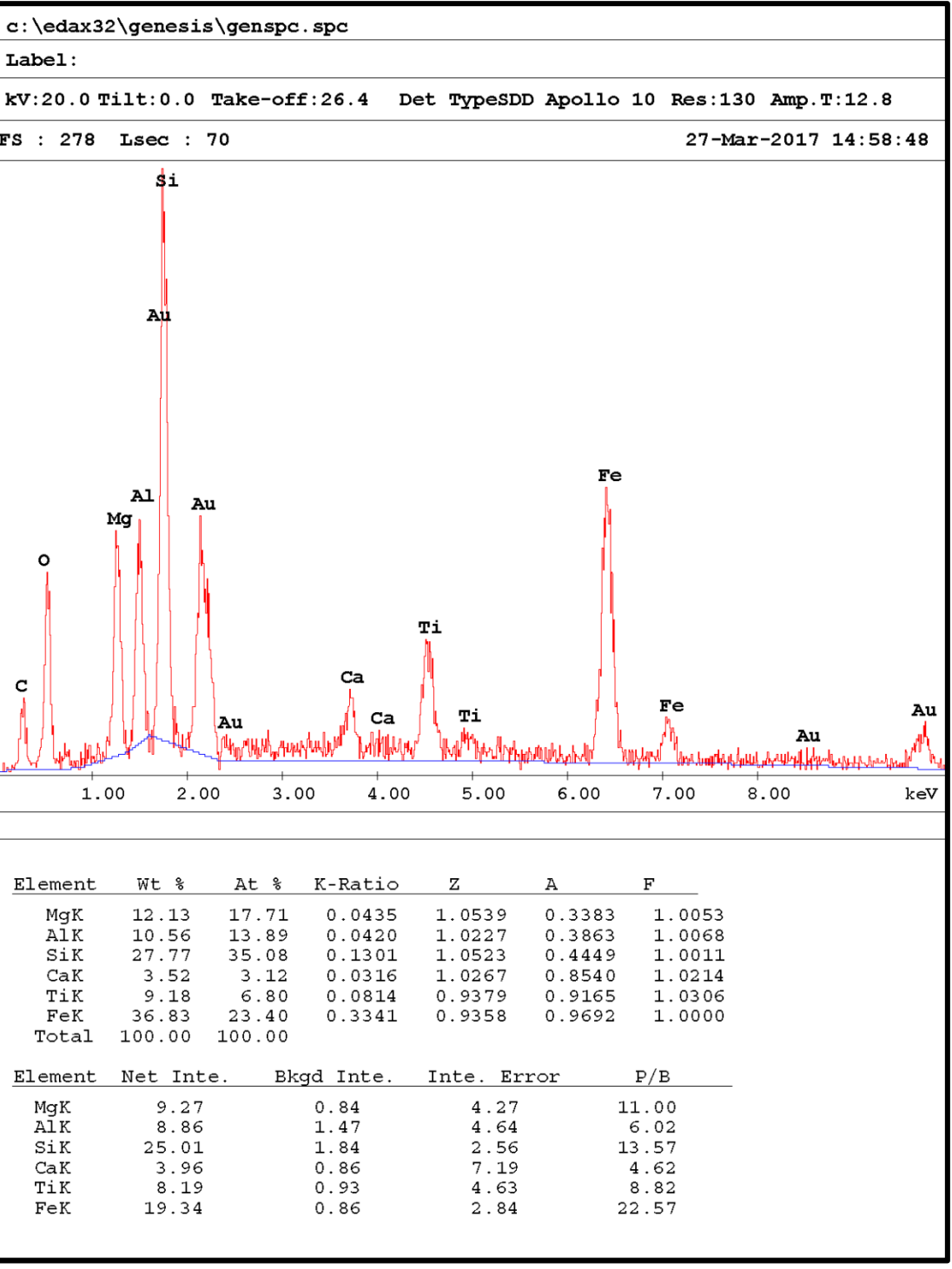


Figure 55: Siliceous grain from GT-16, Figure 21-D